Uranium migration in the Opalinus Clay quantified on the host rock scale with reactive transport simulations

---

Uranmigration im Opalinuston quantifiziert für die Wirtsgesteinsskala mit reaktiven Transportsimulationen

Kumulative Dissertation

zur Erlangung des akademischen Grades

doctor rerum naturalium (Dr. rer. nat.)

in der Wissenschaftsdisziplin Hydrogeologie

eingereicht an der

Mathematisch-Naturwissenschaftlichen Fakultät

der Universität Potsdam

vorgelegt von

Theresa Hennig

Potsdam, 22. Februar 2022

Gutachter

Prof. Dr. Michael Kühn
Deutsches GeoForschungsZentrum GFZ
Department Geochemie
Sektion Fluidsystemmodellierung

und

Universität Potsdam
Mathematisch-Naturwissenschaftliche Fakultät
Institut für Geowissenschaften

Prof. Dr. Thomas Neumann
Technische Universität Berlin
Fakultät VI - Planen Bauen Umwelt
Institut für Angewandte Geowissenschaften

Prof. Dr. Vinzenz Brendler
Helmholtz-Zentrum Dresden-Rossendorf
Institut für Ressourcenökologie
Abteilung Thermodynamik der Actiniden

Tag der Disputation: 01. Juni 2022

Published online on the
Publication Server of the University of Potsdam:
https://doi.org/10.25932/publishup-55270
https://nbn-resolving.org/urn:nbn:de:kobv:517-opus4-552700

Abstract

Humankind and their environment need to be protected from the harmful effects of spent nuclear fuel, and therefore disposal in deep geological formations is favoured worldwide. Suitability of potential host rocks is evaluated, among others, by the retention capacity with respect to radionuclides. Safety assessments are based on the quantification of radionuclide migration lengths with numerical simulations as experiments cannot cover the required temporal (1 Ma) and spatial scales (>100 m).

Aim of the present thesis is to assess the migration of uranium, a geochemically complex radionuclide, in the potential host rock Opalinus Clay. Radionuclide migration in clay formations is governed by diffusion due to their low permeability and retarded by sorption. Both processes highly depend on pore water geochemistry and mineralogy that vary between different facies. Diffusion is quantified with the single-component (SC) approach using one diffusion coefficient for all species and the process-based multi-component (MC) option. With this, each species is assigned its own diffusion coefficient and the interaction with the diffuse double layer is taken into account. Sorption is integrated via a bottom-up approach using mechanistic surface complexation models and cation exchange. Therefore, reactive transport simulations are conducted with the geochemical code PHREEQC to quantify uranium migration, i.e. diffusion and sorption, as a function of mineralogical and geochemical heterogeneities on the host rock scale.

Sorption processes are facies dependent. Migration lengths vary between the Opalinus Clay facies by up to 10 m. Thereby, the geochemistry of the pore water, in particular the partial pressure of carbon dioxide (pCO_2), is more decisive for the sorption capacity than the amount of clay minerals. Nevertheless, higher clay mineral quantities compensate geochemical variations. Consequently, sorption processes must be quantified as a function of pore water geochemistry in contact with the mineral assemblage.

Uranium diffusion in the Opalinus Clay is facies independent. Speciation is dominated by aqueous ternary complexes of U(VI) with calcium and carbonate. Differences in the migration lengths between SC and MC diffusion are with ±5 m negligible. Further, the application of the MC approach highly depends on the quality and availability of the underlying data. Therefore, diffusion processes can be adequately quantified with the SC approach using experimentally determined diffusion coefficients.

The hydrogeological system governs pore water geochemistry within the formation rather than the mineralogy. Diffusive exchange with the adjacent aquifers established geochemical gradients over geological time scales that can enhance migration by up to 25 m. Consequently, uranium sorption processes must be quantified following the identified priority: pCO_2 > hydrogeology > mineralogy.

The presented research provides a workflow and orientation for other potential disposal sites with similar pore water geochemistry due to the identified mechanisms and dependencies. With a maximum migration length of 70 m, the retention capacity of the Opalinus Clay with respect to uranium is sufficient to fulfill the German legal minimum requirement of a thickness of at least 100 m.

Kurzfassung

Zum Schutz von Mensch und Umwelt vor den schädlichen Auswirkungen abgebrannter Brennelemente, wird weltweit die Endlagerung in tiefen geologischen Formationen favorisiert. Daher ist das Rückhaltevermögen potenzieller Wirtsgesteine gegenüber Radionukliden ein wichtiges Kriterium. Sicherheitsbewertungen basieren auf der Quantifizierung der Migration mit numerischen Simulationen, da Experimente die erforderlichen zeitlichen (1 Ma) und räumlichen Skalen (>100 m) nicht abdecken können.

Ziel der Dissertation ist es, die Migration des geochemisch komplexen Radionuklids Uran im potenziellen Wirtsgestein Opalinuston zu bewerten. In Tonformationen wird die Radionuklidmigration aufgrund der geringen Durchlässigkeit von Diffusion bestimmt und durch Sorption verzögert. Beide Prozesse hängen stark von der Porenwassergeochemie und Mineralogie ab, die zwischen verschiedenen Fazies variieren. Die Diffusion wird mit dem Einkomponenten- (SC) und Mehrkomponentenansatz (MC) quantifiziert. Nach dem SC-Ansatz wird ein Diffusionskoeffizient für alle Spezies verwendet, wohingegen mit der MC-Option individuelle Werte zugewiesen und die Interaktion mit der diffusen Doppelschicht berücksichtigt wird. Die Sorption ist mit Hilfe mechanistischer Oberflächenkomplexierungsmodelle und Kationenaustausch integriert. Die Durchführung reaktiver Transportsimulationen mit dem Code PHREEQC ermöglicht die Quantifizierung der Uranmigration, d. h. Diffusion und Sorption, in Abhängigkeit der Mineralogie und Porenwassergeochemie für die Wirtsgesteinsskala.

Sorptionsprozesse sind faziesabhängig. Die Migrationslängen variieren um bis zu 10 m zwischen den Fazies aufgrund von Unterschieden in der Porenwassergeochemie. Dabei ist insbesondere der Partialdruck des Kohlendioxids (pCO_2) entscheidender für die Sorptionskapazität als die Menge an Tonmineralen. Allerdings kompensieren höhere Tonmineralmengen geochemische Schwankungen. Folglich müssen Sorptionsprozesse in Abhängigkeit der Porenwassergeochemie quantifiziert werden.

Urandiffusion ist faziesunabhängig. Die Speziation wird durch aquatische ternäre Komplexe von U(VI) mit Kalzium und Karbonat dominiert. Die Unterschiede in den Migrationslängen zwischen SC- und MC-Diffusion sind mit ± 5 m vernachlässigbar. Die Anwendung des MC-Ansatzes hängt stark von der Qualität und Verfügbarkeit der zugrunde liegenden Daten ab. Diffusionsprozesse können also mit dem SC-Ansatz unter Verwendung experimentell ermittelter Diffusionskoeffizienten quantifiziert werden.

Haupteinflussfaktor auf die Porenwassergeochemie ist das hydrogeologische System und nicht die Mineralogie. Der diffusive Austausch mit den angrenzenden Aquiferen hat über geologische Zeiträume geochemische Gradienten geschaffen, die die Migration um bis zu 25 m verlängern können. Folglich müssen Sorptionsprozesse nach der identifizierten Priorität quantifiziert werden: pCO_2 > Hydrogeologie > Mineralogie.

Die ermittelten Abhängigkeiten dienen als Orientierung für andere potenzielle Endlagerstandorte mit ähnlicher Porenwassergeochemie. Mit einer maximalen Migration von 70 m reicht das Rückhaltevermögen des Opalinustons gegenüber Uran aus, um die deutsche gesetzliche Mindestanforderung von 100 m Mächtigkeit zu erfüllen.

Table of contents

Abstract I

Kurzfassung III

List of figures IX

List of tables XI

List of acronyms and symbols XIII

1 Introduction 1
- 1.1 Learning from nature - the multi-barrier concept . . . 2
  - 1.1.1 The host rock is the natural and final barrier . . . 3
  - 1.1.2 The Opalinus Clay as potential host rock . . . 5
- 1.2 Long-term behaviour of repository systems must be evaluated with numerical simulations . . . 7
  - 1.2.1 Diffusion is the transport process through the host rock clay . . . 7
  - 1.2.2 Sorption on clay minerals retards radionuclide transport . . . 9
  - 1.2.3 Heterogeneous systems require advanced approaches . . . 9
- 1.3 Thesis objectives . . . 13
- 1.4 Structure of the thesis and scientific contribution . . . 13

2 Simulation of diffusive uranium transport and sorption processes in the Opalinus Clay 17
- 2.1 Introduction . . . 17
- 2.2 Methods . . . 19
  - 2.2.1 Geochemical modelling of Opalinus Clay pore water . . . 19
  - 2.2.2 Modelling transport and sorption processes . . . 21
- 2.3 Model calibration . . . 24
- 2.4 Results . . . 24
  - 2.4.1 Speciation calculations of uranium in the Opalinus Clay . . . 24
  - 2.4.2 Uranium migration depending on pore water chemistry . . . 27
  - 2.4.3 Uranium migration as a function of mineral composition . . . 28
- 2.5 Discussion . . . 30
  - 2.5.1 Speciation of uranium in the pore water . . . 30
  - 2.5.2 Governance of pCO_2 on uranium migration . . . 30
  - 2.5.3 Influence of varying mineralogical compositions . . . 32
- 2.6 Conclusions and Outlook . . . 33

3 Surrogate model for multi-component diffusion of uranium through Opalinus Clay on the host rock scale 35
3.1 Introduction . . . 35
3.2 Methods . . . 37
3.2.1 Geochemical system of the Opalinus Clay . . . 38
3.2.2 Integrating sorption processes . . . 38
3.2.3 Modelling multi-component diffusion . . . 40
3.2.4 Modelling single-component diffusion . . . 43
3.3 Model calibration . . . 43
3.4 Results . . . 45
3.4.1 Multi- and single-component simulations on the metre-scale . . . 45
3.4.2 Multi-component diffusion for varying total amounts of minerals on the metre-scale . . . 48
3.4.3 Transfer of multi-component diffusion simulations to the host rock scale . . . 49
3.5 Discussion . . . 50
3.5.1 Differences between single- and multi-component diffusion approach . . . 51
3.5.2 Effect of varying mineralogy on multi-component diffusion . . . 54
3.5.3 Implications for the host rock scale . . . 55
3.6 Conclusions and outlook . . . 56

4 Uranium migration varies on the metre-scale in response to differences of a stability constant 59
4.1 Introduction . . . 59
4.2 Methods . . . 61
4.3 Results . . . 64
4.3.1 Pourbaix diagrams for the speciation of uranium . . . 64
4.3.2 Uranium migration on the host rock scale . . . 65
4.4 Discussion . . . 66
4.5 Conclusions . . . 67

5 Potential uranium migration within the geochemical gradient of the Opalinus Clay system at the Mont Terri 69
5.1 Introduction . . . 69
5.2 Methods . . . 71
5.2.1 Geological and hydrogeological evolution of the Mont Terri anticline . . . 72
5.2.2 Initial model conditions . . . 73
5.2.3 Geochemical system and present-day pore water profiles . . . 75
5.2.4 Incorporated sorption processes . . . 76
5.2.5 Modelling single-component diffusion . . . 77
5.2.6 Modelling multi-component diffusion . . . 78
5.2.7 Uranium source term . . . 79

5.3 Model calibration and validation . . . 79
5.3.1 Chloride profile at Mont Terri . . . 80
5.3.2 Diffusion experiment with uranium . . . 81
5.4 Results . . . 81
5.4.1 Simulation of pore water profiles using single- and multi-component diffusion . . . 81
5.4.2 Simulation of potential uranium migration within a geochemical gradient . . . 84
5.5 Discussion . . . 86
5.5.1 Diffusion and mineral interaction control pore water profiles . . . 86
5.5.2 Geochemical system governs uranium migration . . . 88
5.6 Conclusions and outlook . . . 90

6 Discussion **93**
6.1 Pore water geochemistry governs uranium migration . . . 94
6.2 Data quality affects resulting migration lengths . . . 99
6.3 Predictive power of models must be quantified . . . 104

7 Conclusions and outlook **109**

A Supplementary S-1: Surface parameters and reactions **113**

B Supplementary S-2: Self-diffusion coefficients in water D_w **117**

C Supplementary S-3: Data summary of pore water components **119**

D Supplementary S-4: Adapted stability constant of calcite **121**

E Supplementary S-5: Measured pore water profiles confirmed **123**

Publications of the author **125**

Acknowledgements **127**

Selbstständigkeitserklärung

List of figures

1.1 A multi-barrier system is designed to isolate the spent fuel mainly consisting of uranium from the surface environment 3

1.2 Migration of radionuclides in clay formations depends on the accessibility of the pore space and is retarded by sorption processes 8

2.1 Concept of the one-dimensional diffusion model in PHREEQC applying single-component (SC) diffusion 23

2.2 Calibrated model applicable to quantify uranium diffusion and sorption in the Opalinus Clay with SC diffusion 25

2.3 Pourbaix diagrams of aqueous uranium speciation for the pore water composition of the sandy facies 26

2.4 Trends in modelled pH and pe in the three Opalinus Clay facies (shaly, sandy and carbonate-rich) for varying pCO_2 27

2.5 Uranium concentrations in the pore waters of the three facies after one million years as a function of pCO_2 28

2.6 Uranium migration depending on the mineralogical heterogeneity between the three litho-facies 29

3.1 Conceptual, one-dimensional model of the multi-component (MC) diffusion approach implemented in PHREEQC 42

3.2 MC option can be applied to the Opalinus Clay system as empirical parameter n representing pore space geometry is calibrated 44

3.3 Differences in uranium migration lengths between SC and MC simulations observed in all facies on the metre-scale 45

3.4 Concentrations of calcium, magnesium, chloride, sulphate and uranium in the DDL of the clay minerals in the sandy facies 47

3.5 Uranium migrates farther through the formation with decreasing amount of minerals per kg pore water 48

3.6 Transport parameters calibrated on the metre-scale can be applied to the host rock scale as surrogate for MC diffusion 50

4.1 Log K value of $Ca_2UO_2(CO_3)_3$ complex in the underlying database governs predominant aqueous uranium species in the shaly facies 64

4.2 Migration distances deviate by up to 7 m depending on predominant uranium species (neutral or anionic ternary complex) 66

5.1 Erosion history of the Mont Terri anticline and associated freshwater infiltration into embedding aquifers of Opalinus Clay 72

5.2 Profile of measured chloride concentrations at Mont Terri is used to define the conceptual model with boundary and initial conditions 74

5.3 Measured profiles of pore water components governing uranium sorption decrease from Opalinus Clay towards embedding aquifers 76

5.4 Conceptual model is calibrated for further application against measured chloride profile for SC and MC simulations 80

5.5 Model concept is validated for uranium diffusion and sorption as simulation results coincide with data of diffusion experiment 82

5.6 Measured pore water profiles of Ca^{2+}, Mg^{2+}, pH and pCO_2 confirmed by data-driven and conceptual scenario 83

5.7 Uranium migration is enhanced by the geochemical gradients due to a decrease in sorption capacity associated with ionic strength 85

6.1 Application of constant K_d values leads to an underestimation of migration distances compared to process-based simulations 96

6.2 Updated thermodynamic data changes main species from anionic to neutral affecting calibrated mineral composition and exponent n 102

6.3 Formation of predominantly neutral complexes is associated with a decreased sorption and thus farther uranium migration 104

6.4 Increased pCO_2 in the initial conditions leads to farther uranium migration due to an associated decreased sorption capacity 106

C.1 Concentrations of pore water components used for model calibration decrease towards embedding aquifers 119

E.1 Measured pore water profiles confirmed with SC simulations and initial conditions according to data-driven scenario (1R) 123

E.2 SC simulations of conceptual scenario (2J) coincide with measured pore water profiles except for potassium and sulphate 124

List of tables

2.1 Geochemical and mineralogical input parameters representing the three facies (shaly, sandy and carbonate-rich) in the Opalinus Clay 20

2.2 Percentage of aqueous uranium species in the pore water of the sandy and shaly facies for different pCO_2 26

3.1 Mineralogical and geochemical input parameters representing the three facies in the multi-component (MC) simulations 39

3.2 Hydro-physical input parameters for the scenarios with minimum and maximum amount of minerals per kg pore water for the facies 40

3.3 Transport parameters (K_d and D_e) of all scenarios calibrated from the MC simulations on the metre-scale 47

4.1 Pore water and mineralogical composition of the shaly and sandy facies representing higher and lower clay mineral quantities 62

4.2 Log K value of the neutral ternary uranyl complex governs predominant aqueous species (anionic or neutral ternary complex) 65

5.1 Input concentrations of main pore water components in the embedding aquifers and low permeable layer for the two scenarios 75

6.1 Application of updated thermodynamic data for uranium changes species distribution from predominantly anionic to neutral 103

6.2 Selection of simulations representing the hydrogeological system of the Opalinus Clay at Mont Terri is verified by rRMSE 105

A.1 Summary of surface parameters and reactions as well as cation exchange used for modelling U(VI) sorption onto clay minerals 113

B.1 Summary of the self-diffusion coefficients in water D_w required to apply the MC diffusion approach 117

C.1 Summary of the pore water data from borehole analyses that are used to calibrate the model 120

List of acronyms and symbols

Abbreviations

AtG	Atomgesetz
BASE	Bundesamt für die Sicherheit der nuklearen Entsorgung
BGE	Bundesgesellschaft für Endlagerung mbH
CEC	Cation exchange capacity
CO_2	Carbon dioxide
DDL	Diffuse double layer
HZDR	Helmholtz-Zentrum Dresden-Rossendorf
IAEA	International Atomic Energy Agency
IS mixed	Illite/smectite mixed layers
MC	Multi-component
MC_{max}	MC simulation; maximum amount of rock per kg pore water
MC_{min}	MC simulation; minimum amount of rock per kg pore water
MC_{2Clay}	MC simulation; sorption on illite and montmorillonite
MC_{4Clay}	MC simulation; sorption on illite, montmorillonite, kaolinite and chlorite
Nagra	Nationale Genossenschaft für die Lagerung radioaktiver Abfälle
NEA	Nuclear Energy Agency
OPA	Opalinus Clay
PSI	Paul Scherrer Institut
RMSE	Root mean square error
rRMSE	Relative root mean square error
SC	Single-component
SCM	Surface complexation model
StandAG	Standortauswahlgesetz
TJB	Triassic-Jurassic boundary
1R	Data-driven scenario; pore water composition based on sample taken at Mont Russelin
2D	Two-dimensional
2J	Conceptual scenario; combination of Liassic groundwater from Mont Russelin and Jurassic sea water
3D	Three-dimensional

Latin symbols

C	Concentration of the species in the mobile phase	mol/m^3
c_i	Species concentration in the accessible pore water	mol/m^3
$c_{i,DDL}$	Species concentration in the Donnan pore space	mol/m^3
D_e	Effective diffusion coefficient	m^2/s
d_{DDL}	Thickness diffuse double layer	m
D_p	Pore water diffusion coefficient	m^2/s
D_w	Self-diffusion coefficient in water	m^2/s
F	Faraday constant (96,485)	J/V/eq
I	Ionic strength	mol/L
J_i	Diffusive flux of species i in solution	$mol/m^2/s$
K_d	Distribution coefficient	m^3/kg
n	Empirical correction factor for pore space geometry	-
n_{DDL}	Number of lengths	-
O_i	Experimental value of i-th sample	-
pCO_2	Partial pressure of carbon dioxide	bar
pzc	Point of zero charge	-
R	Gas constant (8.314)	J/K/mol
s	Number of samples	-
SSD	Surface site density	$sites/nm^2$
SSA	Specific surface area	m^2/g
t	Time	s
T	Absolute temperature	K
u_i	Mobility of species i in water	$m^2/s/V$
wc_{wet}	Wet water content	-
X_i	Simulated result of i-th sample	-
x	Spatial coordinate	m
z	Charge number of chemical species	-

Greek symbols

α	Activity of chemical species	mol/m^3
ϵ	Effective (accessible) porosity	-
ϵ_{wc}	Water content porosity	-
μ	Electrochemical potential	J/mol
μ^0	Standard potential	J/mol
ρ_{db}	Dry bulk density	kg/m^3
ρ_{wb}	Wet bulk density	kg/m^3
ψ	Electrical potential of a charged surface	V
ψ_{DDL}	Electrical potential in the DDL	V

Chapter 1

Introduction

One of the most challenging environmental tasks modern society has to face on earth is the disposal of nuclear waste. From the discovery of nuclear fission of uranium isotopes in 1938 (Hahn and Strassmann, 1939a,b) and its theoretical as well as nuclear physical interpretation in 1939 (Frisch, 1939; Meitner and Frisch, 1939), the nuclear era was ushered with the first controlled, self-sustaining nuclear chain reaction in a reactor at the University of Chicago in the frame of the Manhattan project (Hore-Lacy, 2007). Initially investigated for purely military purposes, which ultimately led to the atomic bombs being dropped over Hiroshima and Nagasaki in 1945, civilian use of nuclear power for electricity generation has increasingly moved to the forefront since the 1950's (Hore-Lacy, 2007). By the end of 2020, 442 nuclear power plants were in operation worldwide, including six in Germany[1], with 52 more under construction (IAEA, 2021a,b). To date, the use of nuclear energy has globally generated more than 400,000 t of heavy metal of spent fuel, with the amount increasing by 7,000 t each year (IAEA, 2021b). With the phase out of nuclear power in Germany by the end of 2022 (§ 7 Article 1a AtG[2]), 1,900 containers with highly radioactive waste material will be produced. If the wastes were loaded onto wagons, this would correspond to a train 11 km long (BASE, 2020). However, from the 1950's to the present, e.g. some 70 years later, only three countries (Finland, France and Sweden) of the 173 member states of the International Atomic Energy Agency (IAEA) have the licensing for the construction of disposal facilities under way, with the first in Finland being scheduled to be operational in 2025 (IAEA, 2021b).

The classification of radioactive materials as hazardous waste and concerns about its disposal are related to the increase in their quantity over the years (McKinley et al., 2007). From the initial dilute and disperse options on land or in the sea (McKinley et al., 2007), disposal in deep geological formations is now favoured worldwide to shield human and nature from the harmful effects of ionizing radiation (IAEA, 2003). This requires time periods of up to one million years since only then the radiotoxity of the spent fuel will have fallen below that of the corresponding amount of natural uranium ore (Nagra, 2002a). This means that about two generations have benefited from nuclear energy and will leave a radiating legacy for the next 30,000 generations. The original idea of a few geologists and engineers being able to construct a repository has turned into a much more complex challenge involving biological, chemical, logistical and societal aspects (Alexander et al., 2015).

[1] At the end of 2021, three German power plants were taken out of operation.

[2] Atomgesetz (AtG) in the version promulgated on 15 July 1985 (Federal Law Gazette p. 1565) as last amended by the promulgation of 3 January 2022 (Federal Law Gazette p. 14). URL: https://www.gesetze-im-internet.de/atg/BJNR008140959.html (accessed on 13 June 2022)

1.1 Learning from nature - the multi-barrier concept

Natural systems provide the reference for present-day concepts because repositories are similar to them. Spent nuclear fuel basically consists of uranium (Ewing, 2015; Metz et al., 2012), specifically irradiated UO_2 (Figure 1.1a). Therefore, uranium ores are used as natural analogues as they are mainly composed of the naturally-occurring mineral uraninite (UO_2, Alexander et al., 2015). For instance, the 1.3 billion years old Cigar Lake in Canada is world's second largest uranium ore deposit and offers a unique opportunity to test geochemical models and the associated thermodynamic databases as well as numerical codes (Bruno et al., 1997, 2002; Liu et al., 1996; Smellie and Karlsson, 1999). These are applied to quantify radionuclide migration for conditions assumed in future disposal systems since transport in groundwater and/or pore water is the governing natural process transferring radionuclides from a repository into the surface environment (IAEA, 1999). Moreover, all current concepts use a multi-barrier system analogous to natural ore deposits (Bruno et al., 2002; IAEA, 1999). Technical and geo-technical constructions in the near-field of the repository together with the host rock as the final barrier in the far-field (Figure 1.1b and c) are designed to isolate the radioactive waste from the environment (Bruno et al., 2002; IAEA, 1999, 2003; Nagra, 2002a). At the surface of Cigar Lake, for example, there is no indication for the existence of the uranium ore body since its redox state has been stable over the last billion years due to a high iron(II)-sulphide content. Further, the uranium matrix is surrounded by a clay layer and a host rock several hundred metres thick (Bruno et al., 2002), which can also be found in present concepts (Figure 1.1b and c). However, natural uraninite differs from spent fuel in one crucial aspect, namely the high concentrations of fission products, actinides and actinide daughters (Figure 1.1a) as it has never experienced criticality, unlike the natural reactors at Oklo (Alexander et al., 2015). Natural uraninites can be several millions of years old, as shown by the Cigar Lake example, and are therefore evidence of the longevity and stability of UO_2 in geological environments (Alexander et al., 2015).

Nature showed that isolation, and thus disposal of radioactive material, might work over geological time periods. The natural nuclear fission reactors near Oklo in Africa discovered in 1972 in the open pit of the uranium deposit, offer a worldwide unique opportunity to investigate migration of fission products (Bracke and Gauthier-Lafaye, 2001; Gauthier-Lafaye, 2002). Here, around two billion years ago, nuclear fission reactions spontaneously occurred at a depth of around 3,000 m in 15 reactors of which only the smallest is preserved today (Gauthier-Lafaye, 2002). A 5 m to 20 m thick uraninite layer builds the core of the natural reactors, usually embedded in clay minerals that protected the core against diagenetic and weathering fluids (Gauthier-Lafaye, 2002). Early studies showed that fission or their decay products with low solubility, especially in reducing natural groundwaters, were completely retained (Gauthier-Lafaye, 2002). Based on detailed analyses, the uraninite mineral was identified as most efficient to retain migration of actinides and fission products (Gauthier-Lafaye, 2002). Thus, reducing conditions maintained by iron(II) minerals and organic matter were important.

However, gaseous fission products or such with high solubility have been completely lost from the reactors, even under reducing conditions (Gauthier-Lafaye, 2002). Consequently, the retention capacity governed by geochemistry and mineralogy as well as the thickness of a host rock as the final barrier are of particular relevance for present-day concepts.

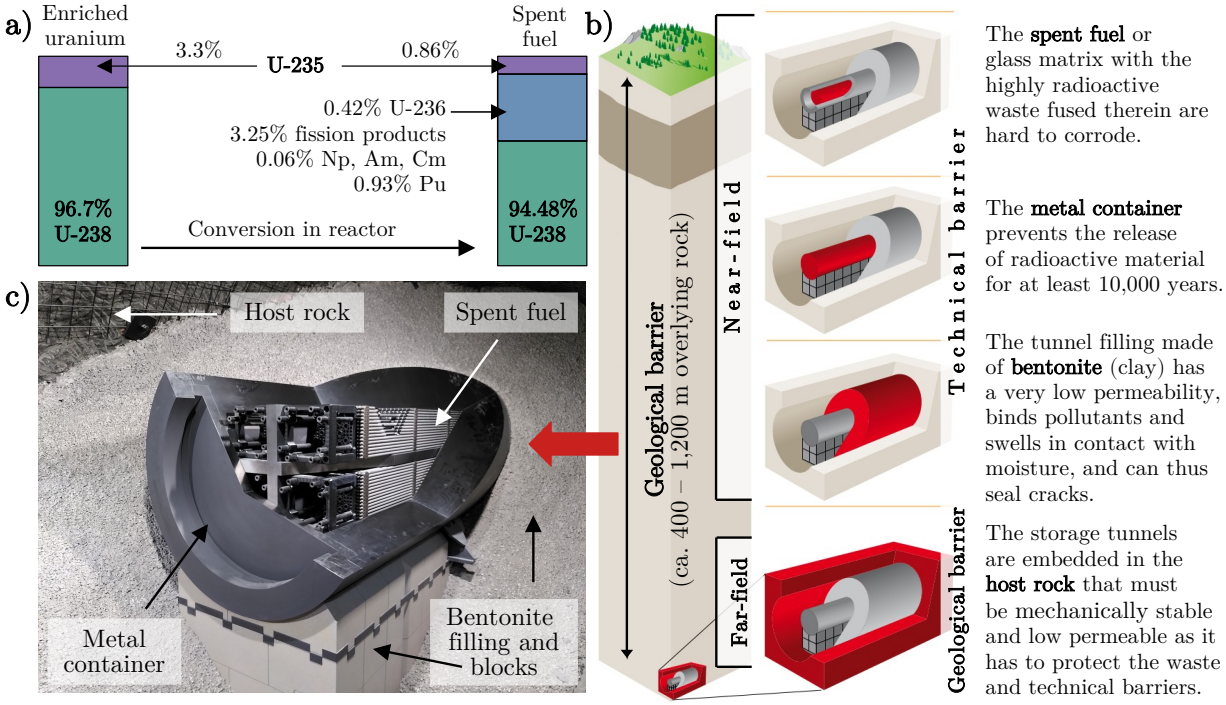

Figure 1.1: A multi-barrier system is designed to isolate the spent fuel from the surface environment. The fuel rods mainly consist of uranium (**a**), here the exemplary composition after use in a light water reactor (Volkmer, 2007). Due to the highly radioactive fission products, the spent fuel needs to be isolated from the surface environment in geological formations, ensured by a combination of technical barriers in the near-field and the host rock as the geological barrier in the far-field (**b**) as shown in the model representation (**c**). Modified from Nagra (2007).

1.1.1 The host rock is the natural and final barrier

The engineered barriers shall retain the radionuclides within the near-field as long as possible by a minimization of their release from the spent fuel as well as their mobility. The fuel rods consist of $UO_{2(s)}$ pellets (Figure 1.1a and b) that are stacked in tubes and cladded with a zirconium alloy material. Both, pellets and cladding material, have a very low solubility in groundwater (Eriksen et al., 2012; Ewing, 2015; Metz et al., 2012). However, the stability of the $UO_{2(s)}$ matrix and surrounding materials can be altered by the operation in a nuclear reactor, for instance, due to the very high temperatures (>1,000 °C) and the ionizing radiation (Carbol et al., 2020; Eriksen et al., 2012; Ewing, 2015; Metz et al., 2012). This, in turn, can increase their solubilty or even lead to failure and release of radionuclides. Therefore, the fuel assemblies are stored in metal containers of several cm-thickness (Figure 1.1b) composed of either carbon steel, a copper-lined nodular iron or a combination of cement and stainless steel to prevent or delay water reaching the fuel

matrix (Carbol et al., 2020; Ewing, 2015; Metz et al., 2012). Contact with groundwater or microbial activity can cause these containers to corrode or fail, whereby the corrosion rate highly depends on the geochemical conditions (Carbol et al., 2020; Leupin et al., 2017a). For this reason, the tunnels are filled with buffer materials such as bentonite, crushed rock salt or concrete that additionally delay water inflow from the host rock into the repository (Metz et al., 2012). Furthermore, bentonite mainly consists of the clay mineral montmorillonite, and thus has a high retention capacity against radionuclides (Baeyens and Bradbury, 2017; Grambow et al., 2006; Philipp et al., 2019). Nevertheless, the buffer material might also undergo alteration and transformation processes. These processes can be caused due to interaction with the outer contacting solution or the other containment materials as well as due to heat generated by the waste packages or radioactive decay. This, in turn, can affect the containment properties, such as a decreased retention capacity (Filipská et al., 2017; Fox et al., 2019). Although extensive research has been done in recent years on the processes inside a repository (Ma et al., 2019; Metz et al., 2012), no one can predict them with 100% accuracy or assure that none of the technical barriers fails. Ultimately, the host rock remains the natural and also final barrier isolating radionuclides from the surface environment.

The ideal host rock is characterized by a high stability over millions of years, practically stagnant groundwater, a geochemically reducing environment and conditions governed by themodynamic equilibrium between pore water and minerals (IAEA, 2003). The host rock virtually provides all of the required retention capacity, and thus only a simple concept would be required (IAEA, 2003). However, such perfect conditions are not present in many countries. Therefore, the multi-barrier concepts differ in the chosen container materials and the host rock itself (Alexander et al., 2015). Worldwide, the favoured host rock types for geological disposal of radioactive wastes are crystalline and salt rocks as well as argillaceous formations (Ewing, 2015; IAEA, 2003; Metz et al., 2012).

Crystalline rocks are preferred, in particular, because of their high stability, low heat sensitivity and low solubility (BGR, 2007; Hedin and Olsson, 2016). A significant disadvantage is the potential occurrence of fractures, which can lead to high permeabilities, and thus enhance radionuclide transport (BGR, 2007). Thus, the primary focus is on the containment within the near-field. The most advanced concept for crystalline rock is the Swedish KBS-3, where a copper canister is used as main barrier to achieve containment over several thousands of years. The canister is additionally surrounded by a buffer material, usually bentonite, to retard radionuclide transport in the event of a container failure, while the crystalline host rock provides the long-term stable environment (Bennett and Gens, 2008; Hedin and Olsson, 2016; Metz et al., 2012). Finland and Canada use similar concepts to the Swedish one (Metz et al., 2012).

Rock salt is characterized by a high thermal conductivity and is practically impermeable to fluids under undisturbed natural conditions (BGR, 2007; von Berlepsch and Haverkamp, 2016). However, a major disadvantage is the high solubility in case water enters into the repository and the low retention capacity with respect to radionuclides (BGR, 2007; von Berlepsch and Haverkamp, 2016).

Thus, a special container has been designed to prevent radionuclide release. The inner cask of the container is made of stainless steel with a thick-walled outer cast iron cask (Metz et al., 2012). Salt formations have been intensively investigated as potential host rock at the Gorleben site in Germany, but also in the USA (von Berlepsch and Haverkamp, 2016).

Clay formations are favourable host rocks because of their very low permeability only allowing diffusion-controlled transport, their high retention capacity against radionuclides and low solubility (BGR, 2007; Grambow, 2016). Among the disadvantages compared to the other host rocks are the low thermal conductivity and the lower mechanical stability (BGR, 2007; Grambow, 2016). However, these disadvantages can be overcome by limiting the maximum temperature outside the canisters, a greater distance between them as well as technical aspects of construction (BGR, 2007; Grambow, 2016). France (Callovo-Oxfordian argillite), Belgium (Boom Clay), Hungary (Boda Claystone Formation) and Switzerland (Opalinus Clay) are focussing on different types of clay formations as potential host rocks in their nuclear disposal concepts (Altmann et al., 2012; Delay, 2019; Grambow, 2016; Metz et al., 2012; Nagra, 2002a; Ortiz et al., 2002).

All three host rock types have their advantages but also disadvantages. The drawbacks can be addressed by technical adjustements in the respective concepts, for example, by using a thicker container made of materials that hardly corrode. What they all have in common is the potential to meet the legal minimum requirements: permeability $<10^{-10}$ m/s, thickness >100 m, burial depth >300 m, sufficient spatial extent for the construction of a repository as well as stable conditions over geological time scales (§ 23 Article 5 StandAG[3]).

1.1.2 The Opalinus Clay as potential host rock

In Germany, all three formation types are present, and thus are considered in the site selection process restarted in 2013 (§ 1 Article 3 StandAG[3]). A first milestone in the procedure was achieved with the publication of the sub-areas interim report by the Bundesgesellschaft für Endlagerung mbH (BGE) in autumn 2020 (BGE, 2020). The BGE is in charge of the site selection procedure in Germany and has identified 54% of the area in Germany as geologically suitable from a stratigraphical point of view. Clay formations account for around 54% of the sub-areas and crystalline and salt rock for 33% and 13%, respectively (BGE, 2020). Thus, clay formations are most abundant in terms of area. The majority of the argillaceous sub-areas are located in northern Germany (Lower Cretaceous Clays) but there are also smaller sub-areas in southern Germany, such as the Opalinus Clay formation (BGE, 2020; Rübel et al., 2007). Consequently, claystones play an important role in the site selection process due to their proportion of area involved and spatial abundance.

[3]Standortauswahlgesetz (StandAG) of 5 May 2017 (Federal Law Gazette p. 1074) as last amended by Article 1 of the Act of 7 December 2020 (Federal Law Gazette p. 2760). URL: https://www.gesetze-im-internet.de/standag_2017/BJNR107410017.html (accessed on 13 June 2022).

The Opalinus Clay, named after the ammonites *Leioceras opalinum* contained therein, is of special relevance as the formation is present in southern Germany and Switzerland, where it has been chosen as suitable host rock for the disposal of the Swiss highly radioactive waste materials (BGR, 2007; Nagra, 2007). For almost 25 years, the Opalinus Clay has been intensively investigated in the underground laboratory Mont Terri located in the Jura mountains in northwestern Switzerland (Bossart et al., 2017; Nagra, 2002a). Additional drilling campaigns at the potential disposal sites and depths provided further information that was compared with findings from Mont Terri for shallower depth. About 180 million years ago, the formation was deposited in a shallow marine environment: the Jurassic sea. It covered an area from the Jura mountains in Switzerland and France as well as the Swiss-German foreland basin and parts of southern Germany (Bossart and Thury, 2008; Nagra, 2002a; Pearson et al., 2003). In the past, it was buried to depths of at least 1,000 m, making it an overconsolidated shale formation with thicknesses ranging from 80 m to 120 m, with local variations (Bossart and Thury, 2008; Lauper et al., 2018; Mazurek et al., 2011; Pearson et al., 2003). The major components are clay minerals with quantities varying between 25 wt.% and 76 wt.% followed by calcite and quartz with the amounts ranging between 7 wt.% and 42 wt.% and 6 wt.% and 32 wt.%, respectively (Pearson et al., 2003). Due to this mineralogical heterogeneity, the Opalinus Clay is subdivided into three litho-facies: the shaly, sandy and carbonate-rich (Lauper et al., 2018; Pearson et al., 2003). Moreover, the inherent clay minerals provide high retention capacities against radionuclides due to their large reactive surface area, what has been demonstrated by many laboratory as well as in-situ experiments (Appelo et al., 2010; Gimmi et al., 2014; Joseph et al., 2011; Leupin et al., 2013). Minor mineral components are pyrite, feldspars, dolomite, siderite and organic carbon (Pearson et al., 2003). The geochemical conditions are controlled by thermodynamic equilibrium between pore water and inherent minerals, especially clay minerals and carbonates (Nagra, 2002a; Pearson et al., 2003; Wersin et al., 2009). Further, the presence of pyrite and siderite is evidence that the pore water is moderately reducing. With porosities between 12% and 20%, the Opalinus Clay contains a significant amount of water, i.e. 120 l/m^3 up to 200 l/m^3 (Bossart and Thury, 2008; Nagra, 2002a). Nevertheless, the pore water is practically immobile because of the filigree pore space microstructure determined by the layered clay minerals (Nagra, 2002a). Measured permeabilities range between $2 \cdot 10^{-14}$ m/s and $1 \cdot 10^{-13}$ m/s for undisturbed as well as disturbed rock due to the self-sealing capacity of the inherent clay minerals. Consequently, diffusion is the dominant transport process for millions of years (Nagra, 2002a), what has been additionally confirmed by modelling pore water profiles measured at Mont Terri and in the deep boreholes (Gimmi et al., 2007; Koroleva and Mazurek, 2009; Mazurek et al., 2011; Nagra, 2002a; Wersin et al., 2018). Moreover, there are no indications that the various glaciations had any impact, and thus the geochemical conditions are considered stable (Nagra, 2002a). Consequently, the suitability of the Swiss Opalinus Clay as host rock for the disposal of radioactive waste was proven based on the results obtained at Mont Terri together with the deep boreholes.

Independent of the chosen host rock and associated concept, all countries pursue the same goal: the isolation of the radioactive waste for several tens of thousands up to one million years. Therefore, the question is always the same: How far do radionuclides migrate through the final barrier, the host rock, within this time frame?

1.2 Long-term behaviour of repository systems must be evaluated with numerical simulations

Performance or safety assessments of a potential repository aim to demonstrate and evaluate the suitability and robustness for a specific host rock and disposal concept or system components according to the state of the art in science and technology (§ 27 Article 2 StandAG[3]). They are required to finally describe and validate the safety case for a specific location. One of the most challenging tasks is thereby to extrapolate the long-term (i.e. ten thousand to a million years) behaviour on the repository scale (>100 m) from the necessarily short-term data on significantly smaller scales of analytical and underground rock laboratories currently available. Accordingly, numerical simulations are indispensable for safety assessments as the required temporal as well as spatial scales cannot be directly addressed by laboratory experiments (StandAG[3], Supplement 2 of § 24 Article 3, Alexander et al., 2015; Kühn et al., 2021). This raises one major question: How can radionuclide migration through a complex and heterogeneous system, like a several hundred metres thick host rock, be modelled?

1.2.1 Diffusion is the transport process through the host rock clay

The dominant transport process in clay formations is molecular diffusion due to their low permeability (Bourg and Tournassat, 2015; Grambow, 2016; Leupin et al., 2017b; Nagra, 2002a). However, transport processes in the pore space are complex because of the electrostatic interaction between the clay mineral surfaces in contact with the pore water. Under the geochemically slightly alkaline conditions in clay formations (Altmann et al., 2012), the surfaces of clay minerals have a negative charge due to their internal structure and the pH-dependent dissociation of protons from the functional hydroxyl groups. This negative surface charge is compensated in a region of the pore water near the surfaces, the so-called diffuse double layer (DDL, Figure 1.2a), by the attraction of cationic and repulsion of anionic species. In case the DDL overlap, this effect is known as anion exclusion (Figure 1.2a). Thereby, the extension of the DDL and hence the anion exclusion decrease with increasing ionic strength of the pore water because the negative surface charge can be shielded better (Altmann et al., 2012; Glaus et al., 2015, 2007; Van Loon et al., 2007; Wigger and Van Loon, 2018). On the contrary, some cationic species have access to the interlayer space between the clay mineral layers (Figure 1.2a), which additionally enhances their diffusive transport in the pore water and the DDL (Glaus et al., 2007). Consequently, the accessibility of the pore space, and thus the diffusive pathways of charged and neutral species, differ and depend on the chemical conditions of the clay system (Altmann et al., 2012; Bourg and Tournassat, 2015; Van Loon et al., 2003b).

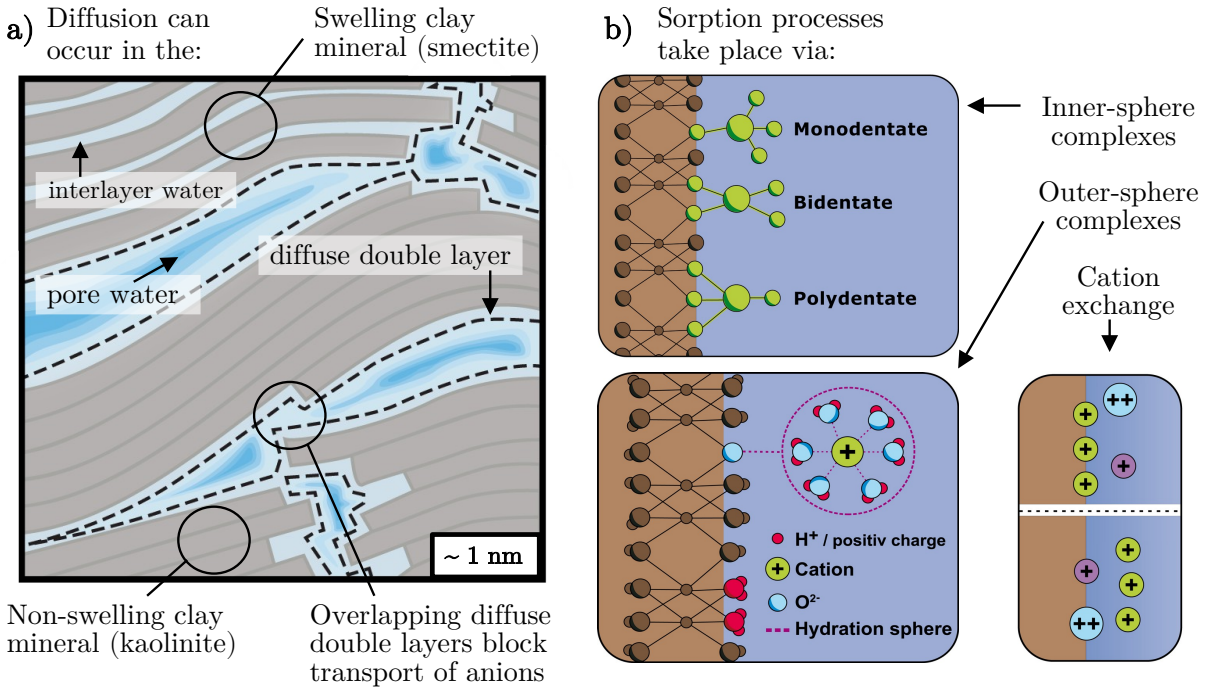

Figure 1.2: Diffusive transport of aqueous species is determined by the pore space accessibility (**a**), and thus depends on the charge (anionic, cationic or uncharged) as exemplarily illustrated for the Opalinus Clay. Migration of radionuclides is retarded by sorption (**b**) via inner- and outer-sphere complexes as well as cation exchange processes. Modified from Nagra (2002b).

The classical approach to determine diffusion lengths are Fick's laws that describe diffusive transport in time and space along a concentration gradient (Altmann et al., 2012; Gratwohl, 1958; Tournassat and Steefel, 2019). To solve numerical simulations based on Fick's laws, the accessible porosity ϵ (-) and the effective diffusion coefficient D_e (m^2/s) of the radionuclide are required (Altmann et al., 2012; Gratwohl, 1958; Tournassat and Steefel, 2019). The D_e accounts for the reduced cross-sectional area available for diffusion in the pore space (Figure 1.2a, Gratwohl, 1958) and is determined for each radionuclide and host rock in laboratory experiments for geochemically and mineralogically controlled conditions (Glaus et al., 2007; Joseph et al., 2013b; Van Loon and Soler, 2003). Since only one radionuclide is considered at a time, Fick's diffusion will be referred to as single-component (SC) diffusion in the following. Due to the acceptable computational costs even on the host rock scale, transport models based on Fick's diffusion are often applied in safety assesments (Nagra, 2002a; Rübel et al., 2007). The variation in diffusive transport of charged and neutral species can be addressed by simply using different experimentally determined D_e (Altmann et al., 2012; Bourg and Tournassat, 2015; Glaus et al., 2015, 2007, 2010; Nagra, 2002a; Soler et al., 2019). Nevertheless, the interaction of radionuclides with the DDL and hence their diffusive transport (Figure 1.2a) strongly depend on the geochemical conditions and mineral composition (Nagra, 2002a; Pearson et al., 2003; Wersin et al., 2009). This means, D_e determined in the laboratory might no longer be applicable outside the experimentally defined conditions. Consequently, heterogeneities on the host rock

scale, such as the facies sequence in the Opalinus Clay, can only be considered with a sufficient amount of previous laboratory experiments covering all potential mineralogical and geochemical conditions.

1.2.2 Sorption on clay minerals retards radionuclide transport

The diffusive transport of radionuclides in clay formations is retarded by sorption processes taking place on the clay mineral surfaces (Altmann et al., 2012). Cation exchange and surface complexation (Figure 1.2b) are the two dominant sorption processes that remove radionuclides from the pore water. Due to their negative surface charge, clay minerals are cation exchanger. Smectites and illites are thereby the clay minerals with the highest cation exchange capacity (CEC), resulting from the isomorphic substitution of the central atoms (Smith, 1997). This means that cations bound to the clay mineral surfaces can easily be exchanged with, for instance, cationic radionuclide species from the pore water solution and vice versa (Figure 1.2b). Thereby, multivalent ions are generally more strongly bound compared to monovalent ions. The other sorption process is the surface complexation on the functional hydroxyl groups located on the basal and edge sites of the clay mineral surfaces. Due to the dis- or association of the bounded protons, the accessible amount of these sorption sites is pH-dependent (Smith, 1997). On the functional groups, sorption can take place via outer-sphere complexes, also known as non-specific sorption, due to electrostatic attraction of the hydrated ions (Figure 1.2b) or via inner-sphere complexes (Smith, 1997). Inner-sphere complexes are also referred to as specific sorption and are based on the exchange of protons by radionuclide species so that the ion is fixed in the surface complex (Figure 1.2b). Cation exchange and surface complexation remove radionuclides from the pore water, and thus decrease their diffusive transport, whereby the geochemical conditions and mineral quantity determine the sorbed concentration.

A simple approach to consider sorption processes in transport simulations is via the distribution coefficient K_d (m^3/kg). The K_d is defined as ratio between the species concentration adsorbed on the solid phase and present in the liquid phase. Usually, K_d values are determined in batch sorption or diffusion experiments for controlled geochemical and mineralogical conditions (Fröhlich et al., 2013; Joseph et al., 2011, 2013a,b; Payne et al., 2013; Soler et al., 2008). In many transport simulations, they are considered to be constant in time and space, which means neither heterogeneities nor dynamic developments of natural systems can be taken into account (Payne et al., 2013). However, sorption of radionuclides highly depend on the present geochemical conditions, especially pH (Smith, 1997; Tournassat et al., 2018). As a consequence, K_d values of an element like uranium can vary by several orders of magnitudes depending on the geochemical conditions in a system (Altmann et al., 2012; Noseck et al., 2018, 2012; Smith, 1997; Stockmann et al., 2017). This means that either many experiments will have to be performed, hopefully covering all possible geochemical and mineralogical conditions, or other more advanced approaches will be required.

1.2.3 Heterogeneous systems require advanced approaches

Migration lengths of radionuclides through claystones result from the quantification of diffusive transport through the pore space and retention on the clay minerals, which is governed by the speciation, and thus by the geochemistry of the pore water. Thus, migration includes both, i.e. diffusion and sorption processes. All these processes and changes associated with natural, dynamic systems cannot be taken into account with classical approaches applying experimentally determined D_e and K_d that are used as constant in time and space. Variations in the mineralogical composition are connected with changes in pore water chemistry due to water-rock interactions, which, in turn, affect the speciation of radionuclides and hence their diffusive transport and sorption behaviour (Amayri et al., 2011; Kim, 2001). This is especially relevant for radionuclides with a complex chemistry, e.g. pH- or redox-dependent, like uranium or plutonium (Amayri et al., 2011; Bourg and Tournassat, 2015; Huang, 2016). Here, geochemical codes, such as PHREEQC (Parkhurst and Appelo, 2013), enable to solve this problem. With PHREEQC, aqueous geochemical calculations can be performed based on the law of mass action, and thus on thermodynamic equilibrium (Parkhurst and Appelo, 2013). This offers a variety of calculations for a defined geochemical system, such as speciation and saturation-index calculations, batch-reactions and one-dimensional transport calculations with reversible and irreversible reactions that include aqueous, mineral, gaseous, solid-solution, surface-complexation and ion-exchange equilibria, as well as specified mole transfers of reactants. Further, kinetically controlled reactions, mixing of solutions and pressure and temperature changes can be taken into account, as well as inverse modelling problems (Parkhurst and Appelo, 2013). For instance, to quantify radionuclide migration with reactive transport simulations, a comprehensive chemical thermodynamic database is required that includes all relevant species of the pore water components and radionuclides, mineral phases, surface complexes and exchangeable species. Reactive transport models numerically solved with geochemical codes, like PHREEQC, provide the possibility to quantify sorption and diffusion processes as a function of the geochemical conditions in the system taking into account dynamic changes.

Natural systems, like the Opalinus Clay formation, are heterogeneous on the host rock scale. Usually, the transport parameters of a radionuclide, D_e and K_d, are determined on the basis of drill cores that are supposed to represent the host rock. Because of mineralogical heterogeneities resulting from the deposition process, the Opalinus Clay is subdivided into the litho-facies shaly, sandy and carbonate-rich (Bossart and Thury, 2008; Pearson et al., 2003). The majority of diffusion and sorption experiments has been done for the shaly facies with a large amount of clay minerals (>50 wt.%, Bossart et al., 2017; Fröhlich et al., 2011; Leupin et al., 2013). Thus, K_d values might not be transferable to the sandy or carbonate-rich facies with lower clay mineral quantities (Pearson et al., 2003). Further, the higher carbonate contents in the carbonate-rich and sandy facies can change the pore water composition compared to the shaly facies (Pearson et al., 2003). For instance, measured pH values

range between 7.0 and 7.5, which, in turn, has an impact on the sorption behaviour (Pearson et al., 2003; Schmeide and Bernhard, 2010; Smith, 1997; Tournassat et al., 2018). This can be addressed by the application of mechanistic surface complexation models (SCM) as implemented in PHREEQC to quantify sorption processes. SCM aim to describe the sorption process analogous to the formation of aqueous complexes. Therefore, the surface complexation reactions (Figure 1.2b) can be described with mass law equations and an algorithm to obtain thermodynamic equilibrium considering the charges on the solid surface and of the adsorbing ions (Churakov and Prasianakis, 2018; Parkhurst and Appelo, 2013; Smith, 1997). The required surface reactions, corresponding stability constants as well as additional parameters describing the surface and complexes are experimentally determined and collected in thermodynamic sorption databases (Bradbury and Baeyens, 2005a,b, 2017; Bradbury et al., 2010; Hartmann, 2010; Noseck et al., 2018; Turner and Sassman, 1996). This emphasizes the need for reliable data and experiments, without which substantial reactive transport modelling is not possible. The mineralogical heterogeneity of the Opalinus Clay facies, and therewith a potential facies dependence of sorption processes, can be quantified by the application reactive transport models and SCM.

Process-based approaches are required to account for changes in mineralogy and pore water geochemistry and their impact on diffusive transport processes. Diffusion in clay formations is governed by the interaction of mobile species with the DDL that envelope the clay minerals to counterbalance their surface charge. The thickness and composition of the DDL are predominantly controlled by the ionic strength and pore water constituents, and thus by the geochemistry (Wigger and Van Loon, 2018). The higher the ionic strength, the better the negative surface charge is shielded by the pore water. As a consequence, the DDL is thinner, with bivalent ions providing stronger shielding than monovalent ions (Wigger and Van Loon, 2018). The mineralogy determines thereby the composition and quantity of the respective clay minerals and hence the net negative surface charge to be shielded. In the Opalinus Clay system, for instance, the shaly facies has a higher ionic strength as well as concentration of bivalent ions compared to the sandy facies (Pearson et al., 2003; Wersin et al., 2009). Consequently, experimentally determined D_e values might not be transferable from one facies to the other. This can be overcome by the application of more process-based approaches, like the multi-component (MC) diffusion (Appelo and Wersin, 2007). With this approach, diffusive transport is calculated separately for each species present in the system considering the individual interaction with the DDL and also interlayer diffusion (Figure 1.2a) as a function of the present geochemical conditions (Appelo et al., 2010; Appelo and Wersin, 2007). Thereby, the speciation of a radionuclide in the modelled system plays an important role, what is determined by the selection of the underlying thermodynamic data. The MC approach has been succesfully applied to model diffusion experiments and pore water profiles as well as to obtain pore water compositions (Appelo et al., 2010, 2008; Appelo and Wersin, 2007; Liu et al., 2011). Nevertheless, a more precise description of transport and sorption processes as a function of the

geochemical conditions is accompanied by an increase of the computational costs and numerical robustness (Churakov and Prasianakis, 2018; Leal et al., 2017b). This may necessitate the development and application of surrogate models, especially at the host rock scale (De Lucia and Kühn, 2013, 2021; Leal et al., 2017a,b; Noseck et al., 2018, 2012; Stockmann et al., 2017). Furthermore, it remains to be seen to what extent the precise consideration of diffusive transport and sorption processes is actually necessary on the host rock scale. What actually is the difference in metres migration length compared to a more simplified approach based, for instance, on Fick's laws applying D_e and K_d values? The MC option in PHREEQC combined with SCM increases the number of equations, and thus the computational costs, but allows for the quantification of diffusive transport and sorption processes as a function of variations in mineralogy and pore water geochemistry associated with the heterogeneities of the Opalinus Clay facies.

For the evaluation of the suitability of a host rock for the disposal of nuclear waste, the entire system must be taken into account. The Opalinus Clay is considered to be almost impermeable, and thus its geochemical conditions as constant. Nevertheless, the formation is influenced by the surrounding formations, i.e. the hydrogeological system, especially on geological time scales. At Mont Terri, measured chloride concentrations decrease from the centre of the formation towards the embedding aquifers that were flushed with freshwater, and thus activated during the Jura folding and associated erosion of overlying stratigraphic layers (Koroleva et al., 2011; Koroleva and Mazurek, 2009; Mazurek et al., 2011, 2009; Pearson et al., 2003). These gradients established due to diffusive exchange over millions of years and are also found at the other locations of the deep boreholes. Here, the low permeable section consisting of Opalinus Clay, Liassic shales and Brown Dogger is even thicker than at Mont Terri (Gimmi et al., 2007; Wersin et al., 2018). Consequently, the geochemical conditions on the host rock scale cannot be considered as constant. In addition to the mineralogical heterogeneity of the facies, the inherent geochemical gradients can thus influence radionuclide migration, which is difficult to assess in experiments anyway and unfeasible for the host rock scale. Therefore, it is important not only to focus on heterogeneities between individual facies, but to always have in mind the impact of the entire hydrogeological system with inherent gradients on radionuclide migration.

1.3 Thesis objectives

For safety assessments of nuclear waste disposals, it is of particular relevance to demonstrate that the thickness of the host rock is sufficient to isolate the radionuclides from the biosphere for at least one million years. Experiments cannot cover the required spatial (>100 m) and temporal scales (1 Ma), and therefore numerical simulations are indispensable. In Switzerland, the Opalinus Clay has been intensively investigated for almost 25 years and has been proven as suitable host rock. It is also present in southern Germany and, consequently, of interest for the German site selection process. Uranium was chosen as example radionuclide for this thesis as it is the main component in spent nuclear fuel and has a complex speciation chemistry. Three main research objectives are derived from the explanations given above, in order to improve the understanding and quantification of uranium migration, i.e. diffusion and sorption, in the Opalinus Clay:

- The **first objective** of this thesis is to evaluate the impact of the mineralogical heterogeneity and associated changes in pore water geochemistry on uranium sorption processes for the three facies of the Opalinus Clay. Therefore, reactive transport models are applied to identify a potential facies dependence on the host rock scale.
- The **second objective** focusses on the identification of a potential facies dependence of diffusion processes by a process-based implementation of the first objective. For this, the multi-component diffusion approach is applied, whereby its relevance for the host rock scale as well as selection of underlying thermodynamic data is evaluated based on the resulting migration lengths.
- The **third objective** is to assess the hydrogeological system and inherent geochemical gradients to understand their impact on uranium migration lengths. This is done by a systematic modelling of the Opalinus Clay formation and surrounding aquifers.

1.4 Structure of the thesis and scientific contribution

This cumulative doctoral thesis consists of four articles that are all published in international, peer-reviewed journals and summarized within the following section. The studies are presented in detail in Chapter 2 to 5. A comprehensive discussion with respect to the main findings is presented in Chapter 6. The conclusions related to the thesis objectives, as well as an outlook for future work, are given in Chapter 7.

The author's contributions to the manuscripts are identical for all four publications, and therefore are listed only once below. As first author, I was responsible for the conceptualization and performing of the research as well as collecting, analysing and illustrating the data and simulation results. Further, I was mainly responsible for the preparation of the manuscript and the revision process. My co-author Michael Kühn supervised my scientific activities and contributed to the development and revision of the manuscripts. The thermodynamic database was provided by Madlen Stockmann, who also supported the conceptualization of the surface complexation modelling.

In **Chapter 2**, diffusion and sorption processes of uranium are quantified on the host rock scale (50 m) with reactive transport simulations following Fick's laws and taking into account the varying mineralogy and associated pore water composition of the three Opalinus Clay facies: shaly, sandy and carbonate-rich. The geochemical system of the investigated rock type is governed by the calcite-carbonate-ion system realized in the simulations by a mineral equilibrium with calcite, dolomite, siderite and pyrite as a function of the partial pressure of carbon dioxide (pCO_2). Measurements of the pCO_2 are associated with uncertainties, and therefore a range typical for clay formations is chosen and its impact on the migration lengths investigated. Based on the resulting migration lengths, a facies dependence of uranium sorption is identified, whereby the geochemistry of the pore water resulting from the interaction with the minerals is more decisive than the quantity of clay minerals. This chapter is published as *"Simulation of diffusive uranium transport and sorption processes in the Opalinus Clay"* in Applied Geochemistry and cited in the following as Hennig et al. (2020).

In **Chapter 3**, the influence of the mineralogical and geochemical heterogeneity in the Opalinus Clay facies on uranium diffusion processes is determined. For this, the process-based multi-component (MC) diffusion approach is applied and resulting distances are compared with findings of single-component (SC) simulations. Uranium is mainly present in anionic ternary uranyl complexes. Therefore, accounting for the interaction of the different uranium species with the diffuse double layers (DDL) of the clay minerals using MC diffusion descreased uranium migration through the formation because of the anion exclusion effect. Due to the high computational costs associated with MC diffusion on the host rock scale, a workflow was developed to calibrate transport parameters, D_e and K_d, from the MC simulations on the metre-scale and apply them as surrogate on the host rock scale. The chapter is published as *"Surrogate model for multi-component diffusion of uranium through Opalinus Clay on the host rock scale"* in Applied Sciences and cited as Hennig and Kühn (2021a) in the following.

In **Chapter 4**, also MC simulations are performed for two scenarios only differing in the stability constant of the ternary uranyl complex $Ca_2UO_2(CO_3)_3$ used in the underlying chemical thermodynamic database. This estimates, what a difference in the value of up to one order of magnitude will ultimately mean for the repository scale in one million years. The constant governs the predominant uranium species in the modelled system, whether it is an anionic or neutral complex, which, in turn, changes the interaction with the DDL, and thus migration. The simulations are performed for the shaly and sandy facies representing the major differences in mineralogy and geochemistry of the pore water. Migration distances deviate between the scenarios because anion exclusion may or may not decrease diffusive transport depending on the predominant species. Thereby, pore water composition determines how strong anions are excluded from the DDL. All in all, the influence of the stability constant is negligible on the host rock scale. This chapter is published as *"Uranium migration through the Swiss Opalinus Clay varies on the metre scale in response to differences of the stability constant of the aqueous, ternary uranyl complex $Ca_2UO_2(CO_3)_3$"* in Advances in Geosciences and referenced as Hennig and Kühn (2021b).

In **Chapter 5**, uranium migration in the hydrogeological system of the Opalinus Clay formation at Mont Terri is modelled. The formation is embedded between aquifers that established pore water gradients over millions of years in the 210 m thick low permeable section due to diffusive exchange. Hence, present-day pore water profiles are modelled in a first step by a data-driven and by a conceptual scenario, both in good agreement with measured data. They are used as starting point for the simulation of uranium migration, which is conducted in a second step. To quantify the impact of these gradients on uranium migration, the distances are compared with the results presented in Hennig et al. (2020). The simulation results demonstrate that depending on the pCO_2 of the system, inherent gradients can significantly enhance uranium migration, and therefore need to be taken into account. The chapter is published as *"Potential uranium migration within the geochemical gradient of the Opalinus Clay system at the Mont Terri"* in Minerals and cited in the following as Hennig and Kühn (2021c).

Chapter 2

Simulation of diffusive uranium transport and sorption processes in the Opalinus Clay

Abstract

Diffusive transport and sorption processes of uranium in the Swiss Opalinus Clay were investigated as a function of partial pressure of carbon dioxide (pCO_2), varying mineralogy in the facies and associated changes in pore water composition. Simulations were conducted in one-dimensional diffusion models on the 100 m-scale for a time of one million years using a bottom-up approach based on mechanistic surface complexation models as well as cation exchange to quantify sorption. Speciation calculations have shown, uranium is mainly present as U(VI), and must therefore be considered as mobile for in-situ conditions. Uranium migrated up to 26 m in both, the sandy and the carbonate-rich facies, whereas in the shaly facies 16 m was the maximum. The main species was the anionic complex $CaUO_2(CO_3)_3^{2-}$. Hence, anion exclusion was taken into account and further reduced the migration distances by 30%. The concentrations of calcium and carbonates reflected by the set pCO_2 determine speciation and activity of uranium and, consequently, the sorption behaviour. Our simulation results allow for the first time to prioritize on the far-field scale the governing parameters for diffusion and sorption of uranium and hence outline the sensitivity of the system. Sorption processes are controlled in descending priority by the carbonate and calcium concentrations, pH, pe and the clay mineral content. Therefore, the variation in pore water composition resulting from the heterogeneity of the facies in the Opalinus Clay formation needs to be considered in the assessment of uranium migration in the far-field of a potential repository.

2.1 Introduction

One of the major challenges for future generations is the long-term disposal of nuclear waste. In Germany and many other countries, humans and nature are to be permanently protected from the harmful effects of these wastes for one million years. According to our current knowledge, deep subsurface geological repositories are the safest way to store especially high-level radioactive waste over such long time periods (IAEA, 2003). The retardation ability of the host rock as natural barrier plays a crucial role in the safety case of a repository. Assessments for periods exceeding a few decades about the future behaviour of the effective containment zone of a host rock are only possible with numerical simulations.

Besides crystalline and salt rock, claystones are favourable host rocks for the geological disposal of nuclear waste due to low permeability and retardation of transport by sorption. Sorption processes are primarily determined by the geochemical conditions (Smith, 1997) influenced by the interaction between pore water and prevailing minerals and need to be quantified to evaluate the safety case of a repository.

In Europe, the Callovo-Oxfordian Clay in France (Delay, 2019), the Boom Clay in Belgium (Ortiz et al., 2002) and the Opalinus Clay in Switzerland (Nagra, 2002b) are investigated as potential formations to dispose high-level radioactive waste. The present study focusses on the Opalinus Clay due to the availability of a comprehensive database elaborated during more than 25 years of scientific activities in the Mont Terri underground research laboratory (Bossart et al., 2017). The formation also occurs in southern Germany, and plays therefore a role in the German search for a repository as well (Hoth et al., 2007). In the Mont Terri region, located in north-western Switzerland, the Opalinus Clay formation is about 160 m thick and was deposited 180 million years ago by sedimentation in a shallow marine environment of the Jurassic sea (Nagra, 2002a; Pearson et al., 2003). Due to the heterogeneity, the formation is subdivided into shaly, sandy and carbonate-rich facies varying in clay mineral content (25 wt.% - 76 wt.%) and pore water composition (Pearson et al., 2003).

The main transport mechanism in the Opalinus Clay is diffusion resulting from the low hydraulic conductivities in the range from 10^{-14} m/s to 10^{-12} m/s (Koroleva et al., 2011; Mazurek et al., 2011; Nagra, 2002a; Pearson et al., 2003). The pore space is primarily defined by the negatively charged clay mineral surfaces leading to a subdivision of the pore water, and thus to different diffusion pathways and behaviour for anionic, cationic and neutral species represented by the effective diffusion coefficient. The theoretical background of these processes has already been described in detail (Appelo et al., 2008; Bradbury and Baeyens, 2003; Nagra, 2002b). Many diffusion experiments with various tracers have been performed in laboratories and in Mont Terri. Results prove the applicability of laboratory diffusion coefficients to the formation (Appelo et al., 2010; Leupin et al., 2017b; Van Loon et al., 2003a, 2004; Wersin et al., 2008).

Uranium with its isotopes *U-235, U-236* and *U-238* is the major component in spent fuel (Ewing, 2015; Metz et al., 2012). We focus here on the migration and speciation of uranium in the far-field (>100 m) of a hypothetical repository, the host rock. Uranium is a redox-sensitive species and in natural systems primarily present in two redox states with different migration behaviour. The oxidized form, U(VI), is mobile compared to the reduced form, U(IV) (Ma et al., 2019; Vodyanitskii, 2011). Migration of U(VI) in the Opalinus Clay is governed by sorption on the different clay minerals (Amayri et al., 2016; Joseph et al., 2011, 2013a,b). U(IV) can be immobilised by precipitation (e.g. UO_2) due to its low solubility. The speciation between U(IV) and U(VI) in the Opalinus Clay is constraint by the redox state and pH, but also by the presence of complexing ligands, and thus ultimately by the composition of the pore water. Especially the presence of dissolved carbon dioxide influences speciation and solubility of uranium (Geckeis et al., 2013; Huang, 2016; Joseph et al., 2011, 2013b; Philipp et al., 2019).

Our aim is to investigate the migration behaviour of uranium in the Opalinus Clay on the 100 m-scale considering the variability of the in-situ geochemical conditions such as partial pressure of carbon dioxide (pCO_2). We apply numerical reactive transport simulations to assess uranium migration towards adjacent groundwater aquifers, depending on the different facies of the Opalinus Clay and resulting variations in pore water composition. For this, we benefit from the knowledge gained from experiments in

the laboratory on the small scale available in the literature and make use of it on the large scale. Hence, our work complements the investigations of the Opalinus Clay as potential host rock for nuclear waste disposal.

2.2 Methods

Simulations are conducted with PHREEQC Version 3 (Parkhurst and Appelo, 2013) using the PSI/Nagra thermodynamic database version 12/07 (Thoenen et al., 2014) including the actual NEA data for U(IV) and U(VI)[1]. This database was updated with actual thermodynamic data for relevant aqueous and solid phases for U(VI) and extended for auxiliary minerals and complexes of other matrix components in the context of a German research project (Noseck et al., 2018) on long-term safety assessments of a repository. In addition, the data as described in Joseph et al. (2013a) for sorption of U(VI) on clay minerals was added to the updated version of the database. The geochemical code PHREEQC is used for the complete speciation calculations of the pore waters and radionuclides for in-situ conditions as well as transport and sorption. A coupling between PHREEQC and the open source programming language R is used to create Pourbaix diagrams of the speciation of uranium in the Opalinus Clay pore water (De Lucia and Kühn, 2013). Since ionic strength (I) of the pore waters in the facies does not exceed 0.5 mol/L (Table 2.1), the Davies approach (Davies, 1962) used for the database is considered appropriate to represent ion-ion interactions (Noseck et al., 2018; Stockmann et al., 2017). The temperature in the Opalinus Clay formation ranges between 13 °C in the Mont Terri region (Pearson et al., 2003) and 45 °C determined from pore water analyses from a depth between 799 m and 833 m below surface from the deep borehole Schlattingen (Wersin et al., 2016) representing the conditions at greater depths compared to Mont Terri. Wersin et al. (2016) showed that the effect of a higher temperature, such as 45 °C, on the solute concentration is <5%. Moreover, diffusion experiments with uranium in Opalinus Clay for different temperatures (25 °C and 60 °C) have shown that an elevated temperature has no significant impact on the migration behaviour (Joseph et al., 2013b). Therefore, we decided to apply the reference temperature according to the database used and perform the calculations for a temperature of 25 °C.

2.2.1 Geochemical modelling of Opalinus Clay pore water

The present pore water composition in the Opalinus Clay is determined by the original marine components and water-rock interactions, such as precipitation and/or dissolution of minerals as well as cation exchange on the clay minerals (Pearson et al., 2003; Wersin et al., 2009). Due to the extended contact time between minerals and pore water, equilibrium between both is assumed

[1] This refers to the chemical thermodynamic data for uranium and other radionuclides published with the first NEA update (Guillaumont et al., 2003). In October 2020, the NEA published the second update (Grenthe et al., 2020). Based on the evaluation of recent data, the stability constants, in particular of the ternary uranyl complexes, were revised and set leading to significant changes in the speciation calculations presented here. To the best of our knowledge, this update has not yet been included in the PSI/Nagra thermodynamic database, but is considered in the discussion part of this dissertation.

(Bradbury and Baeyens, 1997; Pearson et al., 2003, 2011; Wersin et al., 2009). In the simulations, the pore water composition and mineralogy of the facies are represented by analyses from boreholes at Mont Terri. The initial input values are given in Table 2.1. Regarding the pore water composition, the values are averaged for the respective time of the measurement series. To keep the geochemical system preferably simple, only the main cations and anions are considered, whereby charge balance of the analysis (±3%) is adjusted by chloride. The distribution of the clay minerals is adapted in the given range for each borehole to achieve the sum of clay minerals indicated.

Table 2.1: Relevant input parameters representing the three facies: shaly, sandy and carbonate-rich. Concentrations are given as average values from the borehole analyses. The number behind the shaly facies corresponds to the clay mineral content at the sampled location.

Parameter	Unit	Shaly-76 [a,b]	Shaly-61 [c,d]	Sandy [e,f]	Carb-rich [g,h]
pH	-	7.13	7.50	7.40	7.28
Na^+	mmol/L	280.7	229.5	120.8	195.3
K^+	mmol/L	1.93	1.47	0.87	0.73
Mg^{2+}	mmol/L	21.97	16.79	5.91	15.89
Ca^{2+}	mmol/L	18.90	16.03	6.73	16.37
Sr^{2+}	mmol/L	0.46	0.47	0.35	0.44
Fe_{total}	µmol/L	29.62	8.37[d]	9.81[f]	9.81[f]
U_{total}	nmol/L	2.28[d]	2.28[d]	2.52[f]	2.52[f]
Cl^-	mmol/L	326.7	272.8	120.6	242.3
SO_4^{2-}	mmol/L	16.79	12.30	6.94	16.03
PO_4^{3-}	µmol/L	21.65[d]	21.65[d]	10.65[f]	10.65[f]
Alkalinity	mmol/L	3.85	1.24	2.61	2.05
I[i]	mol/L	0.39	0.32	0.16	0.28
Illite	wt.%	20	17	17	8
IS mixed[j]	wt.%	16	12	8	6
Kaolinite	wt.%	30	26	13	8
Chlorite	wt.%	10	6	7	4
∑Clay	wt.%	76	61	45	26
Calcite	wt.%	14	11	17	42
Dolomite	wt.%	n.a.	2	2	3
Siderite	wt.%	1	4	2	2

n.a. = no data available; [a] Vinsot et al. (2008), borehole BPC-C1; [b] Pearson et al. (2003), borehole BPP-1; [c] Wersin et al. (2009), borehole BWS-A1; [d] Pearson et al. (2003), borehole BWS-A1; [e] Wersin et al. (2009), borehole BWS-A3; [f] Pearson et al. (2003), borehole BWS-A3; [g] Pearson et al. (2003), borehole BGP-1; [h] Pearson et al. (2003), borehole EPFL; [i] calculated in PHREEQC for pCO_2 of $10^{-2.2}$ bar; [j] IS mixed = illite/smectite mixed layers

Partial pressure of carbon dioxide (pCO_2) and pH are highly sensitive parameters and coupled through the carbonate equilibria (Pearson et al., 2003; Wersin et al., 2009). The precise determination of the in-situ pCO_2 in the Opalinus Clay formation varies in measurements and values range between $10^{-1.7}$ bar (Vinsot et al., 2008) and $10^{-3.5}$ bar (Pearson et al., 2003) with corresponding pH values between 6.9 and 8.3, respectively. Therefore, we decided to fix pCO_2 in different scenarios in the range between 10^{-2} bar and $10^{-2.5}$ bar. This is recommended for clay rocks and corresponds with values measured in the Opalinus Clay (Gaucher et al., 2010; Lerouge et al., 2015; Vinsot et al., 2008).

With the fixed pCO_2, pH is controlled via an equilibrium with the present carbonates calcite, dolomite and siderite as well as cation exchange of H^+ with the clay minerals (Section 2.2.2). Equilibrium with the clay minerals or other silicates present in the Opalinus Clay, such as quartz or feldspar (Nagra, 2002a; Pearson et al., 2003), is not taken into account as the effect on the pH is negligible compared to the carbonate system. Including equilibrium with the mentioned carbonates also adapts the initial concentrations of calcium, magnesium and iron.

The reactions controlling the redox state in the Opalinus Clay formation the most are still under discussion (Pearson et al., 2003, 2011; Wersin et al., 2009, 2011). However, it is clear that for in-situ conditions the pore water is moderately reducing (Pearson et al., 2011; Wersin et al., 2011). Therefore, an initial E_H value of -227 mV (Bossart and Thury, 2008) is chosen. In the simulations, the redox state is governed by the minerals pyrite and siderite, or respectively by the redox couple SO_4^{2-}/HS^-. This redox couple provides the most consistent results with the measurements (Pearson et al., 2003, 2011; Wersin et al., 2009, 2011).

2.2.2 Modelling transport and sorption processes

The migration of uranium through Opalinus Clay is simulated for each facies perpendicular to bedding for a time period of one million years on a 100 m-scale representing the potential far-field of a repository. In intact Opalinus Clay, diffusion is the only transport mechanism. It is calculated in the model using Fick's law:

$$\epsilon \cdot \frac{\partial C}{\partial t} = \epsilon D_p \cdot \frac{\partial^2 C}{\partial x^2} \tag{2.1}$$

with ϵ (-) as effective porosity, D_p (m^2/s) as pore water diffusion coefficient, C (mol/m^3) as concentration of the species in the mobile phase, t (s) as time and x (m) as spatial coordinate. Effective porosity ϵ (-), wet water content wc_{wet} (-), wet bulk density ρ_{wb} (kg/m^3) as well as dry bulk density ρ_{db} (kg/m^3) are needed to calculate the amount of pore water in each grid cell and the respective amount of sediment per kilogram pore water. The physico-chemical parameters are chosen as 0.16, 0.067, 2,450 kg/m^3 and 2,290 kg/m^3, respectively. These are the averaged values of data from the four boreholes (Table 2.1) based on the results given in Pearson et al. (2003) and coincide with the mean values given in Bossart and Thury (2008) for the Opalinus Clay formation.

We have used a constant porosity throughout the simulation domain, therefore ϵ can be eliminated from Equation 2.1, so that diffusion only depends on D_p. The pore water diffusion coefficient D_p can be derived from the effective porosity ϵ and the effective diffusion coefficient D_e (m^2/s) accounting for the reduced cross-sectional area available for diffusion in porous media via $D_e = \epsilon \cdot D_p$ (Equation 2.1). The D_e for uranium in Opalinus Clay perpendicular to bedding is set to $1.9 \cdot 10^{-12}\,m^2/s$ for all facies, as determined by Joseph et al. (2013b) in a diffusion experiment with U(VI) in Opalinus Clay of the sandy facies. The main species in the experiment was the neutral aquatic uranyl complex $Ca_2UO_2(CO_3)_3$. This results in a D_p for the neutral aquatic uranyl complex of $1.2 \cdot 10^{-11}\,m^2/s$, which is used in the transport equation. Due to the anion exclusion effect, the pore space accessible for anionic species is reduced compared to neutral or cationic species resulting in a lower D_e. However, there is no diffusion experiment in the literature for the anionic uranyl complex in Opalinus Clay. For anionic species, we therefore assume a smaller D_p, what is equivalent to a reduction of D_e as we use a constant, homogeneous porosity. In our approximation, D_p is scaled with factor 0.55 analogous to the reduced accessible porosity of anionic species resulting in $6.53 \cdot 10^{-12}\,m^2/s$. The scaling factor coincides with literature data for the chloride porosity ratio in the Opalinus Clay (Appelo et al., 2010; Bond et al., 2013; Gimmi et al., 2014; Mazurek et al., 2011; Pearson et al., 2003; Wersin et al., 2018, 2017).

Each facies is represented by an one-dimensional finite-difference diffusion model (Figure 2.1) with a spatial resolution of 0.2 m. The grid independence of the model is confirmed by simulations of finer resolution ($x = 0.1$ m). Dirichlet conditions with an uranium concentration of 1 μmol/L are applied to the first grid cell to represent the uranium source term from the failed high-level waste canisters according to Keesmann et al. (2005) and Joseph et al. (2013b). This constraint is a simplification of a nuclear waste disposal concept, and hence our results are to be considered as maximum migration lengths. Neumann boundary conditions are enforced at the last grid cell. After each transport step, the solutions are equilibrated with the carbonates and pyrite to include the interaction of the minerals with the pore water (Figure 2.1).

The Opalinus Clay is a heterogeneous formation consisting of various minerals (Pearson et al., 2003). In our simulations, sorption is considered as bottom-up approach as described by Stockmann et al. (2017) and applied to the Opalinus Clay by Joseph et al. (2013a) for modelling sorption batch experiments. Following this approach, sorption of contaminants in the formation can be determined based on the competitive sorption effect from the individual minerals. In our simulations, we only consider sorption on the clay minerals since the proportion by the other minerals on the total sorption capacity is negligible (<1%). This was proven by previous tests and is also consistent with Bradbury et al. (2010) and Joseph et al. (2013a). The illite/smectite mixed layers are treated as a combination based on the sorption data of the pure clay minerals with a distribution of 50% illite and 50% smectite according to Joseph et al. (2013a). Smectite is the generic term for a group of swellable clay minerals and is not described in detail for the Opalinus Clay formation.

We have chosen montmorillonite as representative mineral of the smectite group since it is the best investigated (Joseph et al., 2013a).

In our simulations, sorption of uranium is quantified with mechanistic surface complexation models (SCM) as well as cation exchange (Kim, 2001). For modelling surface complexation reactions, the two-layer model of Dzombak and Morel (1990) is used. The respective SCM data set (Supplementary S-1) has been successfully applied by Joseph et al. (2013a) to model a sorption experiment with uranium and Opalinus Clay. All surface parameters and reactions are given in the Supplementary S-1. In addition to surface complexation on the clay minerals, we also consider cation exchange of the main cations as well as uranyl-ions on illite and montmorillonite as exchange phases in the model. All cation exchange reactions and corresponding log K are given in the Supplementary S-1.

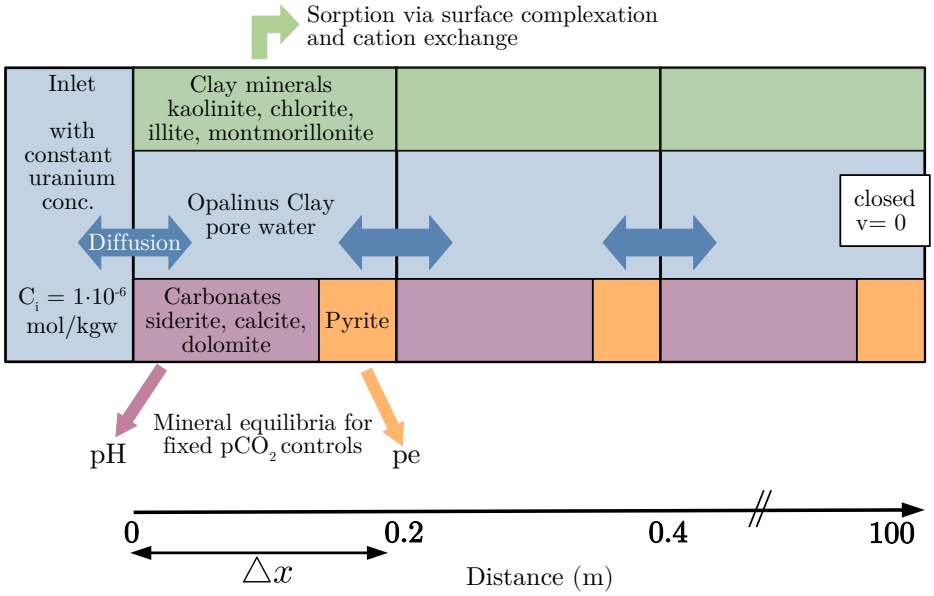

Figure 2.1: Concept of the one-dimensional finite-difference diffusion model.

The remaining net charge of the clay mineral surfaces is compensated by the attraction of counter-ions in a region close to the surface known as the electrical double layer (Tournassat et al., 2015). We apply the diffuse double layer as SCM using the Donnan-approach implemented in PHREEQC as fast and robust method to calculate the averaged composition of the double layer (Parkhurst and Appelo, 2013). In the simulations, the Donnan layer is only used to compensate the remaining net surface charge and not to contribute to the transport. The thickness of the Donnan layer is calculated via the ionic strength I (Table 2.1) according to Wigger and Van Loon (2018). For simplification, the Donnan layer thickness is rounded to 0.5 nm for the carbonate-rich and shaly facies for an ionic strength of 0.4 mol/L. The surfaces and exchanger are initially equilibrated with the pore water solutions. In case sorption of uranium leads to oversaturation, precipitation of amorphous hydrous uraninite ($UO_{2(am,hyd)}$) is enabled during transport simulations. The uranium isotopes are not distinguished,

since no radioactive decay is considered in the simulations. Therefore, effects like the α-recoil induced by α-decay of *U-238* potentially leading to a small-scale enhanced mobility of *U-234* (Pękala et al., 2010, 2009) are excluded. Pękala et al. (2009) have shown that this process only affects the uranium distribution in the Opalinus Clay formation on the cm-scale.

2.3 Model calibration

The diffusion experiment of Joseph et al. (2013b) done with U(VI) and Opalinus Clay is used to test our model concept against experimental data. We have set up a model with a total length of 14.1 mm representing the length of the diffusion cell in the experiment. The model consists of 50 cells because grid size effects have been observed for coarser resolutions. The exact mineralogical composition of the drill core used in the experiment has not been determined. As the diffusion experiment was conducted with sandy Opalinus Clay, we have chosen a clay mineral content of 45 wt.% according to Pearson et al. (2003) and adapted the clay mineral distribution in a calibration procedure to the diffusion curve determined in the experiment. The pore water composition is equal to the one in the experiment containing the main cations and anions. In addition, we assume an uranium background concentration of 2.5 nmol/L (Table 2.1) resulting from the contact of the artificial pore water with the Opalinus Clay sample. This concentration is similar to the conditions measured in the pore water of the sandy facies (Pearson et al., 2003). Calculations have been performed for a pCO_2 of $10^{-3.5}$ bar and 25 °C since the experiment has been done under atmospheric conditions. The pore water composition is controlled by the equilibrium with carbonates and pyrite to adapt pH and pe. Finally, we achieved the best result for a ratio between kaolinite : illite : illite/smectite mixed layers : chlorite of 0.5 : 0.2 : 0.1 : 0.2, respectively. Our results coincide with the experimental data of Joseph et al. (2013b), as shown in Figure 2.2. The relative Root Mean Square Error (rRMSE) is defined as:

$$rRMSE = \sqrt{\frac{1}{s} \sum_{i \epsilon j | O_j > 0}^{s} \left(\frac{O_i - X_i}{O_i} \right)^2} \tag{2.2}$$

with s as number of samples, O_i as experimental values and X_i as simulated results. The rRMSE of our model has been calculated related to the data in Figure 2.2 with a value of 30%, whereby it is important to note that the y-axis is logarithmic. Due to the scattering of the experimental data itself, we consider our model as calibrated.

2.4 Results

2.4.1 Speciation calculations of uranium in the Opalinus Clay

The Pourbaix diagrams were calculated for a pH range from 2 to 10 and for E_H values between -413 mV and 413 mV corresponding to pe of -7 and 7, respectively. As input, the initial solution composition of the sandy facies (Table 2.1) was equilibrated with pyrite and the carbonates for a pCO_2 of $10^{-2.2}$ bar

(Pearson et al., 2003; Wersin et al., 2009). In Figure 2.3a, uranium concentration was set to 1 μmol/L to represent the speciation for higher uranium concentrations as used in the experiments and our simulations. Figure 2.3b shows the speciation for conditions with an uranium concentration of 2.5 nmol/L (Table 2.1) according to the concentrations measured in the sandy facies (Pearson et al., 2003). Phosphate was not considered due to the low concentration in the pore water leading to a minimization of complexing ligands and with it to a better overview in the Pourbaix diagrams. The calculations were performed for atmospheric pressure and temperature conditions. The pH and E_H range observed in the Opalinus Clay pore waters for in-situ conditions are indicated by the dashed box.

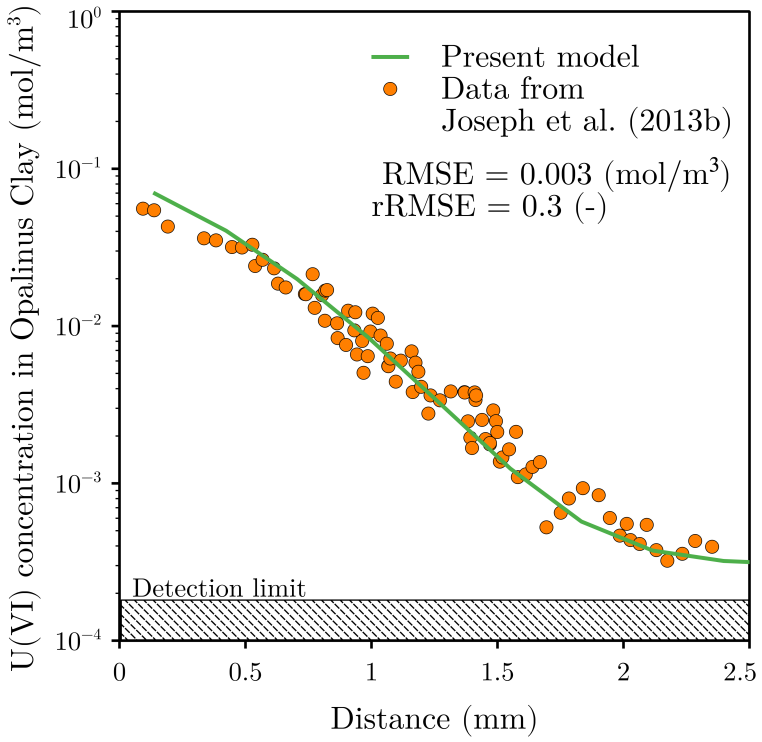

Figure 2.2: Calibrated model applicable to quantify uranium diffusion and sorption in the Opalinus Clay. Model (line) coincides with experimental data (dots) of diffusion experiment done with U(VI) and Opalinus Clay of the sandy facies (Joseph et al., 2013b) for a clay mineral content of 45 wt.%. Ratio between present clay minerals kaolinite : illite : illite/smectite mixed layers : chlorite is set to 0.5 : 0.2 : 0.1 : 0.2, respectively.

As can be seen in Figure 2.3, uranium was mainly present as U(VI) in an anionic Ca-U-CO_3 complex for the moderately reducing conditions applied in the simulations. The species distribution of U(IV) varied for pH>4 depending on the uranium concentration. Table 2.2 shows the remaining species in the pore water of the sandy facies for the minimum and maximum pCO_2. Uranium was more than 90% present as U(VI) distributed among $CaUO_2(CO_3)_3^{2-}$ as main species, $MgUO_2(CO_3)_3^{2-}$ and the neutral uranyl-calcium complex $Ca_2UO_2(CO_3)_3$. A minor part of uranium (<3%) was also present as U(IV) as the conditions were close to the transition to the tetravalent phase. For undisturbed conditions, U(IV) was present as anionic carbonate complex $UCO_3(OH)_3^-$ (Figure 2.3b). A slight increase in the U(IV) fraction could be observed

for a lower pCO_2 of $10^{-2.5}$ bar in combination with a decrease of the amount of U(VI) in the anionic complexes (Table 2.2). However, the changes in species distribution for the minimum and maximum set pCO_2 were less than 1%. The distribution slightly varied (±3%) for the individual facies as can be seen from the values in brackets for the shaly facies (Shaly-76).

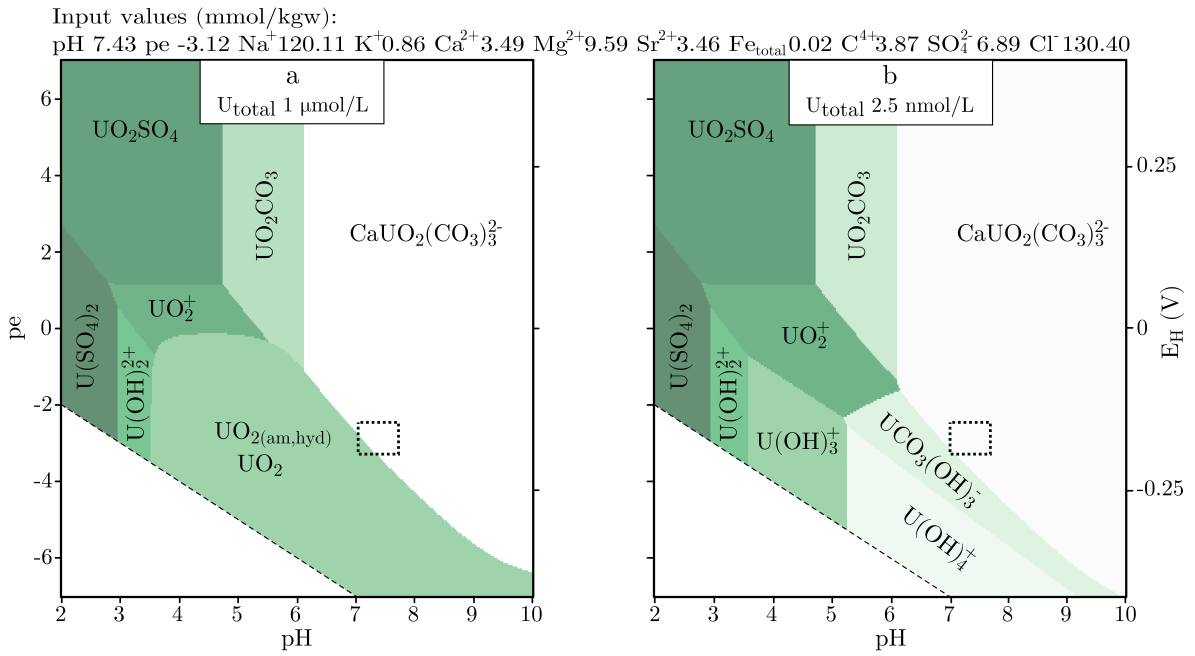

Figure 2.3: In the pH and E_H range observed in the Opalinus Clay formation under in-situ conditions (dashed box), uranium is mainly present as U(VI) in an anionic ternary complex. Pourbaix diagrams of uranium speciation for uranium concentrations of 1 μmol/L (**a**) and 2.5 nmol/L (**b**) in the pore water of the sandy facies of the Opalinus Clay in equilibrium with pyrite and carbonates for an initial pCO_2 of $10^{-2.2}$ bar. Input concentrations are given above in mmol/kgw.

For more strongly reducing redox potentials, the main species turns into U(IV) and solid amorphous uraninite might precipitate with increasing uranium concentration (Figure 2.3). Complexation of uranium was dominated by carbonates for pH>5, whereas complexation with other ligands, like sulphate, became more important for oxidising conditions and pH<5.

Table 2.2: Percentage of aqueous uranium species in the pore water of the sandy facies for a pCO_2 of 10^{-2} bar (A) and $10^{-2.5}$ bar (B). Values of the shaly facies (Shaly-76) are given in brackets.

Species	Valence state	A		B	
$CaUO_2(CO_3)_3^{2-}$	U(VI) in %	69.11	(70.24)	67.91	(69.30)
$MgUO_2(CO_3)_3^{2-}$		15.47	(15.73)	15.20	(15.20)
$Ca_2UO_2(CO_3)_3$		2.72	(5.94)	2.51	(5.77)
$UO_2(CO_3)_3^{4-}$		7.86	(4.89)	8.15	(4.90)
$UCO_3(OH)_3^-$	U(IV) in %	1.03	(1.00)	2.09	(2.06)
$U(OH)_4$		0.05	(0.08)	0.18	(0.28)

2.4.2 Uranium migration depending on pore water chemistry

Uranium migration depending on the geochemical conditions is determined in scenarios for all facies with pCO_2 between 10^{-2} bar and $10^{-2.5}$ bar (Section 2.2.1) since measurements of pCO_2 are associated with a high degree of uncertainty. The pH and pe in the different facies resulting from the respective mineral equilibrium (Section 2.2.1) for a given pCO_2 are shown in Figure 2.4.

The observed pH of 7.1 to 7.6 in the facies depend on the fixed value of pCO_2. In all facies, the same linear behaviour of a decreasing pH with an increasing pCO_2 was observed (Figure 2.4a). The pH values of the facies were very similar for the respective pCO_2 except for the sandy facies, where the pH values were about 0.2 units higher. With increasing pCO_2, the redox potential became less reducing (Figure 2.4b). Values of the pe between -2.7 and -3.3 correspond to an E_H of -160 mV and -195 mV, respectively. The pe in the sandy facies was also about 0.2 units below the pe for the other locations.

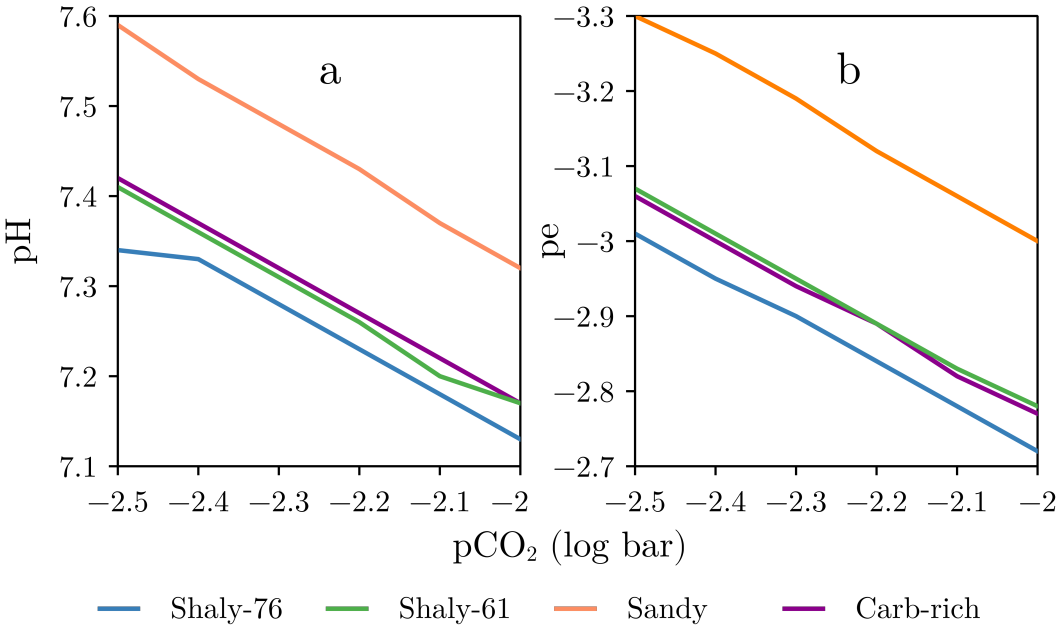

Figure 2.4: pH (**a**) decreases, whereas pe (**b**) increases with pCO_2. Values are given for the pore waters of the three Opalinus Clay facies for the investigated range of pCO_2 between 10^{-2} bar and $10^{-2.5}$ bar. The number behind the shaly facies corresponds to the clay mineral content at the sample location.

The uranium concentrations in the pore water depending on the pCO_2 and resulting composition of the pore water are shown for all facies in Figure 2.5. In all facies, the uranium concentration in the pore water varied according to the pCO_2 resulting in different migration lengths. Figure 2.5 shows that uranium migrated farther into the Opalinus Clay with increasing pCO_2. For example, the difference in migration distance in the shaly facies between a pCO_2 of 10^{-2} bar (16 m) and of $10^{-2.5}$ bar (10 m) was 6 m (Figure 2.5a). In the carbonate-rich facies, the difference in migration distance between a pCO_2 of 10^{-2} bar (26 m) and of $10^{-2.5}$ bar (16 m) was 10 m. Uranium migrated up to 10 m farther into the carbonate-rich facies compared to the shaly facies (Figures 2.5a and b). Migration lenghts varied by 8 m for the second location

in the shaly facies (Figure 2.5c) as well as for the sandy facies (Figure 2.5d) in the investigated range of the pCO_2. The saturation index of uraninite is derived from the uranium concentration in the pore water. No precipitation occurred anywhere along the flow path during the simulation time of one million years in any facies for the investigated geochemical conditions, as the saturation index of the phase remained below 0.

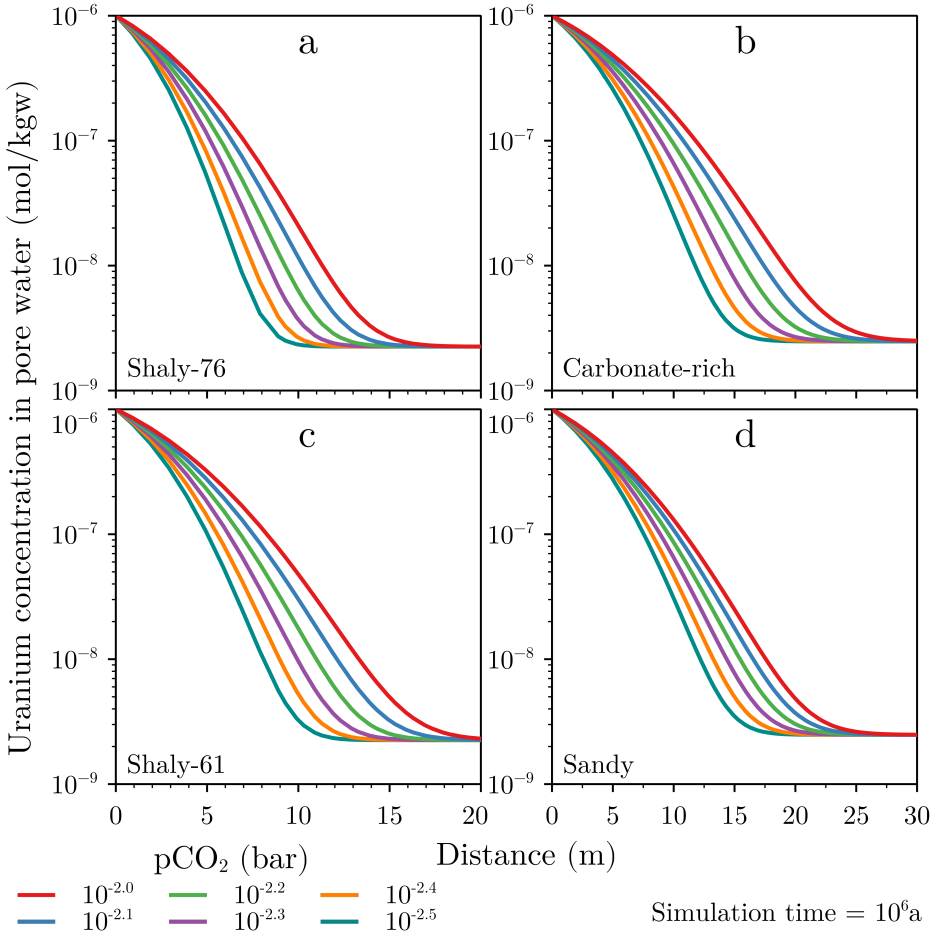

Figure 2.5: With increasing pCO_2, uranium migrates farther through the formation. Concentration of uranium in the pore water of the shaly (**a**, **c**), carbonate-rich (**b**) and sandy (**d**) facies after a simulation time of one million years for pCO_2 between 10^{-2} bar and $10^{-2.5}$ bar. The number behind the shaly facies corresponds to the clay mineral content at the sample location.

2.4.3 Uranium migration as a function of mineral composition

The migration behaviour of uranium depending on the varying mineral composition in the facies of the Opalinus Clay (Table 2.1) was calculated for a fixed pCO_2 of $10^{-2.2}$ bar according to Pearson et al. (2003). The speciation calculations of uranium in the Opalinus Clay have shown that uranium was predominantly present as U(VI) in the anionic complex $CaUO_2(CO_3)_3^{2-}$ (Figure 2.3). Consequently, the anion exclusion effect must be taken into account for the transport simulations. In Figure 2.6a, the dashed lines represent the simulations considering the effect of anion exclusion on the transport process in the different facies of the Opalinus Clay, whereas the solid lines show the results ignoring anion exclusion. For a better overview in Figure 2.6, only the effect of anion exclusion on the uranium conentrations in the pore water is shown.

Migration lengths of uranium in the facies of the Opalinus Clay varied between 13 m (Shaly-76) and 22 m (Carb-rich, Figure 2.6a). The concentrations of uranium in the pore water (Figure 2.6a) as well as sorbed on the solid phase (Figure 2.6b) were almost equal for the sandy and carbonate-rich facies. For the two locations representing the shaly facies, the difference of uranium migration into the formation was approximately 3 m. In all facies, the effect of anion exclusion reduced uranium transport. Uranium diffused between 9 m (Shaly-76, blue dashed line) and 16 m (Carb-rich, purple dashed line). That means, diffusion into the Opalinus Clay was about 30% less taking the effect of anion exclusion into account.

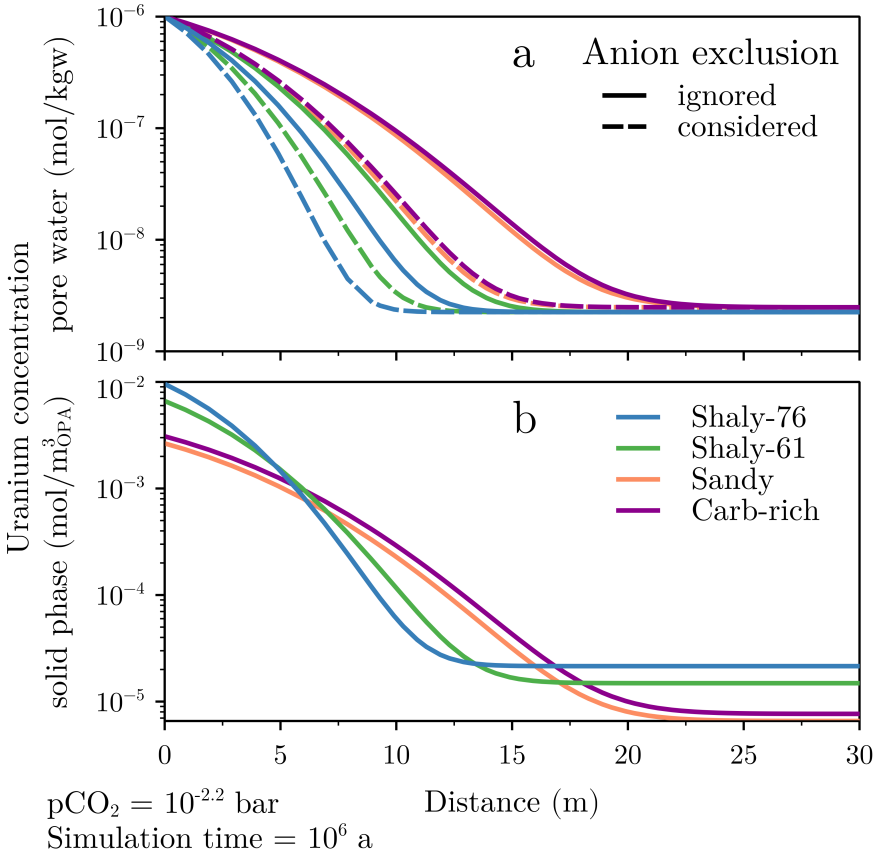

Figure 2.6: Uranium migrated farther through the formation with decreasing clay mineral quantity. Uranium concentrations in the pore water (**a**) and on the solid phase (**b**) are shown for the different facies of the Opalinus Clay after a simulation time of one million years and for a pCO_2 of $10^{-2.2}$ bar. The dashed lines represent the simulations considering the effect of anion exclusion. The number behind the shaly facies corresponds to the clay mineral content at the sample location. OPA = Opalinus Clay.

Sorption onto the shaly facies was twice as high to almost one order of magnitude higher compared to the sandy and carbonate-rich facies. The sorption curves of the shaly facies showed a steeper slope in contrast to the other two facies, which were smoother. Behind the diffusion front (x>20 m), a lower sorption was observed in general in the sandy and carbonate-rich facies in relation to the shaly facies (Figure 2.6b), although background concentration of uranium is slightly higher in the sandy and carbonate-rich facies (Table 2.1).

2.5 Discussion

2.5.1 Speciation of uranium in the pore water

The speciation of uranium in the pore water of the sandy facies of the Opalinus Clay (Table 2.1) equilibrated with pyrite and the carbonates (calcite, dolomite and siderite) is shown in Pourbaix diagrams (Figure 2.3). The calculations were performed for an initial pCO_2 of $10^{-2.2}$ bar and for different uranium concentrations of 1 μmol/L (Figure 2.3a) and 2.5 nmol/L (Figure 2.3b). The primary uranium species, present under the conditions we applied in our simulations, was the anionic complex $CaUO_2(CO_3)_3^{2-}$. About 90% of uranium was present as U(VI) in anionic ternary uranyl complexes (Table 2.2). Therefore, we decided to consider the anion exclusion effect in the transport simulations by reducing the pore water diffusion coefficient D_p (m^2/s).

The geochemistry of the pore water, particularly concentrations of dissolved carbon and calcium as well as pH, define the uranium speciation in the Opalinus Clay. In contrast to our calculated Pourbaix diagrams, the speciation in the diffusion experiment done by Joseph et al. (2013b) was dominated by the neutral aquatic complex $Ca_2UO_2(CO_3)_3$, which was only existent in small quantities in our simulations (3-6%, Table 2.2). This was also the dominating species in other sorption experiments done with U(VI) and Opalinus Clay (Amayri et al., 2016; Joseph et al., 2011, 2013a; Kautenburger et al., 2019). The preponderance of either the neutral $Ca_2UO_2(CO_3)_3$ or the anionic complex $CaUO_2(CO_3)_3^{2-}$ as primary uranium species is sensitive to various geochemical factors such as pH, Ca^{2+} concentration, pCO_2 and also ionic strength (Fox et al., 2006; Tournassat et al., 2018). The deviation between the main species in the experiments and our simulations possibly stems from differences in the geochemistry. For instance, the pore water composition used in the experiments had a higher Ca^{2+} concentration (>0.02 mol/L) and pH (>7.5) in relation to the pore water compositions used in our simulations (Ca^{2+} concentration <0.02 mol/L and pH<7.5, Table 2.1). With increasing Ca^{2+} concentration, the equilibrium of the solution is shifted from the anionic to the neutral complex $Ca_2UO_2(CO_3)_3$ as main species (Dong and Brooks, 2006). Another aspect, which explains the difference in primary species, is the used stability constant ($\log K$) for the neutral ternary uranyl complex in the databases. In Joseph et al. (2013b) a higher $\log K$ taken from Bernhard et al. (2001) is used for the neutral complex, whereas our database is based on the PSI/Nagra thermodynamic database version 12/07 (Thoenen et al., 2014) with a lower $\log K$ resulting in a smaller proportion of the neutral complex in the speciation calculations. These aspects explain the difference of the main species in our simulations compared to the mentioned experiments and emphasize the high influence of the thermodynamic data selection on the results.

2.5.2 Governance of pCO_2 on uranium migration

The pCO_2 controls the calcium and carbonate concentrations as well as pH in the pore waters of the facies via the calcite-carbonate-ion equilibrium. Hence, the pCO_2 has a major influence on the uranium speciation. The pH and pe varied throughout the simulations between 7.1 to 7.6 and -2.7 and -3.3 (E_H of -160 mV and -190 mV, Figure 2.4).

The pH is in line with the pH values determined in the underground rock laboratory Mont Terri mainly ranging from 7 to 8 (Pearson et al., 2003; Wersin et al., 2009). In contrast to the initially set pe of -3.85 (Section 2.2.1) taken from Bossart and Thury (2008), it increased to values between -2.7 and -3.3 due to the equilibration of the pore water with pyrite and siderite. This is in the range of measured values in the Opalinus Clay (Pearson et al., 2003; Vinsot et al., 2008; Wersin et al., 2011). The pH and pe were quite constant because the Opalinus Clay buffers the system via water-rock interactions with the carbonates and pyrite (Wersin et al., 2009). The difference of the calculated pH and pe of the sandy facies from the carbonate-rich and shaly facies (Figure 2.4) is caused by variations in the initial composition of the pore waters. In the sandy facies, the concentrations of Ca^{2+} and Mg^{2+} are about an order of magnitude lower compared to the shaly or carbonate-rich facies (Table 2.1). Due to the greater initial Ca^{2+} and Mg^{2+} concentrations, more CO_2 was dissolved in the equilibrium batch calculations of the carbonate-rich and shaly facies to achieve the given pCO_2 with precipitation of calcite as well as dissolution of siderite and dolomite. A higher concentration of dissolved carbonate results in a decreasing pH. The dissolution of siderite led to higher iron concentrations, and thus pyrite precipitated with an increase in pe. The speciation of the carbonates with the alkali and earth alkali metals also varied with the initial Ca^{2+} and Mg^{2+} concentrations.

Sorption of uranium onto clay minerals strongly depends on the pH. For instance, as the pH rises above 7 and the primary sorption process turns from cation exchange to surface complexation, sorption decreases due to the electrostatic repulsion between the negatively charged uranium species and the negatively charged surfaces of the clay minerals (Cao et al., 2019; Gao et al., 2015; Joseph et al., 2013a; Kim, 2001; Li et al., 2016; Tournassat et al., 2018). Consequently, this should result in a stronger sorption, and thus decreased migration through the formation, for a pCO_2 of 10^{-2} bar with a pH around 7.1 than for a pCO_2 of $10^{-2.5}$ bar with a corresponding pH of around 7.35 (Shaly-76, Figure 2.4). But we observed an increased uranium sorption and hence shorter migration length in the simulations with a higher pH and lower concentration of dissolved carbon dioxide (Shaly-76, Figure 2.5a).

The concentrations of dissolved carbon dioxide and calcium in the system, controlled by the pCO_2 via the carbonate equilibrium, are more decisive for uranium sorption on clay minerals than pH. The reason is the speciation of uranium in the presence of carbonates and calcium due to the formation of neutral or anionic $Ca\text{-}UO_2\text{-}CO_3$ complexes (Figure 2.3). Sorption experiments with uranium under the presence of carbonates showed for a pH above 7 decreased U(VI) sorption on montmorillonite compared to experiments for the same pH range without carbonates (Bachmaf et al., 2008; Philipp et al., 2019; Tournassat et al., 2018), which confirms our findings.

Our results indicate that the influence of the geochemical parameters in solution increases as the clay mineral content decreases. For instance, the difference in migration length between the simulations for the minimum and maximum pCO_2 in the shaly facies was 6 m and 10 m in the carbonate-rich even though the geochemistry of the pore waters were similar (Figure 2.4). Due to the lower clay mineral content and

the associated lower sorption, the difference in extent for the pCO_2 range was greater in the carbonate-rich facies. The simulation results showed that minimal changes in speciation (<1%, Table 2.2) due to a change in pCO_2 had an increasing influence on the transport as clay mineral content decreases (Figures 2.5a and b).

2.5.3 Influence of varying mineralogical compositions

The differences in sorption, and thus transport behaviour of uranium in the facies of the Opalinus Clay, are related to the quantity of clay minerals and hence the number of available sorption sites. For a constant pCO_2 of $10^{-2.2}$ bar, it has been observed that uranium migration varied by 9 m between the three facies of the Opalinus Clay after a simulation time of one million years (Figure 2.6a). Accordingly, a different transport behaviour for uranium was observed in the individual facies. Migration distance of uranium decreased with increasing clay mineral content, and therefore a higher clay mineral content is associated with stronger sorption.

Besides the clay mineral content, the chemistry of the pore waters is also decivise for sorption processes in the Opalinus Clay as it governs the availability of sorption sites and speciation of uranium. In the sandy facies, the concentrations of uranium in the pore water and on the solid phase were similar to the carbonate-rich facies, although the clay mineral content is about 20% higher (Table 2.1). This is caused by the higher pH as well as differences in the calcium and carbonate concentrations compared to the other facies. For this case, unlike we expected, the chemistry resulting from the interaction between pore water and prevailing minerals is more important than the clay mineral content. Based on our results, we can therefore prioritize the known influencing factors for the sorption of uranium in the Opalinus Clay in descending order for the first time: pCO_2, Ca^{2+} concentration, pH, pe and the clay mineral content. Only for large differences in the quantity of clay minerals (>50 wt.%) and similar chemistry, such as carbonate-rich and shaly facies (Table 2.1, Figure 2.4), sorption increases with higher clay mineral contents and ultimately leads to reduced migration. The retardation capacity of the carbonate-rich facies with a clay mineral content of 26 wt.% is still sufficient since uranium did not migrate farther than 26 m after a simulation time of one million years (Figure 2.5). With regard to the minimum requirements for a host rock for nuclear waste disposal as defined, e.g. by the German government (§ 23 Article 5 StandAG[2]), this means that a thickness of 100 m is sufficient to retain uranium within the host rock and keep it away from adjacent aquifers and the human environment.

For the anionic complex, migration is decreased due to the effect of anion exclusion in claystones as considered in the simulations by reducing D_p by a factor of 0.55 analogous to the diffusion-accessible porosity ratio of chloride. This led to a lowering of the transport distance by about 30%. However, this scaling factor determined for chloride may be too large due to the larger ionic radius as well as more negative charge of the anionic ternary uranyl complex compared to chloride (Van Loon et al., 2007, 2018).

[2]Standortauswahlgesetz (StandAG) of 5 May 2017 (Federal Law Gazette p. 1074) as last amended by Article 1 of the Act of 7 December 2020 (Federal Law Gazette p. 2760). URL: https://www.gesetze-im-internet.de/standag_2017/BJNR107410017.html (accessed on 13 June 2022).

For example, in an in-situ diffusion experiment done in the underground laboratory Mont Terri for larger anions a smaller scaling factor was indicated (Gimmi et al., 2014). This would lead to a shorter migration distance for uranium. Gimmi et al. (2014) also showed that a difference in ionic strength, as in the facies at Mont Terri, had no significant influence on the anion exclusion effect, therefore this aspect was not considered further here.

The migration lengths discussed here represent maximum distances. Our model concept and applied boundary conditions simplify a potential nuclear waste disposal. For the future, several engineered barriers have been developed to keep the radionuclides as best as possible inside the repository and with that significantly retard their migration into the host rock (Nagra, 2002a). Besides the influence of these engineered barriers on the source term, the uranium concentration from the canisters is limited and would decrease with time, reducing migration into the Opalinus Clay. Since our focus lies on the migration behaviour in the far-field, i.e. the host rock, we did not take into account those details, what has to be kept in mind when considering our results.

With regard to a real case application, in which disposal of nuclear waste in the Opalinus Clay at a burial depth of around 650 m is intended (Nagra, 2002a), the influence of an increased overburden must not only be considered on the lithostatic pressure influencing, for example, the anisotropy of transport parameters. Since the overburden at Mont Terri is only around 300 m (Bossart and Thury, 2008), a larger load would also have an effect on the hydrostatic pressure in the system, which, in turn, affects the chemical equilibrium between the prevailing minerals and pore water, and thus the composition of the pore water. This is especially the case for the carbonate system (Wersin et al., 2016), which has a high influence on the speciation and hence sorption of uranium in Opalinus Clay as shown in experiments and with our results. The borehole Schlattingen is used to investigate the Opalinus Clay formation at the potential depth for a repository (Nagra, 2014). Our investigated range of pCO_2 covers the partial pressures determined for the location (Lerouge et al., 2015). This indicates that our results could also be applied to greater depths.

2.6 Conclusions and Outlook

Diffusion and sorption processes of uranium in Opalinus Clay were investigated in one-dimensional diffusion models on the 100 m-scale and for a simulation time of one million years for the first time. Calculations were performed in PHREEQC depending on the different mineralogy in the three facies (shaly, sandy and carbonate-rich) and associated changes in pore water composition as a function of partial pressure of carbon dioxide (pCO_2) in the range of 10^{-2} bar and $10^{-2.5}$ bar. Sorption processes were quantified with mechanistic surface complexation models and cation exchange based on a bottom-up approach. Pore water compositions of the facies were based on analyses from boreholes at the underground research laboratory Mont Terri and equilibrated with the carbonates (calcite, dolomite and siderite) as well as pyrite to adapt pH and pe.

Uranium must be regarded as mobile in the geochemical system of the Opalinus Clay with migration depending on the facies. Our speciation calculations have shown that uranium is mainly present as U(VI) as anionic complex $CaUO_2(CO_3)_3^{2-}$ for in-situ conditions. For a constant pCO_2 of $10^{-2.2}$ bar, migration distances varied between the shaly (13 m) and sandy as well as carbonate-rich facies (22 m) about 9 m. This is caused by the clay mineral content and associated number of sorption sites as uranium migration increased with decreasing clay mineral content.

Sorption and with it migration of uranium in the Opalinus Clay is primarily controlled by the calcite-carbonate-ion system and not so much by the clay mineral content. The results of the sandy and carbonate-rich facies showed that for lower clay mineral contents (<50 wt.%) the geochemistry in the pore waters resulting from the interaction with the prevailing minerals is more decisive for the sorption processes compared to the clay mineral content. The pore water composition governs speciation and activities of uranium. This, in turn, results in a differentiated sorption behaviour due to the complexation of uranium with calcium and carbonate that do not sorb or only weakly on clay minerals for the investigated geochemical conditions. Based on our results, we were able to order the known important key parameters for the sorption of uranium in the Opalinus Clay with decreasing priority as follows: dissolved carbon and calcium concentrations, pH, pe and clay mineral content.

Considering only the radionuclide uranium, we conclude that Opalinus Clay in general seems to be a suitable potential host rock for the disposal of spent fuel. Uranium did not migrate farther than 26 m after a simulation time of one million years and for a pCO_2 of $10^{-2.5}$ bar even in the facies with the lowest clay mineral content, the carbonate-rich. With a thickness of 100 m, uranium is retained in the effective containment zone of the host rock and no adjacent groundwater aquifer, and hence the human environment, is reached.

Chapter 3

Surrogate model for multi-component diffusion of uranium through Opalinus Clay on the host rock scale

Abstract

Multi-component (MC) diffusion simulations enable a process-based and more precise approach to calculate transport and sorption compared to the commonly used single-component (SC) models following Fick's law. The MC approach takes into account the interaction of chemical aqueous species in the pore water with the diffuse double layer (DDL) adhering clay mineral surfaces. We studied the shaly, sandy and carbonate-rich facies of the Opalinus Clay. High clay contents dominate diffusion and sorption of uranium. The MC simulations show shorter diffusion lengths than the SC models due to anion exclusion from the DDL. This hampers diffusion of the predominant species $CaUO_2(CO_3)_3^{2-}$. On the one side, species concentrations and ionic strengths of the pore water and on the other side surface charge of the clay minerals control the composition and behaviour of the DDL. For some instances, it amplifies the diffusion of uranium. We developed a workflow to transfer computationally intensive MC simulations to SC models via calibrated effective diffusion and distribution coefficients. Simulations for one million years depict maximum uranium migration lengths between 10 m and 35 m. With respect to the minimum requirement of a thickness of 100 m, the Opalinus Clay seems to be a suitable host rock for nuclear waste disposal.

3.1 Introduction

For the safe disposal of especially highly radioactive waste, emplacement in deep subsurface geological repositories is favoured worldwide to ensure the protection of human and nature from the potential radiation exposure of the waste packages for periods of up to one million years (IAEA, 2003). Claystones are among potential host rocks due to their low permeability. Hence, diffusion is the primary transport process in intact formations (Delay et al., 2007; Mazurek et al., 2008; Nagra, 2002a). Another important and positive aspect of claystones with regard to the disposal of nuclear waste is the high sorption capacity retarding the potential migration of radionuclides.

The diffusive transport through the host rock is quantified with numerical simulations usually using Fick's law (Nagra, 2002a). According to this method, only one diffusion coefficient is used for all species, major and minor ions as well as all radionuclides, in the same way. A more advanced approach is the multi-component (MC) diffusion, where each species in the system is assigned its own diffusion coefficient and transport is calculated separately for the diffuse double layer (DDL) and the free pore water (Appelo et al., 2010; Appelo and Wersin, 2007). The surfaces of clay minerals are charged due to their internal structure and contact to the external pore water.

Dependent on pH of the solution and the hydroxyl groups on the mineral surface the DDL forms, compensating the net surface charge by attraction of counter-ions and repulsion of co-ions (Tournassat et al., 2015). Enhanced transport of counter-ions as well as decreased transport of co-ions occurs in the DDL (Appelo and Wersin, 2007; Nagra, 2002a). As a consequence, anionic, cationic and neutral species show different diffusive migration pattern in clay formations (Altmann, 2008; Appelo et al., 2010).

The Swiss Opalinus Clay is a potential host rock for the disposal of nuclear waste (Nagra, 2002a). The formation has been investigated for the last 25 years in the underground research laboratory Mont Terri and hence offers a comprehensive database (Bossart et al., 2017). Furthermore, the MC diffusion approach has already been successfully applied to the Opalinus Clay to model diffusion experiments, for instance, with caesium, sodium, chloride and tritium (Appelo et al., 2010). The Opalinus Clay is subdivided into shaly, sandy and carbonate-rich facies (Pearson et al., 2003), which differ in their mineralogical composition. As a result of the water rock interaction, the geochemical conditions in the pore waters of the facies vary and impact on sorption and transport of radionuclides (Hennig et al., 2020).

Uranium is one of the main components in spent fuel (Metz et al., 2012), for which we apply diffusion simulations for the far-field ($>$50 m) of a potential host rock to assess its migration behaviour. Uranium is redox sensitive and its speciation between U(IV) and U(VI) is controlled by the pore water composition. In the geochemical system of the Opalinus Clay, uranium is mainly present as anionic as well as neutral ternary uranyl complex bound to calcium and carbonate. In a previous study, the migration of uranium in the Opalinus Clay was assessed in one-dimensional diffusion simulations using Fick's laws as a function of different partial pressures of carbon dioxide (pCO_2) covering the range of measured values for the formation and depending on the mineralogical heterogeneity in the facies (Hennig et al., 2020). The various facies govern the geochemistry of the system especially via the pCO_2, and thus by the carbonate and calcium concentrations as well as the resulting pH through which the anionic ternary uranyl complex $CaUO_2(CO_3)_3^{2-}$ is the predominant species in the system (Hennig et al., 2020). Based on their results Hennig et al. (2020) prioritized the governing parameters for the sorption of uranium in the Opalinus Clay as follows: pCO_2, Ca^{2+} concentration, pH, pe and clay mineral quantity. Furthermore, the effect of anion exclusion on the migration lengths was estimated by an adapted pore water diffusion coefficient, what reduced uranium migration by 30%. The work presented here thus aims to extend the findings of Hennig et al. (2020) by means of the MC approach.

The first focus in the present study was to assess the deviation between the classical single-component (SC) and the MC approach in the diffusion lengths of uranium. We know that sorption processes of uranium are facies dependent (Hennig et al., 2020), hence we investigated and quantified the dependence also for the MC diffusion approach. Many different field and laboratory experiments would be necessary to investigate uranium migration for all geochemical and mineralogical occurrences of the Opalinus Clay. However, those experiments are time-consuming and limited to the metre-scale. In contrast, the safety assessment of a potential nuclear waste repository is required

for the host rock scale and for time frames of several hundred thousands of years, what makes numerical simulations indispensable. Unfortunately, MC diffusion on the host rock scale is associated with a huge computational effort. As a second focus, we therefore developed a workflow using MC simulations on the small scale to calibrate transport parameters, which are then used as surrogate of MC diffusion in the SC approach on the host rock scale for simulation times of up to one million years.

3.2 Methods

For the varying geochemical (Section 3.2.1) and mineralogical conditions (Section 3.2.2) in the facies of the Opalinus Clay, one-dimensional diffusion simulations were performed using the MC diffusion approach (Section 3.2.3) that is implemented in PHREEQC Version 3.5.0 (Parkhurst and Appelo, 2013).

As first step, we quantified the deviation between the MC approach and the SC method using Fick's law (Section 3.2.4) by comparing the calculated migration lengths on the metre-scale, and thus for acceptable computing times. In a second step, we developed a workflow to calibrate and transfer results of MC diffusion simulations on the metre-scale to the host rock scale (far-field) and a simulation time of one million years. For that, we used a distribution coefficient K_d (m^3/kg) and an effective diffusion coefficient D_e (m^2/s). The K_d was calculated from results of PHREEQC (Section 3.2.2) and was then used to calibrate the D_e by applying Fick's laws until the results coincide with the MC simulations. The quality of the workflow was evaluated by comparison with a MC simulation.

The underlying thermodynamic data are described in Hennig et al. (2020) and updated with the self-diffusion coefficients in water D_w (m^2/s, Section 3.2.3, Supplementary S-2[1]) for the uranium species (Kerisit and Liu, 2010; Liu et al., 2011) as well as for the pore water components (Parkhurst and Appelo, 2013). All simulations were performed for a temperature of 25 °C in regard to the database. Elevated temperatures as expected due to heat generated by the high-level waste or relevant for greater depths can be neglected because it is shown that it affects neither the pore water composition (<5% for a temperature of 45 °C, Wersin et al., 2016) nor the migration behaviour of uranium in the Opalinus Clay up to temperatures of 60 °C (Joseph et al., 2013b). All transport simulations were conducted for hydraulic rock properties corresponding to the direction perpendicular to bedding. The uranium source term from the failed high-level waste canisters is represented by a Dirichlet boundary with a constant uranium concentration of 1 μmol/L (Joseph et al., 2013b; Keesmann et al., 2005). Since our focus lies on the migration behaviour of uranium in the far-field, we do not consider the effect of the engineered barriers on the source term (Nagra, 2002a), such as a delay and retention due to the metal canisters or the bentonite filling. This constraint is a simplification of the nuclear waste disposal concept, and hence our results need to be considered as maximum migration lengths. Neumann boundary is applied to the model outlet.

[1] Table S-2 only contains the uranium species that are relevant for the investigated system, i.e. present in concentrations $>10^{-12}$ mol/L, and therefore it has been shortened compared to the published version.

3.2.1 Geochemical system of the Opalinus Clay

The facies of the Opalinus Clay are defined in the simulations based on mineralogical and geochemical data from bore hole logs at Mont Terri (Table 3.1). The concentrations of the main ions in the pore water are averaged for the measurement series and electro neutrality of the solution (±3%) is established via chloride (Hennig et al., 2020). The composition of the pore water stems from marine origin and the interaction with the minerals, such as cation exchange and/or dissolution as well as precipitation (Pearson et al., 2003; Wersin et al., 2009). Due to the geological age of the formation and the associated contact time between minerals and pore water, thermodynamic equilibrium between both is assumed (Bradbury and Baeyens, 1997; Pearson et al., 2003, 2011; Wersin et al., 2009).

The speciation of uranium in the pore water and its sorption on the Opalinus Clay highly depends on the pCO_2 (Hennig et al., 2020) as it controls the concentrations of carbonates and calcium as well as pH in solution (Pearson et al., 2003; Wersin et al., 2009). Measurements of pCO_2 in the Opalinus Clay are associated with a degree of uncertainty (Pearson et al., 2003; Vinsot et al., 2008; Wersin et al., 2011), and therefore we decided to fix it to $10^{-2.2}$ bar as recommended for clay formations with similar mineral assemblages (Lerouge et al., 2015; Pearson et al., 2003, 2011). Depending on pCO_2, the pore waters of the facies are equilibrated with the carbonates calcite, dolomite and siderite to control pH and the concentrations of calcium, magnesium and iron (Gaucher et al., 2010). For the applied pCO_2 of $10^{-2.2}$ bar, uranium is mainly present as anionic ternary uranyl complex $CaUO_2(CO_3)_3^{2-}$ in the pore water (Hennig et al., 2020). For in-situ conditions, the pore water in the Opalinus Clay is moderately reducing (Pearson et al., 2011; Wersin et al., 2011). An initial E_H of -227 mV published by Bossart and Thury (2008) was chosen and governed in the simulations via an equilibrium with the minerals pyrite and siderite. These minerals, or the redox couple SO_4^{2-}/HS^-, provide the most consistent results with measurements (Pearson et al., 2003, 2011; Wersin et al., 2009, 2011).

3.2.2 Integrating sorption processes

The varying mineralogy of the Opalinus Clay is implemented in the simulations with a bottom-up approach (Marques Fernandes et al., 2015; Stockmann et al., 2017). The amount of sorption of contaminants in heterogeneous formations can be determined by the additive sorption on individual minerals. It is quantified with mechanistic surface complexation models (SCM) using the two-layer model of Dzombak and Morel (1990) and cation exchange (Kim, 2001). The respective and proven SCM dataset (Joseph et al., 2013a) with all surface parameters and reactions is given in the Supplementary of Chapter 2 (Supplementary S-1, Hennig et al., 2020). We only consider sorption on the main clay minerals illite, illite/smectite mixed layers, kaolinite and chlorite (Scenario MC_{4Clay}) as the contribution of the other minerals to the total sorption can be neglected (<1%, Hennig et al., 2020). The illite/smectite mixed layers are handled as a combination of the pure clay minerals (illite and smectite) with a proportion of 1:1 (Joseph et al., 2013a). Smectite is a generic term for a group of clay minerals and not further described for the Opalinus Clay. We decided to use montmorillonite as

representative because it is the best investigated (Joseph et al., 2013a). Cation exchange is considered for the main cations and uranyl-ions on illite and montmorillonite as exchange phases (Hennig et al., 2020). The respective reactions are given as well in the Supplementary of Chapter 2 (Supplementary S-1, Hennig et al., 2020). The distribution coefficient K_d (m^3/kg) is defined by the ratio between the amount of a species adsorbed

Table 3.1: Input parameters representing the three facies: shaly, sandy and carbonate-rich. Concentrations are given as average values from the borehole analyses. Shaly-76 and Shaly-61 correspond to the clay mineral content in wt.% at the sampled location.

Parameter	Unit	Shaly-76 [a,b]	Shaly-61 [c,d]	Sandy [e,f]	Carb-rich [g,h]
pH	-	7.13	7.50	7.40	7.28
Na^+	mmol/L	281	230	121	195
K^+	mmol/L	1.93	1.47	0.87	0.73
Mg^{2+}	mmol/L	21.97	16.79	5.91	15.89
Ca^{2+}	mmol/L	18.90	16.03	6.73	16.37
Sr^{2+}	mmol/L	0.46	0.47	0.35	0.44
Fe_{total}	μmol/L	29.62	8.37[d]	9.81[f]	9.81[f]
U_{total}	nmol/L	2.28[d]	2.28[d]	2.52[f]	2.52[f]
Cl^-	mmol/L	327	273	121	242
SO_4^{2-}	mmol/L	16.79	12.30	6.94	16.03
PO_4^{3-}	μmol/L	21.65[d]	21.65[d]	10.65 [f]	10.65[f]
Alkalinity	mmol/L	3.85	1.24	2.61	2.05
I[i]	mol/L	0.38	0.32	0.16	0.28
DDL[j]	nm	0.49	0.54	0.76	0.57
Illite	wt.%	20	17	17	8
IS mixed[k]	wt.%	16	12	8	6
Kaolinite	wt.%	30	26	13	8
Chlorite	wt.%	10	6	7	4
∑Clay	wt.%	76	61	45	26
Calcite	wt.%	14	11	17	42
Dolomite	wt.%	n.a.	2	2	3
Siderite	wt.%	1	4	2	2
Porosity ϵ_{wc}	-	0.166[l]	0.162	0.137[m]	0.155
Wet water content wc_{wet}	-	0.068[l]	0.070	0.055[m]	0.063
Dry bulk density ρ_{db}	kg/m^3	2,290[l]	2,280	2,365[m]	2,320
Wet bulk density ρ_{wb}	kg/m^3	2,458[l]	2,456	2,498[m]	2,480

n.a. = no data available; [a] Vinsot et al. (2008), borehole BPC-C1; [b] Pearson et al. (2003), borehole BPP-1; [c] Wersin et al. (2009), borehole BWS-A1; [d] Pearson et al. (2003), borehole BWS-A1; [e] Wersin et al. (2009), borehole BWS-A3; [f] Pearson et al. (2003), borehole BWS-A3; [g] Pearson et al. (2003), borehole BGP-1; [h] Pearson et al. (2003), borehole EPFL; [i] calculated in PHREEQC for a pCO_2 of $10^{-2.2}$ bar; [j] thickness Donnan-layer, calculated via ionic strength (Wigger and Van Loon, 2018); [k] IS mixed, illite/smectite mixed layers; [l] Pearson et al. (2003), borehole BWS-A6; [m] Pearson et al. (2003), borehole BWS-E3

on the solid phase and the amount present in the liquid phase. The K_d is calculated in PHREEQC for each facies depending on the geochemical and mineralogical conditions following Stockmann et al. (2017). In the literature, sorption of uranium on Opalinus Clay is commonly modelled using only the clay minerals illite and montmorillonite (Bradbury and Baeyens, 2005a,b; Bradbury et al., 2005; Hartmann et al., 2008). We followed that approach and assessed the effect of various mineral compositions on the resulting migration length (Scenario MC_{2Clay}).

Porosity, bulk density and water content vary for each facies (Pearson et al., 2003). These parameters influence the simulation results as they define the amount of pore water per volume unit Opalinus Clay and the amount of clay minerals per kilogram pore water. Therefore, we performed various scenarios of MC diffusion simulations for the minimum and maximum amount of rock per kilogram pore water (Scenarios MC_{min} and MC_{max}, Table 3.2) as well as with different clay mineral compositions (Scenarios MC_{4Clay} and MC_{2Clay}).

Table 3.2: Water content porosity (ϵ_{wc}), dry and wet bulk density (ρ_{db} and ρ_{wb}) as well as wet water content (wc_{wet}) used for the scenarios with the minimum and maximum amount of rock per kilogram pore water for the facies of the Opalinus Clay (Pearson et al., 2003).

Parameter	Shaly-76		Shaly-61		Sandy		Carb-rich	
	Min	Max	Min	Max	Min	Max	Min	Max
Water content porosity ϵ_{wc} (-)	0.191	0.141	0.191	0.141	0.177	0.130	0.171	0.155
Wet water content wc_{wet} (-)	0.051	0.086	0.051	0.086	0.053	0.078	0.053	0.075
Dry bulk density ρ_{db} (kg/m^3)	2,230	2,410	2,230	2,410	2,260	2,400	2,280	2,400
Wet bulk density ρ_{wb} (kg/m^3)	2,420	2,530	2,420	2,530	2,440	2,530	2,450	2,530
Rock per kg pore water (kg_{rock}/kg_{pw})	11.55	16.95	11.55	16.95	12.36	18.17	13.20	15.24

3.2.3 Modelling multi-component diffusion

In contrast to Fick's laws, the transport of species in the MC diffusion approach is not based on a concentration gradient but on the electrochemical potential μ (Appelo et al., 2010, 2008; Appelo and Wersin, 2007; Parkhurst and Appelo, 2013):

$$\mu = \mu^0 + RTln\alpha + zF\psi \tag{3.1}$$

with μ^0 the standard potential (J/mol), R the gas constant (8.314 J/K/mol), T the absolute temperature (K), α the activity (mol/m^3), z the charge number (-), F the Faraday constant (96,485 J/V/eq) and ψ the electrical potential of a charged surface (V). This enables calculation of the diffusive flux in uncharged (free pore water) and charged regions (DDL) of the clay minerals or the interlayer space between the clay layers. Appelo et al. (2010) successfully applied the approach for the Opalinus Clay to model a diffusion experiment with neutral, cationic and anionic species. Furthermore, it was used to obtain the pore water composition in the Callovo-Oxfordian clay rock (Appelo et al., 2008).

The diffusive flux of a species in solution J_i (mol/m^2/s) as result of the chemical and electrical potential gradients becomes (Appelo, 2007; Appelo et al., 2010; Appelo and Wersin, 2007; Parkhurst and Appelo, 2013):

$$J_i = -\frac{u_i c_i}{|z_i|F}\frac{\partial \mu_i}{\partial x} - \frac{u_i z_i c_i}{|z_i|}\frac{\partial \psi}{\partial x} \tag{3.2}$$

with u_i the mobility in water (m^2/s/V), c_i as species concentration in the accessible pore water (mol/m^3) and x as spatial coordinate (m). The mobility of species i in Equation 3.2 is related to the self-diffusion coefficient in water $D_{w,i}$ (m^2/s):

$$u_i = D_{w,i} \cdot \frac{|z_i|F}{RT} \tag{3.3}$$

Due to the different transport velocities of ions, a charge with an associated potential is created, and thus the gradient of the electrical potential ($\partial\psi/\partial x$) in Equation 3.2. The electrical potential in Equation 3.1 stems from a charged surface, and is therefore fixed without inducing any electrical current. Accordingly, both potentials may differ from each other (Appelo, 2007; Appelo et al., 2010; Appelo and Wersin, 2007; Parkhurst and Appelo, 2013). If there is no electrical current, $\sum z_i J_i = 0$. This zero-charge flux condition allows to eliminate the electrical potential gradient ($\partial\psi/\partial x$) from Equation 3.2 by expressing it as a function of the other terms in Equation 3.2 (Appelo et al., 2010; Appelo and Wersin, 2007; Parkhurst and Appelo, 2013). Any charge imbalance that may, for instance, exist in the DDL is maintained by the zero-charge flux condition and hence the equation is also valid, if the solution is not electrically neutral.

Within PHREEQC, the diffusive flux for every species present in the system is calculated as the sum of the transport in the pore water as well as in the DDL for the MC option. Conceptually, the porous medium within a model element is subdivided along its length in paired cells for each mineral present (Figure 3.1). Accordingly, each pair of cells consists of a charge-balanced solution, the free pore water, and a charged surface with a DDL. In the case of negatively charged surfaces, cations are enriched in the DDL to compensate the remaining net surface charge and anions are excluded. Consequently, the pore space accessible for anions is reduced and so their diffusive flux. This is known as the anion exclusion effect. In the simulations, anion exclusion is controlled by the composition and amount of water in the DDL. The composition of the DDL is calculated as average using the fast and robust method of the Donnan approximation implemented in PHREEQC (Parkhurst and Appelo, 2013), which assumes a single potential for the DDL as an entity (Appelo and Wersin, 2007):

$$c_{i,DDL} = c_i \cdot exp\left(\frac{-z_i F \psi_{DDL}}{RT}\right) \tag{3.4}$$

with $c_{i,DDL}$ the concentration of species i in the Donnan pore space (mol/m^3) and ψ_{DDL} the potential in the DDL (V) to ensure zero charge of the paired cells. The potential of the Donnan volume ψ_{DDL} is adapted to counterbalance the surface

charge (Parkhurst and Appelo, 2013). Hence, the concentrations in the DDL are linked to the concentrations in the free pore water c_i (mol/m^3) and the surface charge that must be neutralized (Appelo, 2017). The thickness of the DDL is determined via the ionic strengths (I, Table 2.1, Wigger and Van Loon, 2018). MC diffusive transport in a model element is calculated by explicit finite differences for each interface among the cells and summed up for the diffusive transport between two model elements. A more detailed description of the approach can be found in Appelo and Wersin (2007), Appelo (2007) and Appelo et al. (2010).

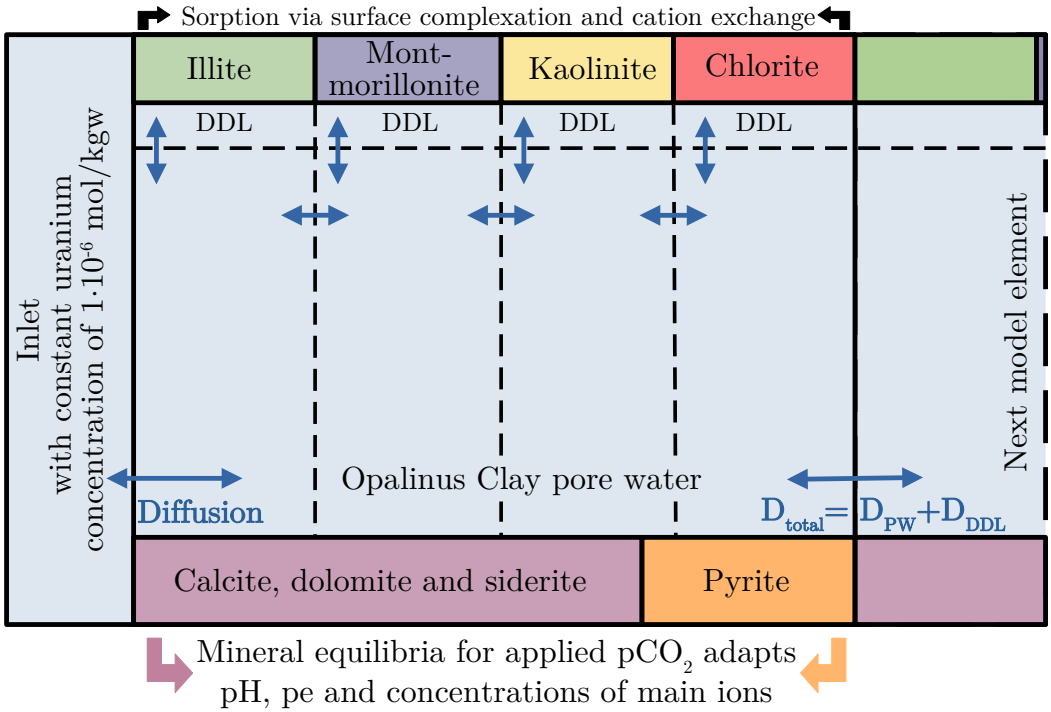

Figure 3.1: Concept of the one-dimensional finite-difference diffusion model in PHREEQC applying the multi-component approach.

In porous media, diffusive transport is impeded by tortuosity of the pores, the reduced cross-sectional area available for diffusion and the pore sizes (Gratwohl, 1958), which is reflected by the effective diffusion coefficient D_e (m^2/s). PHREEQC assumes that a model element exclusively contains water (Parkhurst and Appelo, 2013), and therefore the pore water diffusion coefficient D_p (m^2/s) is applied instead to calculate the diffusive flux. Equation 3.5 gives the relation between D_p and D_e. In PHREEQC, D_p is derived analogous to Archie's law via the D_w (m^2/s), the accessible porosity ϵ (-) and an empirical exponent n (-):

$$\frac{D_e}{\epsilon} = D_p = D_w \cdot \epsilon^n \tag{3.5}$$

The empirical exponent n is a constant, medium-specific parameter (Van Loon et al., 2007) and needs to be determined for the Opalinus Clay (Section 3.3) to use the MC approach in PHREEQC. In order to individually calculate the diffusive flux for each species present in the system, D_w must be assigned in the database. The D_w of all relevant uranyl species were calculated by molecular-dynamic simulations

and are taken from Kerisit and Liu (2010) as well as from Liu et al. (2011). In the case of a missing D_w for an uranium species, the diffusion coefficient of a chemically similar one was chosen to be used instead. All other necessary D_w stem from the database *phreeqc.dat* provided with PHREEQC (Parkhurst and Appelo, 2013). The selected D_w are given in the Supplementary S-2[1].

On the metre-scale, MC simulations were performed for each facies (Table 3.1, Section 3.2.1) as well as for varying mineral quantities and compositions (Table 3.2, Section 3.2.2) for models of 1 m with a spatial resolution of 0.01 m and a simulation time of 100 years. Simulations on the host rock scale were conducted for each facies with a model of 50 m and a spatial resolution of 0.5 m and a simulation time of one million years. Grid independence of the diffusion models on both scales was confirmed by simulations with finer resolutions.

3.2.4 Modelling single-component diffusion

The classical SC diffusion simulations were conducted in Python-based diffusion models for each facies using Fick's laws and finite-differences. The spatial resolution is 0.005 m on the small scale (1 m) and 0.25 m on the far-field scale (50 m) to ensure grid independence. Sorption is considered via the distribution coefficient K_d calculated for every facies in the MC simulation, as described in Section 3.2.2. Since only one diffusion experiment with uranium in Opalinus Clay of the sandy facies is given in the literature (Joseph et al., 2013b), this D_e is used for all facies in the SC simulations. The D_e was determined in the experiment for a temperature of 25 °C and perpendicular to bedding with $1.9 \cdot 10^{-12}$ m^2/s (Joseph et al., 2013b). Porosities are taken from Table 3.1.

3.3 Model calibration

The medium-specific parameter n required for the MC diffusion approach to determine the D_e for every species (Equation 3.5) was calibrated using an experiment with U(VI) and Opalinus Clay of the sandy facies (Joseph et al., 2013b). We set up a model equal to the one presented in Hennig et al. (2020) with the additional application of the MC diffusion approach. For the diffusion experiment, the precise composition of the minerals was not determined. Therefore, the mineral composition used here is based on the results given in Hennig et al. (2020) for a clay mineral content of 45 wt.% corresponding to the sandy facies (Pearson et al., 2003): 23 wt.% kaolinite, 9 wt.% illite, 4 wt.% illite/smectite mixed layers and 9 wt.% chlorite (Section 2.3). The parameter n was varied until the best coincidence between the MC diffusion simulations and the experimental data was achieved. For the simulations considering sorption on all clay minerals (MC_{4Clay}: illite, montmorillonite, chlorite and kaolinite), an exponent n of 2.6 was determined, whereas for the model concept with only two clay minerals (MC_{2Clay}: illite and montmorillonite) the best match between experimental and modelled data was observed for an n of 2.1. Both results and the experimental data are shown in Figure 3.2.

In the literature, values for the medium-specific parameter n of 2.4 (Van Loon et al., 2018) and 2.5 (Mazurek et al., 2009, 2008; Van Loon et al., 2003b) are given for Opalinus Clay, which is in line with the value n = 2.6 of our MC_{4Clay} concept. For bentonite mainly consisting of montmorillonite, a value of n = 1.9 can be found (Van Loon and Mibus, 2015), which is similar to the MC_{2Clay} concept with only illite and montmorillonite as clay minerals and an exponent n = 2.1. However, the experimental data can be reproduced as shown in Figure 3.2. The relative Root Mean Square Errors (rRMSE, Equation 2.2) are calculated in relation to the experimental data. The values for the rRMSE are 28% for an n = 2.6 (MC_{4Clay}) and 27% for a n = 2.1 (MC_{2Clay}). Due to the scattering of the data, we consider our model concepts for the exponents n = 2.6 (MC_{4Clay}) and n = 2.1 (MC_{2Clay}) as best fit and calibrated for further application.

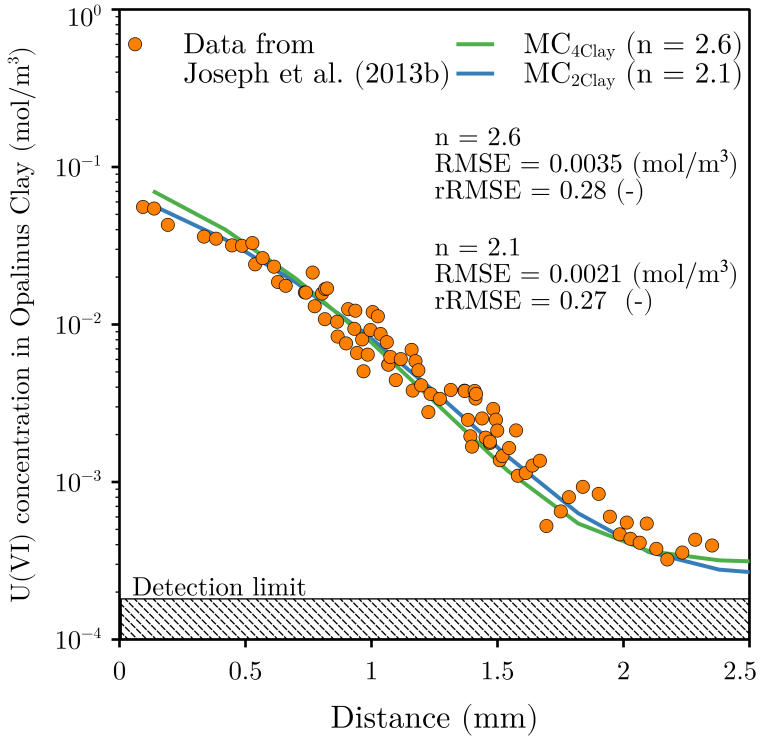

Figure 3.2: The multi-component (MC) diffusion approach can be applied to the Opalinus Clay system as the empirical parameter n that is used as a correction factor for the pore space geoemetry is calibrated. For the model concept considering all clay minerals (kaolinite, illite, montmorillonite and chlorite) for sorption (MC_{4Clay}, green line), the modelled results match with the experimental data (dots) of the diffusion experiment with U(VI) and Opalinus Clay of the sandy facies for an exponent n of 2.6. For the model taking into account only the two clay minerals illite and montmorillonite (MC_{2Clay}, blue line), n is 2.1.

3.4 Results

3.4.1 Multi- and single-component simulations on the metre-scale

The difference between MC and SC diffusion was determined depending on mineralogical and geochemical variations in the facies of the Opalinus Clay (Table 3.1) by quantifying and comparing the resulting migration lengths of uranium. MC diffusion simulations were performed for two model concepts (MC_{4Clay} and MC_{2Clay}), which differ in the clay minerals considered for sorption, to identify the effect of the clay mineral composition on the migration lengths. For all facies, the results of the MC simulations for the two model concepts as well as the SC simulations are shown in Figure 3.3.

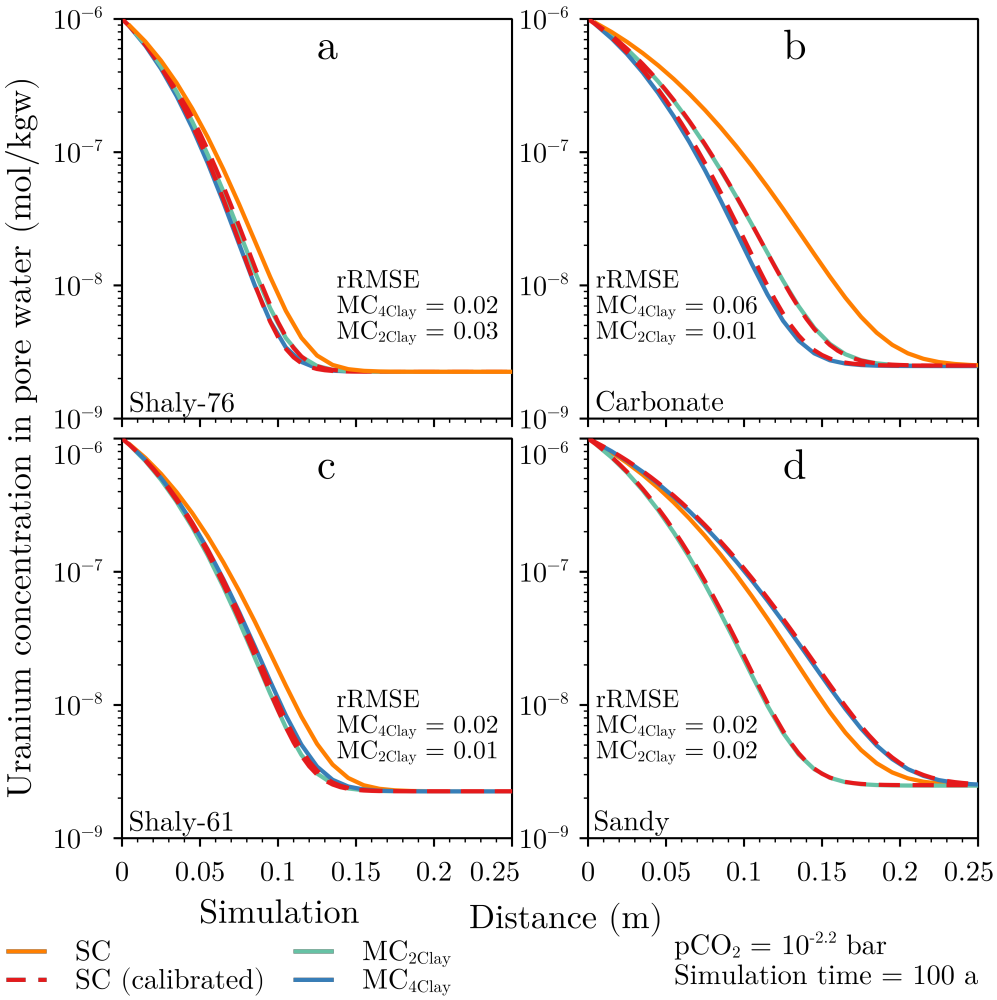

Figure 3.3: Differences in uranium migration lengths between SC and MC simulations are observed in all facies. Concentration of uranium in the pore water of the shaly (**a** and **c**), carbonate-rich (**b**) and sandy facies (**d**) for the MC diffusion (MC_{2Clay}, light blue line, and MC_{4Clay}, dark blue line) as well as the SC approach (SC, orange line). The red, dotted lines represent the results of the simulations based on the SC approach using the K_d and D_e calibrated from the MC simulations. The rRMSE indicates the deviation between the simulations with the calibrated parameters and the respective MC simulation. The number behind the shaly facies corresponds to the clay mineral content in wt.%.

Differences in the migration length between the MC and SC approach are obvious in all facies. After a simulation time of 100 years, the maximum migration lengths determined with the MC diffusion approach ranged from 0.12 m in the shaly (MC_{4Clay}, Figure 3.3a) up to 0.24 m in the sandy facies (MC_{4Clay}, Figure 3.3d). Using the SC diffusion approach, the migration lengths varied between 0.14 m in the shaly (Figure 3.3a) and 0.23 m in the carbonate-rich facies (Figure 3.3b). In the shaly and carbonate-rich facies, uranium migrated less far into the Opalinus Clay in the MC simulations compared to SC, whereas in the sandy facies it was opposite. The difference in migration lengths in a facies between the two approaches varied from around 0.07 m less (Figure 3.3b) up to 0.02 m farther (Figure 3.3d) into the formation using the MC approach with four clay minerals (MC_{4Clay}).

Consideration of only two (MC_{2Clay}) instead of four clay minerals (MC_{4Clay}) for sorption in the MC simulations led to a farther migration of uranium into the model, and thus reduced the difference between MC and SC in the shaly (Shaly-76) as well as carbonate-rich facies (Figure 3.3a and c). However, uranium still migrated less far into the Opalinus Clay compared to the SC approach. For the second mineral composition representing the shaly facies (Shaly-61), uranium migration was roughly 0.01 m less far into the formation, when using only two clay minerals (MC_{2Clay}, Figure 3.3c). In the sandy facies, the migration lengths changed from 0.02 m farther to 0.08 m less into the formation in the MC simulations compared to the SC (Figure 3.3d).

The results of the MC simulations could be reproduced with the SC approach using the calculated K_d and calibrated D_e given in Table 3.3 with a deviation between 1% and 6% (average 2%) between the calibrated SC and the MC simulations. In the experiment, a K_d of $0.025\,m^3/kg$ was identified (Joseph et al., 2013b). All of our calculated K_d values are an order of magnitude smaller and decrease with the clay mineral content, with only a minimal difference in sorption between the sandy and carbonate-rich facies despite the fact that 20 wt.% more clay minerals are in the sandy facies (Table 3.3). It is to be highlighted that the K_d values (Table 3.3) of the shaly facies are more than twice as large compared to the sandy and carbonate-rich facies. For all facies, the K_d values and hence sorption were slightly reduced using the MC_{2Clay} scenario. The calibrated D_e range from $1 \cdot 10^{-12}\,m^2/s$ to $2.25 \cdot 10^{-12}\,m^2/s$ (Table 3.3) for the MC_{4Clay} scenario, and thus the experimentally determined value of $1.9 \cdot 10^{-12}\,m^2/s$ from the diffusion experiment of Joseph et al. (2013b) is within our range. The MC_{2Clay} scenario only slightly increases the D_e for the carbonate-rich facies, whereas in the sandy and shaly facies (Shaly-61) it leads to a reduction. For the location with the highest clay mineral content (Shaly-76), the D_e is equal for both scenarios.

The composition of the DDL was calculated for each clay mineral dependent on the geochemical conditions in a facies using the Donnan approximation implemented in PHREEQC. The total amount of water in the DDL is distributed mainly via illite (72–79%) and montmorillonite (15–20%), followed by kaolinite (5–9%) and chlorite (0.3–0.5%) as a result of the geochemical conditions and mineral composition. The concentrations in the DDL of the clay minerals are shown in Figure 3.3 for calcium and magnesium (Figure 3.4a), sulphate and chloride (Figure 3.4b and c) and uranium (Figure 3.4d).

Table 3.3: Calibrated transport parameters, K_d (10^{-3} m^3/kg) and D_e (10^{-12} m^2/s), from the different scenarios of the MC diffusion simulations on the metre-scale and after a simulation time of 100 years for the facies of the Opalinus Clay.

Scenario	Parameter	Shaly-76	Shaly-61	Sandy	Carb-rich
MC_{4Clay}	K_d	4.04	3.09	1.55	1.43
	D_e	1.50	1.60	2.25	1.00
MC_{max}	K_d	4.04	3.09	1.55	1.43
	D_e	1.00	1.10	2.00	1.00
MC_{min}	K_d	4.04	3.09	1.55	1.43
	D_e	2.20	2.65	4.50	1.25
MC_{2Clay}	K_d	3.64	2.71	1.10	1.29
	D_e	1.50	1.40	0.80	1.15

As the distribution of the different species across the DDL differs only in absolute numbers, we decided to give the results exemplary only for the sandy facies. The highest uranium concentration across the DDL was observed in chlorite (Figure 3.4d). This also applied to sulphate (Figure 3.4b), except for the sample Shaly-76. For this mineral composition, the highest sulphate concentrations were found in the DDL of illite. The other ions, such as chloride, calcium or magnesium, were mainly located in the DDL of illite (Figure 3.4a and b). The concentrations of uranium, magnesium and calcium in the DDL of chlorite decreased along the x-axis, while the sulphate and chloride concentrations simultaneously increased (Figure 3.4).

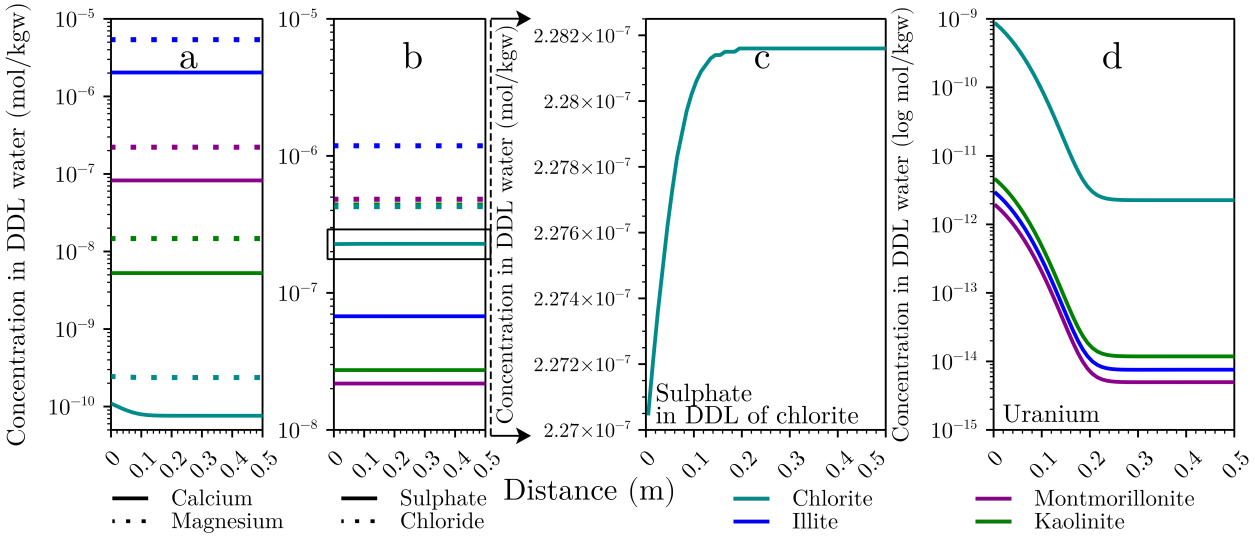

Figure 3.4: In the diffuse double layer of chlorite, concentrations of uranium, calcium and magnesium decrease along the x-axis, while concentrations of sulphate and chloride simultaneously increase. Concentrations of calcium and magnesium (**a**), sulphate and chloride (**b**, **c**) and uranium (**d**) in the DDL of the clay minerals for the sandy facies after a simulation time of 100 years and for a pCO_2 of $10^{-2.2}$ bar. For better clarity, the concentration of sulphate in the DDL of chlorite is given in **c** as close-up of **b**.

3.4.2 Multi-component diffusion for varying total amounts of minerals on the metre-scale

The migration of uranium as a function of the variability of hydro-physical parameters, e.g. porosity or dry bulk density, and the resulting amounts of minerals within a facies of the Opalinus Clay were simulated in minimum and maximum scenarios (MC_{max} and MC_{min}, Table 3.2) using MC diffusion simulations (MC_{4Clay}) on the metre-scale. The effect of the total mineral amount on the migration lengths was quantified by comparison with the MC simulations based on the averaged data given in Table 3.1. From the results of the MC simulations, K_d was calculated and D_e calibrated to reproduce the MC simulations with the SC approach. Figure 3.5 shows the results of the MC simulations for the minimum and maximum total amount of rock for all facies as well as the SC simulations using the calibrated transport parameters.

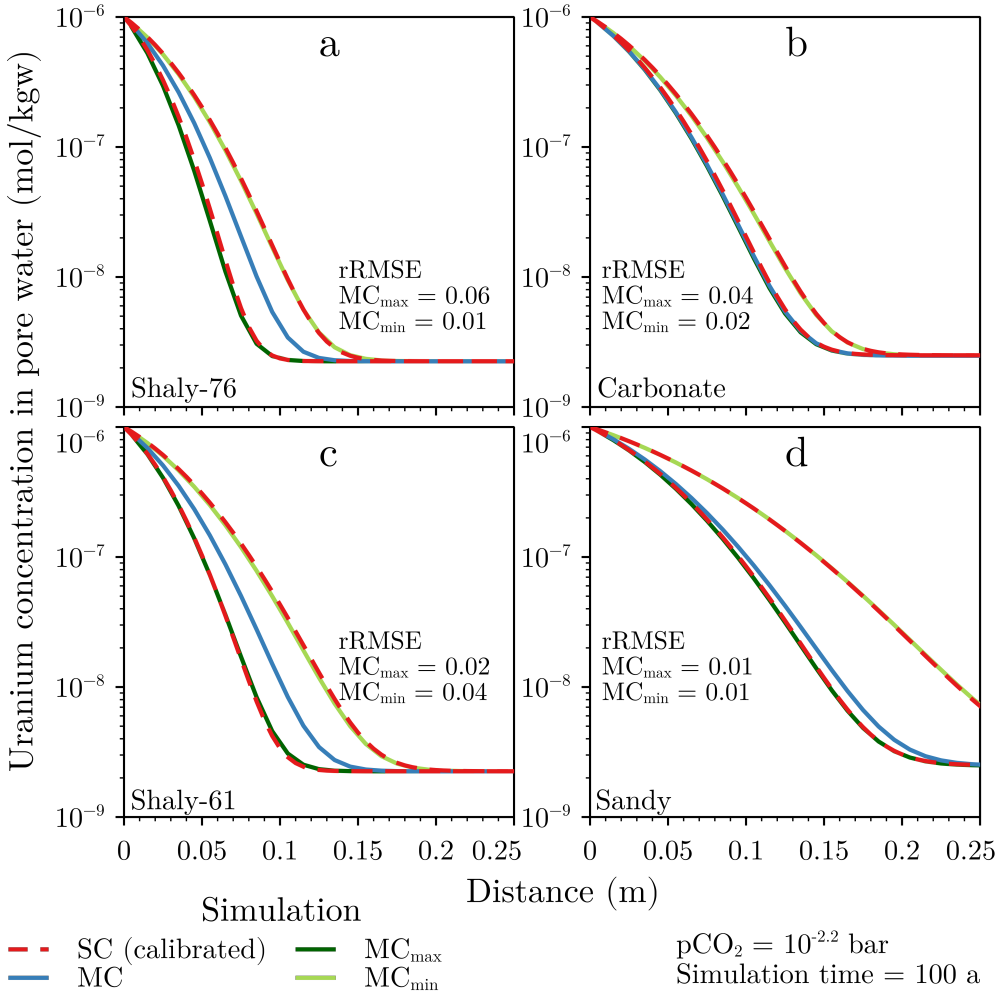

Figure 3.5: Uranium migrates farther through the formation in all facies with decreasing amount of minerals per kg pore water. Concentration of uranium in the pore water of the shaly (**a**,**c**), carbonate-rich (**b**) and sandy facies (**d**) for the scenarios with minimum (MC_{min}, 12–13 kg_{rock}/kg_{pw}, light green line), maximum (MC_{max}, 15–18 kg_{rock}/kg_{pw}, dark green line) and average total amount of rock per kg pore water (MC, 14–17 kg_{rock}/kg_{pw}, blue line). The red, dotted lines represent the results of the simulations based on the SC approach with the K_d and D_e calibrated from the MC simulations.

In all facies, uranium migrated farther into the formation for the MC_{min} scenario. After a simulation time of 100 years, the maximum migration length of 0.35 m was determined in the sandy facies (Figure 3.5d). The difference in migration distance between the two scenarios for the total amount of rock per kg pore water ranged from 0.02 m in the carbonate-rich facies (Figure 3.5b) to 0.13 m in the sandy facies (Figure 3.5d). In Figure 3.5b and d, the migration lengths of the maximum scenarios are similar to the simulations using the averaged values of the hydro-physical parameters. For all scenarios and facies, MC simulations could be reproduced with the calibrated transport parameters with a deviation between 1% and 6% (average 3%) between SC and MC simulation (Figure 3.5).

The K_d and D_e for the scenarios presented in Figure 3.5 are given in Table 3.3. The calculated K_d values are unaffected by the variation in total mineral amount, whereas especially the calibrated D_e of the MC_{min} more than doubles in some cases compared to the value of $1.9 \cdot 10^{-12}$ (m^2/s) determined in the diffusion experiment of Joseph et al. (2013b). The D_e of all scenarios showed the least variation from each other in the carbonate-rich and the highest in the sandy facies.

3.4.3 Transfer of multi-component diffusion simulations to the host rock scale

The applicability of K_d and D_e calibrated from the 1 m-model to the host rock scale (50 m) was evaluated by comparison with a MC simulation (MC_{4Clay}). The other scenarios (MC_{max}, MC_{min} and MC_{2Clay}) were calculated using the SC approach and the calibrated parameters given in Table 3.3 to quantify the influence of the mineral composition and total amount on the host rock scale. All results on the host rock scale are shown in Figure 3.6.

After a simulation time of one million years, migration lengths of uranium for the MC_{4Clay} scenario varied in the facies between 13 m (Figure 3.6a) and 24 m (Figure 3.6d). For all facies, the MC simulations could be reproduced on the host rock scale with the K_d and D_e calibrated on the small scale with an average deviation of 3% (rRMSE MC_{4Clay}, Figure 3.6). Considering two (MC_{2Clay}) or four (MC_{4Clay}) clay minerals for sorption did not significantly influence the migration of uranium in the shaly and carbonate-rich facies (Figure 3.6a and c), whereas in the sandy facies it reduced uranium migration by 8 m, from 24 m (MC_{4Clay}, Figure 3.6d) to 16 m (MC_{2Clay}, Figure 3.6d). The scenarios for the minimum and maximum total amount of minerals per kg pore water led to differences in the migration lengths between 2 m (Figure 3.6b) and 13 m (Figure 3.6d). Depending on the total amount of rock, maximum migration lengths of uranium ranged from 10 m in the shaly (MC_{max}, Figure 3.6a) to 35 m in the sandy facies (MC_{min}, Figure 3.6d).

The computing times for the individual scenarios in Table 3.3 varied on the metre-scale between 1 h and 2 h for the MC approach and a few seconds for the SC calculations. On the host rock scale, the MC simulations required a computing time between 5 h and 6 h (6 h = 21,600 s), whereas the SC simulations were done in a few seconds (<10 s). This provides a time saving of four orders of magnitude (factor of $2 \cdot 10^4$).

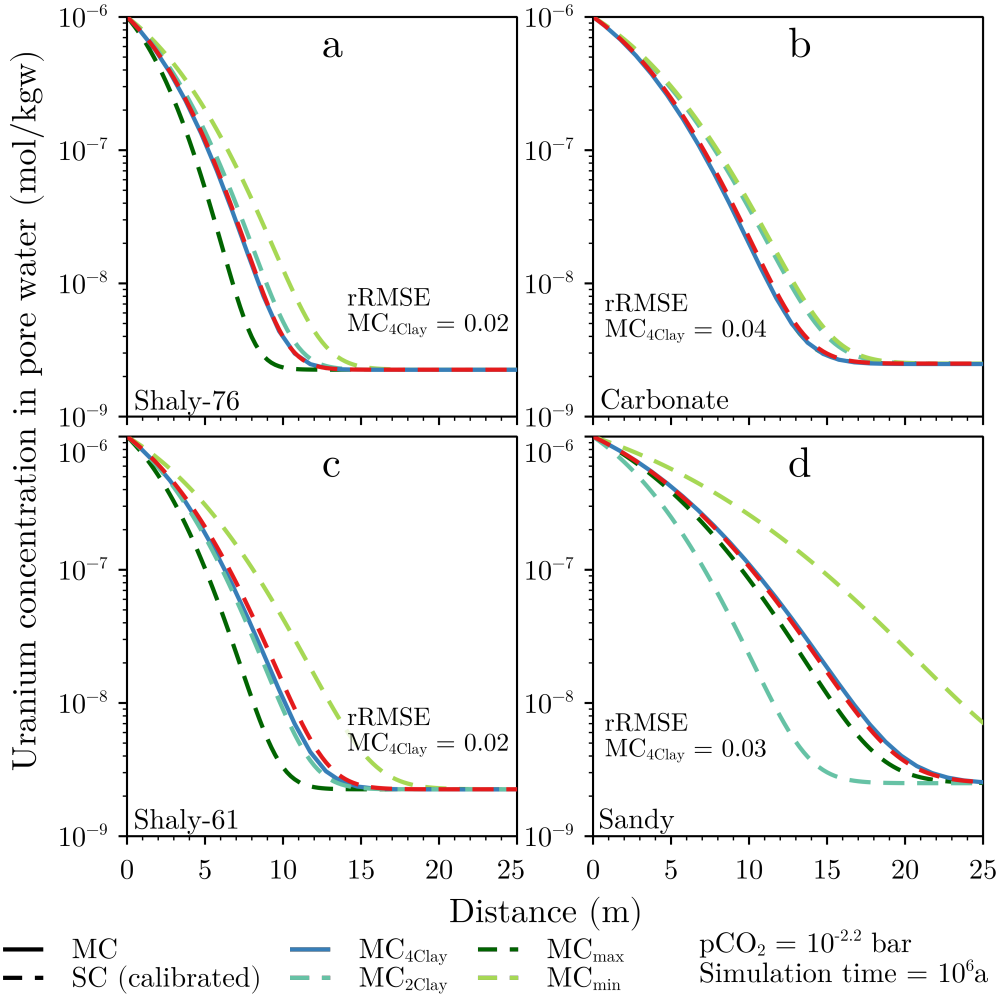

Figure 3.6: Transport parameters calibrated on the metre-scale can be applied to the host rock scale as surrogate for MC diffusion. Concentration of uranium in the pore water of the shaly (**a**,**c**), carbonate-rich (**b**) and sandy facies (**d**) for the scenarios with minimum (MC_{min}, light green line), maximum (MC_{max}, dark green line) and average total amount of rock per kg pore water (MC, blue line) as well as for the concepts considering four (MC_{4Clay}) and two clay minerals (MC_{2Clay}) for sorption. Dotted lines mean that the SC approach with the calibrated K_d and D_e was used, with red representing the results for the MC_{4Clay} scenario for better visibility. Only MC_{4Clay} (blue line) is based on the MC diffusion approach.

3.5 Discussion

From the study of Hennig et al. (2020) we know that sorption processes, and thus migration of uranium in the Opalinus Clay, are controlled by the calcite-carbonate-ion system. The authors identified the governing parameters in descending priority as follows: pCO_2, Ca^{2+} concentration, pH, pe and clay mineral quantity. Hence, geochemistry is more decisive for uranium sorption than the clay mineral content, whereby its influence increases with decreasing amount of clay minerals. This, in turn, results in a facies dependence of uranium sorption as the heterogeneous mineralogy in the facies leads to differences in the composition of the pore water as a result of water rock interactions. As our geochemical system is identical to the one of Hennig et al. (2020), these findings are also valid here. Furthermore, Hennig et al. (2020) estimated that anion exclusion reduces the migration lengths of uranium by 30%.

3.5.1 Differences between single- and multi-component diffusion approach

Based on the migration lengths of uranium, differences between the SC and MC diffusion approach were quantified on the metre-scale. For the MC_{4Clay} concept, uranium migrated less far into the model for all facies using the MC approach except for the sandy facies, where it migrated farther (MC_{4Clay}, Figure 3.3). We presume that not only sorption processes of uranium are facies dependent in the Opalinus Clay (Hennig et al., 2020), but also the diffusive transport. The difference is the DDL enveloping the clay mineral surfaces in the calculation with the MC approach.

The effect of anion exclusion reduces uranium migration in the MC diffusion approach. In our simulations, the anionic complex $CaUO_2(CO_3)_3^{2-}$ is the predominant species in the pore water of the Opalinus Clay because of the geochemical system (Hennig et al., 2020). Due to the negatively charged surfaces of the clay minerals mainly cations are enriched in the respective DDL decreasing the accessible pore space for anionic species, and thus reducing their diffusive transport (Appelo and Wersin, 2007; Van Loon et al., 2007, 2003a). For the MC_{4Clay} simulations, anion exclusion decreased uranium diffusion by about 0.02 m in the shaly and 0.07 m in the carbonate-rich facies corresponding to about 14% and 30% reduction compared to SC, respectively (Figure 3.3). Thus, for the shaly facies, our results contradict the estimate of Hennig et al. (2020) that migration lengths are reduced by 30% due to anion exclusion. However, the estimate applies for the carbonate-rich facies. The accessible pore space directly depends on the ionic strength of the pore water with a decreasing thickness of the DDL with increasing ionic strength (Van Loon et al., 2007; Wigger and Van Loon, 2018). Therefore, anion exclusion and with it the deviation in migration lengths between the SC and MC approach are different in the shaly and carbonate-rich facies (Figure 3.3a and c). Due to the lower ionic strength in the carbonate-rich compared to the shaly facies, the DDL is about 0.1 nm thicker (Shaly-76 and Carb-rich, Table 3.1), and thus anion exclusion is stronger. Accordingly, the deviation between both approaches should be the greatest in the sandy facies with the thickest DDL (Table 3.1). However, in the case of the sandy facies, uranium migrates farther instead of less into the model for the MC_{4Clay} simulation compared to the SC (Figure 3.3d). Only for the MC_{2Clay} scenario the sandy facies compares with the others as uranium migration is also reduced by 0.08 m, equivalent to about 30%. Therefore, anion exclusion is only one of the effects that explains the deviation in migration lengths between the two approaches. For the shaly as well as carbonate-rich facies, uranium migration is overestimated using the SC approach due to anion exclusion. A general estimate, how strong anion exclusion reduces the migration lengths cannot be made because of the dependence on the pore water chemistry. However, the reduced migration length due to anion exclusion determined here is an estimate for other clay formations with similar geochemistry and mineralogy.

Uranium mainly sorbs on illite and montmorillonite. The investigated model concepts, MC_{4Clay} and MC_{2Clay}, differ in their composition of clay minerals selected (Section 3.2.2). MC_{4Clay} is considered with the four clay minerals chlorite, kaolinite,

illite and montmorillonite, whereas in the MC_{2Clay} model only the minerals illite and montmorillonite are taken into account for sorption. The K_d values calculated in PHREEQC, and thus the sorption capacity of the individual facies (Table 3.3), decrease with the amount of illite and montmorillonite and hence the clay content in general (Table 3.1). Accordingly, the sample Shaly-76 has the highest sorption capacity followed by Shaly-61, sandy and carbonate-rich with the lowest (MC_{4Clay}, Table 3.3). Comparing the K_d values of both concepts (MC_{4Clay} and MC_{2Clay}, Table 3.3), it becomes clear that the contribution of chlorite and kaolinite to the uranium sorption is only about 10% in the carbonate-rich as well as in the shaly facies and about 30% in the sandy facies. Consequently, the majority of uranium is retained by illite and montmorillonite. From this point of view, one could say that illite and montmorillonite are sufficient to be considered to describe the sorption of uranium with a respective uncertainty for the shaly and carbonate-rich facies. However, this does not apply for the sandy facies as the contribution of chlorite and kaolinite to uranium sorption is in that case much larger with 30%. As already discussed by Hennig et al. (2020), sorption in the sandy facies is only slightly larger than in the carbonate-rich due to the geochemistry of the pore water (e.g. pH and Ca^{2+} concentration), although in the sandy facies are about 20 wt.% more clay minerals present. This also applies to our calculated K_d values of both facies (Table 3.3) and indicates that the contribution of kaolinite and chlorite to uranium sorption in the sandy facies is increased due to the pore water composition. Thus, we can confirm the findings of Hennig et al. (2020) on the facies dependence of uranium sorption in the Opalinus Clay and the governing role of the pore water geochemistry on sorption processes.

Chlorite plays a geochemical key role for the diffusive uranium transport using the MC diffusion approach. Due to the determined point of zero charge (pzc) of 9.5 for the chlorite used here (Zorn, 2000) and the corresponding SCM data for uranium (Arnold et al., 2001), the mineral surface is positively charged in the pH range present in the facies of the Opalinus Clay as a result of the interaction between pore water and prevailing minerals for the applied pCO_2 (Hennig et al., 2020). This leads to an enrichment of anionic species, such as the predominant anionic ternary uranyl complex, in the DDL to compensate the remaining net surface charge, and thus the highest uranium concentrations could be observed in the DDL of chlorite (Figure 3.4d). This, in turn, affects the migration behaviour of uranium as the accessible pore space is increased instead of decreased compared to the clay minerals with a negative surface charge. The contribution of chlorite to the total transport of uranium depends on the thickness of the DDL, and thus on the ionic strength of the pore water. A lower ionic strength means a thicker DDL and in the case of the chlorite used here an enhanced diffusion of uranium instead of an intensified effect of anion exclusion as it would be the case for the clay minerals with negatively charged surfaces. Therefore, a farther uranium migration into the formation was observed in the sandy facies for the MC_{4Clay} simulation compared to SC and hence counteracts anion exclusion (Figure 3.3d). Without chlorite (MC_{2Clay}, Figure 3.3d), the anion exclusion effect is fully effective. This emphasizes the important role of chlorite within the system, especially for the migration of

uranium or other anionic radionuclides, such as selenite, in the sandy facies. However, the thermodynamic data used here are based on investigations of an almost pure chlorite sample taken from a granite fracture in the Swiss rock laboratory Grimsel (Arnold et al., 2001; Zorn, 2000). It serves for us as an analogue because chlorite from the Opalinus Clay has not yet been studied in detail. It therefore remains unclear, whether chlorite from Grimsel and Mont Terri actually correspond in their chemical properties. For instance, a pzc<7 would result in a negatively charged surface for the geochemical conditions and turn around the behaviour of the system. In this case, the determined migration lengths would correspond to the MC_{2Clay} scenarios. Accordingly, a detailed characterization of the clay minerals in the Opalinus Clay and of their individual properties is essential and indicates the need for further research.

The sulphate concentration in the pore water limits the contribution of chlorite to uranium migration. In addition to uranium, other anions from the pore water, such as chloride or sulphate, are also enriched in the DDL of chlorite to compensate the positively charged surface of the mineral. Chloride ions are mainly present in the DDL of illite, whereas for sulphate, similar to for uranium, the highest concentrations have been observed in the DDL of chlorite (Figure 3.4b and d). Due to the same negative charge of two, both anions compete with each other in the DDL. This was also determined by the concentrations along the x-axis. With decreasing uranium concentration in the DDL of chlorite, the sulphate concentration simultaneously increases (Figure 3.4c and d). Accordingly, a higher initial sulphate concentration in the pore water (Table 3.1) is associated with a potentially lower uranium concentration in the DDL of chlorite, and thus less impact of chlorite on the diffusive uranium transport (Figure 3.3). This also explains the difference between the simulations MC_{4Clay} and MC_{2Clay} between the individual facies. Due to the higher initial concentrations of sulphate in the Shaly-76 and carbonate-rich facies (Table 3.1), chlorite does not contribute significantly to the uranium transport and so mineral selection only affects sorption (Figure 3.3a and b). On the contrary, the lower sulphate concentration in the pore waters for the sample Shaly-61 and of the sandy facies (Table 3.1) enable an enhanced uranium transport via the chlorite DDL (Figure 3.3c and d). Consequently, the chlorite DDL accelerates uranium migration only for low sulphate concentrations.

Besides sulphate, the concentrations of calcium and magnesium in the pore water are also decisive for the influence of the DDL on uranium migration. For instance, Wigger and Van Loon (2018) observed in anion diffusion experiments that the negative surface charge was more strongly shielded at the same ionic strength by bivalent cations, such as calcium, compared to monovalent ones, such as sodium. Consequently, the anion exclusion effect is reduced by a higher concentration of bivalent cations (Wigger and Van Loon, 2018). In relation to our results, this means that the anion exclusion effect in the sandy facies is intensified by the lower concentrations of bivalent cations in the pore water compared to the other facies (Table 3.1) in addition to the thicker DDL. In that way, the geochemistry in the pore waters governs how strong the different DDL affect uranium migration. Thus, we confirm the findings of Hennig et al. (2020) that the geochemistry is more decisive than the clay minerals.

Furthermore, we can supplement that the geochemistry of the pore water not only controls sorption processes, but also the diffusive transport of uranium in the Opalinus Clay. Our results also provide indications for the migration of uranium or other anionic radionuclides in clay formations with similar mineralogy and underline the importance of a detailed determination of the pore water and the geochemical system for each potential site.

3.5.2 Effect of varying mineralogy on multi-component diffusion

The variation of the total mineral amount led to significant differences in the migration lengths. The assumptions inherent in the models regarding the hydro-physical parameters cause uncertainties in the results since they determine the amount of rock per kg pore water, and thus sorption as well as the accessible pore space. Therefore, we studied in minimum and maximum scenarios for the total amount of rock per kg pore water (Section 3.2.2) on the metre-scale the migration lengths.

The distribution coefficient K_d is unaffected by the variation in the total amount of minerals. In all facies, the K_d was the same for the minimum and maximum scenarios (MC_{max} and MC_{min}, Table 3.3), although the total amount of minerals differed by up to 6 kg per kg pore water within a facies (Table 3.2). The K_d indicates the ratio between sorbed and dissolved species for a defined mineral composition and pore water chemistry. As long as identical proportions of the individual clay minerals are used in the simulations, the total amount of minerals has no influence on the K_d. However, the total amount of sorbed uranium is affected by this and so is the migration length. In many sorption experiments, it has been observed how strongly uranium sorption depends on the chemical properties of the pore water, such as pH or carbonate concentration (Joseph et al., 2013a; Philipp et al., 2019; Tournassat et al., 2018). Furthermore, for the Opalinus Clay, we showed that the pore water chemistry is more decisive for the sorption of uranium than the quantity of clay minerals.

Changing amounts of minerals directly lead to changes in the amount of water in the DDL and in the pore space. For all facies, a farther uranium migration into the formation was observed for the minimum scenario (Figure 3.5). On the one hand, this is related to the reduced quantity of minerals available for sorption. However, as long as the pore water chemistry does not change, the sorption capacity is only slightly affected. On the other hand, the variation in migration for the investigated scenarios is much more affected due to changes of the total amount of water in the DDL with the mineral quantity. A smaller amount of minerals means, for instance, less water in the DDL of the negatively charged surfaces. Consequently, anion exclusion is attenuated and uranium migrates farther into the formation. This also applies for other clay formations. Furthermore, more pore space for diffusive transport is available in the minimal scenarios compared to the maximum scenario. Concerning the calibrated transport parameters K_d and D_e for the different scenarios (Table 3.3), it becomes clear that the total amount of minerals constrains transport within the facies. It is important to note that the averaged values of the hydro-physical parameters for the locations representing the sandy as well as carbonate-rich facies (Table 3.1) are very similar to the maximum

values for the respective facies (Table 3.2). Therefore, the calculated migration lengths are also almost identical for the reference (MC_{4Clay}) and the maximum scenario (MC_{max}). Thus, the priority list for uranium sorption in the Opalinus Clay described by Hennig et al. (2020) can also be confirmed for the diffusion and supplemented with the hydro-physical parameters as follows: pCO_2, Ca^{2+} concentration, pH, pe, hydro-physical parameters and the amount of clay minerals.

3.5.3 Implications for the host rock scale

We developed a workflow to set-up surrogate models on the metre-scale for efficient application on the host rock scale. As the previously investigated MC scenarios could be reproduced on the metre-scale with the SC approach using the calibrated K_d and D_e (Figures 3.3 and 3.5), the application to the host rock scale was evaluated by comparison with a representative MC simulation for each facies and for a simulation time of one million years (Figure 3.6). The MC_{4Clay} simulations could be reproduced on the host rock scale with the transport parameters calibrated on the small scale with a deviation between 2% and 4% (Figure 3.6).

Scale invariance enables the application of the calibrated K_d and D_e from the metre-scale to the host rock scale. The properties of a state and chemical processes remain largely or exactly the same and universality is given. Based on our presented modelling workflow, transport parameters for varying mineralogy and chemistry can therefore be determined. Since SC simulations using the calibrated transport parameters only required a few seconds (<10 s) of computing time, this represents time saving on the order of 10^4 for the host rock scale compared to full complexity MC simulations, which require up to 6 h (= 21,600 s). This improvement enables performing 'MC' diffusion simulations on the host rock scale, for instance, for a sequence of facies or in 2D models with acceptable computing times and without numerous previous experiments otherwise required.

Uranium migration in Opalinus Clay is facies dependent and its migration length is constrained by the rock type itself (shaly, sandy and carbonate-rich), as well as by the respective internal heterogeneity of varying mineral amounts and compositions. On the host rock scale, this results in an offset of up to 25 m between the shaly facies with a maximum amount of clays and the sandy facies with a minimum amount of clays (Figure 3.6a and d). Within the sandy facies, for instance, variations in porosity and bulk densities led to a deviation between the migration lengths of up to 13 m (Figure 3.6d). In contrast, the migration lengths in the shaly facies varied by 5 m (Figure 3.6a) and in the carbonate-rich one even only by 2 m (Figure 3.6b). Due to the high amount of clay minerals in the shaly facies, heterogeneities are compensated, whereas in the carbonate-rich variations in the hydro-physical parameters are less effective because of the low clay content in combination with the pore water composition. In the case of the sandy facies, the heterogeneity within the individual facies causes a higher uncertainty regarding the migration lengths compared to the shaly and carbonate-rich. Our simulation results demonstrate the effect of hydro-physical parameters and the amount of clay minerals on migration, especially on the transport

properties. This influence of heterogeneity on transport properties does not only apply to the Opalinus Clay, but it is likely that this is also the case for any other clay formation. In any case, detailed measurements are required because facies or clay formations in general can vary immensely in their properties on the dm-scale, e.g. for the Opalinus Clay through clay layers within the sandy facies and vice versa (Lauper et al., 2018). It is shown for the sandy facies, compared the shaly and carbonate-rich ones, that with decreasing clay content within the rock, the variation in mineral composition and its effect on the pore water chemistry and with that on the transport behaviour of uranium increases.

On the host rock scale, it becomes obvious that the shaly facies is best suited for the disposal of nuclear waste followed by the carbonate-rich and sandy ones due to the shorter migration lengths. The high amount of clay minerals in the shaly facies (>50 wt.%) dominates diffusion and sorption processes, and hence better compensates chemical and mineralogical heterogeneities compared to the other facies, which is apparent from the shorter migration lengths and their smaller span. This also means that the SC approach is sufficient for the shaly as well as carbonate-rich facies since the deviation in the migration lengths for the two approaches, but also by the mineralogical heterogeneity itself, is negligible. However, the use of the SC approach for the sandy facies results in an over- or underestimation of maximum migration length, and hence implies a high degree of uncertainty, especially due to the mineralogical heterogeneity. Nevertheless, uranium is still retained in any case within the effective containment zone of a potential host rock with a thickness of 100 m, and hence the Opalinus Clay fulfills the minimum requirements for a potential disposal site (§ 23 Article 5 StandAG[2]).

Due to the decisive role of the pore water geochemistry in the system, the migration lengths determined here cannot be directly transferred to other sites. However, the insights on the MC diffusion of uranium in clay formations gained here, e.g. the role of the chlorite DDL and the sulphate concentration, can be taken as directions for future works and other sites since uranium is one of the most important radionuclides for the long-term safety of a potential repository. The modular structure of our concept (pore water composition and mineralogy) offers the opportunity to use this workflow for other potential sites or radionuclides, if all data are available.

3.6 Conclusions and outlook

The significance of multi-component (MC) compared to single-component (SC) diffusion approaches was shown within one-dimensional simulations on the metre as well as on the host rock scale for uranium diffusive transport and sorption in Opalinus Clay depending on varying mineralogy and pore water geochemistry. The MC approach enables a process-based description of diffusive transport as it takes into account the interaction of the involved chemical aqueous species with the diffuse double layers (DDL) adhering the clay mineral surfaces. Due to the huge computational effort of MC diffusion simulations on the host rock scale, a surrogate model based

[2]Standortauswahlgesetz (StandAG) of 5 May 2017 (Federal Law Gazette p. 1074) as last amended by Article 1 of the Act of 7 December 2020 (Federal Law Gazette p. 2760). URL: https://www.gesetze-im-internet.de/standag_2017/BJNR107410017.html (accessed on 13 June 2022).

on a distribution coefficient K_d (m^3/kg) and an effective diffusion coefficient D_e (m^2/s) was developed with a workflow to calibrate the parameters on the metre-scale and transfer them as pseudo-MC diffusion to larger scales.

The three facies (shaly, sandy and carbonate-rich) were represented by analyses from boreholes at the underground research laboratory Mont Terri in Switzerland. Pore water geochemistry was controlled by a constant partial pressure of carbon dioxide (pCO_2) and mineral equilibria with dolomite, calcite as well as siderite and pyrite. The resulting pore water chemistry is facies dependent and varies with the individual mineral assemblage significantly affecting sorption as well as the diffusive transport.

In the MC diffusion approach implemented in PHREEQC, diffusion coefficients are determined analogous to Archie's law, and hence the medium specific parameter n had to be calibrated for our model. We did this successfully by means of a diffusion experiment with Opalinus Clay and uranium (Joseph et al., 2013b). Based on a bottom-up approach, surface complexation and cation exchange are used to implement sorption processes.

A high clay content (>50 wt.%), such as in the shaly facies of the Opalinus Clay, dominates diffusion and sorption processes of uranium with short migration lengths of 10 m to 19 m within one million years depending on their heterogeneity. The MC simulations show shorter migration lengths than the SC models but the differences with less than one metre are almost neglectable. For the carbonate-rich facies, migration lengths are 16 m to 18 m using the MC approach with 7 m difference between MC and SC. The simplified SC model overestimates the migration length of uranium. For the sandy facies, it depends on the selected mineral composition, if the MC under- or overestimates the SC simulations by 8 m or 2 m, respectively. The migration length ranges between 16 m and 35 m. Considering the clay minerals illite, montmorillonite, chlorite and kaolinite for sorption, the calculated K_d values ranged between 0.004 m^3/kg for Shaly-76 with the highest clay mineral content and 0.0014 m^3/kg for the carbonate-rich with the lowest. The K_d of the sandy facies with a value of 0.0016 m^3/kg is only slightly higher despite the 20 wt.% more clay minerals compared to the carbonate-rich highlighting the increasing influence of geochemistry on sorption with decreasing amount of clay minerals.

Variations in migration of uranium in the MC approach can be attributed to the different pore water compositions in the facies in combination with the DDL on the clay mineral surfaces. A high ionic strength reduces the thickness of the DDL, and thus the accessible pore space for diffusion is increased. Further, the pore water geochemistry interacts with the charged mineral surfaces. Negatively charged surfaces attract cations and exclude anions to or from the DDL. This is known as anion exclusion effect. The accessible pore space is reduced and the migration of the anions is hampered. This is the reason the MC simulations show shorter diffusions lengths of up to 30% compared to the SC models. A higher concentration of bivalent cations in the pore water shields the negative surface charge of the clay minerals better, and hence decreases anion exclusion. The latter is the case within the shaly facies of the Opalinus Clay and reduces the effect of anion exclusion. This, in combination with a higher ionic strength, reduces the migration length in the

shaly facies by 14% compared to SC. Conversely, positively charged mineral surfaces attract anions. This is the case for chlorite for the studied geochemical system of the Opalinus Clay as it attracts, e.g. the predominant uranium species $CaUO_2(CO_3)_3^{2-}$. This means an increased accessible pore space for uranium enhancing the diffusive transport compared to the other clay minerals illite, montmorillonite and kaolinite with negatively charged surfaces. This is the reason, why simulations for the sandy facies show increased migration lengths for MC compared to SC models. As anion with the same negative charge, sulphate competes with the anionic ternary uranyl complex in the DDL of chlorite. Therefore, a higher sulphate concentration in the pore water reduces the enhancing influence of chlorite on the uranium transport as can be seen for the shaly and carbonate-rich facies.

Hydro-physical parameters, such as porosity or bulk densities, have an impact on the migration lengths as assessed in scenarios with varying total amounts of rock per kg pore water. These parameters determine the ratio between rock and pore water within the pore space, and thus control the amount of water in the DDL. Uranium migration can be significantly enhanced by the variation in hydro-physical rock properties in combination with an appropriate composition of the pore water, i.e. a low concentration of sulphate and bivalent cations. Calibrated D_e for uranium varied for the facies between $8 \cdot 10^{-13}\,m^2/s$ and $4.5 \cdot 10^{-12}\,m^2/s$. Therefore, uranium diffusion and sorption in the Opalinus Clay is governed in descending priority by pCO_2, Ca^{2+} concentration, pH, pe, the hydro-physical parameters and the amount of clay minerals.

Due to the high computational costs of MC diffusion simulations, they are inefficient for larger and more complex models such as on the host rock scale. Therefore, we developed a surrogate. Based on the results of the MC simulations on the metre-scale, we determined K_d and D_e and showed that they can successfully be applied to the host rock scale and required simulation times up to one million years. In that way, we achieved a time saving on the order of 10^4. Consequently, a detailed description of pore water chemistry and hydro-physical properties from field or laboratory studies in combination with our workflow using MC diffusion simulations is a powerful tool to quantify uranium migration on the host rock scale for varying mineralogy and geochemistry of potential repository sites in other clay formations. Our workflow offers the possibility for pseudo-MC diffusion simulations applied for complex 2D as well as 3D models accounting for anisotropy and heterogeneity of facies, which will be required in performance assessments of a repository. Further, with the help of our approach, the design of diffusion experiments can be assisted. After a simulation time of one million years, the maximum determined migration length of uranium was 35 m in the sandy facies. With respect to the minimum requirement of a thickness of 100 m, the Opalinus Clay seems to be a suitable host rock as it effectively retains the radionuclide uranium and no adjacent aquifer is reached.

Chapter 4

Uranium migration varies on the metre-scale in response to differences of a stability constant

Abstract

The simulation of uranium migration through the Swiss Opalinus Clay is used as an example to quantify the influence of varying values of a stability constant in the underlying thermodynamic database on the migration lengths for the repository scale. Values for the stability constant of the neutral ternary uranyl complex $Ca_2UO_2(CO_3)_3$ differ in literature by up to one order of magnitude. Within the studied geochemical system, either the neutral or the anionic complex $CaUO_2(CO_3)_3^{2-}$ is the predominant one depending on the chosen value for the neutral complex. This leads to a changed interaction with the diffuse double layers (DDL) enveloping the clay minerals, and thus can potentially influence the diffusive transport of uranium. Hence, two identical scenarios only differing in the value for the stability constant of the $Ca_2UO_2(CO_3)_3$ complex were applied in order to quantify and compare the migration lengths of uranium on the host rock scale (50 m) after a simulation time of one million years. We ran multi-component diffusion simulations for the shaly and sandy facies in the Opalinus Clay. A difference in the stability constant of 1.33 log units changes the migration lengths by 5 m to 7 m for the sandy and shaly facies, respectively. The deviation is caused by the anion exclusion effect. However, with a maximum diffusion distance of 22 m, the influence of the stability constant of the $Ca_2UO_2(CO_3)_3$ complex on uranium migration in the Opalinus Clay is negligible on the host rock scale.

4.1 Introduction

Safety of a repository is based to a large extent on the isolation of the radioactive waste within a suitable host rock (IAEA, 2003). Clay rocks provide an option due to their high retention capacity against radionuclides and very low hydraulic conductivity only allowing diffusive transport. However, diffusion processes in clay formations are complex due to the diffuse double layers (DDL) enveloping the clay minerals and the associated different migration behaviour for cationic, anionic and neutral species (Appelo et al., 2010; Appelo and Wersin, 2007; Van Loon and Soler, 2003). The DDL compensates the net surface charge resulting from the contact between pore water and external surfaces of the clay minerals by attraction of counter-ions and repulsion of co-ions and affects thereby their diffusive transport (Wersin et al., 2008). Therefore, determination of the speciation of an element in the pore water is crucial to quantify migration distances precisely.

To cover the spatial and temporal scales required for safety assessments, reactive transport simulations are a powerful tool to quantify transport of sorbing radionuclides considering the geochemical conditions within the system. They are based to a large extent on the use of chemical thermodynamic databases. Consequently, in addition to completeness, the selection of the data itself is also important as often various values dependend on the applied experimental conditions are given in literature (Mühr-Ebert et al., 2019; Thoenen et al., 2014). Because varying stability constants within the law of mass action change the overall aqueous species distribution and predominant species, the maximum migration distance of a radionuclide through a clay formation might be affected.

In the present study, we assess this influence for the example of uranium, one of the main components in spent fuel, in the Swiss Opalinus Clay, a potential host rock for the disposal of nuclear waste. For this, we perform multi-component (MC) diffusion simulations on the host rock scale (50 m) accounting for the interaction with the DDL as well as for the mineralogical heterogeneity between the shaly and sandy facies. In this geochemical system, uranium is mainly present as U(VI) in ternary uranyl complexes with calcium and carbonate (Hennig et al., 2020).

In previous numerical studies (Hennig and Kühn, 2021a; Hennig et al., 2020) that used the PSI/Nagra thermodynamic database (Thoenen et al., 2014) with a $\log K$ of 29.22 for the neutral complex (Equation 4.1), the anionic complex (Equation 4.2) was the predominant species in the geochemical system of the Opalinus Clay.

$$2\,Ca^{2+} + UO_2^{2+} + 3\,CO_3^{2-} \rightleftharpoons Ca_2UO_2(CO_3)_3\,(aq)\;log\,K\;=\;29.22 \tag{4.1}$$

$$Ca^{2+} + UO_2^{2+} + 3\,CO_3^{2-} \rightleftharpoons CaUO_2(CO_3)_3^{2-}\,(aq)\;log\,K\;=\;27.18 \tag{4.2}$$

In contrast, in a sorption experiment done for the same system (Joseph et al., 2011), a value of 30.55 for the $\log K$ of the neutral complex (Bernhard et al., 2001) was used in the speciation calculations leading to the neutral complex as predominant one. Both complexes, anionic and neutral, cannot be clearly distinguished by the methods usually applied in experiments (Mühr-Ebert et al., 2019). Moreover, Guillaumont et al. (2003) remarked that the constant of Bernhard et al. (2001) is not precise since the analysis indicates large experimental errors. Therefore, it was not used for the PSI/Nagra database (Thoenen et al., 2014). Thus, the uncertainty regarding the predominant uranium species in the geochemical system of the Opalinus Clay remains.[1]

With our one-dimensional, MC diffusion models we quantify the influence of the thermodynamic constant of one of the main aqueous uranium species in the studied system, the neutral ternary uranyl complex $Ca_2UO_2(CO_3)_3$, on the maximum migration

[1] With the second update of the NEA on the chemical thermodynamics of uranium (Grenthe et al., 2020), the stability constants for the neutral as well as anionic ternary uranyl complex were set based on the evaluation of recent data. To the best of our knowledge, this update has not yet been included in the PSI/Nagra thermodynamic database (Thoenen et al., 2014) but is considered in the discussion part of this chapter (Section 4.4) as well as in Chpater 6.

length by using two different values for the log K in the underlying thermodynamic database. With this, we demonstrate, what the difference regarding the selected value for the stability constant means in metre on the host rock scale after one million years.

4.2 Methods

Simulations were performed with the MC option in PHREEQC Version 3.5.0 (Parkhurst and Appelo, 2013). The thermodynamic data is based on the PSI/Nagra database version 12/07 (Thoenen et al., 2014). The Davies approach (Davies, 1962) is used for the database to represent ion-ion interactions (Noseck et al., 2018; Stockmann et al., 2017) as ionic strength of the pore waters in the facies does not exceed 0.5 mol/L (Table 4.1). As already described in Hennig et al. (2020) and Hennig and Kühn (2021a), it was updated and supplemented with the sorption data for the hydroxo-complexes of uranium on the inherent clay minerals (Table 4.1) as well as the self-diffusion coefficients in water D_w (m^2/s) required to apply the MC option (Supplementary S-1 and S-2). This means, the uranium carbonate complexes dominating the speciation in the studied system (Hennig et al., 2020; Joseph et al., 2013b) were not taken into account for sorption (Supplementary S-1). Consequently, the diffusive transport of uranium complexes and their interaction with the DDL governed by the ionic strength becomes more important, what is accounted for by the MC option in PHREEQC. In line with the database, all simulations were conducted for a temperature of 25 °C as it has been shown that elevated temperatures, for instance, relevant for greater depths (Nagra, 2002a), can be neglected (Hennig and Kühn, 2021a; Hennig et al., 2020). Neither it significantly changes the pore water composition (<5% for a temperature of 45 °C, Wersin et al., 2016), nor it affects uranium migration up to temperatures of 60 °C (Joseph et al., 2013b). The Pourbaix diagrams (Section 4.3.1) were created with a coupling between PHREEQC and the open source programming language R (De Lucia and Kühn, 2013, 2021).

The model applied here is based on the concepts presented in Hennig et al. (2020) and Hennig and Kühn (2021a). Simulations were performed for the shaly and sandy facies of the Opalinus Clay representing higher and lower clay mineral quantities (76 wt.% and 45 wt.%) as well as major differences in the pore water composition as this primarily governs uranium sorption and migration. The initial input parameters are based on analyses from boreholes at the underground research laboratory Mont Terri (Switzerland) and are given in Table 4.1.

The geochemical behaviour of the Opalinus Clay system, and thus speciation as well as sorption of uranium highly depend on the calcite-carbonate-ion system (Hennig et al., 2020; Pearson et al., 2003; Wersin et al., 2009). Therefore, we decided to fix the partial pressure of carbon dioxide (pCO_2) to $10^{-2.2}$ bar, what corresponds to measured values and is recommended for clay formations with similar mineralogy as the Opalinus Clay (Gaucher et al., 2010; Lerouge et al., 2015; Pearson et al., 2003, 2011; Vinsot et al., 2008). An initial E_H of −227 mV published by Bossart and Thury (2008) was chosen to represent the moderately reducing in-situ conditions (Pearson et al., 2011; Wersin et al., 2011). The pH, pe and the concentrations of the

main ions are controlled by means of the fixed pCO_2 via an equilibrium with the present carbonates (calcite, dolomite and siderite) as well as pyrite. The redox couple SO_4^{2-}/HS^- provides the most consistent results with measured values (Pearson et al., 2003, 2011; Wersin et al., 2009, 2011).

Table 4.1: Input parameters representing the shaly and sandy facies. Concentrations are given as average values from borehole analyses.

Parameter	unit	Shaly[a,b]	Sandy[c,d]
pH	-	7.13	7.40
Na^+	mmol/L	280.7	120.8
K^+	mmol/L	1.93	0.87
Mg^{2+}	mmol/L	21.97	5.91
Ca^{2+}	mmol/L	18.90	6.73
Sr^{2+}	mmol/L	0.46	0.35
Fe_{total}	μmol/L	29.62	9.81[d]
U_{total}	nmol/L	2.52[d]	2.52[d]
Cl^-	mmol/L	326.7	120.6
SO_4^{2-}	mmol/L	16.79	6.94
Alkalinity	mmol/L	3.85	2.61
I[e]	mol/L	0.39	0.16
DDL[f]	nm	0.49	0.76
Illite	wt.%	20	17
Illite/smectite mixed layers	wt.%	16	8
Kaolinite	wt.%	30	13
Chlorite	wt.%	10	7
∑Clay total	wt.%	76	45
Calcite	wt.%	14	17
Dolomite	wt.%	n.a.	2
Siderite	wt.%	1	2
Porosity ϵ_{wc}	-	0.166[g]	0.137[h]
wet water content wc_{wet}	-	0.068[g]	0.055[h]
dry bulk density ρ_{db}	kg/m^3	2290[g]	2365[h]
wet bulk density ρ_{wb}	kg/m^3	2458[g]	2498[h]

n.a. = no data available; [a] Vinsot et al. (2008), borehole BPC-C1; [b] Pearson et al. (2003), borehole BPP-1; [c] Wersin et al. (2009), borehole BWS-A3; [d] Pearson et al. (2003), borehole BWS-A3; [e] calculated in PHREEQC; [f] thickness Donnan layer, calculated via ionic strength (Wigger and Van Loon, 2018); [g] Pearson et al. (2003), borehole BWS-A6; [h] Pearson et al. (2003), borehole BWS-E3

Each facies is represented by an one-dimensional diffusion model consisting of 100 cells a 0.5 m (= 50 m) and corresponds to the transport direction perpendicular to the bedding. Grid independence was confirmed by simulations with finer resolution (0.25 m). Numerical stability is ensured by the Neumann criteria. The source term, e.g. from the high-level waste canisters, is represented by a Dirichlet boundary condition with a constant uranium concentration of 1 μmol/L (Joseph et al., 2013b;

Keesmann et al., 2005), whereas a Neumann boundary is applied to the model outlet. Since our focus lies on the influence of a stability constant on the migration length in the host rock, we do not consider the interaction with the engineered barriers. Hence, our results have to be considered as maximum diffusion lengths.

Sorption is quantified with mechanistic surface complexation models (SCM) using the two-layer model of Dzombak and Morel (1990) as well as cation exchange (Kim, 2001) following the bottom-up approach as described in Marques Fernandes et al. (2015) and Stockmann et al. (2017). The respective and proven dataset (Joseph et al., 2013a) with all surface parameters and reactions can be found in the Supplementary of Chapter 2 (Supplementary S-1). In line with previous work (Bradbury and Baeyens, 2005a,b; Bradbury et al., 2005, 2010; Hartmann et al., 2008), sorption of uranium in the Opalinus Clay is modelled using only the clay minerals illite (Na-illite, Bradbury and Baeyens, 2005a) and montmorillonite (Na-montmorillonite, Bradbury and Baeyens, 2005b) as representative for the smectite group.

With the MC option in PHREEQC, diffusion is calculated individually for each aqueous species present in the system as sum of transport in the pore water as well as in the DDL via the electrochemical potential (Appelo et al., 2010; Appelo and Wersin, 2007; Parkhurst and Appelo, 2013). For this, PHREEQC uses the pore water diffusion coefficient D_p (m^2/s) that is derived for each species analogous to Archie's law via the self-diffusion coefficient in water D_w (m^2/s), the accessible porosity ϵ (-) and an empirical exponent n (-):

$$D_p = D_w \cdot \epsilon^n \tag{4.3}$$

The exponent n is a constant, medium-specific parameter (Van Loon et al., 2007) that needs to be determined for the specific host rock to account for the pore space geometry. Hennig and Kühn (2021a) calibrated their model by means of a diffusion experiment with uranium and Opalinus Clay (Joseph et al., 2013b). The best result was obtained for a value of $n = 2.1$, which we also used here. Anion exclusion is controlled by the amount of water in the DDL, derived here from the ionic strength (Wigger and Van Loon, 2018), and the water composition, which is calculated as average using the Donnan approximation implemented in PHREEQC (Parkhurst and Appelo, 2013). Further details on the model concept and the underlying equations can be found in Parkhurst and Appelo (2013), Appelo et al. (2010) and Appelo and Wersin (2007) as well as Hennig and Kühn (2021a).

Scenario 1 is in line with the PSI/Nagra database (Thoenen et al., 2014) using the stability constant determined by Kalmykov and Choppin (2000) with a $\log K = 29.22$, what leads to the predominance of the anionic complex $CaUO_2(CO_3)_3^{2-}$, as already shown in Hennig et al. (2020). For Scenario 2, we have chosen the value obtained by Bernhard et al. (2001) with a $\log K = 30.55$ since it was used for the speciation calculations in the diffusion experiment, on which the calibration of the parameter n is based (Joseph et al., 2013b).

4.3 Results

4.3.1 Pourbaix diagrams for the speciation of uranium

The Pourbaix diagrams were created using the pore water composition of the shaly facies (Table 4.1) that was initially equilibrated with the carbonates as well as pyrite for a pCO_2 of $10^{-2.2}$ bar. From the Pourbaix diagrams, the predominant aqueous species can be read for a range of pH and pe conditions. In addition to the species shown in Figure 4.1, the element under consideration, here uranium, can of course also be present in the form of further aquatic species in smaller proportion (Table 4.2). Speciation calculations were performed for standard pressure and temperature conditions (1 bar, 25 °C) and a pH range from 2 to 10 as well as for E_H values between -413 mV and 413 mV corresponding to pe of -7 and 7, respectively. Figure 4.1a (Scenario 1) shows the aqueous speciation of uranium in the Opalinus Clay pore water of the shaly facies using the $\log K = 29.22$ according to the PSI/Nagra database, whereas in Figure 4.1b (Scenario 2) the $\log K$ was exchanged by the value of 30.55 determined by Bernhard et al. (2001). The dashed box marks the pH and E_H range observed in the Opalinus Clay. The Pourbaix diagrams for the pore water composition of the sandy facies (Figure 2.3) are identical with the ones shown in Figure 4.1 and were already published in Hennig et al. (2020).

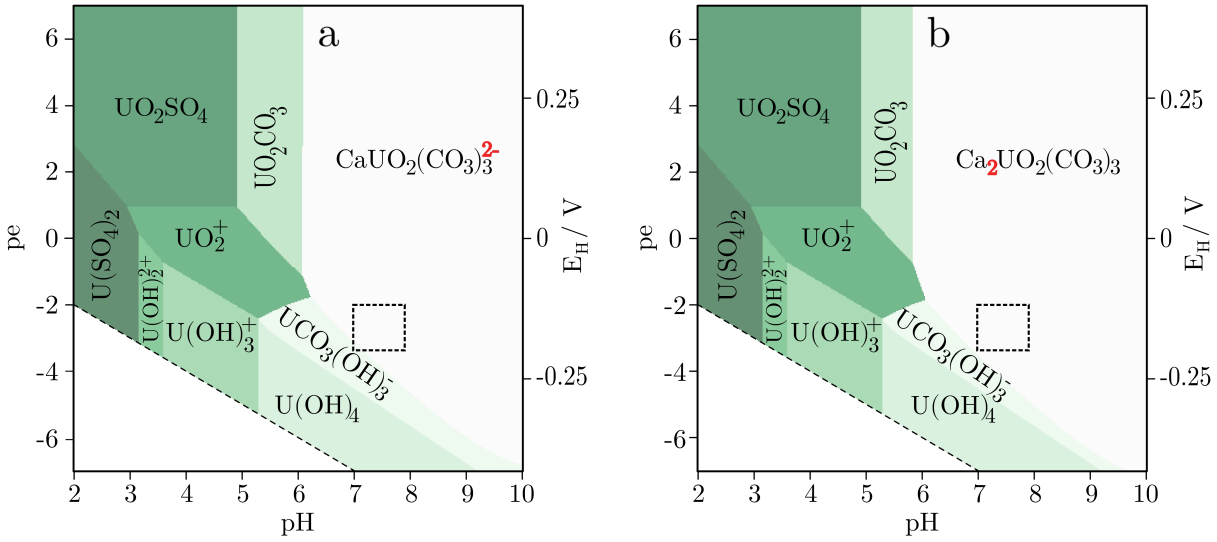

Figure 4.1: Predominant aqueous uranium species (neutral or anionic complex) depends on the $\log K$ value of the $Ca_2UO_2(CO_3)_3$ complex in the underlying database. Pourbaix diagrams for the aqueous uranium speciation in the pore water of the shaly facies with an uranium background concentration of 2.52 μmol/L either using the $\log K = 29.22$ given in the PSI/Nagra database (**a**) for the neutral ternary uranyl complex or the value of 30.55 (**b**) obtained by Bernhard et al. (2001). The main change in speciation is highlighted by the red numbers. The pore water was initially equilibrated with the carbonates and pyrite for a pCO_2 of $10^{-2.2}$ bar and calculations were performed for standard pressure and temperature conditions (1 bar, 25 °C). The dashed box marks the pH and E_H range measured in-situ in the Opalinus Clay formation.

From Figure 4.1 it becomes clear that uranium is mainly present as U(VI) complexes with calcium and carbonate in the pH and pe range observed in the Opalinus Clay, whereby the chosen log K for the neutral ternary uranyl complex governs uranium speciation in the modelled system. Depending on the selected value, either the ternary anionic uranyl complex $CaUO_2(CO_3)_3^{2-}$ (Scenario 1, Figure 4.1a) is the predominant species or the neutral one $Ca_2UO_2(CO_3)_3$ (Scenario 2, Figure 4.1b). A minor part (<2%) is present as U(IV) as the in-situ conditions are close to the transition to the tetravalent state. Table 4.2 gives the distribution of uranium among the main species in the pore water of the shaly as well as sandy facies. The relative proportions of the species do not differ significantly (<1%) within the pH and E_H range marked by the dashed box in Figure 4.1.

For Scenario 1, the percentage distribution of uranium among the individual species is similar in both facies. The main species is the anionic complex with calcium, followed by the anionic complex with magnesium $MgUO_2(CO_3)_3^{2-}$ and minor parts of the neutral complex as well as $UO_2(CO_3)_3^{4-}$. Whereas for the second scenario, the proportion of the neutral complex increases in the sandy facies but the anionic one is still the dominant. In the shaly facies, the neutral complex is predominant as can be seen in Figure 4.1b.

Table 4.2: Percentage of uranium species in the pore water of the shaly facies for the scenario with log K = 29.22 (Scenario 1) and for the value of 30.55 (Scenario 2). Values of the sandy facies are given in brackets.

Species	Scenario 1 in %	Scenario 2 in %
$Ca_2UO_2(CO_3)_3$	6 (3)	57 (37)
$CaUO_2(CO_3)_3^{2-}$	70 (69)	32 (45)
$MgUO_2(CO_3)_3^{2-}$	16 (15)	7 (10)
$UO_2(CO_3)_3^{4-}$	5 (8)	2 (5)

4.3.2 Uranium migration on the host rock scale

The difference of the uranium migration as a function of the predominant species was determined for the shaly and sandy facies of the Opalinus Clay by comparing the distances on the host rock scale (50 m) after a simulation time of one million years. Figure 4.2 shows the results for the shaly (Figure 4.2a) and the sandy (Figure 4.2b) facies, whereby Scenario 1 is represented by the solid line and Scenario 2 by the dashed line.

For the two considered scenarios, migration distances of uranium varied after a simulation time of one million years between 13 m (Scenario 1) and 20 m (Scenario 2) in the shaly facies (Figure 4.2a). In the sandy facies (Figure 4.2b), it were 17 m (Scenario 1) and 22 m (Scenario 2). Thus, the difference between both scenarios and with that the influence of the predominant species on the maximum migration distance is stronger in the shaly facies. With a maximum distance of 22 m, uranium migrated the farthest in the sandy facies, although the difference to the shaly facies with a maximum of 20 m is only small.

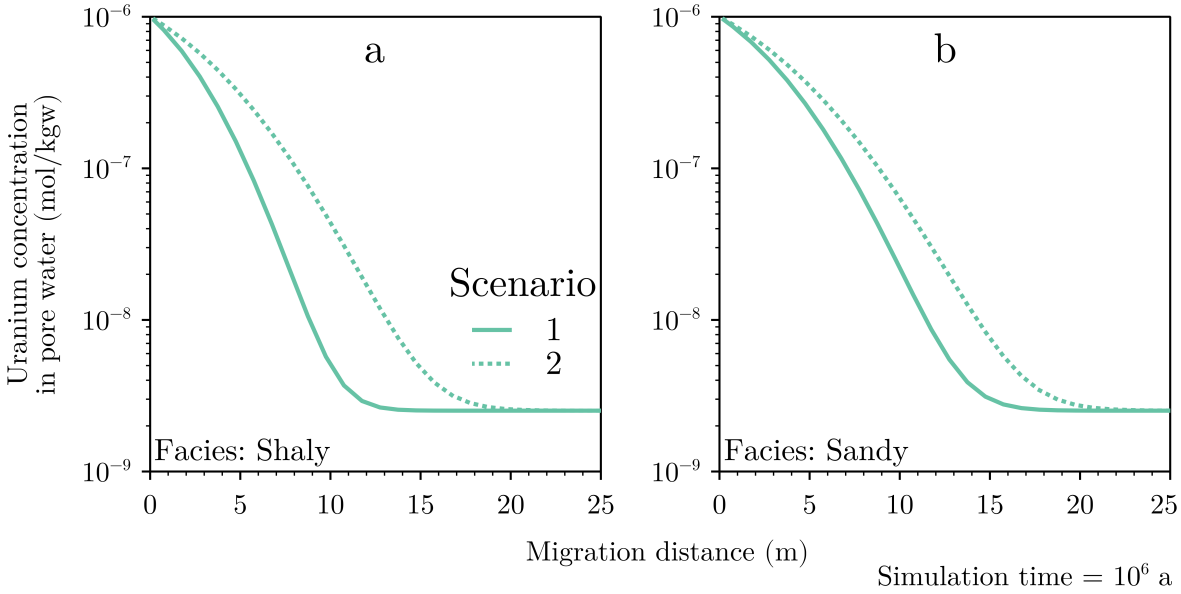

Figure 4.2: Migration distances deviate by up to 7 m depending on the predominant uranium species (neutral or anionic ternary complex). Uranium pore water concentrations in the shaly (**a**) and sandy facies (**b**) of the Opalinus Clay after a simulation time of one million years. The solid line shows the results for Scenario 1 using $\log K = 29.22$ for the neutral ternary uranyl complex and the dashed line represents the results for Scenario 2 with $\log K = 30.55$.

4.4 Discussion

Based on the diffusion lengths of uranium after one million years, the influence of the stability constant for the neutral ternary uranyl complex $Ca_2UO_2(CO_3)_3$ on the migration behaviour was quantififed with one-dimensional MC diffusion simulations in two scenarios and for different geochemical conditions as present in the shaly and sandy facies of the Opalinus Clay. For Scenario 1, the value according to the PSI/Nagra database (Thoenen et al., 2014) was chosen resulting in the anionic ternary uranyl complex with calcium as predominant species (Figure 4.1a) and less migration into the Opalinus Clay formation in both facies (solid line, Figure 4.2) compared to Scenario 2. Here, a higher value determined by Bernhard et al. (2001) was applied, and hence the thermodynamic equilibrium of the pore water was shifted towards the neutral ternary uranyl complex as predominant species (Figure 4.1b) with an associated farther migration of uranium. In metres, this means a difference between both scenarios of 7 m and 5 m in the shaly and sandy facies, respectively.

The effect of anion exclusion hampers uranium migration. The predominant species in the modelled system, e.g. anionic or neutral, governs the interaction with the DDL of the clay minerals. Due to their crystallographic structure, the surfaces of the clay minerals are negatively charged, what is compensated by the attraction of cationic species in the DDL and repulsion of anionic ones (Van Loon et al., 2007, 2003b). This decreases the accessible (effective) pore space for anionic species leading to slower diffusion. Thus, the effect of anion exclusion explains the difference between the two investigated scenarios. The intensity of anion exclusion is thereby determined by the ionic strength of the pore water. With decreasing ionic strength, the thickness of the DDL increases and

hence the effect of anion exclusion (Wersin et al., 2018, 2008; Wigger and Van Loon, 2018). This, in turn, implies that the difference in migration lengths between the two scenarios should be greater for the sandy facies with the lower ionic strength and associated thicker DDL compared to the shaly (Table 4.1). However, unlike our expectations, we observed the opposite. This means, additional factors also play a role as the difference between the scenarios for the two facies shows.

Calcium concentration in the pore water, and hence the geochemical composition itself, controls uranium speciation stronger than selection of thermodynamic data. From previous numerical studies, we know that the pore water composition, mainly pCO_2 and calcium concentration, and with that the geochemical conditions in the facies of the Opalinus Clay govern uranium sorption (Hennig et al., 2020) and transport processes Hennig and Kühn (2021a). This also applies here. Due to the lower initial calcium concentration in the sandy compared to the shaly facies (Table 4.1), the thermodynamic equilibrium of the pore water results in a governing anionic complex, even for Scenario 2. It is simply not enough calcium present in solution to completely shift the species distribution towards the neutral complex, as twice as much is required to form the complex. This is also reflected by the aqueous species distribution of uranium for Scenario 2 in the sandy facies (values in brackets, Table 4.2). Therefore, the variant influence of the stability constant on the uranium migration lengths is explained by the major differences of the pore water composition for the two facies.

With the second update on the chemical thermodynamics of uranium of the Nuclear Energy Agency (NEA, Grenthe et al., 2020), the discussion about the value for the stability constant of the neutral ternary complex $Ca_2UO_2(CO_3)_3$ was settled. Within this review, new studies have been discussed and evaluated and the log K of Endrizzi and Rao (2014) with a value of 30.8 has been selected as the most precise one published to-date. This value is even higher as the one of Bernhard et al. (2001) used for Scenario 2 ($\log K = 30.55$). This, in turn, means for uranium speciation in the geochemical system of the Opalinus Clay that the neutral ternary complex is the predominant one and migration lengths of uranium correspond more to the results of Scenario 2 or probably even greater.

4.5 Conclusions

The influence of data selection for the underlying chemical database on the migration length in the Swiss Opalinus Clay was tested using the example of the thermodynamic data for uranium. As required for safety assessments of potential repositories, the migration distance after one million years was quantified for the host rock scale. We have investigated the effect of two different values for the thermodynamic stability constant of a predominant uranium species as given in the literature. Our speciation calculations have shown that uranium is mostly present as U(VI) with calcium and carbonate. Depending on the chosen value for the stability constant of the neutral ternary uranyl complex $Ca_2UO_2(CO_3)_3$, the predominant species in the pH and pe range observed in the Opalinus Clay is either the neutral or the anionc complex $CaUO_2(CO_3)_3^{2-}$. Hence, with our multi-component (MC) diffusion simulations

accounting for the interaction of different charged species with the diffuse double layers (DDL) enveloping the clay minerals, we wanted to answer the question: What does the uncertainty regarding the thermodynamic data mean in metre of the migration distance on the host rock scale (50 m) after one million years? For this, we set up two scenarios identical except for the applied value for the stability constant of the neutral complex.

Simulations were performed for the shaly and sandy facies representing main differences in the pore water composition and clay mineral content as it has been shown that uranium sorption is mainly governed by the present geochemical conditions, namely pCO_2, calcium concentration, pH and pe, and less by the quantity of clay minerals. Uranium sorption on the clay minerals is decreased due to the formation of ternary complexes with calcium, magnesium and carbonate. Hence, the geochemical system in the facies is controlled by a fixed pCO_2 of $10^{-2.2}$ bar and mineral equilibria with the carbonates (calcite, dolomite and siderite) as well as pyrite governing the concentrations of the main ions, pH and pe.

For the shaly facies, maximum migration distances after one million years were 13 m (Scenario 1, $\log K = 29.22$) and 20 m (Scenario 2, $\log K = 30.55$) for the scenario with the anionic and neutral complex as predominant species, respectively. In the sandy facies, the diffusion lengths were 17 m and 22 m, correspondingly. The difference in the migration lengths of the two considered scenarios can be explained by the effect of anion exclusion, and hence by the predominant species. Due to the negatively charged surfaces of the clay minerals, anions are excluded from the DDL, and thus their accessible pore space and so their diffusive transport are diminished. Consequently, the larger the proportion of the anionic complex, the more is uranium diffusion through the facies hampered by the anion exclusion effect. The intensity of anion exclusion depends thereby on ionic strength as it governs the amount of water in the DDL. A lower ionic strength as in the sandy facies, for instance, is associated with a thicker DDL, and thus stronger anion exclusion. Accordingly, the difference between the two scenarios should potentially be the largest in the sandy facies. However, the influence of the stability constant on the migration lengths, and thus on the difference between the two scenarios, is less in the sandy facies compared to the shaly facies. Due to the lower initial calcium concentration in the sandy facies, the anionic complex is predominant for both scenarios.

With this, we quantified the effect of the stability constant of the $Ca_2UO_2(CO_3)_3$ complex on the maximum migration length of uranium and demonstrated, what a difference of 1.33 log units means in metre on the host rock scale, e.g. 5 m and 7 m for the sandy and shaly facies, respectively. However, as uranium is still retained within the formation with a thickness of around 160 m and no adjacent aquifer is reached, the effect is negligible in the geochemical system of the Opalinus Clay for the host rock scale. Furthermore, our results can serve as reference for clay formations with similar geochemistry, in case that speciation of uranium, and thus migration, is dominated by calcium and carbonate.

Chapter 5

Potential uranium migration within the geochemical gradient of the Opalinus Clay system at the Mont Terri

Abstract

Transport properties of potential host rocks for nuclear waste disposal are typically determined in laboratory or in-situ experiments under geochemically controlled and constant conditions. Such a homogeneous assumption is no longer applicable on the host rock scale as can be seen from the pore water profiles of the potential host rock Opalinus Clay at Mont Terri (Switzerland). The embedding aquifers are the hydrogeological boundaries that established gradients in the 210 m thick low permeable section through diffusive exchange over millions of years. Present-day pore water profiles were confirmed by a data-driven as well as by a conceptual scenario. Based on the modelled profiles, the influence of the geochemical gradient on uranium migration was quantified by comparing the distances after one million years with results of common homogeneous models. Considering the heterogeneous system, uranium migrated up to 24 m farther through the formation depending on the source term position within the gradient and on the partial pressure of carbon dioxide (pCO_2) of the system. Migration lengths were almost equal for single- (SC) and multi-component (MC) diffusion. Differences can predominantly be attributed to changes in the sorption capacity, whereby pCO_2 governs how strong uranium migration is affected by the geochemical gradient. Thus, the governing parameters for uranium migration in the Opalinus Clay can be ordered in descending priority: pCO_2, geochemical gradients, mineralogical heterogeneity.

5.1 Introduction

The protection of future generations and their environment from effects of highly radioactive waste requires the isolation of the, e.g. spent fuel in deep geological repositories in a suitable host rock (IAEA, 2003). Clay formations are one of the preferred host rocks because they have high retention capacities with respect to radionuclides due to the large reactive surface area of the inherent minerals and provide very low permeabilities, only allowing diffusive transport.

The retardation of radionuclide migration has been demonstrated for claystones, like the Opalinus Clay (Switzerland), in many laboratories as well as in-situ experiments, usually applying constant and homogeneous (geochemical) experimental conditions (Leupin et al., 2017b; Van Loon et al., 2003b, 2004; Wersin et al., 2008). However, for many radionuclides it has been shown that sorption and migration are affected by geochemistry and can deviate by one or more orders of magnitude (Hennig and Kühn, 2021a; Ma et al., 2019; Noseck et al., 2012). Hence, the transport parameters determined in experiments may no longer be applicable in the case of changing geochemical conditions.

On the host rock scale, a formation is not homogeneous. Therefore, numerical process coupling is required in order to give quantitative robust statements as the "homogeneous" results of the small-scale experiments are not easily transferable. Besides the hydro-physical and chemical properties governing transport of radionuclides, the overall thickness of the potential host rock plays a crucial role to ensure the enclosure of the radioactive material for times of up to one million years. In Germany and Switzerland, for instance, where the Opalinus Clay is present, a thickness of at least 100 m is a minimum criteria (§ 23 Article 5 StandAG[1], Nagra, 2002a). On the one hand, the heterogeneity is given by variations in the mineralogical composition due to the deposition process. Reasons for differences in the pore water composition are water-rock-interactions. On the other hand, chemical heterogeneities developed as a result of diffusive exchange of waters with adjacent formations. Due to the large spatial and temporal scales to be considered, numerical simulations are indispensable for safety assessments of potential repositories to quantify radionuclide migration.

The Opalinus Clay is subdivided into three lithological units: the shaly, sandy and carbonate-rich facies (Lauper et al., 2018; Pearson et al., 2003; Wersin et al., 2009). Furthermore, present-day pore water profiles are characterised on the host rock scale by a geochemical gradient across the entire thickness (Figures 5.1–5.3) as a result of the exchange with adjacent permeable formations (Mazurek et al., 2011; Pearson et al., 2003). The current hydrogeological boundaries are represented by aquifers at the footwall (Liassic limestone) and hanging wall (Dogger limestone, Figure 5.1). As discussed in the comprehensive study of Mazurek et al. (2011), the shape and gradients of the profiles of chloride as conservative tracer (no mineral interaction) as well as of helium and the stable water isotopes can be explained by diffusion and the activation times of the surrounding aquifers. This leads to the following questions: Do geochemical gradients affect radionuclide migration? If so, how much?

In the present study, we assess the influence of measured geochemical gradients on potential radionuclide migration of uranium as one of the main components in spent fuel (Metz et al., 2012) in the hydrogeological system of the Opalinus Clay formation in the Mont Terri region. From previous numerical studies (Hennig and Kühn, 2021a; Hennig et al., 2020), we know that uranium speciation is controlled by the pore water composition and that it is mainly present in anionic and neutral complexes with calcium, magnesium and carbonate, e.g. $Ca_2UO_2(CO_3)_3$, $CaUO_2(CO_3)_3^{2-}$, $MgUO_2(CO_3)_3^{2-}$. Moreover, sorption as well as diffusion processes of uranium in the geochemical system are governed by the partial pressure of carbon dioxide (pCO_2), Ca^{2+} concentration, pH, pe, the hydro-physical parameters and the clay mineral quantity (Hennig and Kühn, 2021a). With fully coupled reactive transport models, we quantify uranium migration under consideration of the pore water geochemistry in the hydrogeological framework of the potential host rock Opalinus Clay.

[1]Standortauswahlgesetz (StandAG) of 5 May 2017 (Federal Law Gazette p. 1074) as last amended by Article 1 of the Act of 7 December 2020 (Federal Law Gazette p. 2760). URL: https://www.gesetze-im-internet.de/standag_2017/BJNR107410017.html (accessed on 13 June 2022).

In the first step, we modelled the chloride profile presented in Mazurek et al. (2011) and extended their work with the profiles of other pore water components, e.g. calcium, sodium, magnesium or strontium, based on the comprehensive geochemical database given in Pearson et al. (2003) and Wersin et al. (2009) to calibrate our model. The basic idea is to match and initialise our simulations with the present-day profiles of the pore water components.

In the second step, we add uranium as prospective repository to the calibrated model and simulate the migration lengths for a time span of one million years. Important part of the study is the comparison of single-component (SC) with multi-component (MC) diffusion to determine the respective influence of geochemical gradients. In contrast to the SC simulations based on Fick's laws, the MC approach accounts for the interaction of charged species with the diffuse double layers (DDL) of the clay mineral surfaces. The migration distances of uranium after a simulation time of one million years were compared with the results presented in Chapter 2 (Hennig et al., 2020) that were obtained for a geochemically constant, and thus homogeneous, Opalinus Clay system with SC simulations. In that way, we account for the first time for the influence of changing geochemical conditions on sorption as well as the diffusive transport and we quantify the uncertainty of transport parameters of uranium on the host rock scale.

5.2 Methods

Reactive transport simulations were applied to quantify uranium migration considering diffusion and sorption processes as well as interaction with the inherent minerals depending on the geochemical gradient in the Opalinus Clay formation at the Mont Terri. Based on the geological evolution of the Mont Terri anticline (Section 5.2.1), the initial conditions (Section 5.2.2) were chosen and the geochemical system was defined (Section 5.2.3) to match as first step the present-day pore water profiles (Section 5.2.3) as calibration for our model concept. The one-dimensional simulations were conducted on the host rock scale (approx. 200 m) with PHREEQC Version 3.5.0 (Parkhurst and Appelo, 2013) to consider the geochemical conditions to quantify sorption (Section 5.2.4) and diffusion applying the SC method following Fick's law (Section 5.2.5) as well as the implemented MC approach (Section 5.2.6). In the second step, we added an uranium source term to the system (Section 5.2.7) to assess the migration under a geochemical gradient for one million years.

The underlying thermodynamic data are based on the PSI/Nagra database version 12/07 (Thoenen et al., 2014) with the extensions and updates described in Hennig et al. (2020) and Hennig and Kühn (2021a). Details are given in the corresponding Supplementary (Supplementary S-1 and S-2). All simulations were conducted for the reference temperature of 25 °C. Previous studies showed that temperature variations, e.g. due to uplift of the formation, changes of the surface temperature or heat generated by the radioactive waste, have only a minor effect on the modelled chloride profile (Mazurek et al., 2011, 2009). Furthermore, uranium migration in the Opalinus Clay (up to temperatures of 60 °C, Joseph et al., 2013b) as well as the concentrations of

the pore water components (<5% for a temperature of 45 °C, Wersin et al., 2016) are not significantly affected by elevated temperatures. The hydraulic rock properties correspond to the direction perpendicular to bedding for all transport simulations. Dirichlet boundaries are applied to the model outlets. All models have a spatial resolution of 2 m. Grid independence is ensured by simulations of finer resolution and numerical stability by the Neumann criteria.

5.2.1 Geological and hydrogeological evolution of the Mont Terri anticline

The Mont Terri anticline is located in northwestern Switzerland in the canton of Jura between the cities St. Ursanne and Courgenay, which are connected by a motorway tunnel constructed through the core of the anticline (Figure 5.1). The Mont Terri consists of Triassic and Jurassic limestones, marls and shales with the Opalinus Clay formation embedded (Figure 5.1). The formation accessed by an underground laboratory (Bossart and Thury, 2008; Pearson et al., 2003) has an overburden of around 300 m. The maximum overburden in the past is estimated with at least 1,000 m (Bossart and Thury, 2008; Mazurek et al., 2011; Pearson et al., 2003). Thus, the Opalinus Clay is an overconsolidated shale formation deposited about 180 Ma ago in the Lower Aalenian in a shallow marine environment of the Jurassic sea covering an area from the Jura mountains in Switzerland and France as well as the Swiss-German foreland basin and parts of Southern Germany (Bossart and Thury, 2008; Pearson et al., 2003).

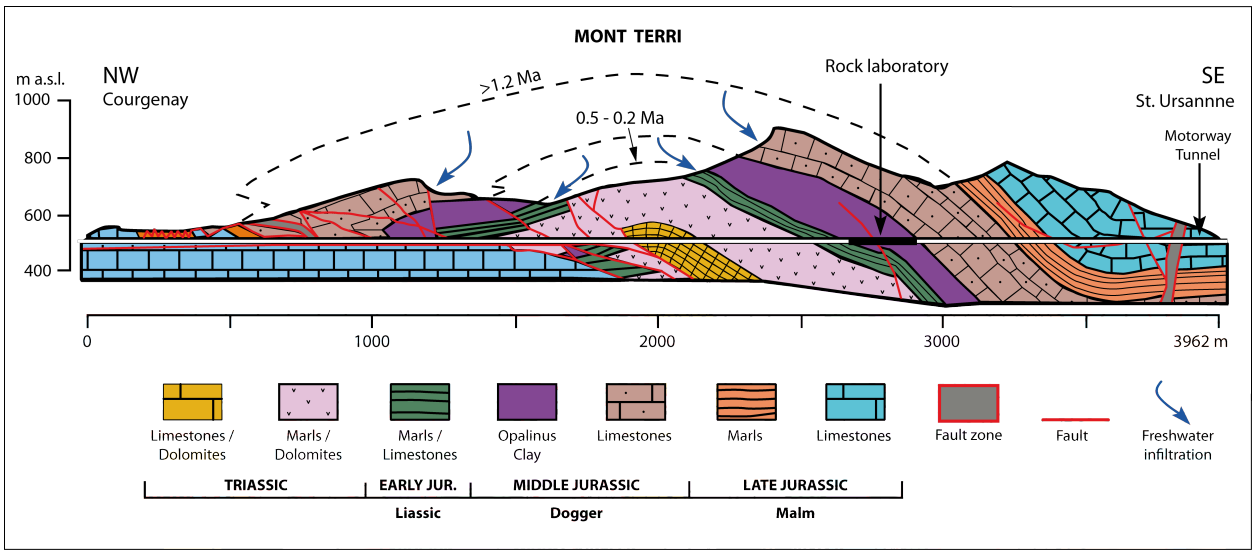

Figure 5.1: Erosion history of the Mont Terri anticline and associated freshwater infiltration into the embedding aquifers, and thus activation of the current hydrogeological boundaries of the Opalinus Clay system, is indicated in the geological profile by the blue arrows. Modified from Freivogel and Huggenberger (2003).

In the studied area, the total thickness of the low permeable section is 210 m. It consists of 50 m of Liassic shales (Obtusus Clay, Posidonia Shale and Jurensis Marl) and the 160 m thick Opalinus Clay (Figure 5.1) with an alternating sequence of its facies shaly, sandy, and carbonate-rich (Mazurek et al., 2011; Pearson et al., 2003).

The hydrogeological boundary at the footwall is the Liassic Gryphaea limestone. The hanging wall boundary (Figure 5.1) is defined by the contact between Opalinus Clay and the limestones of the Lower Dogger (Mazurek et al., 2009; Pearson et al., 2003). Hence, the Opalinus Clay is an aquiclude sandwiched between two aquifers (Bossart and Thury, 2008). According to Pearson et al. (2003) and Mazurek et al. (2011), freshwater infiltration into both aquifers and with that the activation of the current hydrogeological boundaries of the system was only possible after uplift of the entire sequence due to the folding of the Jura mountains about 10 Ma ago and the subsequent erosion of the overlying stratigraphic layers. Therefore, onset of freshwater infiltration first occurred in the upper aquifer of the Dogger between 10 Ma and 1.2 Ma before today (Figure 5.1, Mazurek et al., 2011). Only after erosion of the overlying Opalinus Clay and Liassic shales, the aquifer at the footwall was activated between 0.5 Ma and 0.2 Ma ago leading to a substantial time lag of freshwater infiltration into both aquifers, and thus to the associated asymmetric shape of the pore water components (Figures 5.2a and 5.3). It is important to note that the observed profiles for chloride, helium as well as the stable water isotopes could be reproduced and understood with diffusion as sole transport process (Mazurek et al., 2011). More details on the hydrogeological evolution of the Opalinus Clay can be found in Mazurek et al. (2011, 2009) and Pearson et al. (2003) as well as in the Swiss Safety Report (Nagra, 2002a).

5.2.2 Initial model conditions

The total simulation time was six million years with the Dogger aquifer being active during the entire time and the Liassic aquifer only for the last 0.5 million years (Figure 5.2b). The initial conditions for the following simulations were based on the findings discussed in the comprehensive study of Mazurek et al. (2011).

The observed chloride profile (Figure 5.2a, Pearson et al., 2003) suggests bleeding of chloride from the low permeable sequence into the bounding aquifers. This, in turn, means the initial chloride concentration must have been equal or even higher compared to the maximum value of around 14 g/L observed today (Mazurek et al., 2011; Pearson et al., 2003). Based on their model calculations, Mazurek et al. (2011) discussed that the initial chloride concentration must have been between 14 g/L and 24 g/L with the best fit for an initial concentration of 18.4 g/L. This value was determined from a sampling of stagnant groundwater from the Liassic aquifer at the nearby Mont Russelin, where the Liassic has no surface contact and is protected within the core of the anticline shielded by the overlying formations like the Opalinus Clay (Koroleva and Mazurek, 2009). Therefore, the water samples at Mont Russelin were interpreted to represent chemical signatures that were not affected by exchange with aquifers (Koroleva and Mazurek, 2009; Mazurek et al., 2011).

For our simulations, we need the initial concentrations of the main pore water components (e.g. Na^+, Cl^-, K^+, Ca^{2+}, Mg^{2+}, Sr^{2+}, SO_4^{2-}) before the activation of the bounding aquifers. We elaborated two scenarios as given in Table 5.1 in order to model the pore water profiles observed at Mont Terri (Section 5.2.3), assuming that the waters determined at Mont Russelin are considered as unaffected.

Hence, the pore water concentrations obtained from squeezing a sample from the Opalinus Clay in the core of the Mont Russelin anticline (Koroleva and Mazurek, 2009) with a chloride concentration of around 18.9 g/L were used for the first scenario (Scenario 1R, data-driven, Table 5.1). The second scenario (Scenario 2J, conceptual, Table 5.1) is based on sampled stagnant groundwater from the Liassic aquifer at Mont Russelin (Koroleva and Mazurek, 2009) according to Mazurek et al. (2011). However, only the values for chloride, sodium and strontium can be used due to a contamination with cement during sampling. We assume that the concentrations for calcium and magnesium in particular have been altered. For the other components, the sea water concentrations according to the time of deposition in the Jurassic were chosen (Horita et al., 2002) as already discussed in Mazurek et al. (2009). The water compositions of the bounding aquifers stem from seepage samples taken in the Mont Terri tunnel close to the rock laboratory (Pearson et al., 2003). The concentrations of the main ions are given as well in Table 5.1 as averaged values of the corresponding measurement campaign. More details can be found in the Supplementary S-3.

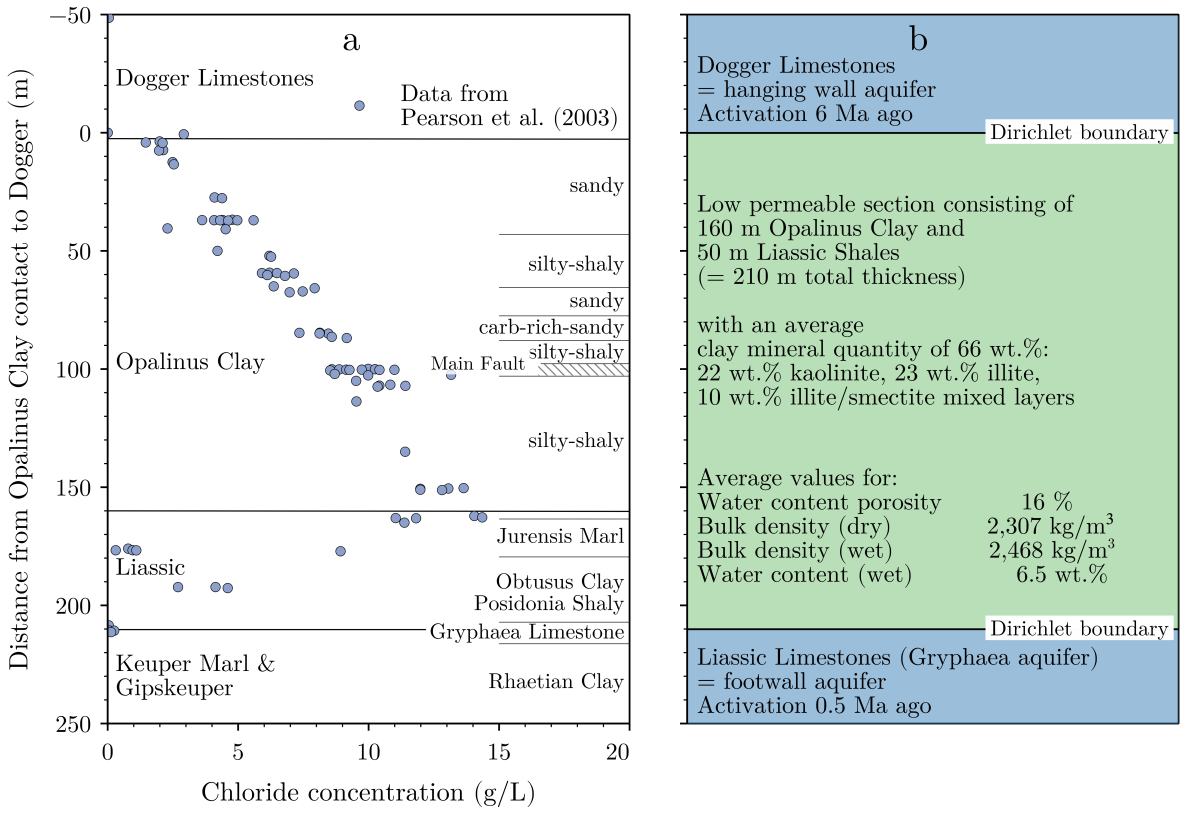

Figure 5.2: Profile of measured chloride concentrations at Mont Terri (**a**) is used to define the conceptual model (**b**) with boundary and initial conditions. The shape of the profile in the low permeable section (Liasic shales and Opalinus Clay) is the result of the time lag in freshwater infiltration into the bounding aquifers, e.g. the Dogger and Liassic limestones. The y-axis is the distance perpendicular to the contact between Opalinus Clay and Dogger limestones. Modified from Pearson et al. (2003).

Table 5.1: Concentrations of the main ions (mmol/L) for the two scenarios regarding the initial conditions prior to activation of the aquifers as well as for the present-day waters of bounding aquifers in the Dogger and Liassic. Scenario 1R (data-driven) is based on a sample from the Opalinus Clay taken at Mont Russelin (Koroleva and Mazurek, 2009). Scenario 2J (conceptual) is a combination of Liassic groundwater at Mont Russelin (Koroleva and Mazurek, 2009) and Jurassic sea water (indicated by *, Horita et al., 2002).

Parameter	Scenario 1R	Scenario 2J	Dogger limestone	Liassic limestone
Na^+	402	413	0.8	1.3
Cl^-	522	508	0.08	0.2
Ca^{2+}	46	26*	1.9	2.1
Mg^{2+}	41	33*	2.7	0.7
SO_4^{2-}	31	14*	0.9	0.5
K^+	1.2	10.2*	0.4	0.1
Sr^{2+}	0.8	0.6	0.2	0.03

5.2.3 Geochemical system and present-day pore water profiles

The geochemical system of the Opalinus Clay is governed by the calcite-carbonate-ion system and hence by the pCO_2 (Pearson et al., 2003; Wersin et al., 2009). This, in turn, controls speciation and migration of uranium (Hennig et al., 2020), and therefore the pCO_2 needs to be fixed. We took the atmospheric pCO_2 at the time of deposition close to the Triassic-Jurassic boundary (TJB) about 200 Ma ago. At the TJB, the carbon dioxide concentration in the atmosphere increased up to values between 2,000 ppm and 2,500 ppm and remained elevated for some time before it decreased again to the previous value of 1,000 ppm (Steinthorsdottir et al., 2011). The exact time frame is uncertain, and therefore we selected two scenarios for the pCO_2 with 2,000 ppm and 1,000 ppm corresponding to $10^{-2.7}$ bar (Scenario A) and 10^{-3} bar (Scenario B), respectively. Depending on the applied pCO_2, the initial pore water compositions were equilibrated with calcite and dolomite to control pH and with siderite and pyrite to govern the redox state within the system as these minerals are most consistent with measured values (Pearson et al., 2003, 2011; Wersin et al., 2009, 2011). The initial values for the pH and pe were 8.2 according to today's sea water (Marion et al., 2011) and -3.85, respectively. The latter is equivalent to an E_H of -227 mV as published for Mont Terri (Bossart and Thury, 2008). The equilibrium of the mineral assemblage also controls the concentrations of the main cations calcium, magnesium, and iron. The ratio between the ions, e.g. the Mg/Ca ratio, is thereby determined by the stability constants usually used for pure minerals resulting in this case to a Mg/Ca ratio of around 0.8. However, at Mont Terri higher Mg/Ca ratios were observed ranging between 0.9 and 1.3 (Pearson et al., 2003) resulting from the exchange of calcium with magnesium ions on the surface of the calcite lattice (Möller and De Lucia, 2020). The incorporation of magnesium led to an increased solubility of calcite compared to the pure mineral. Therefore, the stability constant of calcite has been adapted in the applied thermodynamic

database according to the approach presented in Möller and De Lucia (2020) based on the Mg/Ca ratio measured in the pore water of the Opalinus Clay at Mont Russelin (Koroleva and Mazurek, 2009). The adapted log K is about 0.2 log units higher, as can be seen in the Supplementary S-4, leading to a Mg/Ca ratio of 1.3. With the outlined constraints, we defined the geochemical system of the Opalinus Clay in our model concept as a function of the pCO_2 around the time of deposition.

Calcium, magnesium, pCO_2 and pH are the governing parameters for uranium speciation and hence sorption (Hennig et al., 2020) as well as diffusion (Hennig and Kühn, 2021a). Therefore, only these profiles are exemplarily shown for the other pore water components (Figure 5.3). The applied geochemical data stems from various borehole analyses at the underground research laboratory taken from the comprehensive studies of Pearson et al. (2003) and Wersin et al. (2009). The underlying data and all other profiles can be found in the Supplementary S-3.

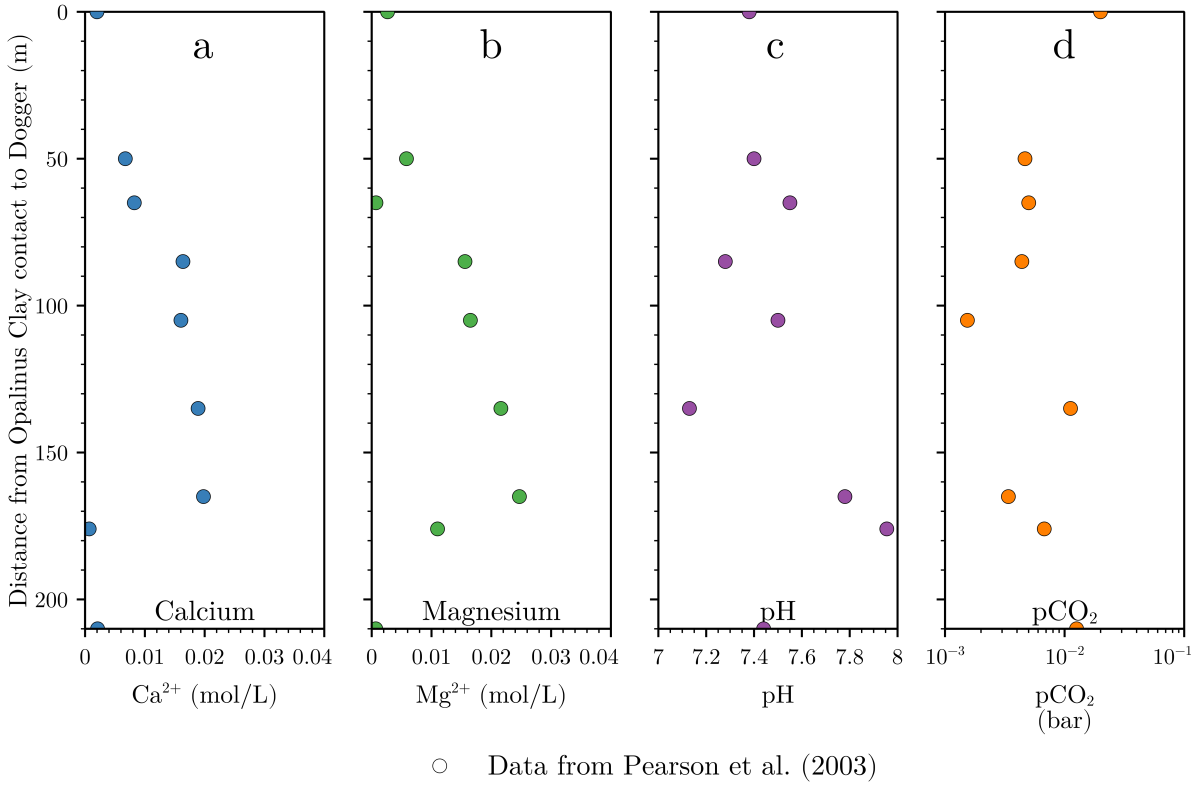

Figure 5.3: Measured profiles of pore water components governing uranium sorption, i.e. calcium (**a**), magnesium (**b**), pH (**c**) and pCO_2 (**d**), decrease from Opalinus Clay towards embedding aquifers. The data stems from borehole analyses at the underground laboratory Mont Terri. The y-axis is the distance perpendicular to the contact between Opalinus Clay and Dogger limestones.

5.2.4 Incorporated sorption processes

Sorption processes were integrated in the simulations via a bottom-up approach by the additive sorption on the individual minerals present in the formation (Marques Fernandes et al., 2015; Stockmann et al., 2017) using mechanistic surface complexation models (SCM) based on the two-layer model of Dzombak and Morel (1990) as well as cation exchange. The applied and proven dataset (Joseph et al., 2013a)

is given in the Supplementary of Chapter 2 (Hennig et al., 2020) together with all required surface parameters and reactions (Supplementary S-1). Not all present minerals contribute equally to the total uranium sorption (Hennig et al., 2020). Hence, we only consider sorption on the clay minerals kaolinite, illite and illite/smectite mixed layers that were handled as a 1:1 combination of the pure minerals illite and smectite. Smectite is a generic term for a group of clay minerals, for which we have chosen montmorillonite as the best investigated representative (Joseph et al., 2013a), and is not further described for the Opalinus Clay. Illite and montmorillonite are the exchange phases for the main cations as well as uranyl-ions (Hennig et al., 2020; Kim, 2001). The respective reactions are also given in the Supplementary of Chapter 2 (Supplementary S-1, Hennig et al., 2020). Sorption is quantified via the distribution coefficient K_d (m^3/kg) calculated in PHREEQC following Stockmann et al. (2017) as ratio between the amount of a species absorbed on the solid phase and the amount present in the liquid phase.

Since geochemistry of the pore water is more decisive for uranium sorption and migration in the Opalinus Clay than the quantity of clay minerals, we decided to use a mean of 66 wt.% clay minerals for the entire low permeable sequence with 22 wt.% kaolinite, 23 wt.% illite and 10 wt.% illite/smectite mixed layers (Bossart and Thury, 2008; Reisdorf et al., 2016). Accordingly, we have also chosen averaged values for porosity 0.16 (-), wet water content 0.065% as well as for dry and wet bulk density 2,307 kg/m^3 and 2,468 kg/m^3 (Pearson et al., 2003), respectively. These parameters are needed to calculate the amount of pore water per volume unit Opalinus Clay and hence the amount of clay minerals per kilogram pore water.

5.2.5 Modelling single-component diffusion

In the SC simulations, diffusive transport is quantified based on Fick's laws. Accordingly, one diffusion coefficient is used for all pore water components in the same way. To model the profiles, we use the effective diffusion coefficient D_e of chloride with $4.6 \cdot 10^{-12}$ m^2/s (Mazurek et al., 2011; Van Loon et al., 2003a) as it is a conservative tracer. Further, the chloride profile is used to calibrate our model (Section 5.3.1). For the subsequent uranium migration, the D_e of uranium is used that was determined with a value of $1.9 \cdot 10^{-12}$ m^2/s in an experiment with Opalinus Clay of the sandy facies (Joseph et al., 2013b). Transport modelling in PHREEQC is based on the assumption that a model element solely contains water (Parkhurst and Appelo, 2013). Consequently, the pore water diffusion coefficient D_p (m^2/s) must be applied instead, which can be derived from the effective porosity ϵ (-) and the D_e accounting for the reduced cross-sectional area available for diffusion in porous media via $D_e = \epsilon \cdot D_p$ (Equation 5.1). Considering a ratio of anion- to water-accessible porosity of 0.54 due to the anion exclusion effect (Mazurek et al., 2011; Van Loon et al., 2003a), this results in a $D_p = 5.3 \cdot 10^{-11}$ m^2/s for chloride. In the uranium diffusion experiment, a neutral ternary uranyl complex was the dominant species resulting in a $D_p = 1.2 \cdot 10^{-11}$ m^2/s used in the simulations.

5.2.6 Modelling multi-component diffusion

The MC approach implemented in PHREEQC is based on the electrochemical potential. This enables the calculation of diffusive transport in porous media with uncharged regions and charged regions (Appelo and Wersin, 2007; Parkhurst and Appelo, 2013) as, for instance, present in claystones like the Opalinus Clay with the (free) pore water and the DDL, respectively. The approach has already been successfully applied to the Opalinus Clay to model a diffusion experiment with different charged species (Appelo et al., 2010) as well as with uranium (Hennig and Kühn, 2021a). Detailed descriptions of the approach and underlying equations can be found in Appelo and Wersin (2007), Appelo et al. (2010), Hennig and Kühn (2021a) as well as in the PHREEQC manual (Parkhurst and Appelo, 2013).

With the MC option in PHREEQC, the diffusive flux is calculated separately for each species present in the system as the sum of diffusion in the pore water and the DDL. This is conceptually implemented by dividing a model element along its length in paired cells for each mineral defined so that each pair consists of a charge-balanced solution (free pore water) and a charged surface with a DDL. The diffusive transport within a model element is calculated by explicit finite differences for each interface among the paired cells and then summed up to determine the exchange between two model elements. In the underlying thermodynamic database, each species is assigned its own self-diffusion coefficient in water D_w (m^2/s) that is needed to derive the corresponding D_p analogous to Archie's law:

$$\frac{D_e}{\epsilon} = D_p = D_w \cdot \epsilon^n \tag{5.1}$$

where n is an empirical exponent (Van Loon et al., 2007) that needs to be determined for a specific medium, here Opalinus Clay (Section 5.3). The D_w for the pore water components were taken from the phreeqc.dat provided with PHREEQC (Parkhurst and Appelo, 2013) and for the uranium species from the works of Kerisit and Liu (2010) as well as Liu et al. (2011), as described in Chapter 3 (Hennig and Kühn, 2021a). All details can be found in the corresponding Supplementary (Supplementary S-2).

The net surface charge of the clay minerals is compensated within the area of the DDL by the enrichment of counter-ions and repulsion of co-ions, which accordingly reduces their pore space and hampers their diffusive transport compared to counter-ions. In the case of negatively charged surfaces of the clay minerals, this effect is known as anion exclusion (Appelo and Wersin, 2007; Van Loon et al., 2003a; Wigger et al., 2018). Therefore, the amount of water and hence the thickness of the DDL as well as the composition govern anion exclusion. We use the fast and robust method of the Donnan approximation implemented in PHREEQC that assumes a single potential for the DDL as entity to calculate the composition within the DDL as average (Parkhurst and Appelo, 2013). The thickness of the DDL is controlled by the ionic strength of the pore water (Appelo et al., 2010; Appelo and Wersin, 2007; Wigger et al., 2018).

With decreasing ionic strength according to the chloride concentration and the geochemical gradient towards the bounding aquifers, the thickness of the DDL increases. Therefore, we have decided to use the Debye-length option in PHREEQC (Parkhurst and Appelo, 2013) to determine the thickness of the DDL (d_{DDL}, Equation 5.2) as a function of the ionic strength (I, Equation 5.2). With this option, the d_{DDL} (m) is calculated as product of a defined number of lengths (n_{DDL}) times the Debye length (Appelo and Wersin, 2007; Wersin et al., 2018). Based on I (mol/L) and d_{DDL} given in Hennig and Kühn (2021a) for the three facies of the Opalinus Clay (Table 3.1), we determined n_{DDL} with a value of 1 according to:

$$d_{DDL} = \frac{3.09 \cdot 10^{-10}}{\sqrt{I}} n_{DDL} \tag{5.2}$$

where the number $3.09 \cdot 10^{-10}$ is a factor dependent on the dielectric constant and temperature and valid at a temperature of 25 °C (Wersin et al., 2018).

5.2.7 Uranium source term

The uranium source term to mimic the failed high-level waste canisters is integrated by a mineral equilibrium with amorphous, hydrated uraninite $UO_{2(am,hyd)}$. Thereby, the saturation index is chosen to achieve a concentration of around 1 μmol/L (Joseph et al., 2013b; Keesmann et al., 2005). The potential repository is placed in one case in the centre of the model at a depth of 100 m below contact between Dogger limestones and Opalinus Clay and in the other case at a depth of 150 m, i.e. the transition from Opalinus Clay to Liassic shales with the highest chloride concentrations (Figures 5.2 and 5.4). We would like to emphasize that our results need to be considered as maximum diffusion lengths. We assume a very simplified nuclear waste disposal concept and do not consider the effect of the engineered barriers on the source term as, for instance, a delay and retention due to the metal canisters or the bentonite filling (Nagra, 2002a). We focus on the migration behaviour of uranium in the far-field taking into account the geochemical gradient within the low permeable section.

Present-day uranium concentrations deviate between $6.0 \cdot 10^{-10}$ mol/L and $2.3 \cdot 10^{-9}$ mol/L in the pore waters of the low permeable section as well as in the surrounding aquifers (Pearson et al., 2003). The background concentrations were established in the model by an undersaturation with regard to $UO_{2(am,hyd)}$ together with the mineral equilibria with the carbonates and pyrite (Section 5.2.3).

5.3 Model calibration and validation

First, our model was calibrated against the chloride profile measured in the field (Figure 5.2a) with the outlined initial and boundary conditions (Section 5.2.2) using the SC approach (Section 5.2.5). Otherwise, it would be pointless to consider the other pore water components or MC diffusion. Subsequently, the exponent n required for the MC diffusion (Equation 5.1, Section 5.2.6) was determined based on the SC simulations. Both results are presented in Section 5.3.1. Secondly, the model was validated against a diffusion laboratory experiment with uranium and Opalinus Clay of the sandy facies

(Joseph et al., 2013b) applying the SC as well as MC diffusion approach with the calibrated exponent n (Section 5.3.2).

5.3.1 Chloride profile at Mont Terri

The chloride profile given in Pearson et al. (2003) is used to calibrate our model and test the underlying concept with initial and boundary conditions (Section 5.2.2). The main assumption is that the entire low permeable sequence (Liassic shales and Opalinus Clay) had a uniform initial chloride concentration of around 18.4 g/L (Mazurek et al., 2011), e.g. corresponding to around 0.5 mol/L (Table 5.1). Due to erosion, the surrounding aquifers were activated, and thus flushed with freshwater leading to a diffusive exchange with the embedded clays (Figure 5.1, Section 5.2.1). Total simulation time was six million years with the footwall aquifer only being active for the last 0.5 million years (Figure 5.2b). The initial chloride concentrations of both scenarios are (very) similar with values of 18.9 g/L (1R, data-driven) and 18.4 g/L (2J, conceptual, Table 5.1). We therefore present only the results of Scenario 1R as the chloride profiles of both scenarios do not differ significantly. The deviation of our model in relation to the measured data is quantified by the relative Root Mean Square Error (rRMSE, Equation 2.2). Due to the scattering of the data, the rRMSE were calculated with logarithmised values. Figure 5.4 shows that the chloride profile can be well reproduced using the SC approach with a rRMSE of 13%.

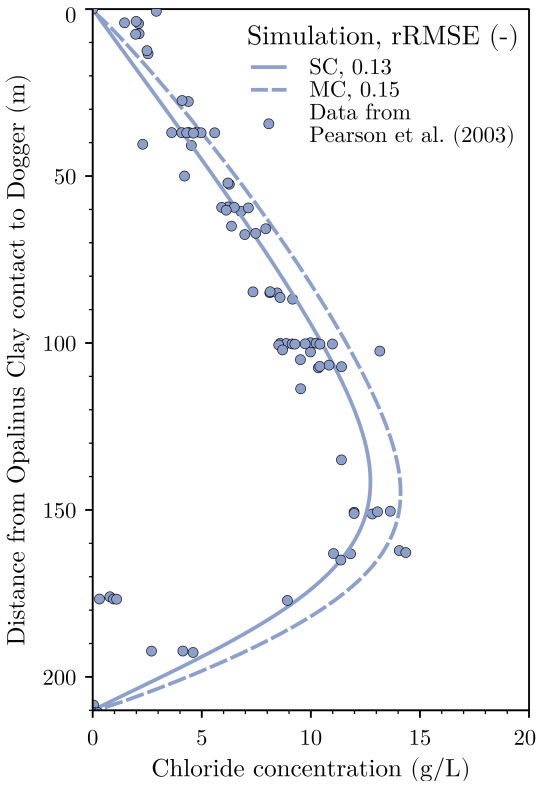

Figure 5.4: Model calibrated for further application. The chloride profile (dots) was reproduced (rRMSE≤15%) for the data-driven scenario (1R) with an initial chloride concentration of around 18.9 g/L using the SC (solid line) as well as the MC diffusion approach (dashed line). Best match using MC diffusion was achieved for an exponent n = 2.

Based on the SC results, the parameter n required for the MC diffusion to determine the D_e for every species (Equation 5.1, Section 5.2.6) was varied until the best match between MC simulation results and measured data was achieved with $n = 2$ and an associated rRMSE of 15%. In literature, values of the medium-specific parameter n vary between 2 and 2.5 for the Opalinus Clay, especially for anionic species (Mazurek et al., 2011, 2009, 2008; Van Loon et al., 2018, 2003a). Thus, our calibrated parameter falls into the respective range. Compared to the SC simulations, diffusion of chloride towards the aquifers is slightly lower for the MC approach resulting in higher maximum values across the modelled profile. However, the profile still coincides very well with the measured data as shown in Figure 5.4. Therefore, we consider our model concept for the SC and MC approach with $n = 2$ as calibrated for further application and extension with the other pore water components.

5.3.2 Diffusion experiment with uranium

The diffusion experiment with uranium and Opalinus Clay of the sandy facies (Joseph et al., 2013b) is used to verify our model concept in terms of incorporated transport and sorption processes against laboratory data to quantify migration of uranium. The spatial resolution, initial and boundary conditions of the model are equal to the one used in Chapter 2 (Hennig et al., 2020). Here, we consider sorption on the clay minerals kaolinite, illite and the illite/smectite mixed layers (Section 5.2.4) for the SC and MC diffusion approach (Section 5.2.5 and 5.2.6). The mineralogy used here is based on the results given in Hennig et al. (2020) for a clay mineral content of 45 wt.% (23 wt.% kaolinite, 9 wt.% illite and 4 wt.% illite/smectite mixed layers) corresponding to the sandy facies (Pearson et al., 2003). Figure 5.5 shows the modelled diffusion experiment applying the SC (solid line) as well as MC approach (dashed line). The experimental data were well reproduced by the SC as well as by the MC diffusion simulations with rRMSEs of 29% and 40%, respectively. Due to the scattering of the data itself, we consider our conceptual model as calibrated, and thus applicable to quantify uranium diffusion and sorption on the host rock scale (Hennig and Kühn, 2021a; Hennig et al., 2020).

5.4 Results

5.4.1 Simulation of pore water profiles using single- and multi-component diffusion

Present-day profiles of Ca^{2+}, Mg^{2+}, pH and pCO_2 were modelled applying SC and MC diffusion simulations for two scenarios differing in the composition of the initial pore water (Table 5.1). For Scenario 1R (data-driven), concentrations measured from samples of the Opalinus Clay at the Mont Russelin were used, where the Liassic aquifer has no contact with meteoric water and the pore water is therefore considered as unaffected. Scenario 2J (conceptual) was a combination of measured values from Liassic groundwater at Mont Russelin (Cl^-, Na^+ and Sr^{2+}) and Jurassic sea water (Ca^{2+}, Mg^{2+}, K^+ and SO_4^{2-}). For both scenarios, the geochemical system was governed in the simulations by a mineral equilibrium with carbonates and pyrite for pCO_2 of $10^{-2.7}$ bar (A) and 10^{-3} bar (B)

according to the atmospheric pCO_2 during the time of deposition (Section 5.2.3). The results for Scenario 1R are given in Figure 5.6a–d and for Scenario 2J in Figure 5.6e–h.

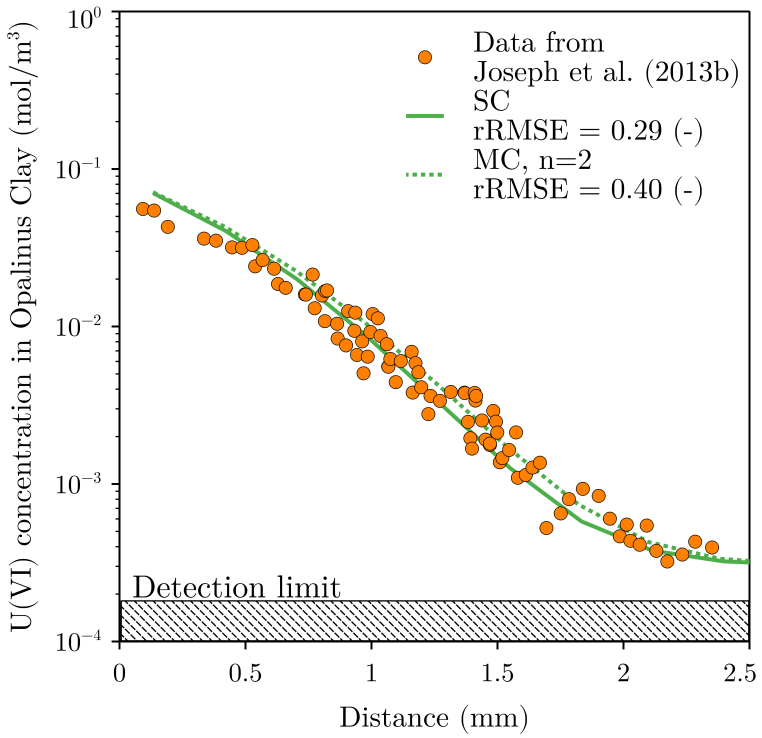

Figure 5.5: The model is validated for uranium sorption and diffusion. SC (solid line) as well as MC (dashed line, n = 2) simulation results coincide with the laboratory data (dots) of the diffusion experiment with U(VI) and Opalinus Clay using a mineral composition of 23 wt.% kaolinite, 9 wt.% illite and 4 wt.% illite/smectite mixed layers.

The simulated pore water profiles of Ca^{2+}, Mg^{2+}, pH and pCO_2 coincide especially well with measured data using the initial pore water composition according to the Opalinus Clay at Mont Russelin (Scenario 1R, Figure 5.6a–d) and applying SC diffusion (solid line). Only the concentrations of Mg^{2+} were about 0.003 mol/L higher in relation to the observed values (Figure 5.6b). The application of MC diffusion (dashed line) increased modelled concentrations for Ca^{2+} (around 0.006 mol/L) as well as Mg^{2+} compared to the SC results (Figure 5.6a and b). Especially Mg^{2+} deviates even more with about 0.01 mol/L compared to the measured data using MC diffusion. The profiles of pH were almost equal for SC and MC diffusion (Figure 5.6c), whereas pCO_2 values were up to 0.3 log units lower in the MC simulations compared to SC (Figure 5.6d). The hydrogeological opening of the aquifers was reflected in the profiles of pH and pCO_2 by a wave-like signal close to the model boundaries. Best results for pH were obtained for an initial pCO_2 of $10^{-2.7}$ bar (A) resulting in a pCO_2 of around $10^{-2.3}$ bar within the low permeable section. The profiles of Ca^{2+} and Mg^{2+} were unaffected by the variation in pCO_2 (A and B). Results of the other pore water components are given in the Supplementary S-5 (Figure E.1).

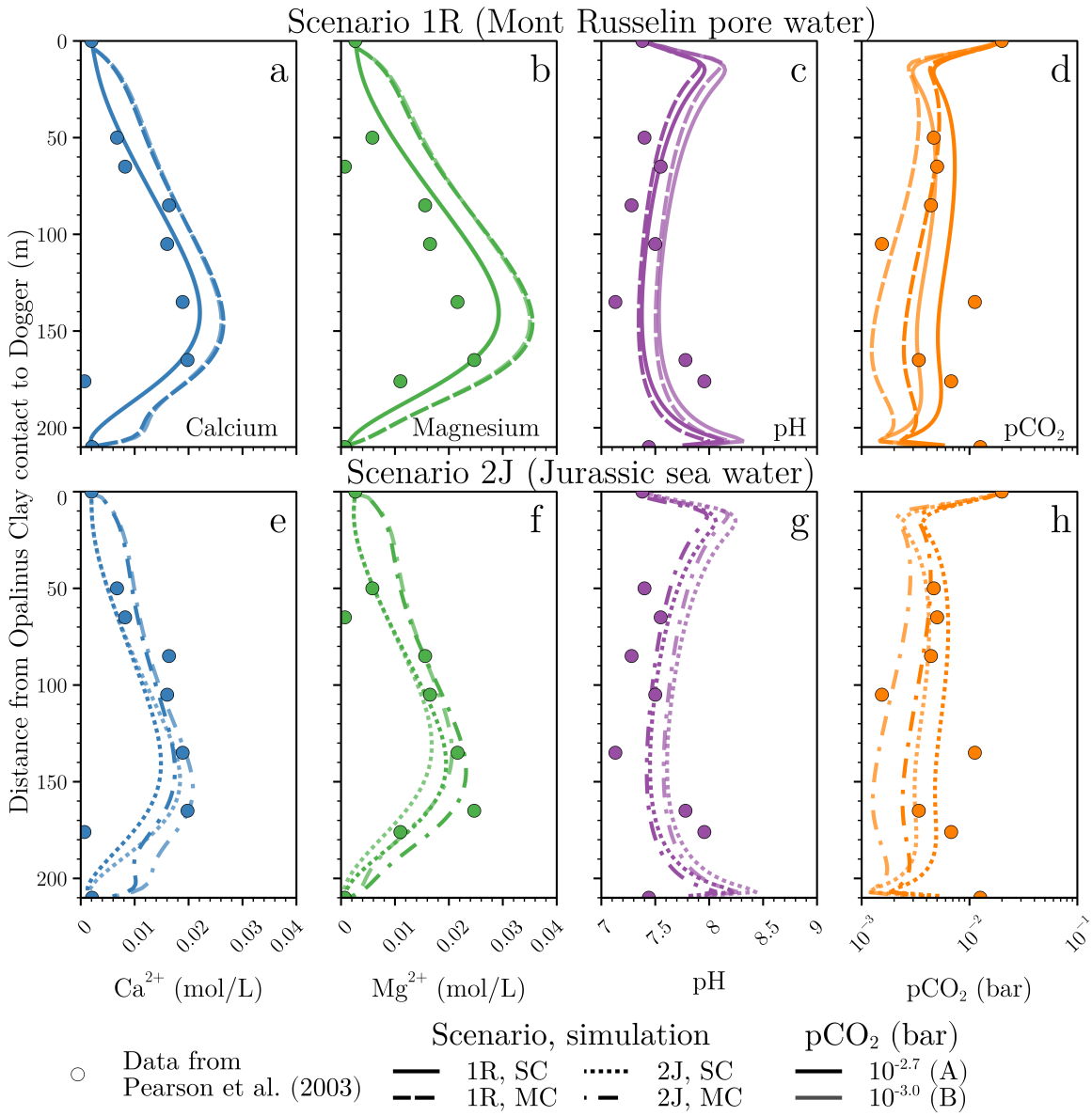

Figure 5.6: Pore water profiles of Ca^{2+} (**a**, **e**), Mg^{2+} (**b**, **f**), pH (**c**, **g**) and pCO_2 (**d**, **h**) were confirmed using the initial concentrations according to the data-driven scenario (1R, a–d) and the conceptual scenario (2J, e–h) applying SC (solid and dotted lines) as well as MC diffusion (dashed and dash-dotted lines). Initial pore waters were equilibrated with calcite, dolomite, siderite as well as pyrite for pCO_2 of $10^{-2.7}$ bar (A) and 10^{-3} bar (B). Total simulation time was six million years with the footwall aquifer only being active for the last 0.5 million years. The data stem from borehole analyses at the underground laboratory Mont Terri (Pearson et al., 2003).

Using the combination of Jurassic sea water and Liassic groundwater as initial composition (Scenario 2J, Figure 5.6e–h), the resulting profiles match better with the observed data applying MC diffusion (dash-dotted line) in contrast to Scenario 1R. However, maximum concentrations of Ca^{2+} and Mg^{2+} (Figure 5.6e and f) were up to 0.003 mol/L lower compared to measured values. Using SC (dotted line), maximum concentrations in the modelled profiles were even lower with differences of up to 0.008 mol/L. The profiles of pH and pCO_2 were almost equal to those of Scenario 1R. Best results for pH were also obtained for an initial pCO_2 of $10^{-2.7}$ bar (A).

Applying MC diffusion, this led to a pCO_2 of around $10^{-2.55}$ bar within the low permeable section. In contrast to Scenario 1R (Figure 5.6a and b), increasing the initial pCO_2 to $10^{-2.7}$ bar (A) was associated with lower Ca^{2+} and higher Mg^{2+} concentrations (Figure 5.6e and f) compared to simulations with an initial pCO_2 of 10^{-3} bar (B). Results of the other pore water components are given in the Supplementary S-5 (Figure E.2).

From a purely visual ranking, best matches between modelled and measured data were observed for the simulations SC-1R-A and MC-2J-A. Therefore, they were selected for the subsequent investigations of uranium migration. Furthermore, best results were obtained for both scenarios using an initial pCO_2 of $10^{-2.7}$ bar (A) according to the atmospheric pCO_2 around the TJB 200 Ma ago.

5.4.2 Simulation of potential uranium migration within a geochemical gradient

Potential migration of uranium within a geochemical gradient was simulated for the hydrogeological system of the Opalinus Clay at the Mont Terri based on present-day pore water profiles within the 210 m thick low permeable section (Section 5.2.1). As described above (Section 5.4.1), best results for the modelled profiles were obtained with the simulations SC-1R-A and MC-2J-A (Figure 5.6). Two different locations for the potential repository were investigated. One in the centre of the low permeable section at a distance of around 100 m from the contact between Opalinus Clay and Dogger limestone (Figure 5.7a) and the other at a distance of around 150 m (Figure 5.7b) close to the transition between Opalinus Clay and Liassic shales with the highest chloride concentrations (Figure 5.4). Figure 5.7c displays the distribution coefficients K_d (m^3/kg, Section 5.2.4) of uranium for the two scenarios. The boundary conditions were kept constant during the simulation with both aquifers at the model outlets active (Figure 5.2b). The impact of the geochemical gradient on uranium migration was quantified by comparison with previous SC simulations of homogeneous models (red lines, Figure 5.7) as a function of pCO_2 (Hennig et al., 2020). For best comparison between both, simulation runs with most similar pCO_2 for the systems were chosen (Figure 2.5). This means, results of Scenario 1R-A (average $pCO_2 = 10^{-2.3}$ bar, Figure 5.6d) were projected onto simulations for a pCO_2 of 10^{-2} bar and 2J-A (average $pCO_2 = 10^{-2.55}$ bar, Figure 5.6h) with simulations for a pCO_2 of $10^{-2.5}$ bar.

Uranium migrated farther through the formation in the heterogeneous simulations taking into account the geochemical gradient compared to the homogeneous model with similar pCO_2 (red lines, Figure 5.7a and b). Migration distances from the potential repository located 100 m below the contact Opalinus Clay and Dogger limestone (Figure 5.7a) towards the hanging wall aquifer (Dogger) ranged between 25 m (SC, Scenario 2J-A, purple dotted line) and 50 m (SC and MC, Scenario 1R-A, cyan lines). Distances towards the footwall aquifer (Liassic) were 20 m (SC and MC, Scenario 2J-A, purple lines) and 40 m (SC and MC, Scenario 1R-A, cyan lines). Compared to the migration lengths of the homogeneous models with maximum distances between 16 m (red dashed line, Figure 5.7) and 26 m (red solid line, Figure 5.7),

the geochemical gradients enhanced uranium migration into the formation between +4 m (Scenario 2J-A, in relation to the red, dotted line with 16 m) and +24 m (Scenario 1R-A, reference to the red, solid line with 26 m). Consequently, differences between migration lengths of homogeneous and heterogeneous models were less pronounced for Scenario 2J-A compared to 1R-A. Moreover, uranium migrated farther through the formation towards the Dogger limestones and, for Scenario 1R-A, twice as far as for Scenario 2J-A. No significant deviations in migration distances between SC and MC simulations were observed.

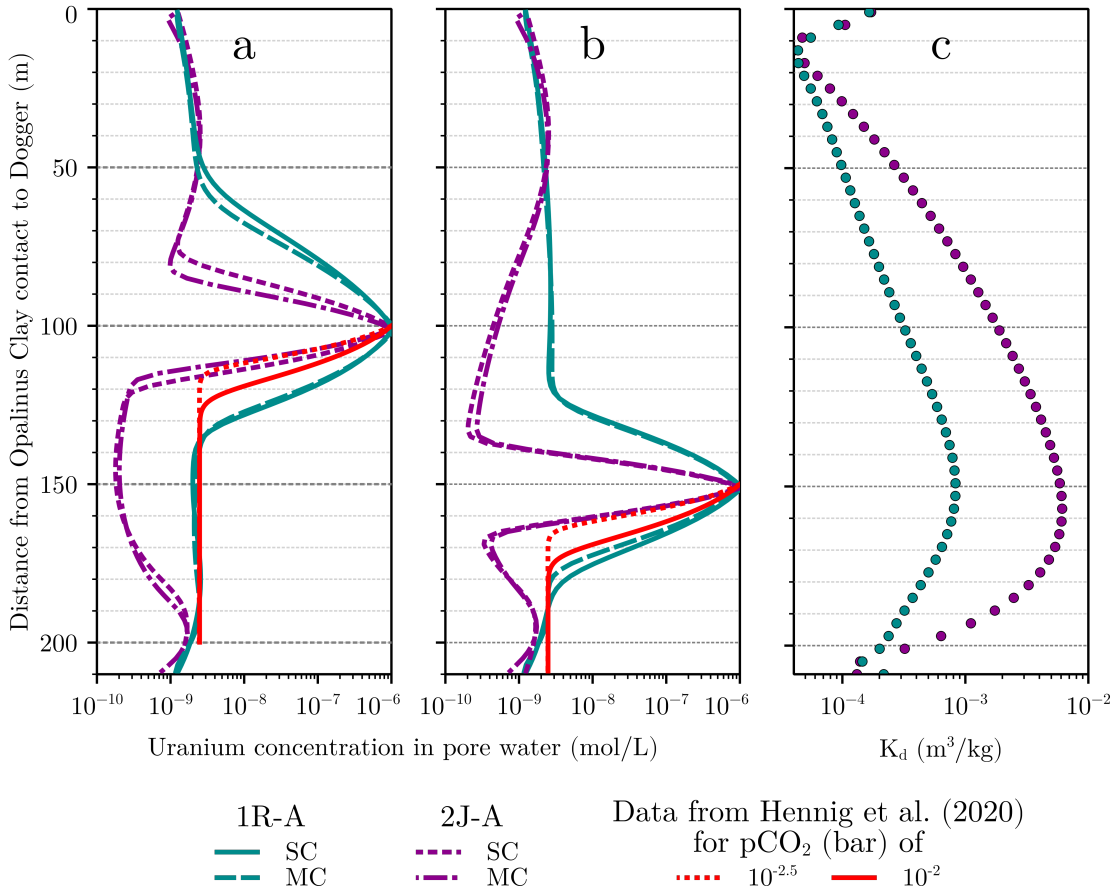

Figure 5.7: Migration of uranium in the Opalinus Clay formation is increased by +4 m to +24 m for heterogeneous systems compared to homogeneous models (red line, Hennig et al., 2020). The uranium source term representing a potential repository was located at a distance of 100 m (**a**) and 150 m (**b**) below the contact Opalinus Clay and Dogger limestone (y-axis). SC and MC simulations were performed for Scenario SC-1R-A (solid and dashed line) and MC-2J-A (dotted and dash-dotted line) and the corresponding distribution coefficients K_d (m^3/kg) of uranium between pore water and mineral phases (**c**) were given.

For the second location of the potential repository at 150 m below contact Opalinus Clay and Dogger (Figure 5.7b), distances towards the Dogger aquifer ranged between 15 m (SC and MC, Scenario 2J-A, purple lines) and 30 m (SC and MC, Scenario 1R-A, cyan lines). Towards the Liassic aquifer, distances were 20 m (SC and MC, Scenario 2J-A, purple lines) and 35 m (SC, Scenario 1R-A, solid cyan line). Compared to Figure 5.7a, migration distances from the peak of the geochemical gradient were thus decreased by up to -20 m. However, uranium migration was still enhanced by the gradients compared

to homogeneous models. Uranium concentrations close to the model outlets were below the natural background concentration (red lines, Figure 5.7a and b).

Figure 5.7c shows the distribution coefficients K_d (m^3/kg) for both scenarios. Values for Scenario 1R-A (cyan symbols) ranged from $4 \cdot 10^{-5}\,m^3/kg$ up to $8 \cdot 10^{-4}\,m^3/kg$. For Scenario 2J-A (purple symbols), K_d values differed between $4 \cdot 10^{-5}\,m^3/kg$ and $6 \cdot 10^{-3}\,m^3/kg$ with up to one order of magnitude larger compared to Scenario 1R-A at the same depth. For both scenarios, a gradient in K_d values towards the aquifers can be observed with the highest values at a depth of around 160 m.

5.5 Discussion

Speciation of uranium in the Opalinus Clay, and thus sorption and diffusion, are governed by the calcite-carbonate-ion system as we know from the study of Hennig et al. (2020). With their simulations, the authors showed that the geochemistry of the system, predominantly pCO_2, Ca^{2+} concentration and pH, is more decisive for uranium migration than the quantity of clay minerals (Chapter 2). For instance, an increase in pCO_2 is associated with higher concentrations of carbonate, Ca^{2+} and Mg^{2+} in the pore water decreasing sorption of uranium due to changes in the chemical speciation (Hennig et al., 2020). This, in turn, means that changes of the geochemical conditions directly influence the migration behaviour of uranium. As we consider the same geochemical system here, these findings are also valid for the presented results. Transport parameters determined for homogeneous conditions in the laboratory might no longer be applicable on the host rock scale (Hennig and Kühn, 2021a). Therefore, we extended the studies of Mazurek et al. (2011) concerning the chloride profile at Mont Terri and included all other pore water components to quantify the influence of geochemical gradients on uranium migration for the host rock scale and a simulation time of one million years.

5.5.1 Diffusion and mineral interaction control pore water profiles

Profiles of Ca^{2+}, Mg^{2+}, pH and pCO_2 were modelled for two different initial pore water compositions (Scenario 1R and 2J) comparing SC and MC diffusion. Measured values within the hydrogeological system of the Mont Terri were reproduced with both scenarios, the data-driven (1R) and conceptual (2J). The initial pore waters were equilibrated with the carbonates and pyrite as a function of different pCO_2 with best results obtained for both scenarios for an initial pCO_2 of $10^{-2.7}$ bar (A). This value corresponds to the atmospheric pCO_2 around the TJB, prior to the time of deposition. The best matches between measured data and modelled profiles were obtained with the SC simulations of Scenario 1R-A and MC diffusion of 2J-A. For both scenarios, application of MC diffusion resulted in higher concentrations of Ca^{2+} and Mg^{2+} as well as lower pCO_2 values compared to the SC simulations, although the initial states of SC and MC diffusion were identical. An increase in pCO_2 was associated with higher Mg^{2+} and lower Ca^{2+} concentrations as well as pH compared to simulations with lower pCO_2, whereas Ca^{2+} and Mg^{2+} profiles of Scenario 1R were unaffected by the variation in pCO_2.

Smaller pore water diffusion coefficients D_p (m^2/s) of the individual species decrease exchange between aquifers and Opalinus Clay using MC diffusion. In the SC simulations, the reference of the D_p is the one of Cl^- with $5.3 \cdot 10^{-11}$ m^2/s (Section 5.2.5). For the MC approach, the applied D_p of Ca^{2+} and Mg^{2+} were with values of $2 \cdot 10^{-11}$ m^2/s and $1.8 \cdot 10^{-11}$ m^2/s, respectively smaller. This, in turn, explains the higher concentrations within the low permeable section due to a reduced diffusive transport towards the aquifers. Of course, this does not only apply for the diffusive transport towards the aquifers and out of the Opalinus Clay, but also in the opposite direction, from the aquifers into the formation. For instance, the pCO_2 values of the surrounding aquifers were higher compared to the initial state of the low permeable section. Therefore, HCO_3^- migrated from the aquifers into the formation leading to an increase of pCO_2 within the low permeable section, especially close to the model outlets. Due to the smaller D_p of HCO_3^- with $3 \cdot 10^{-11}$ m^2/s in the MC simulations, less HCO_3^- diffused into the formation resulting in lower pCO_2 values of the MC simulations compared to SC for the same initial state. Due to the more recent exchange with the Liassic aquifer, the lowest pCO_2 values were observed at a depth of around 160 m corresponding to the contact between Opalinus Clay and Liassic shales with the highest chloride concentrations (Figures 5.3 and 5.6d and h).

Pore water concentrations of Ca^{2+} and Mg^{2+} are governed by the Mg/Ca ratio set by the selected stability constants of the carbonates and not as much by the initial values. The applied scenarios differ considerably for some of the initial concentrations (Table 5.1). For instance, the Ca^{2+} concentration within Scenario 2J is only about half of that of 1R. Nevertheless, the measured Ca^{2+} profile is reproduced by both scenarios in similar way. The deviations of the modelled profiles of Scenario 2J correspond thereby with values of 0.008 mol/L for SC and 0.003 mol/L for MC to less than 50% in relation to the measured data and to the results of Scenario 1R. The governing mineral equilibria are set by calcite and dolomite. The stability constant of calcite has been adapted in the underlying database to account for the incorporation of magnesium into the crystal structure (Möller and De Lucia, 2020). To determine this, the ion ratio of the chemical signatures found in the Opalinus Clay pore waters at Mont Russelin (Section 5.2.3) were used resulting in initial Mg/Ca ratios of around 1.37 and 1.36 for Scenarios 1R and 2J, respectively. This is the reason why variations of pCO_2 of the mineral equilibria only affect the Ca^{2+} and Mg^{2+} concentrations of Scenario 2J with an original Mg/Ca ratio of 1.27 (Table 5.1). Since Scenario 1R is based on the same pore water as used for the determination of the stability constant, the investigated pCO_2 results in almost equal concentrations of Ca^{2+} and Mg^{2+} to reach thermodynamic equilibrium. Only pH is significantly affected as more or less CO_2 needs to be dissolved in the system to keep the Mg/Ca ratio for the applied pCO_2 in equilibrium with the carbonates. In further numerical experiments (not shown) using the original log K of the database for pure calcite, resulting Ca^{2+} and Mg^{2+} concentrations were always too low. The determined Mg/Ca ratios between 1 and 1.3 coincide with present-day ratios at Mont Terri (Pearson et al., 2003). Consequently, in addition to the plausible choice of initial

concentrations, the selection of the underlying thermodynamic data is also decisive for the mineral equilibria.

We have therefore shown with our simulations that present-day pore water profiles within the hydrogeological system at Mont Terri are understood on the one hand with a data-based concept (Scenario 1R). On the other hand, the same results are achieved starting with an estimate of the initial conditions derived from the geological evolution of the formation (Scenario 2J), especially considering process-based MC simulations as closer to reality of diffusion in claystones. Whether this approach is transferable to formations with a similar geochemical system and known geology, but without location specific geochemical data, will be examined in future works.

5.5.2 Geochemical system governs uranium migration

Geochemical pore water gradients in heterogenous systems increase the migration length from an uranium source in the Opalinus Clay. We quantified the impact of the measured and simulated geochemical gradient on the migration lengths of uranium with +4 m (Scenario 2J-A) and +24 m (Scenario 1R-A, Figure 5.7a and b) for the hydrogeological system of the Opalinus Clay at Mont Terri in relation to homogeneous, meaning geochemically constant, SC models (Chapter 2, Hennig et al., 2020). Simulations were performed using SC as well as MC models, whereby both SC models, homogeneous and heterogeneous, were used with a D_e of $1.9 \cdot 10^{-12}\,m^2/s$ experimentally determined for uranium in the Opalinus Clay by Joseph et al. (2013b). Thereby, the comparison between homogeneous and our heteregenous SC simulations showed the influence of the geochemical gradients on the sorption capacity. The deviations between heterogeneous MC and SC simulations additionally demonstrate the impact on diffusion. However, as there were no significant differences between MC and SC simulations on the host rock scale (±5 m, Figure 5.7a and b), the differences in migration lengths can be attributed to the geochemical gradient and associated changes in the sorption capacity. This means experimentally determined D_e can be used in SC models for the host rock scale. However, this does not apply for the respective K_d values.

Uranium migrates farther in the formation considering the geochemical gradients due to an associated decrease in sorption capacity from the peak of the concentration gradient towards the embedding aquifers. From a conceptual point of view, the K_d in the homogeneous simulations is constant over the whole model length, and thus the ratio between sorbed and transported uranium from one model element to the next is the same with every transport step. In contrast, the K_d between two model elements differs in the heterogeneous simulations. From the highest values at a depth of around 160 m below contact Opalinus Clay and Dogger limestone it decreases by up to one order of magnitude towards the aquifers (Figure 5.7c). This means that with each transport step towards the aquifers, proportionally less uranium is sorbed, and thus more is transported by diffusion, compared to the homogeneous model with constant K_d. One important parameter for the sorption of uranium on clay minerals is the pH (Hennig et al., 2020), which also provides the geochemical explanation for the changes in K_d within the gradients.

The pH controls speciation of uranium as well as the charge of the functional groups on the clay mineral surfaces (Li et al., 2016; Saleh and Yun, 2017). With rising pH above 7, sorption of uranium on clay minerals decreases due to changes in the sorption processes from cation exchange to surface complexation (Joseph et al., 2013a; Kim, 2001; Li et al., 2016; Tournassat et al., 2018). Further, the negative surface charge of the clay minerals also increases, and thus negatively charged species are more repelled. As uranium is predominantly present in anionic and neutral complexes with Ca^{2+} and Mg^{2+} in the investigated geochemical system (Hennig and Kühn, 2021a; Hennig et al., 2020), less uranium is sorbed with rising pH as the proportion of these complexes additionally increases (Saleh and Yun, 2017). Within the modelled pH profiles (Figure 5.6c and g), the lowest values were observed at a depth of around 160 m (pH = 7.4). From that point, values of pH increases towards the aquifers by up to 0.7 log units (pH = 8.1) before they decrease again. The K_d profiles were opposed to the pH, accordingly (Figure 5.7c). Moreover, as pH is above 7, sorption of uranium increases with ionic strength due to changes in the electrochemical interaction (Li et al., 2016; Tournassat et al., 2018). The ionic strength governs the thickness of the DDL that compensates the negative surface charge of the clay minerals by the attraction of cations. This means with decreasing ionic strength, the thickness of the DDL increases, and thus the repulsion of negatively charged species (Appelo and Wersin, 2007; Wersin et al., 2018). This also explains, why the migration lengths for the two investigated locations as well as towards the Dogger and Liassic aquifer differ (Figure 5.7a and b). Consequently, the location of a potential repository within a geochemical gradient is important as uranium migrates farther with decreasing gradients compared to the opposite direction.

The pCO_2 of the system is more decisive for the migration length of uranium than the geochemical gradient. The differences between homogeneous and heterogeneous simulations and with that the impact of the geochemical gradient on uranium migration lengths were at maximum +9 m and less pronounced for Scenario MC-2J-A compared to +24 m for Scenario SC-1R-A, although the pore water profiles, especially pH, were almost identical (Figure 5.6). Further, K_d values of Scenario 1R-A were roughly an order of magnitude lower compared to 2J-A (Figure 5.7c) so that uranium migrated twice as far (Figure 5.7a and b). This can be explained by the difference in pCO_2 of around 0.25 log units between both scenarios (Figure 5.6d and h). With increasing concentration of dissolved carbonate in the system, sorption of uranium decreases due to the formation of ternary complexes (Bachmaf et al., 2008; Fox et al., 2006; Philipp et al., 2019; Tournassat et al., 2018) as already discussed by Hennig et al. (2020). This, in turn, means the lower the pCO_2 value of the considered system, the higher are the associated sorption capacities for uranium and the influence of the geochemical gradient on the migration lengths is consequently diminished as can be seen in our simulation results (Figure 5.7a). However, the influence of the gradient becomes more dominant with increasing pCO_2. For instance, uranium migrated farther in the heterogeneous simulations for a pCO_2 of around $10^{-2.3}$ bar compared to the homogeneous models with a pCO_2 of 10^{-2} bar.

Accordingly, the priority list for uranium migration in the Opalinus Clay (pCO_2 > Ca^{2+} > pH > pe > hydro-physical parameters > amount of clay minerals) provided by Hennig and Kühn (2021a) can be confirmed and revised as follows: pCO_2 > hydrogeological system and inherent geochemical gradient > mineralogy (heterogeneity and clay mineral quantity). Moreover, experimentally determined K_d values can not be applied to complex heterogeneous hydrogeological systems like the Opalinus Clay at Mont Terri.

5.6 Conclusions and outlook

Heterogeneous models with resulting geochemical gradients significantly influence the migration of uranium in terms of increased migration lengths. The impact of a geochemical gradient on uranium diffusion and sorption was shown in one-dimensional simulations for the hydrogeological system of the Opalinus Clay at the Mont Terri anticline (Switzerland) with single- (SC) and multi-component (MC) diffusion approaches by comparing the migration lengths with homogeneous, e.g. geochemically constant, SC models. In contrast to SC models, where one diffusion coefficient is used for all species, with the MC approach, each species in the system is assigned its own diffusion coefficient, and thus a more process-based description of diffusive transport is enabled. For this, an empirical medium-specific parameter needs to be calibrated, which we did successfully by means of present-day pore water data and a laboratory diffusion experiment with uranium and Opalinus Clay. Sorption processes were integrated via surface complexation and cation exchange using a bottom-up approach and quantified by means of the distribution coefficient K_d (m^3/kg). By comparing the migration lengths of the SC models, homogeneous and heterogeneous, the influence of the geochemical gradient on uranium sorption can be determined and on diffusion by the heterogeneous SC and MC results. Numerical simulations are required to quantify diffusion of uranium for a heterogeneous system on the repository scale.

The hydrogeological system needs to be conceptualised and calibrated first before the subsequent uranium migration within a geochemical gradient can be quantified for a simulation time of one million years. The Opalinus Clay and Liassic shales are part of a 210 m thick low permeable section embedded between Dogger (hanging wall) and Liassic aquifers (footwall). Both aquifers form the current hydrogeological boundaries of the system. Erosion of the anticline in certain areas led to flushing of the aquifers with freshwater and subsequent diffusive exchange with the pore waters of the low permeable section. The Dogger aquifer was activated about six million years and the Liassic 0.5 million years ago resulting in an asymmetric pore water profile within the Opalinus Clay and geochemical pore water gradients.

Present-day pore water data from comprehensive borehole analyses at the underground laboratory Mont Terri were used to calibrate various models. Two scenarios for the composition of the pore water prior to activation of the aquifers were used. Scenario 1R (data-driven) is based on Opalinus Clay pore water from the nearby Mont Russelin, where the aquifers have and had no contact with meteoric water and the pore waters are therefore considered as unaffected representing unchanged

chemical signatures since deposition. Scenario 2J (conceptual) is a combination of Liassic groundwater from Mont Russelin and Jurassic sea water according to the time of deposition of the Opalinus Clay 180 Ma ago. The pore waters were initially equilibrated depending on pCO_2 with the inherent carbonates (calcite, dolomite, and siderite) as well as pyrite governing pH, redox state and concentrations of main ions of the system. Due to the uncertainty regarding the atmospheric pCO_2 around the time of deposition, two values were used. The pCO_2 of case A was $10^{-2.7}$ bar corresponding to the value around the Triassic-Jurassic-Boundary (TJB) 200 Ma ago and for case B a pCO_2 of 10^{-3} bar was used according to post-TJB values. The application of MC diffusion resulted in higher concentrations of Ca^{2+} and Mg^{2+} as well as lower pCO_2 values compared to the SC simulations due to differences in the D_e (m^2/s), and thus a decreased diffusive exchange between aquifers and low permeable section. Accordingly, best visual match between observed and modelled profiles were obtained for the simulations SC-1R-A and MC-2J-A and were therefore selected for the subsequent uranium migration. Pore water profiles were reproduced solely by diffusive exchange between aquifers and Opalinus Clay for both scenarios and an initial pCO_2 of $10^{-2.7}$ bar. Our results thus indicate that the pCO_2 in the Opalinus Clay corresponds to old signatures of the TJB.

Migration lengths of homogeneous and heterogeneous models deviated, what can be attributed to changes in the sorption considering the geochemical gradients. No significant differences between heterogeneous MC and SC simulations ($\pm$5 m) were observed. Therefore, the geochemical gradient has only a minor influence on diffusion and major on sorption processes. This implies that uranium migration in the Opalinus Clay can be adequately quantified with SC models using experimentally determined diffusion coefficients, but this does not apply to the respective K_d values.

Depending on the location of a potential repository within the geochemical gradient, uranium migrated between +4 m and +24 m farther through the formation compared to homogeneous models due to a decreased sorption capacity associated with the gradients. Two different depths of a potential repository within the geochemical gradients were investigated. One in the centre of the low permeable section with maximum migration distances of 50 m and 40 m towards the Dogger and Liassic aquifer (Scenario 1R-A) and the other around the peak of the concentration gradient with migration lengths of 30 m and 35 m (Scenario 1R-A), respectively. Consequently, with increasing ionic strength, more uranium is sorbed on the clay minerals, and thus migrates less far through the formation. The thickness of the diffuse double layers (DDL) compensating the negative surface charge of the clay minerals depends on ionic strength. The more ions are dissolved in the pore water, the thinner is the DDL and ions can sorb on the functional groups of the clay minerals. Besides the ionic strength, sorption is mainly governed by the pH profile as values increase towards the aquifers. A rise in pH is associated with a decrease in uranium sorption due to changes in the speciation and sorption process. The proportion of anionic and neutral ternary uranyl complexes increases with pH, and thus less uranium is available for sorption. Furthermore, the sorption processes change from cation exchange to surface complexation and the negative surface is amplified by an increase in pH leading to stronger repulsion of negatively charged species

from the surfaces. Therefore, ionic strength and pH of the geochemical gradient govern uranium sorption and lead to a decrease in K_d about one order of magnitude with the gradient towards the aquifers. Consequently, experimental determined K_d values cannot be applied for the entire host rock in heterogeneous system because the geochemistry of the system strongly impacts sorption processes.

The influence of the geochemical gradient on uranium sorption, and thus its migration lengths, increases with pCO_2 values of the system. The migration lengths of Scenario 1R-A were twice as far as for Scenario 2J-A with maximum distances of 25 m and 20 m towards the Dogger and Liassic aquifer, respectively. Moreover, the difference between migration lengths was less pronounced for Scenario 2J-A with a maximum of $+9$ m in relation to 1R-A with $+24$ m. The reason for this is the approximately 0.2 log units difference in pCO_2 between Scenario 1R-A with a value of $10^{-2.3}$ bar and 2J-A with $10^{-2.55}$ bar. The pCO_2 of the considered geochemical system is the most controlling factor for uranium sorption processes in the Opalinus Clay. With increasing pCO_2, sorption of uranium decreases due to the formation of the ternary uranyl complexes. Therefore K_d values of 2J-A with maximum values of $6 \cdot 10^{-3}$ m^3/kg were almost an order of magnitude larger compared to 1R-A with $8 \cdot 10^{-4}$ m^3/kg. Accordingly, the influence of the geochemical gradient decreases for pCO_2 values $< 10^{-2.5}$ bar as sorption increases. Therefore, the governing parameters for uranium migration can be ordered in descending priority: pCO_2 $>$ hydro-geological system and inherent geochemical gradients $>$ mineralogy (heterogeneity and clay quantity).

The sensitivity of uranium sorption processes requires a precise description and quantification of the geochemical system for future performance assessments. Otherwise, the uncertainty in maximum migration length can be several tens of metres. However, the uranium concentration close to the aquifers were below or equal the background concentration, and thus the bounding aquifers were not reached and uranium is effectively retained within the host rock. Whether our findings can be transferred to other potential clay formations needs to be examined in detail in future works. Nevertheless, our findings provide orientation and a workflow for similar geochemical systems.

Chapter 6

Discussion

A precise quantification of radionuclide transport on the host rock scale is essential for assessments of potential disposal concepts to provide safety for time periods of up to one million years. Due to the spatial and temporal scales, numerical simulations are indispensable to determine migration lengths, here of uranium as the main component in spent fuel through the potential host rock Opalinus Clay. Accordingly, diffusion retarded by sorption on the inherent clay minerals governs the resulting migration distances, whereby both processes depend on mineralogy and pore water geochemistry. The presented reactive transport models apply for the first time advanced approaches to the host rock scale in order to account for heterogeneous mineralogical and geochemical conditions. These include single- (SC) and multi-component (MC) diffusion in combination with surface complexation models (SCM) and cation exchange. The publications presented in the previous chapters provide new insights in the understanding of uranium diffusion and sorption as well as their governing parameters, and thus improve the quantification of migration lengths in natural, heterogeneous systems. The main research objectives of the current thesis are:

(1) to evaluate the impact of the mineralogical and geochemical heterogeneities between the three Opalinus Clay litho-facies on uranium sorption processes,

(2) to identify a potential facies dependence of diffusion processes by a process-based implementation of the first objective and

(3) to assess the hydrogeological system and inherent geochemical gradients of the Opalinus Clay formation to understand their impact on uranium migration lengths.

It became clear that migration lengths are governed by the geochemistry of the pore water, in particular the partial pressure of carbon dioxide (pCO_2), and less by the mineralogy. Thereby, sorption rather than diffusion processes are primarily affected by heterogeneities. The following points arise for the discussion of the main findings to quantify uranium migration through the Opalinus Clay:

- An accurate geochemical description of the system is essential (Section 6.1).
- The quality of data underlying a model must be determined (Section 6.2).
- The accuracy and predictive power of models must be quantified (Section 6.3).

Recommendations for performance assessments of potential disposal sites in clay formations result from the discussion of the main findings that might also contribute, for instance, in the site selection process in Germany.

6.1 Pore water geochemistry governs uranium migration

Reactive transport simulations are used in order to evaluate the impact of mineralogical heterogeneities between the three Opalinus Clay litho-facies (shaly, sandy and carbonate-rich) on uranium migration, i.e. diffusion and sorption processes, within one million years. Process-based approaches, such as SC, MC, SCM and cation exchange, are applied to quantify uranium migration on the host rock scale taking into account mineralogical and associated geochemical heterogeneities (Hennig and Kühn, 2021a; Hennig et al., 2020) as well as the impact of the hydrogeological system (Hennig and Kühn, 2021c). In all publications and simulations presented in the previous chapters, migration lengths were primarily determined by the geochemistry of the pore water rather than clay mineralogy (Hennig and Kühn, 2021a,c; Hennig et al., 2020). Thereby, the geochemical conditions in the Opalinus Clay formation are determined by water-rock interactions, whereby the geochemical framework is primarily governed by the diffusive exchange with the embedding aquifers, i.e. the hydrogeological system itself (Hennig and Kühn, 2021c). Ultimately, the pCO_2 of the system is the key parameter, and thus also relevant for laboratory experiments. Modelling uranium migration in the Opalinus Clay, a facies dependence of sorption rather than of diffusion processes stems from changes in the geochemical conditions as a result of the hydrogeological system with its inherent gradients, and therefore the controlling parameters can be ordered as follows: pCO_2, hydrogeological system and mineralogy (Hennig and Kühn, 2021c; Hennig et al., 2020).

Geochemistry of the pore water has a major impact on sorption and minor on diffusion processes. Due to the complex chemistry, uranium is mainly present in the Opalinus Clay as U(VI) in anionic and/or neutral ternary complexes with calcium, magnesium and carbonate (Figure 2.3 and Table 2.2). Thereby, the charge of the complexes determines the interaction with the diffuse double layers (DDL) on the clay mineral surfaces, and thus the diffusive transport pathways (Figure 1.2). In other words, diffusion of anionic species is hampered by anion exclusion effects, whereas for neutral ones this is not the case. To take these interactions as a function of geochemical variations into account, process-based approaches are required, like the MC option implemented in PHREEQC. However, these approaches are associated with an increased computational effort. Accordingly, one research question addressed in the current thesis was, what does the application of the MC approach ultimately mean in metres difference compared to SC simulations, and thus how relevant is MC actually on the host rock scale. For this purpose, MC simulations were performed as a function of clay mineral compostion (Figure 3.3), variations in the hydro-physical parameters (Figure 3.5) as well as of the hydrogeological system (Figure 5.7) and compared with SC simulations in terms of migration lengths after one million years. Thereby, it has been shown that migration lengths differ between the two approaches due to anion exclusion effects and that they depend on the pore water geochemistry of the facies. Furthermore, the hydro-physical parameters govern migration lengths as they determine the quantity of rock per kg pore water, and thus the amount of water in the pore space as well as in the DDL (Section 3.5.2). Considering the facies individually,

migration lengths depend on the chosen hydro-physical parameters and can deviate by >10 m between the SC and MC approach (Figure 3.6). Thereby, a higher amount of clay minerals, such as in the shaly facies, is associated with a stronger compensation of variations in geochemistry (Section 2.5.2 and 3.5.3). From this point of view, one could say that MC is relevant for the host rock scale. However, taking into account the hydrogeological system of the Opalinus Clay at Mont Terri with the inherent geochemical gradients migration lengths between MC and SC simulations only deviate by ±5 m, whereas the difference to homogeneous, i.e. geochemically constant, simulations can be several tens of metres (Figure 5.7). This emphasizes that geochemistry primarily affects sorption rather than diffusion processes as distances of SC and MC simulations are almost equal in the heterogeneous system (Section 5.5.2). Therefore, the SC approach is sufficient to quantify uranium diffusion processes on the host rock scale. Moreover, the data availability and quality is very important for the MC approach and affects the resulting distances, what will be discussed in detail in Section 6.2. Consequently, uranium diffusion processes can be adequately quantfied with experimentally determined effective diffusion coefficients D_e (m^2/s) and SC models as differences to process-based MC simulations are negligible on the host rock scale but this does not apply to the respective distribution coefficients K_d (m^3/kg), and thus to sorption processes.

The application of constant sorption parameters in diffusion models lead to an underestimation of uranium migration distances (Figure 6.1). In the study of Hennig and Kühn (2021c), the impact of the hydrogeological system on uranium migration was considered with a maximum distance of 50 m after one million years. As discussed above, migration lengths differ between SC and MC diffusion only by ±5 m on the host rock scale. Therefore, the K_d plays a major role for simulations following Fick's laws. For instance, uranium migrated only about 5 m through the formation using the K_d determined by Joseph et al. (2013b) with a value of 0.025 m^3/kg (red, solid line, Figure 6.1), which clearly deviates from the maximum of 50 m (green line, Figure 6.1). In Hennig and Kühn (2021c), K_d values are given for the two investigated scenarios, the data-driven (1R) based on a sample taken from the Opalinus Clay at Mont Russelin and the conceptual one (2J) that combines Liassic groundwater from Mont Russelin and Jurassic sea water (Section 5.2.2). Even the application of the maximum K_d values results in an underestimation of uranium migration lengths of about 10 m (red, dashed and dotted lines, Figure 6.1) compared to the respective fully coupled transport model with SCM and cation exchange (purple and green lines, Figure 6.1). Consequently, mechanistic approaches like SCM and cation exchange are required to quantify sorption as a function of geochemical changes since application of constant K_d values lead to shorter migration distances.

Sorption processes of uranium are facies dependent due to differences in pore water geochemistry that are governed by the hydrogeological system. The sorption capacity varies between the individual facies as can be seen from the migration lengths based on SC simulations presented in Figure 2.6 as well as from the calculated K_d values given in Table 3.3. Unlike as expected, the facies dependence is predominantly governed by the geochemical composition of the pore water rather than

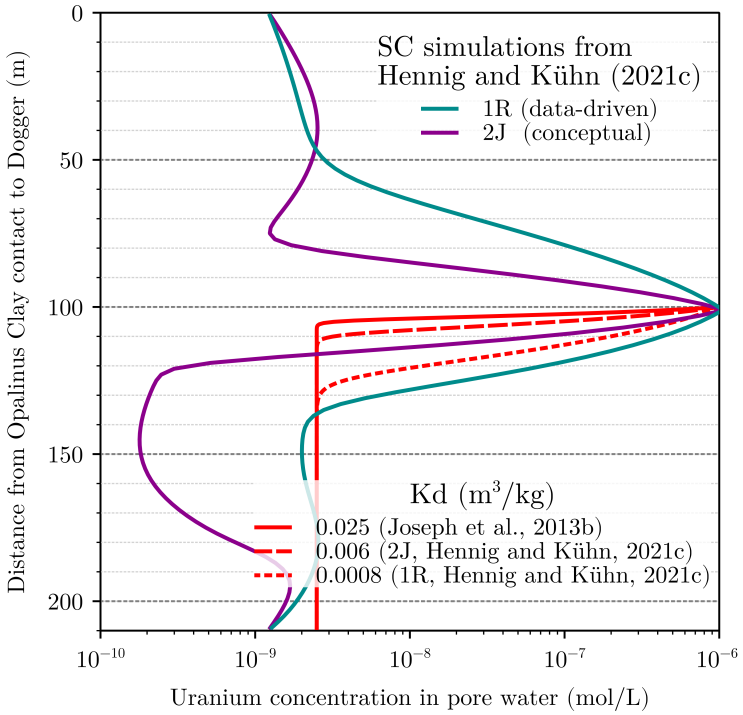

Figure 6.1: Application of constant K_d values, experimentally determined (red, solid line, Joseph et al., 2013b) or calculated with PHREEQC (red, dashed and dotted lines, Hennig and Kühn, 2021c), leads to an underestimation of migration distances compared to fully coupled reactive transport simulations (green and purple lines, Hennig and Kühn, 2021c).

by clay mineralogy, whereby pCO_2 is the most important parameter (Hennig et al., 2020). On the one hand, the composition of the pore water is a result of the original marine components, water-rock interactions such as precipitation and/or dissolution of minerals, and thus the deposition process itself (Pearson et al., 2003; Wersin et al., 2009). On the other hand, considering the whole system and not only individual facies, the diffusive exchange with the waters of the embedding aquifers governs over millions of years the geochemical conditions in the low permeable section (Hennig and Kühn, 2021c; Mazurek et al., 2011; Pearson et al., 2003). The inherent gradients established by the hydrogeological system can be observed, for example, in almost all profiles of pore water components (Figure 5.3 and Supplementary S-5) measured at the underground laboratory Mont Terri (Pearson et al., 2003). Only the profiles of pH and pCO_2 fluctuate within the formation with no pronounced gradient towards the aquifers (Figure 5.3). This indicates a buffer capacity of the clay formation since both parameters are coupled via the calcite-carbonate-ion system (Pearson et al., 2003; Wersin et al., 2009). Furthermore, all profiles could be confirmed by pure diffusion (Figure 5.6 and Supplementary S-5) without taking into account any water-rock interaction during the transport simulations (Section 5.2). Moreover, uranium sorption capacity, namely the K_d values, decrease with the concentrations of the pore water components, and thus ionic strength, by up to one order of magnitude over the >200 m thick low permeable section (Figures 5.2a and 5.7). The pCO_2 governs thereby how strong K_d values decrease with

ionic strength (Figures 5.6 and 5.7). In other words, geochemical differences between the facies due to mineralogical heterogeneities are overlaid over geological time scales by the influence of the adjacent aquifers, whereby pCO_2 determines how strongly the hydrogeological system ultimately affects sorption capacity, and thus facies dependence.

Within the Opalinus Clay formation, geochemical gradients are pronounced to different degrees. The results presented in Hennig and Kühn (2021c) are based on simulations of the Mont Terri anticline. This location is not considered for the disposal of radioactive waste due to its specific geological structure resulting from the Jura folding and asscoiated erosion history of the anticline (Mazurek et al., 2011; Pearson et al., 2003; Thury and Bossart, 1999). The potential disposal sites are located in areas that are tectonically more stable. Therefore, one could say that no geochemical gradients are to be expected there, and thus no enhanced uranium migration. Nevertheless, geochemical gradients within the Opalinus Clay were also determined at other locations. The nearby Mont Russelin anticline, for instance, was eroded less than Mont Terri so that the footwall aquifer in the Liassic has no surface contact. Nevertheless, measured chloride concentrations decrease towards the overlying Dogger, i.e. the hanging wall aquifer (Koroleva et al., 2011). Moreover, gradients can be found even at tectonically calmer areas, where the Opalinus Clay is not directly embedded between aquifers, for instance, at the sites of the exploratory drilling boreholes Benken and Schlattingen (Mazurek et al., 2009; Nagra, 2014; Wersin et al., 2018, 2016). Although the gradients at Benken and Schlattingen are less pronounced compared to the ones at Mont Terri, the geochemical conditions change across the >250 m thick, low permeable section consisting of the Lias and the Dogger with the Opalinus Clay. Accordingly, it can be assumed for both locations that K_d values will also decrease with ionic strength, and therefore cannot be taken as constant. Consequently, selective indivual explorations cannot represent the host rock and its system as a whole. This highlights that the respective hydrogeological system determines the scale to be considered and must be taken into account in any case.

The increase in computational costs associated with fully coupled reactive transport models may require a speed-up of simulations through, for instance, development of surrogate models or application of machine learning. The computational costs of reactive transport models increase with the complexity of the modelled system, i.e. the amount of components and reactions, and with the discretization refinement of the domain (De Lucia and Kühn, 2013; Leal et al., 2017a). Natural systems, like the Opalinus Clay formation, are heterogeneous on the host rock scale, and thus complex. Consequently, geochemical conditions may change over the spatial and temporal scales considered for the geological disposal of nuclear waste so that computational limits can be reached with common reactive transport models. As outlined above, this is of special relevance for the quantification of sorption processes. For this, different approaches were recently developed. For instance, the Smart K_d-approach uses pre-calculated K_d matrices based on SCM and cation exchange so that the appropriate value is then used in the transport simulation depending on the respective geochemistry (Noseck et al., 2018, 2012; Stockmann et al., 2017).

By this, the amount of equations to be solved is reduced, while it allows at the same time to consider sorption processes as a function of geochemistry. However, this requires precise knowledge of the modelled system and the expected fluctuations. Other approaches are the development of so-called surrogate models (De Lucia and Kühn, 2013, 2021) or the application of on-demand machine learning techniques (Leal et al., 2020) to solve geochemical reactions. Surrogate models reflect the behaviour of the studied geochemical system based on statistical methods (De Lucia and Kühn, 2013, 2021). They are trained with a data set containing the relevant in- and output information of the system, and thus many calculations are required in advance to teach the surrogate. For the on-demand machine learning approach, no previous training is necessary to obtain a reliable surrogate (Leal et al., 2017a, 2020). A full calculation is performed with the reactive transport model and the in- and output of all system components are stored as well. If the result of the new calculation can be estimated based on a Taylor approximation of already performed simulations, no new fully coupled simulation is required (Leal et al., 2017a). If this is not the case, the full simulation is performed again. Time saving is achieved since interpolation from stored conditions is much faster than setting up and solving a full geochemical system. Both approaches are associated with a significant programming effort and knowledge in addition to the understanding of the geochemical system, the time needed to train and set up the machine learning framework and they are limited to only simple systems, so far. For the one-dimensional system with only one radionuclide, investigated within this thesis, the application of these approaches was not considered to be justified compared to the full reactive transport model with SCM and cation exchange that are needed anyway. For more complex systems with more than one radionuclide in two- or even three-dimensional transport simulations, machine learning approaches become more relevant.

The key role of geochemistry, in particular the pCO_2, is the connecting line in the presented thesis. Concerning the main objectives of the thesis, a facies dependence of uranium sorption rather than of diffusion processes was identified. Nevertheless, the facies dependence results from the interaction between Opalinus Clay and the embedding aquifers, e.g. the hydrogeological system, and not from mineralogical heterogeneities as initially expected. Accordingly, a process-based description and hence quantification of sorption processes is indispensable. Consequently, the SC approach together with SCM and cation exchange is a powerful tool to quantify uranium migration, i.e. diffusion and sorption, in the Opalinus Clay and is therefore recommended, for instance, to be used in performance and/or safety assessments. The gained insights are not directly transferable to other potential disposal sites. However, the identified dependencies and mechanisms give implications, for instance, for the German site selection process since they are possibly also valid for clay formations with similar geochemistry. Based on the simulations, a priorization of governing paramaters was identified (pCO_2 > hydrogeology > mineralogy), and thus demonstrates how important a precise knowledge of the pCO_2 and hence of the calcite-carbonate-ion system at the potential disposal site are to quantify uranium migration.

6.2 Data quality affects resulting migration lengths

All simulations were conducted with PHREEQC (Parkhurst and Appelo, 2013), and therefore all speciation and complexation reactions are based on equations following the law of mass action and the underlying thermodynamic data sets. The relevant reactions and respective stability constants are contained in a comprehensive chemical thermodynamic database. The chosen SCM data determine thereby the charge of the surface and hence the composition of the DDL as well as they define the complexes that are considered for sorption. With the MC option, diffusion coefficients are derived analogous to Archie's law (Parkhurst and Appelo, 2013; Van Loon et al., 2007). Accordingly, the self-diffusion coefficient in water D_w (m^2/s), the accessible porosity ϵ (-) and the empirical, medium-specific parameter n (Section 3.2.3, Equation 3.5) are required or need to be calibrated, respectively. The empirical exponent n is a correction factor to account for the pore space geometry in porous media, also known as tortuosity and constrictivity (Boving and Grathwohl, 2001; Van Loon and Mibus, 2015). Consequently, the availability, quality and selection of data has a direct impact on the results, i.e. migration lengths of uranium (Hennig and Kühn, 2021b).

With the MC approach, calculations of diffusive transport hinge on the availability of the D_w for all species. Radionuclides with a complex speciation chemistry like uranium require many D_w. However, some of them are challenging to be determined due to the co-existence of various species under most experimental conditions (Guillaumont et al., 2003; Kerisit and Liu, 2010). Therefore, the D_w selected for the uranium species stem from molecular dynamic simulations (Kerisit and Liu, 2010; Liu et al., 2011). Thereby, similar species have the same value because of the lack of data (Supplementary S-2[1]). This might explain the difference of only ± 5 m between the migration lengths of SC and MC simulations, and thus the small impact of MC on the host rock scale (Figure 5.7). However, the D_w of the most relevant, aqueous uranium species in the studied system (i.e. $CaUO_2(CO_3)_3^{2-}$, $Ca_2UO_2(CO_3)_3$ and $MgUO_2(CO_3)_3^{2-}$, Table 2.2) differ only slightly (Kerisit and Liu, 2010). Accordingly, the impact of the other species on the total diffusion length is negligible since uranium is predominantly present as U(VI) in an anionic ternary uranyl complex with calcium (>65%, Table 2.2). Besides these aspects, the pore diffusion coefficient D_p (m^2/s) is ultimately used in the transport simulation and calculated via $D_p = D_w \cdot \epsilon^n$ (Equation 3.5). Consequently, D_p highly depends on the calibrated exponent n, and thus on the underlying SCM data set, as porosities are taken as constant within a model. In other words, the D_p of the predominant species decrease with increasing n. For instance, the difference between calculated and experimentally determined D_p (Joseph et al., 2013b), and with that between SC and MC simulations, is only small for n=2 and a porosity of 0.16, whereby it increases with the value of n. Consequently, the impact of MC diffusion on the resulting migration lengths not only depends on the availability of all D_w, but also on the SCM data set describing the pore space structure and interaction via the calibrated exponent n.

[1] Table S-2 only contains the uranium species that are relevant for the investigated system, i.e. present in concentrations $>10^{-12}$ mol/L, and therefore it has been shortened compared to the published version.

The migration length of a species determined with the MC approach depends on the charge of the considered surfaces and associated DDL composition, and thus on the chosen SCM data set and individual surface parameters. The calibrated exponents n vary within this thesis with values between 2 (Section 5.3) and 2.6 (Section 3.3). This can be explained by the composition of clay minerals that were considered for sorption. In Chapter 3, two scenarios were investigated (Section 3.2.2), once with all four clay minerals (illite, montmorillonite, chlorite and kaolinite) and the other with only two (illite and montmorillonite). Based on the resulting migration lengths of the scenarios, chlorite was identified to be of special relevance for uranium diffusion processes due to the positively charged surface in the studied geochemical system and associated enhanced transport of anionic species (Section 3.5.1), like the predominant ternary uranyl complex (Figure 2.3). However, the selection of clay minerals was revised (Hennig and Kühn, 2021b,c). In an internal discussion with colleagues from the Helmholtz-Zentrum Dresden-Rossendorf (HZDR), who provided the underlying thermodynamic database, it has been worked out that the SCM data of chlorite is not reliable. Consequently, chlorite was excluded from the simulations presented in Chapter 4 and 5. This explains the different values for the calibrated exponent n within this thesis with the MC option as well as the initially identified facies dependence of uranium diffusion processes (Section 3.5.1) in addition to sorption (Hennig et al., 2020). Accordingly, the different migration lengths determined with SC and MC simulation are solely allocated to anion exclusion effects (Figure 3.3, Section 3.5.1). The simulations taking into account the hydrogeological system (Chapter 5) showed that diffusion processes are not facies dependent since migrations lengths of SC and MC simulations were with $\pm 5\,\mathrm{m}$ almost the same at the host rock scale ($>200\,\mathrm{m}$, Figure 5.7, Section 5.5.2). This emphasizes that the application of MC diffusion is associated with many uncertainties strongly affecting the resulting migration lengths. Moreover, the approach is probably not practicable for a performance assessment due to the computational cost. Consequently, the SC approach is recommended to determine uranium migration lengths since MC diffusion is associated with an increase in computational costs and many uncertainties, such as the SCM data.

Values for stability constants vary in the literature, what has a direct impact on the speciation (Figure 4.1), and thus on the migration distances (Figure 4.2). The chemical thermodynamic database underlying the presented simulations is based on the Nagra/PSI database (Thoenen et al., 2014) that uses the data published with the first update of the Nuclear Energy Agency (NEA, Guillaumont et al., 2003) for the uranium species. Accordingly, the anionic ternary uranyl complex $CaUO_2(CO_3)_3^{2-}$ is the dominant species in the modelled geochemical system (Hennig et al., 2020). However, the neutral ternary uranyl complex $Ca_2UO_2(CO_3)_3$ becomes the predominant species with increasing value for the associated stability constant (Figure 4.1) as presented in Chapter 4. This, in turn, means a farther uranium migration through the formation (Figure 4.2) because diffusion is no longer hampered by anion exclusion (Section 4.4). As indicated in Thoenen et al. (2014), the chosen values for the stability constants of the ternary uranyl complexes were placeholders in the Nagra/PSI database

since no better data was available at that time. With the second NEA update of thermodynamic data for uranium (Grenthe et al., 2020), this discussion has been set. A value ($\log K = 30.8$, Endrizzi and Rao, 2014) even higher as the one used in Chapter 4 ($\log K = 30.55$, Bernhard et al., 2001) is chosen as the most precise one published to-date (Grenthe et al., 2020). To be consistent within this thesis, the Nagra/PSI database (Thoenen et al., 2014), and thus the data of the first NEA update (Guillaumont et al., 2003), was used throughout all published manuscripts. However, Chapter 4 gives implications, how the data published with the second NEA update (Grenthe et al., 2020) will affect migration distances (Figure 4.2). With increasing proportion of the neutral ternary uranyl complex in the species distribution determined by the underlying stability constants, uranium migrates farther through the formation as anion exclusion effects decrease.

The impact of the second NEA update for the thermodynamic data of uranium (Grenthe et al., 2020) on the migration lengths is shown, for the sake of completeness, in the following by means of the simulations of the hydrogeological system presented in Chapter 5 (Hennig and Kühn, 2021c). First, the model needs to be re-calibrated against the diffusion experiment of Joseph et al. (2013b) before it can be applied in a second step to model uranium migration in the hydrogeological system of the Opalinus Clay at Mont Terri. As can be seen in Figure 6.2, the modelled (blue lines) and experimental data (orange dots) coincide from a visual point of view quite well. Best results were obtained for a clay mineral composition of 18 wt.% kaolinite, 20 wt.% illite, 10 wt.% illite/smectite mixed layers (blue, solid line, Figure 6.2). However, the deviations between experimental and modelled data represented by the relative Root Mean Square Errors (rRMSE, Equation 2.2) are high with a maximum of 45%. This can be explained by the scattering of the data. Compared to the simulations based on the Nagra/PSI database (green lines, Figure 6.2) as presented in Hennig and Kühn (2021c), the deviation between modelled and experimental data increased with the second NEA update and is also the highest within this thesis (Figure 2.2, 3.2 and 5.5 with maximum rRMSE of 30%, 28% and 40%, respectively).

The clay mineral quantities need to be adjusted for the calibration against the diffusion experiment (Joseph et al., 2013b), as the application of the thermodynamic data published in Grenthe et al. (2020) changes speciation, and thus sorption, compared to Hennig and Kühn (2021c). In Hennig and Kühn (2021c), a composition of 23 wt.% kaolinite, 9 wt.% illite and 4 wt.% illite/smectite mixed layers was used (green, solid line, Figure 6.2). Hence, both calibrations differ in their clay mineral composition (see above-mentioned values). This is caused by the change in species distribution (Table 6.1), which is exemplary given for the pore water composition of the shaly facies using the data of Grenthe et al. (2020) compared to the values published in Hennig and Kühn (2021b) with the data according to the Nagra/PSI database (Thoenen et al., 2014). As can be read from the percentages (Table 6.1), the predominant species changes from the anionic to almost only the neutral ternary uranyl complex $Ca_2UO_2(CO_3)_3$. Due to the stronger complexation of uranium with calcium and carbonate to the neutral ternary complex, less uranyl-ions are in total available to sorb on the clay minerals and, consequently, sorption decreases.

This, in turn, means the clay mineral quantities need to be adapted to achieve the same sorption capacity, and thus to coincide with the experimental data. This is also the case for the exponent n that had to be slightly increased to a value of 2.1 (blue, dashed line, Figure 6.2), what corresponds to the calibrated exponent of the scenario considering only illite and montmorillonite for sorption (MC_{2Clay}, Figure 3.2). However, the rRMSE is with 45% (blue, dashed line, Figure 6.2) about 20% higher ($rRMSE_{MC_{2Clay}} = 27\%$, Figure 3.2). The charge change of the predominant species alters sorption and interaction with the DDL of the clay minerals, what lead to an adjustement in mineral composition and exponent n in the calibration process as anion exclusion no longer hampers uranium diffusion.

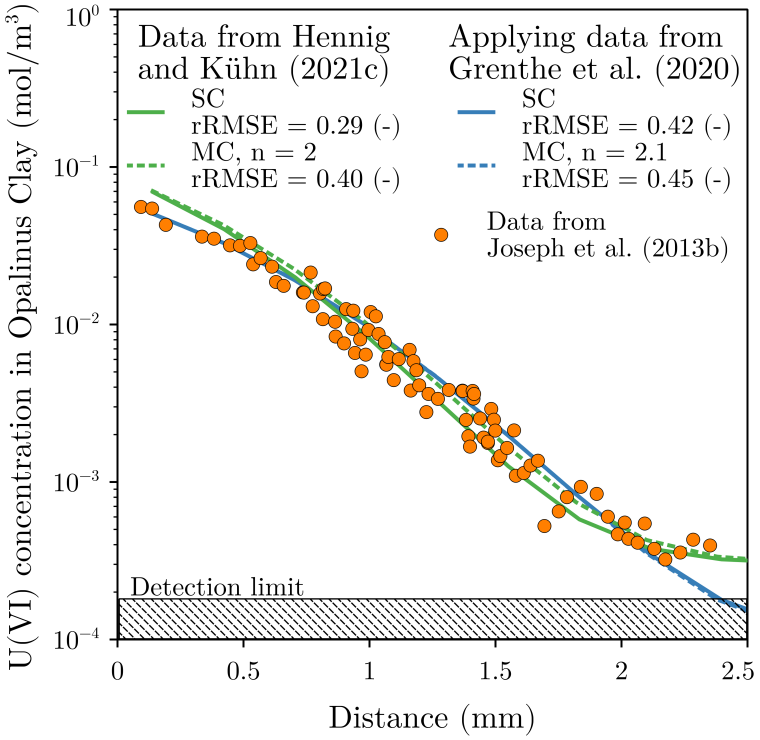

Figure 6.2: The model concept needs to be calibrated again and again. The application of the second NEA update for thermodynamic uranium data (Grenthe et al., 2020) changes the predominant species from the anionic complex $CaUO_2(CO_3)_3^{2-}$ (green lines, Hennig and Kühn, 2021c) to the neutral one $Ca_2UO_2(CO_3)_3$ (blue lines). Accordingly, the clay mineral compostion as well as the medium-specific parameter n need to be re-calibrated for the SC (solid lines) and MC simulations (dashed lines). Best results were obtained for n = 2.1 and a mineral composition of 18 wt.% kaolinite, 20 wt.% illite, 10 wt.% illite/smectite mixed layers.

The charge of the predominant species governs the interaction with the DDL, and thus has a direct impact on the migration lengths on the host rock scale. This impact is exemplarily shown in Figure 6.3a (blue lines) based on the SC simulations presented in Chapter 5 (green lines, Hennig and Kühn, 2021c). As can be seen from the results for the data-driven scenario (1R, solid lines, Figure 6.3a), the charge change of the predominant uranium species from the anionic ternary complex (green lines) to the neutral one (blue lines) lead to migration distances after a simulation time of one million years of 70 m and 60 m towards the Dogger and Liassic, respectively.

Compared to the results presented in Figure 5.7a (50 m and 40 m towards Dogger and Liassic, Hennig and Kühn, 2021c), uranium migrates by up to 20 m farther through the Opalinus Clay formation. For the conceptual scenario (2J, dashed lines, Figure 6.3a), uranium migration is enhanced by up to 15 m compared to the results presented in Figure 5.7a (25 m and 20 m towards Dogger and Liassic, Hennig and Kühn, 2021c). Nevertheless, uranium is retained within the Opalinus Clay formation with a thickness of at least 100 m as concentrations close to the aquifers do not increase (Figure 6.3a). The MC simulations (not shown here) deviated from the SC simulations in a similar way to the results presented in Figure 5.7, by ±5 m for both scenarios (Hennig and Kühn, 2021c). This further emphasizes that regardless of the underlying thermodynamic data determining the predominant species, and thus the interaction with the DDL, the differences in the migrations lengths between the scenarios can be primarily attributed to sorption rather than diffusion processes as the same D_e was used for all SC simulations in Figure 6.3a. The associated profiles of the K_d values underline this once again (Figure 6.3b). Due to the application of the thermodynamic data published with the second NEA update (Grenthe et al., 2020), the sorption capacity significantly decreases for both scenarios (blue lines, Figure 6.3b) compared to the simulations of Hennig and Kühn (2021c) using the data of the first NEA update (green lines, Figure 6.3b, Guillaumont et al., 2003). As already outlined above, this is caused by changes in the species distribution. Less uranyl-ions are in total available for sorption (Supplementary S-1) since uranium increasingly forms ternary complexes. Consequently, it is not only decisive, whether the predominant species is anionic or neutral and, accordingly, whether anion exclusion effects are effective or not but also how strongly and how many complexes are formed as this governs the amount of uranium available for sorption.

Table 6.1: The species distribution changes from predominantly anionic to neutral ternary complexes with the application of the second NEA update for thermodynamic uranium data (Grenthe et al., 2020) compared to the values published in Hennig and Kühn (2021b) using the data of the first NEA update (Guillaumont et al., 2003). Percentage of main uranium species are exemplarily given for the pore water composition of the shaly facies.

Distribution	**Species in % using data according to**	
	Hennig and Kühn (2021b)	Grenthe et al. (2020)
$CaUO_2(CO_3)_3^{2-}$	70	10
$MgUO_2(CO_3)_3^{2-}$	16	2
$Ca_2UO_2(CO_3)_3$	6	88
$UO_2(CO_3)_3^{4-}$	5	0.5

The underlying data ultimately determine the migration distances of numerical simulations. MC diffusion simulations improve the understanding of diffusion processes of complex radionuclides, like uranium, and their interaction with clay minerals. However, the approach requires a large set of different data that is not always available in sufficient quality. Further, it is associated with huge computational costs,

especially on the host rock scale. As migration lengths of MC simulations do not differ significantly from SC simulations, the latter is recommended to quantify uranium migration in performance assessments of potential disposal sites. The underlying thermodynamic data governs speciation and, in turn, the amount of uranium available for sorption, and thus ultimately the migration distances with differences of up to 20 m.

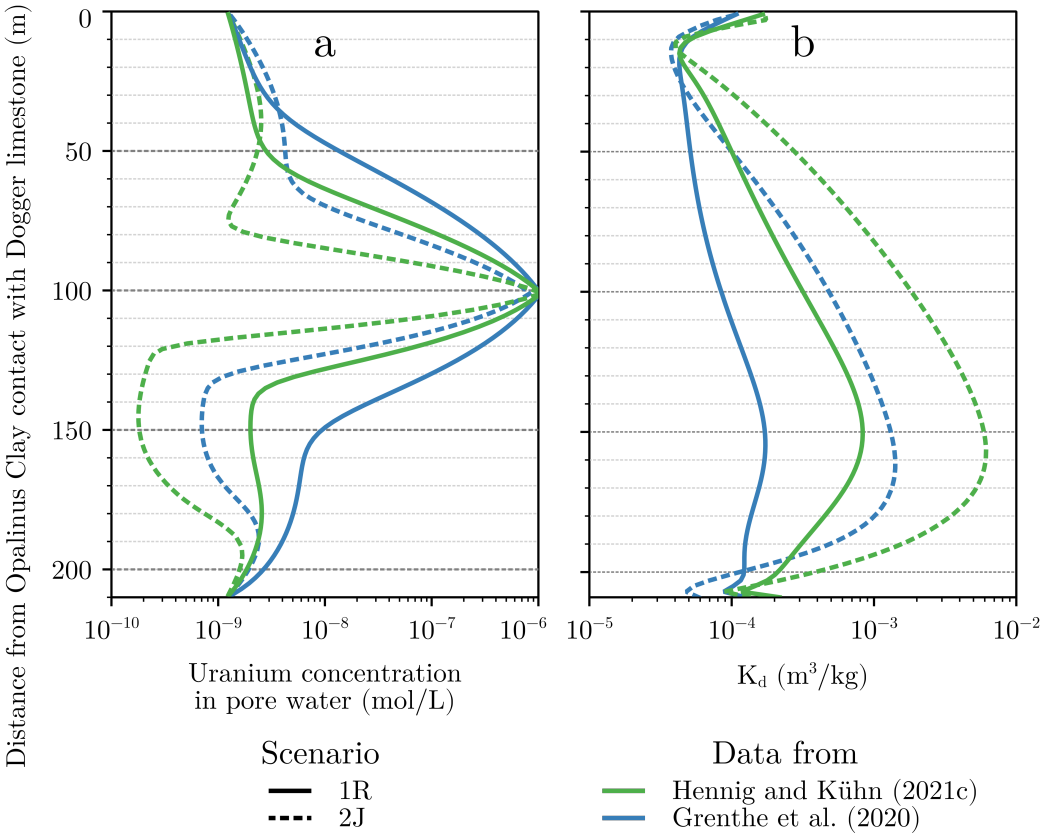

Figure 6.3: Changes in the uranium speciation alter the sorption behaviour, and thus migration lengths. For the data-driven (1R, solid lines) as well as conceptual (2J, dashed lines) scenario, uranium migration (**a**) is enhanced by several tens of meters due to the formation of predominantly neutral ternary complexes (blue lines) following the data of Grenthe et al. (2020) compared to the results of Hennig and Kühn (2021c), where speciation is dominated by the anionic complex (green lines). This is caused by a decrease in sorption capacity (**b**).

6.3 Predictive power of models must be quantified

Any model, no matter how complex, is useless, if the meaningfulness or predictive power with respect to, for instance, experimental data cannot be or has not been quantified. For this reason, the rRMSE has been used in this thesis as a measure to provide an indicator how large the simulations deviate from the corresponding experimental data. In Chapter 5, the selection of scenarios used to model uranium migration in the hydrogeological system of the Mont Terri anticline (Figure 5.6) was only done on the basis of a visual ranking between modelled and measured data (Section 5.4.1). At this point, the scenario selection is to be verified with the rRMSE (Table 6.2) that are calculated with logarithmized values due to the scattering of the data, and thus to be less sensitive to outliers.

A purely visual ranking is not sufficient to evaluate model quality or rank different simulations. The rRMSE is a measure to evaluate the deviation between measured and modelled data, and thus helps to identify the best match from different scenarios. The pore water profiles of Ca^{2+}, Mg^{2+}, pH and pCO_2 are exemplarily used for all pore water components (Figure 5.6) because these are the parameters governing uranium sorption processes (Hennig and Kühn, 2021c; Hennig et al., 2020). Based on the visual ranking (Section 5.4.1), the simulations SC-1R-A and MC-2J-A were selected as best results for the data-driven (1R) and conceptual approach (2J), respectively. Taking into account the rRMSE (Table 6.2), it is consistent with the visual ranking for the data-driven approach. For the conceptual scenario, however, the selection must be corrected. The rRMSE clearly show that best results were obtained with the simulation SC-2J-A. Based on the rRMSE, the scenario selection can therefore be confirmed for the data-driven approach (1R), but must be revised for the conceptual one (2J), what highlights the importance of providing a measure in order to evaluate the quality of a model or to rank different scenarios among each other.

Table 6.2: The rRMSE supports the selection of scenarios used to quantify the impact of geochemically heterogeneous conditions on uranium migration (Hennig and Kühn, 2021c). The rRMSE are calculated with logarithmized values due to the scattering of the data. A data-driven (1R) and conceptual (2J) scenario have been used to model the hydrogeological evolution of the Mont Terri anticline. Simulations were performed for different pCO_2, $10^{-2.7}$ bar (A) and 10^{-3} bar (B), with the respective best result printed **bolded**.

Scenario	Simulation	Ca^{2+}	Mg^{2+}	pH	pCO_2
1R-A	SC	0.143	**0.151**	**0.035**	**0.123**
	MC	0.171	0.190	0.038	0.152
1R-B	SC	**0.142**	**0.151**	0.041	0.139
	MC	**0.142**	0.190	0.043	0.228
2J-A	SC	**0.140**	**0.123**	0.037	**0.122**
	MC	0.153	0.154	**0.036**	0.164
2J-B	SC	0.147	0.136	0.048	0.150
	MC	0.147	0.155	0.046	0.224

The initial conditions to quantify uranium migration in the hydrogeological system of the Opalinus Clay changed for the conceptual approach (2J) due to the correction of the starting scenario (from MC-2J-A to SC-2J-A, Figure 5.6e–h). What this ultimately means for the uranium migration lengths as well as for the K_d values is shown in Figure 6.4 (green lines). For comparison, the simulation results using the original initial conditions are also shown (purple lines, Figure 6.4). As can be seen in Figure 6.4a, uranium migrates farther through the formation due to the changed initial conditions. With 50 m and 40 m towards the Dogger and Liassic, respectively, migration distances now correspond to the results of the data-driven approach (1R, green lines, Figure5.7a). This is also the case for the associated K_d values (green dots, Figure 6.4b) that significantly decreased due to the

changed initial conditions. As a result of the corrected initial conditions, less uranium sorbs on the clay minerals, which ultimately lead to farther migration distances.

The pCO_2 of the system is the most important parameter governing uranium sorption processes. The initial conditions of the two scenarios differ with respect to the maximum concentrations of the Ca^{2+} and Mg^{2+} profiles (SC-1R-A and SC-2J-A, Figure 5.6), i.e. concentrations of the data-driven (1R) are higher compared to the conceptual (2J). However, the migration lengths are the same, namely 50 m and 40 m towards the Dogger and Liassic, respectively (Figures 5.7a and 6.4a). In contrast, the profiles of pH and pCO_2 are similar. Due to the correction of the starting profiles for the conceptual scenario, the pCO_2 increases from an average of $10^{-2.55}$ bar to almost $10^{-2.3}$ bar (from MC-2J-A to SC-2J-A, Figure 5.6e–h). As a consequence, more ternary complexes are formed (Hennig and Kühn, 2021c; Hennig et al., 2020). This, in turn, decreases uranium sorption capacity (Figure 6.4b), and thus leading to farther migration through the formation. Consequently, the pCO_2 is the parameter ultimately governing the migration behaviour on the host rock scale as it determines speciation, and thus the sorption capacity.

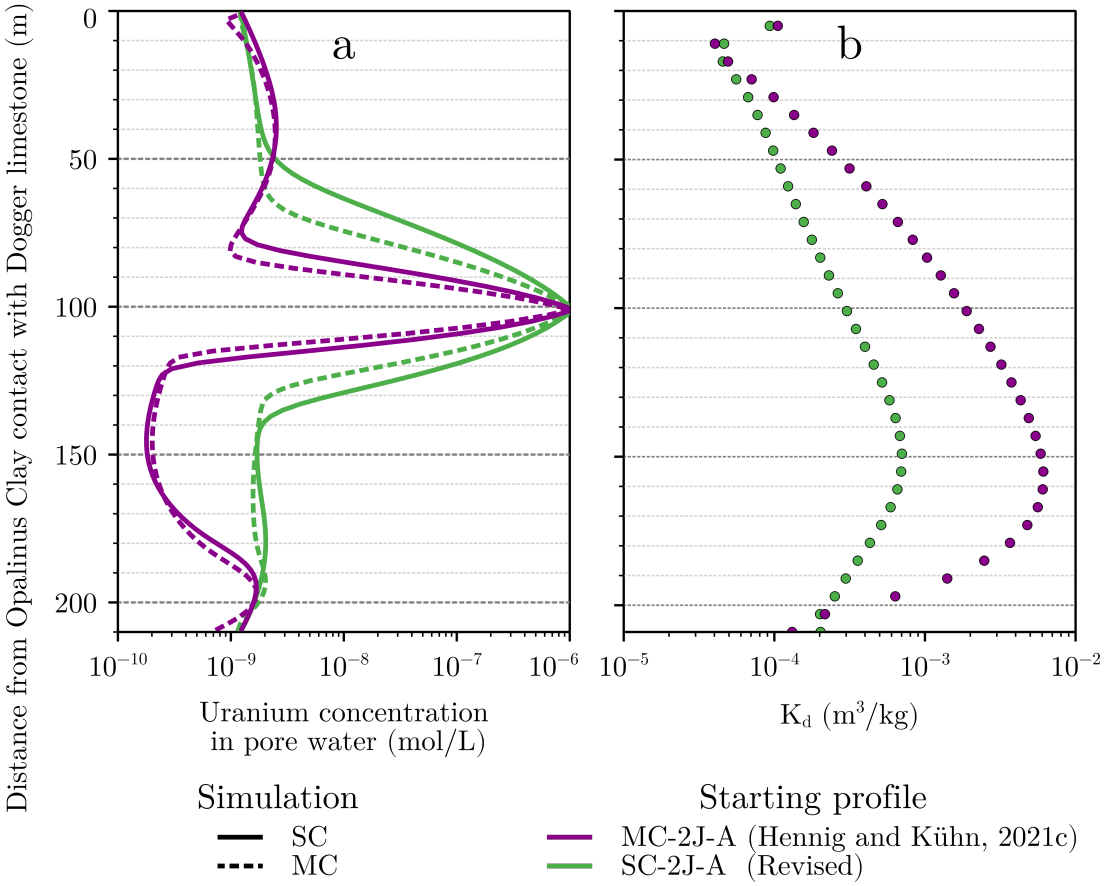

Figure 6.4: Uranium migrates farther through the formation due to an increase in pCO_2 associated with the correction of the initial conditions. As a result, more ternary complexes are formed decreasing the sorption capacity. Uranium concentrations in the pore water (**a**) as well as corresponding K_d values (**b**) are shown for the results of the conceptual scenario (2J, purple) according to Hennig and Kühn (2021c) and the corrected initial conditions (green).

The revision of the scenario selection due to the application of the rRMSE as a measure to compare different scenarios with each other emphasizes how important a quality control for the model under study is. Visually, it is not possible to make a statement about, whether, for instance, the migration distance deviates in the end by ±5% or ±100% or which scenario coincides best with the data. Consequently, it is indispensable in performance assessments to validate the conceptual models by means of experimental or measured data with corresponding error indication or to support a scenario selection with an appropriate measure.

The migration lengths of uranium resulting from reactive transport simulations depend on the model concept, underlying thermodynamic data and applied approaches. The pCO_2 was identified as key parameter for the quantification of uranium sorption processes, and thus migration lengths (Section 6.1). As a function of pCO_2, for instance, resulting migration lengths differed after one million years by up to 25 m in the hydrogeological system of the Mont Terri anticline (Figure 5.7a) and by up to 10 m in the geochemically and mineralogically homogeneous and constant simulations of the three facies (Figure 2.5). Taking into account the hydrogeological system with its inherent geochemical gradients, uranium migrated up to 25 m farther compared to homogeneous simulations (Figure 5.7a). However, the impact of the geochemically heterogeneous system strongly depends on pCO_2. Mineralogical heterogeneities between the three litho-facies led to differences in the resulting migration lengths of 10 m due to associated changes in pore water geochemistry (Figure 2.5). In addition to the geochemical and mineralogical aspects, the underlying thermodynamic data also play an important role as they determine speciation, and thus sorption (Section 6.2). For instance, migration lengths differed by 20 m (Figure 6.3a) using the thermodynamic data of the first or second NEA update for uranium (Grenthe et al., 2020; Guillaumont et al., 2003). In contrast, the application of SC or MC diffusion led to differences of only ±5 m (Figure 5.7a and b). Therefore, the SC approach is considered as adequate and recommended to quantify uranium diffusion on the host rock scale (Section 5.6 and 6.1). With the simulations presented in the current thesis, the uncertainty associated with the model conceptualization and selection of underlying data is demonstrated by the range of migration lengths. All in all, maximum migration distance of uranium through the Opalinus Clay is 70 m (Figure 6.3a). The German legal minimum requirements for potential host rocks of nuclear waste disposal specify a thickness of at least 100 m (§ 23 Article 5 StandAG). This, in turn, means the retention capacity of the Opalinus Clay with respect to uranium is sufficient since no adjacent aquifer is reached. Therefore, it is essential for future safety assessments to know and understand the calcite-carbonate-ion system as well as the hydrogeology at the potential disposal site and to further improve the determination of thermodynamic data, as they are the basis for reactive transport simulations. Otherwise, resulting migration lengths are associated with uncertainties in the order of several tens of metres, e.g. in the investigated case of up to 25 m. Accordingly, the priorization of parameters controlling uranium sorption as given in Hennig and Kühn (2021c) can be confirmed and further substantiated by the impact on the resulting migration lengths: pCO_2 > hydrogeological system > mineralogy.

Chapter 7

Conclusions and outlook

The suitability of a potential disposal site for highly radioactive waste mainly consisting of uranium is evaluated in performance and/or safety assessments by means of the radionuclide migration lengths through the host rock within one million years. Among the favoured host rocks are clay formations, like the Opalinus Clay, due to their low permeability so that radionuclide transport is only possible via diffusion. Diffusive transport in the Opalinus Clay is mainly governed by the interaction of the individual species with the diffuse double layers (DDL) enveloping the clay mineral surfaces to counterbalance their negative surface charge. Thereby, diffusion is retarded by the high sorption capacity with respect to radionuclides resulting from the large reactive surface area of the clay minerals. In this context, numerical simulations are indispensable due to the required spatial and temporal scales and enable quantification of migration, i.e. diffusion and sorption, in different ways. Complexity of available approaches varies from simplified methods following Fick's laws, referred to as single-component (SC) diffusion, where experimentally determined transport parameters, like effective diffusion D_e (m^2/s) and distribution coefficients K_d (m^3/kg), are used to more process-based applying mechanistic surface complexation models (SCM) and/or multi-component (MC) diffusion. With this, migration in the pore space of clay formations can be calculated, even for radionuclides with a complex chemistry like uranium.

The Opalinus Clay is characterised on the host rock scale by mineralogical and geochemical heterogeneities. The investigated formation is subdivided into three litho-facies (shaly, sandy and carbonate-rich) due to variations in mineralogy resulting from the deposition process itself. Moreover, at the location of the underground research laboratory Mont Terri (Switzerland), the hydrogeological system is defined by the surrounding aquifers that influence the geochemical conditions over the entire thickness. This, in turn, has a direct impact on the migration behaviour of uranium. Thus, migration lengths need to be quantified as a function of both variables. Therefore, aim of the present thesis is to improve the understanding and quantification of diffusion as well as sorption processes of uranium in clay formations, like the Opalinus Clay, on the host rock scale by evaluating the impact of mineralogical and geochemical heterogeneities on the migration lengths for a time period of one million years. Accordingly, the three main research objectives of the present research are to identify a potential (1) facies dependence of sorption as well as (2) of diffusion processes that result from variations in mineralogy and associated pore water geochemistry and, further, (3) to understand and evaluate the impact of the hydrogeological system and its inherent geochemical gradients on the migration behaviour of uranium using the example of the Opalinus Clay at Mont Terri.

Sorption processes are facies dependent. SCM are applied in one-dimensional SC simulations to quantify uranium sorption on clay minerals as a function of changing geochemical and mineralogical conditions between the facies as well as of different partial pressures of carbon dioxide (pCO_2) due to uncertainties associated with measurements (Chapter 2). The individual facies are represented by borehole analyses from Mont Terri. Migration distances vary by up 10 m between the facies, whereby the shaly facies has the highest retention capacity with respect to uranium. Noticeable was the sorption capacity of the carbonate-rich, which was almost equal compared to the sandy facies, despite a difference in the clay mineral content of about 20 wt.%. This can be explained by the pore water chemistry of the carbonate-rich facies that is similar to the shaly facies. Accordingly, the geochemistry of the pore water is more decisive for uranium sorption than the amount of clay minerals. Nevertheless, a higher clay mineral quantity (>50 wt.%), such as in the shaly facies, is associated with a better compensation against geochemical variations. Consequently, uranium sorption capacity is controlled by the geochemical conditions of the pore water in contact with the mineral assembladge. In particular, the following geochemical parameters govern uranium speciation, and thus sorption processes, with descending priority: $pCO_2 > Ca^{2+} > pH > pe$.

Diffusion processes of uranium in the Opalinus Clay are facies independent, and therefore can be well described on the host rock scale by an experimentally determined diffusion coefficient. To identify a facies dependence of diffusion processes, various one-dimensional simulations were conducted on the host rock scale applying the process-based MC diffusion approach, meaning each species in the system is assigned its own diffusion coefficient. Thereby, the interaction with the DDL, mineralogical and geochemical variations of the three facies (Chapter 3) as well as the entire hydrogeological system (Chapter 5) were taken into account. By comparing resulting migration lengths with almost identical simulations, except for the use of the SC approach, it has been demonstrated that uranium diffusion processes are not facies dependent as distances differed by only ± 5 m (Chapter 5). Variations in the resulting migration lengths between the individual facies as well as within the entire hydrogeological system can primarily be attributed to changes in the sorption capacity. Moreover, migration distances determined with MC diffusion highly depend on the quality and availability of the underlying data, especially the parameters describing the surfaces. In addition, it has been shown that the application of the MC approach to the host rock scale is associated with a huge computational effort, and therefore it is not recommended for potential performance assessments focussing on more than only one radionuclide. Consequently, uranium diffusion can be adequately quantified on the host rock scale with the SC approach using D_e determined from the laboratory or the field, but this does not apply to the respective K_d value.

The geochemistry of the pore water governs sorption processes and is determined by the hydrogeological system itself. Pore water geochemistry stems on the one hand from water-rock interactions, and thus is associated with mineralogical variations. On the other hand, it has been demonstrated that the interaction with the embedding aquifers, i.e. diffusive exchange over millions of years, established gradients,

and thus governs the geochemical conditions over the entire low permeable section consisting at Mont Terri of the Opalinus Clay and Liassic shales (Chapter 5). Due to these gradients, uranium migration is enhanced by up to +25 m compared to geochemically constant (homogeneous) simulations. Thus, the hydrogeological system is a decisive factor in the quantification of uranium migration. As geochemical conditions in potential clay formations can always be affected by aquifers, especially over geological time scales, the entire hydrogeological system has to be taken into account for the quantification of radionuclide migration. Beyond that, it has been demonstrated that the pCO_2 of the system plays the key role as there can be differences in the resulting migration lengths of up to 25 m depending on the respective value. Accordingly, the following aspects need to be considered quantifying uranium migration on the host rock scale: pCO_2 > hydrogeological system with inherent gradients > mineralogy.

In general, migration distances resulting from reactive transport simulations highly depend on the amount of uranium available for sorption, and thus from speciation. Speciation of uranium in the Opalinus Clay is characterised by the formation of ternary complexes, especially with calcium and carbonate. On the one hand, this is governed by the geochemistry of the pore water. On the other hand, the underlying thermodynamic data play an important role. The selected stability constants determine, which complexes are ultimately formed, for example, whether they are anionic or neutral (Chapter 4). This, in turn, has a direct impact on the migration distances. Speciation defines the amount of uranium available for sorption and if the formed complexes are excluded from the DDL due to electrostatic repulsion or not. In other words, whether anion exclusion effects are active or not. For instance, the change in speciation from predominantly anionic to neutral ternary complexes by the update of the thermodynamic data for uranium lead to an offset of 20 m due to associated significant differences in the sorption capacity. Accordingly, migration distances are ultimately governed by the underlying thermodynamic data as they control speciation as a function of the geochemical conditions in the pore water, and thus the amount of uranium sorbed on the clay minerals.

With the presented simulations, uranium migration was quantified for the first time on the host rock scale, thus new insights were gained in the migration behaviour for the example of the Swiss Opalinus Clay. Depending on the predominant species, anionic or neutral ternary complex, maximum migration distances after a simulation time of one million years are 50 m and 70 m, respectively. With regard to the German minimum legal requirement of a thickness of at least 100 m (§ 23 Article 5 StandAG[1]), the Opalinus Clay thus shows sufficient retention capacity with respect to uranium. The priorisation (pCO_2 > hydrogeological system > mineralogy) identified for the example of the Opalinus Clay is also applicable to other potential disposal sites with similar geochemistry, as this is the decisive factor quantifying uranium migration. Thus, the findings obtained in the frame of the present thesis contribute to the site selection process in Germany as they provide an orientation and workflow for systems with similar geochemical conditions.

[1]Standortauswahlgesetz (StandAG) of 5 May 2017 (Federal Law Gazette p. 1074) as last amended by Article 1 of the Act of 7 December 2020 (Federal Law Gazette p. 2760). URL: https://www.gesetze-im-internet.de/standag_2017/BJNR107410017.html (accessed on 13 June 2022).

The obtained achievements give implications for future laboratory experiments or modelling studies in the frame of performance assessments. As the pCO_2 is the decisive factor, in-situ values of potential disposal sites or ranges typical for clay formations should be taken into account in future works. In this context, it would be very interesting to verify, whether K_d values measured for in-situ pCO_2 correspond to those modelled in this work. Migration distances strongly depend on the underlying data. Therefore, the compilation of comprehensive data sets, in particular surface parameters to apply SCM, should be paid special attention and be further developed. Furthermore, the presented simulations are time-consuming although only one radionuclide was considered. Thus, the further development of machine learning approaches to quantify especially sorption processes as a function of changing geochemical conditions is essential. In addition, future work should assess the transferability of the findings to other clay formations, for example, in France, Belgium or northern Germany.

References

Alexander W. R., Reijonen H. M. and McKinley I. G. (2015): Natural analogues: studies of geological processes relevant to radioactive waste disposal in deep geological repositories. *Swiss Journal of Geosciences* 108, 75–100. DOI: 10.1007/s00015-015-0187-y

Altmann S., Tournassat C., Goutelard F., Parneix J. C., Gimmi T. and Maes N. (2012): Diffusion-driven transport in clayrock formations. *Applied Geochemistry* 27 (2), 463–478. DOI: 10.1016/j.apgeochem.2011.09.015

Altmann S. (2008): 'Geo'chemical research: a key building block for nuclear waste disposal safety cases. *Journal of Contaminant Hydrology* 102 (3-4), 174–179. DOI: 10.1016/j.jconhyd.2008.09.012

Amayri S., Drebert J., Fröhlich D. R., Kaplan U., Kratz J. V., Reich T., Stöbener N., Trautmann N. and Wunderlich T. (2011): Migration of actinides in natural clay: interaction of neptunium and plutonium with natural clay. *Final Report (contract number: 02E10166)*. Mainz, Germany: University of Mainz.

Amayri S., Fröhlich D. R., Kaplan U., Trautmann N. and Reich T. (2016): Distribution coefficients for the sorption of Th, U, Np, Pu, and Am on Opalinus Clay. *Radiochimica Acta* 104 (1), 33–40. DOI: 10.1515/ract-2015-2409

Appelo C. A. J. (2007): Multi-component diffusion in clays. *Water pollution in natural porous media at different scales. Assessment of fate, impact and indicators*. Ed. by L. Candela, L. Vadilo, P. Aagaard, E. Bedbur, M. Trevisan, M. Vanclooster, P. Viotti and J. A. López-Geta. Madrid, Spain: Instituto Geológico de España. Chap. 1, 3–13.

Appelo C. A. J. (2017): Solute transport solved with the Nernst-Planck equation for concrete pores with 'free' water and a double layer. *Cement and Concrete Research* 101, 102–113. DOI: 10.1016/j.cemconres.2017.08.030

Appelo C. A. J., Van Loon L. R. and Wersin P. (2010): Multi-component diffusion of a suite of tracers (HTO, Cl, Br, I, Na, Sr, Cs) in a single sample of Opalinus Clay. *Geochimica et Cosmochimica Acta* 74 (4), 1201–1219. DOI: 10.1016/j.gca.2009.11.013

Appelo C. A. J., Vinsot A., Mettler S. and Wechner S. (2008): Obtaining the pore water composition of a clay rock by modelling the in- and out-diffusion of anions and cations from an in-situ experiment. *Journal of Contaminant Hydrology* 101 (1-4), 67–76. DOI: 10.1016/j.jconhyd.2008.07.009

Appelo C. A. J. and Wersin P. (2007): Multi-component diffusion modelling in clay systems with application to the diffusion of tritium, iodide and sodium in Opalinus Clay. *Environmental Science and Technology* 41 (14), 5002–5007. DOI: 10.1021/es0629256

Arnold T., Zorn T., Zänker H., Bernhard G. and Nitsche H. (2001): Sorption behaviour of U(VI) on phyllite: experiments and modelling. *Journal of Contaminant Hydrology* 47 (2-4), 219–231. DOI: 10.1016/S0169-7722(00)00151-0

Bachmaf S., Planer-Friedrich B. and Merkel B. J. (2008): Effect of sulphate, carbonate, and phosphate on the uranium(VI) sorption behaviour onto bentonite. *Radiochimica Acta* 96 (6), 359–366. DOI: 10.1524/ract.2008.1496

Baeyens B. and Bradbury M. H. (2017): The development of a thermodynamic sorption data base for montmorillonite and the application to bentonite. *Nagra Technical Report* NTB 17-13. Wettingen and Villingen, Switzerland: Nagra and PSI. URL: https://www.nagra.ch/en/download-centre (accessed on 16 February 2022)

BASE (2020): Suche:x nach einem Endlager für hochradioaktive Abfälle. *Broschüre*. Berlin, Germany: Bundesamt für die Sicherheit der nuklearen Entsorgung. URL: https://www.endlagersuche-infoplattform.de (accessed on 16 February 2022)

BENNETT D. G. and GENS R. (2008): Overview of European concepts for high-level waste and spent fuel disposal with special reference waste container corrosion. *Journal of Nuclear Materials* 379 (1-3), 1–8. DOI: 10.1016/j.jnucmat.2008.06.001

BERNHARD G., GEIPEL G., REICH T., BRENDLER V., AMAYRI S., NITSCHE H. and NITSCHE H. (2001): Uranyl(VI) carbonate complex formation: validation of the $Ca_2UO_2(CO_3)_3$(aq.) species. *Radiochimica Acta* 89 (8), 511–518. DOI: 10.1524/ract.2001.89.8.511

BGE (2020): Zwischenbericht Teilgebiete gemäß §13 StandAG. Peine, Germany: Bundesgesellschaft für Endlagerung mbH. URL: https://www.bge.de/de/endlagersuche/zwischenbericht-teilgebiete/ (accessed on 17 February 2022)

BGR (2007): Nuclear waste disposal in Germany - Investigation and evaluation of regions with potentially suitable host rock formations for a geologic nuclear repository. Hannover/Berlin, Germany: Bundesanstalt für Geowissenschaften und Rohstoffe.

BOND A. E., BENBOW S., WILSON J., MILLARD A., NAKAMA S., ENGLISH M., MCDERMOTT C. and GARITTE B. (2013): Reactive and non-reactive transport modelling in partially water saturated argillaceous porous media around the ventilation experiment, Mont Terri. *Journal of Rock Mechanics and Geotechnical Engineering* 5 (1), 44–57. DOI: 10.1016/j.jrmge.2012.06.001

BOSSART P., BERNIER F., BIRKHOLZER J., BRUGGEMAN C., CONNOLLY P., DEWONCK S., FUKAYA M., HERFORT M., JENSEN M., MATRAY J.-M., MAYOR J. C., MOERI A., OYAMA T., SCHUSTER K., SHIGETA N., VIETOR T. and WIECZOREK K. (2017): Mont Terri rock laboratory, 20 years of research: introduction, site characteristics and overview of experiments. *Swiss Journal of Geosciences* 110, 3–22. DOI: 10.1007/s00015-016-0236-1

BOSSART P. and THURY M. (2008): Characteristics of the Opalinus Clay at Mont Terri. *Reports of the Swiss Geological Survey, no. 3: Mont Terri Rock Laboratory - Project, Programme 1996 to 2007 and Results*. Wabern, Switzerland. Chap. Annex 4.

BOURG I. C. and TOURNASSAT C. (2015): Self-diffusion of water and ions in clay barriers. *Developments in Clay Science*. Vol. 6. Elsevier. Chap. 6, 189–226. DOI: 10.1016/B978-0-08-100027-4.00006-1

BOVING T. B. and GRATHWOHL P. (2001): Tracer diffusion coefficients in sedimentary rocks: correlation to porosity and hydraulic conductivity. *Journal of Contaminant Hydrology* 53 (1-2), 85–100. DOI: 10.1016/S0169-7722(01)00138-3

BRACKE G. and GAUTHIER-LAFAYE F. (2001): Migration of fissiogenic Sm in fractures at the natural fission reactor site of Bangombé and effects of neutron capture on remote samples. *Engineering Geology* 61 (2-3), 131–144. DOI: 10.1016/S0013-7952(01)00043-6

BRADBURY M. H. and BAEYENS B. (1997): Derivation of in-situ Opalinus Clay pore water compositions from experimental and geochemical modelling studies. *Nagra Technical Report* NTB 97-07. Wettingen, Villigen and Würenlingen, Switzerland: Nagra and PSI. URL: https://www.nagra.ch/en/download-centre (accessed on 16 February 2022)

BRADBURY M. H. and BAEYENS B. (2003): Pore water chemistry in compacted re-saturated MX-80 bentonite. *Journal of Contaminant Hydrology* 61 (1-4), 329–338. DOI: 10.1016/S0169-7722(02)00125-0

BRADBURY M. H. and BAEYENS B. (2005a): Experimental and modelling investigations on Na-illite: acid-base behaviour and the sorption of strontium, nickel, europium and uranyl. *Nagra Technical Report* NTB 04-02. Wettingen and Villigen, Switzerland: Nagra and PSI. URL: https://www.nagra.ch/en/download-centre (accessed on 16 February 2022)

BRADBURY M. H. and BAEYENS B. (2005b): Modelling the sorption of Mn(II), Co(II), Ni(II), Zn(II), Cd(II), Eu(III), Am(III), Sn(IV), Th(IV), Np(V) and U(VI) on montmorillonite: linear free energy relationships and estimates of surface binding constants for some selected heavy metals and actinide. *Geochimica et Cosmochimica Acta* 69 (4), 875–892. DOI: 10.1016/j.gca.2004.07.020

BRADBURY M. H. and BAEYENS B. (2017): The development of a thermodynamic sorption data base for illite and the application to argillaceous rocks. *Nagra Technical Report* NTB 17-14. Wettingen and Villigen, Switzerland: Nagra and PSI. URL: https://www.nagra.ch/en/download-centre (accessed on 16 February 2022)

BRADBURY M. H., BAEYENS B., GECKEIS H. and RABUNG T. (2005): Sorption of Eu(III)/Cm(III) on Ca-montmorillonite and Na-illite. Part 2: surface complexation modelling. *Geochimica et Cosmochimica Acta* 69 (23), 5403–5412. DOI: 10.1016/j.gca.2005.06.031 (accessed on 16 February 2022)

BRADBURY M. H., BAEYENS B. and THOENEN T. (2010): Sorption databases for generic Swiss argillaceous, crystalline and calcareous rock systems. *PSI Report* no. 10-03. Villingen, Switzerland: PSI.

BRUNO J., CASAS I., CERA E. and DURO L. (1997): Development and application of a model for the long-term alteration of UO_2 spent nuclear fuel test of equilibrium and kinetic mass transfer models in the cigar lake ore deposit. *Journal of Contaminant Hydrology* 26 (1-4), 19–26. DOI: 10.1016/S0169-7722(96)00054-X

BRUNO J., DURO L. and GRIVÉ M. (2002): The applicability and limitations of thermodynamic geochemical models to simulate trace element behaviour in natural waters. Lessons learned from natural analogue studies. *Chemical Geology* 190 (1-4), 371–393. DOI: 10.1016/S0009-2541(02)00126-2

CAO X., ZHENG L., HOU D. and HU L. (2019): On the long-term migration of uranyl in bentonite barrier for high-level radioactive waste repositories: the effect of different host rocks. *Chemical Geology* 525, 46–57. DOI: 10.1016/j.chemgeo.2019.07.006

CARBOL P., WEGEN D. H., WISS T., FORS P., JEGOU C. and SPAHIU K. (2020): Spent nuclear fuel as waste material. *Comprehensive nuclear materials*. Ed. by R. J. KONINGS and R. E. STOLLER. Second Edition. Oxford, UK: Elsevier. Chap. 6.13, 347–386. DOI: 10.1016/B978-0-12-803581-8.10374-1

CHURAKOV S. V. and PRASIANAKIS N. I. (2018): Review of the current status and challenges for a holistic process-based description of mass transport and mineral reactivity in porous media. *American Journal of Science* 318 (9), 921–948. DOI: 10.2475/09.2018.03

DAVIES C. W. (1962): Ion association. Washington, USA: Butterworths.

DAVIS J. A. and KENT D. B. (1990): Surface complexation modelling in aqueous geochemistry. *Mineral-water interface geochemistry. Reviews in Mineralogy 23*. Ed. by M. HOCHELLA and A. WHITE. Washington: Mineralogical Society of America. Chap. 5, 177–260.

DE LUCIA M. and KÜHN M. (2013): Coupling R and PHREEQC: efficient programming of geochemical models. *Energy Procedia* 40, 464–471. DOI: 10.1016/j.egypro.2013.08.053

DE LUCIA M. and KÜHN M. (2021): Geochemical and reactive transport modelling in R with the RedModRphree package. *Advances in Geosciences* 56, 33–43. DOI: 10.5194/adgeo-56-33-2021

DELAY J. (2019): Synthesis of 20 years research, development and demonstration in Andra's underground research laboratory in Bure for Cigéo Project - France. *Andra Technical Document* ID:DRPAS3.

DELAY J., REBOURS H., VINSOT A. and ROBIN P. (2007): Scientific investigation in deep wells for nuclear waste disposal studies at the Meuse/Haute Marne underground research laboratory, northeastern France. *Physics and Chemistry of the Earth* 32 (1-7), 42–57. DOI: 10.1016/j.pce.2005.11.004

DONG W. and BROOKS S. C. (2006): Determination of the formation constants of ternary complexes of uranyl and carbonate with alkaline earth metals (Mg^{2+}, Ca^{2+}, Sr^{2+} and Ba^{2+}) using anion exchange method. *Environmental Science and Technology* 40 (15), 4689–4695. DOI: 10.1021/es0606327

DZOMBAK D. A and MOREL F. M. M. (1990): Surface complexation modelling: hydrous ferric oxide. New York, USA: Jon Wiley and Sons.

ENDRIZZI F. and RAO L. (2014): Chemical speciation of uranium(VI) in marine environments: complexation of calcium and magnesium ions with $[(UO_2)(CO_3)_3]^{4-}$ and the effect on the extraction of uranium from sea water. *Chemistry - A European Journal* 20 (44), 14499–14506. DOI: 10.1002/chem.201403262

ERIKSEN T. E., SHOESMITH D. W. and JONSSON M. (2012): Radiation induced dissolution of UO_2 based nuclear fuel - A critical review of predictive modelling approaches. *Journal of Nuclear Materials* 420 (1-3), 409–423. DOI: 10.1016/j.jnucmat.2011.10.027

EWING R. C. (2015): Long-term storage of spent nuclear fuel. *Nature Materials* 14, 252–257. DOI: 10.1038/nmat4226

FILIPSKÁ P., ZEMAN J., VŠIANSKÝ D., HONTY M. and ŠKODA R. (2017): Key processes of long-term bentonite-water interaction at 90 °C: mineralogical and chemical transformations. *Applied Clay Science* 150, 234–243. DOI: 10.1016/j.clay.2017.09.036

FOX P. M., DAVIS J. A. and ZACHARA J. M. (2006): The effect of calcium on aqueous uranium(VI) speciation and adsorption to ferrihydrite and quartz. *Geochimica et Cosmochimica Acta* 70 (6), 1379–1387. DOI: 10.1016/j.gca.2005.11.027

FOX P. M., TINNACHER R. M., CHESHIRE M. C., CAPORUSCIO F., CARRERO S. and NICO P. S. (2019): Effects of bentonite heating on U(VI) adsorption. *Applied Geochemistry* 109, 104392. DOI: 10.1016/j.apgeochem.2019.104392

FREIVOGEL M. and HUGGENBERGER P. (2003): Modellierung bilanzierter Profile im Gebiet Mont Terri – La Croix (Kanton Jura). *Reports of the FOWG, Geology Series, no 4.: Mont Terri Project – Geology , paleohydrology and stress field of the Mont Terri region*, 7–44.

FRISCH O. R. (1939): Physical evidence for the division of heavy nuclei under neutron bombardment. *Nature* 143, 276. DOI: 10.1038/143276a0

FRÖHLICH D. R., AMAYRI S., DREBERT J. and REICH T. (2011): Sorption of neptunium(V) on Opalinus Clay under aerobic/anaerobic conditions. *Radiochimica Acta* 99 (2), 71–77. DOI: 10.1524/ract.2011.1798

FRÖHLICH D. R., AMAYRI S., DREBERT J. and REICH T. (2013): Influence of humic acid on neptunium(V) sorption and diffusion in Opalinus Clay. *Radiochimica Acta* 101 (9), 553–560. DOI: 10.1524/ract.2013.2059

GAO Y., SHAO Z. and XIAO Z. (2015): U(VI) sorption on illite: effect of pH, ionic strength, humic acid and temperature. *Journal of Radioanalytical and Nuclear Chemistry* 303, 867–876. DOI: 10.1007/s10967-014-3385-6

GAUCHER E. C., LASSIN A., LEROUGE C., FLÉHOC C., MARTY N., BENOÎT H., TOURNASSAT C., ALTMANN S., VINSOT A. and BUSCHAERT S. (2010): CO_2 partial pressure in clayrocks: a general model. *Water-Rock Interaction WRI-13*, 855–858.

GAUTHIER-LAFAYE F. (2002): 2 billion year old natural analogues for nuclear waste disposal: the natural nuclear fission reactors in Gabon (Africa). *Comptes Rendus Physique* 3 (7-8), 839–849. DOI: 10.1016/S1631-0705(02)01351-8

GECKEIS H., LÜTZENKIRCHEN J., POLLY R., RABUNG T. and SCHMIDT M. (2013): Mineral-water interface reactions of actinides. *Chemical Reviews* 113 (2), 1016–1062. DOI: 10.1021/cr300370h

GIMMI T., LEUPIN O. X., EIKENBERG J., GLAUS M. A., VAN LOON L. R., WABER H. N., WERSIN P., WANG H. A. O., GROLIMUND D., BORCA C. N., DEWONCK S. and WITTEBROODT C. (2014): Anisotropic diffusion at the field scale in a 4-year multi-tracer diffusion and retention experiment - I: insights from the experimental data. *Geochimica et Cosmochimica Acta* 125, 373–393. DOI: 10.1016/j.gca.2013.10.014

GIMMI T., WABER H. N., GAUTSCHI A. and RÜBEL A. (2007): Stable water isotopes in pore water of Jurassic argillaceous rocks as tracers for solute transport over large spatial and temporal scales. *Water Resources Research* 43 (4). DOI: 10.1029/2005WR004774

GLAUS M. A., AERTSENS M., APPELO C. A. J., KUPCIK T., MAES N., VAN LAER L. and VAN LOON L. R. (2015): Cation diffusion in the electrical double layer enhances the mass transfer rates for Sr^{2+}, Co^{2+} and Zn^{2+} in compacted illite. *Geochimica et Cosmochimica Acta* 165, 376–388. DOI: 10.1016/j.gca.2015.06.014

GLAUS M. A., BAEYENS B., BRADBURY M. H., JAKOB A., VAN LOON L. R. and YAROSHCHUK A. (2007): Diffusion of ^{22}Na and ^{85}Sr in montmorillonite: evidence of interlayer diffusion being the dominant pathway at high compaction. *Environmental Science and Technology* 41 (2), 478–485. DOI: 10.1021/es061908d

GLAUS M. A., FRICK S., ROSSÉ R. and VAN LOON L. R. (2010): Comparative study of tracer diffusion of HTO, $^{22}Na^{+}$ and $^{36}Cl^{-}$ in compacted kaolinite, illite and montmorillonite. *Geochimica et Cosmochimica Acta* 74 (7), 1999–2010. DOI: 10.1016/j.gca.2010.01.010

GRAMBOW B., FATTAHI M., MONTAVON G., MOISAN C. and GIFFAUT E. (2006): Sorption of Cs, Ni, Pb, Eu(III), Am(III), Cm, Ac(III), Tc(IV), Th, Zr and U(IV) on MX-80 bentonite: an experimental approach to assess model uncertainty. *Radiochimica Acta* 94 (9-11), 627–636. DOI: 10.1524/ract.2006.94.9-11.627

GRAMBOW B. (2016): Geological disposal of radioactive waste in clay. *Elements* 12 (4), 239–245. DOI: 10.2113/gselements.12.4.239

GRATWOHL P. (1958): Diffusion in natural porous media: contaminant transport, sorption/desorption and dissolution kinetics. Ed. by P. CHATWIN. London, UK: Kluwer Academic Publishers.

GRENTHE I., GAONA X., PLYASUNOV A. V., RAO L., RUNDE W., GRAMBOW B., KONINGS R. J. M., SMITH A. L. and MOORE E. E. (2020): Second update on the chemical thermodynamics of uranium, neptunium, plutonium, americium and technecium. *Chemical Thermodynamics* no. 14. Boulogne-Billancourt, France: OECD Nuclear Energy Agency.

GUILLAUMONT R., FANGHÄNEL T., NECK V., FUGER J., PALMER D. A., GRENTHE I. and RAND M. H. (2003): Update on the chemical thermodynamics of uranium, neptunium, plutonium, americium and technetium. *Chemical Thermodynamics* no. 5. Issyles-Moulineaux, France: OECD Nuclear Energy Agency.

HAHN O. and STRASSMANN F. (1939a): Nachweis der Entstehung aktiver Bariumisotope aus Uran und Thorium durch Neutronenbestrahlung; Nachweis weiterer aktiver Bruchstücke bei der Uranspaltung. *Naturwissenschaften* 27, 89–95. DOI: 10.1007/BF01488988

HAHN O. and STRASSMANN F. (1939b): Über den Nachweis und das Verhalten der bei der Bestrahlung des Urans mittels Neutronen entstehenden Erdalkalimetalle. *Naturwissenschaften* 27, 11–15. DOI: 10.1007/BF01488241

HARTMANN E. (2010): Sorption von Ln(III)/An(III) und U(VI) an Tonmineralen und natürlichen Tongesteinen. Ph.D. thesis, Karlsruher Institute of Technology KIT. URL: http://d-nb.info/1007310103/ (accessed on 16 February 2022)

HARTMANN E., GECKEIS H., RABUNG T., LÜTZENKIRCHEN J. and FANGHÄNEL T. (2008): Sorption of radionuclides onto natural clay rocks. *Radiochimica Acta* 96 (9-11), 699–707. DOI: 10.1524/ract.2008.1556

HEDIN A. and OLSSON O. (2016): Crystalline rock as a repository for Swedish spent nuclear fuel. *Elements* 12 (4), 247–252. DOI: 10.2113/gselements.12.4.247

HENNIG T. and KÜHN M. (2021a): Surrogate model for multi-component diffusion of uranium through Opalinus Clay on the host rock scale. *Applied Sciences* 11 (2), 786. DOI: 10.3390/app11020786

HENNIG T. and KÜHN M. (2021b): Uranium migration through the Swiss Opalinus Clay varies on the metre scale in response to differences of the stability constant of the aqueous , ternary uranyl complex $Ca_2UO_2(CO_3)_3$. *Advances in Geosciences* 56, 97–105. DOI: 10.5194/adgeo-56-97-2021

HENNIG T. and KÜHN M. (2021c): Potential uranium migration within the geochemical gradient of the Opalinus Clay system at the Mont Terri. *Minerals* 11 (10), 1087. DOI: 10.3390/min11101087

HENNIG T., STOCKMANN M. and KÜHN M. (2020): Simulation of diffusive uranium transport and sorption processes in the Opalinus Clay. *Applied Geochemistry* 123, 104777. DOI: 10.1016/j.apgeochem.2020.104777

HORE-LACY I. (2007): History of nuclear energy. *Nuclear Energy in the 21st Century*. Chap. 9, 139–151. DOI: 10.1016/b978-012373622-2/50012-x

HORITA J., ZIMMERMANN H. and HOLLAND H. D. (2002): Chemical evolution of sea water during the Phanerozoic: implications from the record of marine evaporites. *Geochimica et Cosmochimica Acta* 66 (21), 3733–3756. DOI: 10.1016/S0016-7037(01)00884-5

HOTH P., WIRTH H., REINHOLD K., BRÄUER V., KRULL P. and FELDRAPPE H. (2007): Endlagerung radioaktiver Abfälle in tiefen geologischen Formationen Deutschlands - Untersuchung und Bewertung von Tongesteinsformationen. Berlin/Hannover, Germany: Bundesanstalt für Geowissenschaften und Rohstoffe.

HUANG H. H. (2016): The E_H-pH diagram and its advances. *Metals* 6 (1), 23. DOI: 10.3390/met6010023

IAEA (1999): Use of natural analogues to support radionuclide transport models for deep geological repositories for long lived radioactive wastes. *IAEA TECDOC Series* no. 1109. Vienna, Austria: International Atomic Energy Agency. URL: https://www.iaea.org/publications/search/type/tecdoc-series (accessed on 16 February 2022)

IAEA (2003): Scientific and technical basis for the geological disposal of radioactive wastes. *Technical Report Series* no. 413. Vienna, Austria: International Atomic Energy Agency.

URL: https://www.iaea.org/publications/search/type/technical-reports-series (accessed on 16 February 2022)

IAEA (2021a): Nuclear power reactors in the world - 2021 Edition. *Reference Data Series* no. 2. Vienna, Austria: International Atomic Energy Agency. URL: https://www.iaea.org/publications/search/type/reference-data-series (accessed on 16 February 2022)

IAEA (2021b): Spent fuel performance assessment and research - Final report of a coordinated research project (SPAR-IV). *IAEA TECDOC Series* no. 1975. Vienna, Austria: International Atomic Energy Agency. URL: https://www.iaea.org/publications/search/type/tecdoc-series (accessed on 16 February 2022)

JOSEPH C., SCHMEIDE K., SACHS S., BRENDLER V., GEIPEL G. and BERNHARD G. (2011): Sorption of uranium(VI) onto Opalinus Clay in the absence and presence of humic acid in Opalinus Clay pore water. *Chemical Geology* 284 (3-4), 240–250. DOI: 10.1016/j.chemgeo.2011.03.001

JOSEPH C., STOCKMANN M., SCHMEIDE K., SACHS S., BRENDLER V. and BERNHARD G. (2013a): Sorption of U(VI) onto Opalinus Clay: effects of pH and humic acid. *Applied Geochemistry* 36, 104–117. DOI: 10.1016/j.apgeochem.2013.06.016

JOSEPH C., VAN LOON L. R., JAKOB A., STEUDTNER R., SCHMEIDE K., SACHS S. and BERNHARD G. (2013b): Diffusion of U(VI) in Opalinus Clay: influence of temperature and humic acid. *Geochimica et Cosmochimica Acta* 109, 74–89. DOI: 10.1016/j.gca.2013.01.027

KALMYKOV S. and CHOPPIN G. R. (2000): Mixed $Ca^{2+}/UO_2^{2+}/CO_3^{2-}$ complex formation at different ionic strengths. *Radiochimica Acta* 88 (9-11), 603–608. DOI: doi:10.1524/ract.2000.88.9-11.603

KAUTENBURGER R., BRIX K. and HEIN C. (2019): Insights into the retention behaviour of europium(III) and uranium(VI) onto Opalinus Clay influenced by pore water composition, temperature, pH and organic compounds. *Applied Geochemistry* 109, 104404. DOI: 10.1016/j.apgeochem.2019.104404

KEESMANN S., NOSECK U., BUHMANN D., FEIN E. and SCHNEIDER A. (2005): Modellrechnungen zur Langzeitsicherheit von Endlagern in Salz- und Granitformationen. GRS-206. Cologne, Germany: Gesellschaft für Anlagen- und Reaktorsicherheit (GRS) mbH.

KERISIT S. and LIU C. (2010): Molecular simulation of the diffusion of uranyl carbonate species in aqueous solution. *Geochimica et Cosmochimica Acta* 74 (17), 4937–4952. DOI: 10.1016/j.gca.2010.06.007

KIM S. J. (2001): Sorption mechanism of U(VI) on a reference montmorillonite: binding to the internal and external surfaces. *Journal of Radioanalytical and Nuclear Chemistry* 250, 55–62. DOI: 10.1023/A:1013212130177

KOROLEVA M., ALT-EPPING P. and MAZUREK M. (2011): Large-scale tracer profiles in a deep claystone formation (Opalinus Clay at Mont Russelin, Switzerland): implications for solute transport processes and transport properties of the rock. *Chemical Geology* 280 (3-4), 284–296. DOI: 10.1016/j.chemgeo.2010.11.016

KOROLEVA M. and MAZUREK M. (2009): Natural tracer profile Mont Russelin (NT) experiment: natural tracer profiles in the Mont Russelin anticline. *Technical Note* TN 2006-24. St. Ursanne and Bern, Switzerland: Mont Terri Project and University of Bern.

KÜHN M., HENNIG T., HEIDBACH O. and SCHECK-WENDEROTH M. (2021): Modelle simulieren die Zukunft. *System Erde* 11 (2), 30–35. DOI: 10.48440/GFZ.syserde.11.02.5

KULIK D. A. (2002): Sorption modelling by Gibbs energy minimisation: towards a uniform thermodynamic database for surface complexes of radionuclides. *Radiochimica Acta* 90 (9-11), 815–832. DOI: 10.1524/ract.2002.90.9-11_2002.815

LAUPER B., JAEGGI D., DEPLAZES G. and FOUBERT A. (2018): Multi-proxy facies analysis of the Opalinus Clay and depositional implications (Mont Terri rock laboratory, Switzerland). *Swiss Journal of Geosciences* 111, 383–398. DOI: 10.1007/s00015-018-0303-x

LEAL A. M. M., KULIK D. A. and SAAR M. O. (2017a): Ultra-fast reactive transport simulations when chemical reactions meet machine learning: chemical equilibrium. *arXiv: Optimization and Control*. EPRINT: https://arxiv.org/abs/1708.04825. (accessed on 16 February 2022)

LEAL A. M. M., KULIK D. A., SMITH W. R. and SAAR M. O. (2017b): An overview of computational methods for chemical equilibrium and kinetic calculations for geochemical and reactive transport modelling. *Pure and Applied Chemistry* 89 (5), 597–643. DOI: 10.1515/pac-2016-1107

LEAL A. M. M., KYAS S., KULIK D. A. and SAAR M. O. (2020): Accelerating reactive transport modelling: on-demand machine learning algorithm for chemical equilibrium calculations. *Transport in Porous Media* 133, 161–204. DOI: 10.1007/s11242-020-01412-1

LEROUGE C., BLESSING M., FLEHOC C., GAUCHER E. C., HENRY B., LASSIN A., MARTY N., MATRAY J., PROUST E., RUFER D., TREMOSA J. and VINSOT A. (2015): Dissolved CO_2 and alkane gas in clay formations. *Procedia Earth and Planetary Science* 13, 88–91. DOI: 10.1016/j.proeps.2015.07.021

LEUPIN O. X., WERSIN P., GIMMI T., METTLER S., RÖSLI U., MEIER O., NUSSBAUM N. C., VAN LOON L. R., SOLER J. M., EIKENBERG J., FIERZ T., VAN DORP F., BOSSART P., PEARSON F. J., WABER H. N., DEWONCK S., FRUTSCHI M., CHAUDAGNE G. and KICZKA M. (2013): DR (diffusion & retention) experiment. *Technical Report* TR 2011-01. St. Ursanne, Switzerland: Mont Terri Project.

LEUPIN O. X., BERNIER-LATMANI R., BAGNOUD A., MOORS H., LEYS N., WOUTERS K. and STROES-GASCOYNE S. (2017a): Fifteen years of microbiological investigation in Opalinus Clay at the Mont Terri rock laboratory (Switzerland). *Swiss Journal of Geosciences* 110, 343–354. DOI: 10.1007/s00015-016-0255-y

LEUPIN O. X., VAN LOON L. R., GIMMI T., WERSIN P. and SOLER J. M. (2017b): Exploring diffusion and sorption processes at the Mont Terri rock laboratory (Switzerland): lessons learned from 20 years of field research. *Swiss Journal of Geosciences* 110, 391–403. DOI: 10.1007/s00015-016-0254-z

LI S., WANG X., HUANG Z., DU L., TAN Z., FU Y. and WANG X. (2016): Sorption and desorption of uranium(VI) on GMZ bentonite: effect of pH, ionic strength, foreign ions and humic substances. *Journal of Radioanalytical and Nuclear Chemistry* 308, 877–886. DOI: 10.1007/s10967-015-4513-7

LIU C., SHANG J. and ZACHARA J. M. (2011): Multi-species diffusion models: a study of uranyl species diffusion. *Water Resources Research* 47 (12). DOI: 10.1029/2011WR010575

LIU J., YU J. W. and NERETNIEKS I. (1996): Transport modelling in the natural analogue study of the Cigar Lake uranium deposit (Saskatchewan, Canada). *Journal of Contaminant Hydrology* 21 (1-4), 19–34. DOI: 10.1016/0169-7722(95)00029-1

MA B., CHARLET L., FERNANDEZ-MARTINEZ A., KANG M. and MADÉ B. (2019): A review of the retention mechanisms of redox-sensitive radionuclides in multi-barrier systems. *Applied Geochemistry* 100, 414–431. DOI: 10.1016/j.apgeochem.2018.12.001

MARION G. M., MILLERO F. J., CAMÕES M. F., SPITZER P., FEISTEL R. and CHEN C.-T. A. (2011): pH of sea water. *Marine Chemistry* 126 (1-4), 89–96. DOI: 10.1016/j.marchem.2011.04.002

MARQUES FERNANDES M., VÉR N. and BAEYENS B. (2015): Predicting the uptake of Cs, Co, Ni, Eu, Th and U on argillaceous rocks using sorption models for illite. *Applied Geochemistry* 59, 189–199. DOI: 10.1016/j.apgeochem.2015.05.006

MAZUREK M., ALT-EPPING P., BATH A., GIMMI T., WABER H. N., BUSCHAERT S., DE CANNIÈRE P., DE CRAEN M., GAUTSCHI A., SAVOYE S., VINSOT A., WEMAERE I. and WOUTERS L. (2011): Natural tracer profiles across argillaceous formations. *Applied Geochemistry* 26 (7), 1035–1064. DOI: 10.1016/j.apgeochem.2011.03.124

MAZUREK M., ALT-EPPING P., BATH A., GIMMI T. and WABER H. (2009): Natural tracer profiles across argillaceous formations: the CLAYTRAC Project. NEA no. 62. Paris, France: OECD Nuclear Energy Agency, 365.

MAZUREK M., GAUTSCHI A., MARSCHALL P., VIGNERON G., LEBON P. and DELAY J. (2008): Transferability of geoscientific information from various sources (study sites, underground rock laboratories, natural analogues) to support safety cases for radioactive waste repositories in argillaceous formations. *Physics and Chemistry of the Earth* 33 (Supplement 1), S95–S105. DOI: 10.1016/j.pce.2008.10.046

MCKINLEY I. G., RUSSELL ALEXANDER W. and BLASER P. C. (2007): Development of geological disposal concepts. *Radioactivity in the Environment* 9, 41–76. DOI: 10.1016/S1569-4860(06)09003-6

MEITNER L. and FRISCH O. R. (1939): Disintegration of uranium by neutrons: a new type of nuclear reaction. *Nature* 143, 239–240. DOI: 10.1038/143239a0

METZ V., GECKEIS H., GONZÁLEZ-ROBLES E., LOIDA A., BUBE C. and KIENZLER B. (2012): Radionuclide behaviour in the near-field of a geological repository for spent nuclear fuel. *Radiochimica Acta* 100 (8-9), 699–713. DOI: 10.1524/ract.2012.1967

MÖLLER P. and DE LUCIA M. (2020): The impact of Mg^{2+} ions on equilibration of Mg-Ca carbonates in groundwater and brines. *Geochemistry* 80 (2), 125611. DOI: 10.1016/j.chemer.2020.125611

MÜHR-EBERT E. L., WAGNER F. and WALTHER C. (2019): Speciation of uranium: compilation of a thermodynamic database and its experimental evaluation using different analytical techniques. *Applied Geochemistry* 100, 213–222. DOI: 10.1016/j.apgeochem.2018.10.006

NAGRA (2002a): Project Opalinus Clay - Safety Report. Demonstration of disposal feasibility for spent fuel, vitrified high-level waste and long-lived intermediate-level waste (Entsorgungsnachweis). *Nagra Technical Report* NTB 02-05. Wettingen, Switzerland: Nagra. URL: https://www.nagra.ch/en/download-centre (accessed on 16 February 2022)

NAGRA (2002b): Projekt Opalinuston: Synthese der geowissenschaftlichen Untersuchungsergebnisse. Entsorgungsnachweis für abgebrannte Brennelemente, verglaste hochaktive sowie langlebige mittelaktive Abfälle. *Nagra Technical Report* NTB 02-03. Wettingen, Switzerland: Nagra. URL: https://www.nagra.ch/en/download-centre (accessed on 16 February 2022)

NAGRA (2007): Spuren der Zukunft. *Nagra Themenhefte* no. 1. Wettingen, Switzerland: Nagra.

NAGRA (2014): SGT Etappe 2: Vorschlag weiter zu untersuchender geologischer Standortgebiete mit zugehörigen Standortarealen für die Oberflächenanlage. *Nagra Technical Report* NTB 14-02. Wettingen, Switzerland: Nagra. URL: https://www.nagra.ch/en/download-centre (accessed on 16 February 2022)

NOSECK U., BRENDLER V., BRITZ S., STOCKMANN M., FRICKE J., RICHTER C., LAMPE M., GEHRKE A. and FLÜGGE J. (2018): Smart K_d-concept for long-term safety assessments: extension towards more complex applications. GRS-500. Cologne and Dresden, Germany: GRS and HZDR.

NOSECK U., BRENDLER V., FLÜGGE J., STOCKMANN M., BRITZ S., LAMPE M., SCHIKORA J. and SCHNEIDER A. (2012): Realistic integration of sorption processes in transport codes for long-term safety assessments. GRS-297. Cologne and Dresden, Germany: GRS and HZDR.

ORTIZ L., VOLCKAERT G. and MALLANTS D. (2002): Gas generation and migration in Boom Clay, a potential host rock formation for nuclear waste storage. *Engineering Geology* 64 (2-3), 287–296. DOI: 10.1016/S0013-7952(01)00107-7

PARKHURST D. L. and APPELO C. A. J. (2013): Description of input and examples for PHREEQC Version 3 — A computer program for speciation, batch-reaction, one-dimensional transport, and inverse geochemical calculations. *Book 6 - Modelling techniques*. Chap. A43, 497. URL: https://pubs.usgs.gov/tm/06/a43/pdf/tm6-A43.pdf (accessed on 16 February 2022)

PAYNE T. E., BRENDLER V., COMARMOND M. J. and NEBELUNG C. (2011): Assessment of surface area normalisation for interpreting distribution coefficients (K_d) for uranium sorption. *Journal of Environmental Radioactivity* 102 (10), 888–895. DOI: 10.1016/j.jenvrad.2010.04.005

PAYNE T. E., BRENDLER V., OCHS M., BAEYENS B., BROWN P. L., DAVIS J. A., EKBERG C., KULIK D. A., LUTZENKIRCHEN J., MISSANA T., TACHI Y., VAN LOON L. R. and ALTMANN S. (2013): Guidelines for thermodynamic sorption modelling in the context of radioactive waste disposal. *Environmental Modelling and Software* 42, 143–156. DOI: 10.1016/j.envsoft.2013.01.002

PEARSON F. J., ARCOS D., BATH A., BOISSON J.-Y., FERNÁNDEZ A. M., GÄBLER H. E., GAUCHER E. C., GAUTSCHI A., GRIFFAULT L., HERNÁN P. and WABER H. N. (2003): Mont Terri Project – Geochemistry of water in the Opalinus Clay formation at the Mont Terri rock laboratory. *Reports of the FOWG, Geology Series* no. 5. Bern, Switzerland: Federal Office for Water and Geology (FOWG).

PEARSON F. J., TOURNASSAT C. and GAUCHER E. C. (2011): Biogeochemical processes in a clay formation in-situ experiment: part E - Equilibrium controls on chemistry of pore water from the Opalinus Clay, Mont Terri underground research laboratory, Switzerland. *Applied Geochemistry* 26 (6), 990–1008. DOI: 10.1016/j.apgeochem.2011.03.008

PĘKALA M., KRAMERS J. D. and WABER H. N. (2010): ^{234}U / ^{238}U activity ratio disequilibrium technique for studying uranium mobility in the Opalinus Clay at Mont Terri, Switzerland. *Applied Radiation and Isotopes* 68 (6), 984–992. DOI: 10.1016/j.apradiso.2010.02.009

PĘKALA M., KRAMERS J. D., WABER H. N., GIMMI T. and ALT-EPPING P. (2009): Transport of ^{234}U in the Opalinus Clay on centimetre to decimetre scales. *Applied Geochemistry* 24 (1), 138–152. DOI: 10.1016/j.apgeochem.2008.09.013

PHILIPP T., SHAMS ALDIN AZZAM S., ROSSBERG A., HUITTINEN N., SCHMEIDE K. and STUMPF T. (2019): U(VI) sorption on Ca-bentonite at (hyper)alkaline conditions – Spectroscopic investigations of retention mechanisms. *Science of the Total Environment* 676, 469–481. DOI: 10.1016/j.scitotenv.2019.04.274

REISDORF A. G., HOSTETTLER B., JAEGGI D., DEPLAZES G., BLÄSI H., MORARD A., FEIST-BURKHARDT S., WALTSCHEW A., DIETZE V. and MENKFELD-GFELLER U. (2016): Litho- and biostratigraphy of the 250 m-deep Mont Terri BDB-1 borehole through the Opalinus Clay and bounding formations. *Technical Report* TR 2016-02. St-Ursanne, Switzerland: Mont Terri Project.

RÜBEL A., BECKER D.-A. and FEIN E. (2007): Radionuclide transport modelling - Performance assessment of repositories in clays. GRS-228. Cologne, Germany: Gesellschaft für Anlagen- und Reaktorsicherheit (GRS) mbH.

SALEH A. S. and YUN J. I. (2017): Equilibrium and kinetics of calcium–uranyl–carbonate adsorption on silica nanoparticles. *Journal of Radioanalytical and Nuclear Chemistry* 314, 93–103. DOI: 10.1007/s10967-017-5395-7

SCHMEIDE K. and BERNHARD G. (2010): Sorption of Np(V) and Np(IV) onto kaolinite: effects of pH, ionic strength, carbonate and humic acid. *Applied Geochemistry* 25 (8), 1238–1247. DOI: 10.1016/j.apgeochem.2010.05.008

SMELLIE J. A. T. and KARLSSON F. (1999): The use of natural analogues to assess radionuclide transport. *Engineering Geology* 52 (3-4), 193–220. DOI: 10.1016/S0013-7952(99)00006-X

SMITH K. S. (1997): Metal sorption on mineral surfaces: an overview with examples relating to mineral deposits. *The environmental geochemistry of mineral deposits: part A: processes, techniques and health issues, part B: case studies and research topics*. Society of Economic Geologists. DOI: 10.5382/Rev.06.07

SOLER J. M., SAMPER J., YLLERA A., HERNÁNDEZ A., QUEJIDO A., FERNÁNDEZ M., YANG C., NAVES A., HERNÁN P. and WERSIN P. (2008): The DI-B in-situ diffusion experiment at Mont Terri: results and modelling. *Physics and Chemistry of the Earth* 33 (Supplement 1), S196–S207. DOI: 10.1016/j.pce.2008.10.010

SOLER J. M., STEEFEL C. I., GIMMI T., LEUPIN O. X. and CLOET V. (2019): Modelling the ionic strength effect on diffusion in clay. The DR-A experiment at Mont Terri. *ACS Earth and Space Chemistry* 3 (3), 442–451. DOI: 10.1021/acsearthspacechem.8b00192

STEINTHORSDOTTIR M., JERAM A. J. and MCELWAIN J. C. (2011): Extremely elevated CO_2 concentrations at the Triassic/Jurassic boundary. *Palaeogeography, Palaeoclimatology, Palaeoecology* 308 (3-4), 418–432. DOI: 10.1016/j.palaeo.2011.05.050

STOCKMANN M., SCHIKORA J., BECKER D. A., FLÜGGE J., NOSECK U. and BRENDLER V. (2017): Smart K_d-values, their uncertainties and sensitivities - Applying a new approach for realistic distribution coefficients in geochemical modelling of complex systems. *Chemosphere* 187, 277–285. DOI: 10.1016/j.chemosphere.2017.08.115

THOENEN T., HUMMEL W., BERNER U. and CURTI E. (2014): The PSI/Nagra chemical thermodynamic database 12/07. *PSI Report* no. 14-04. Villigen, Switzerland: Paul Scherrer Institute. URL: https://www.psi.ch/en/les/database (accessed on 16 February 2022)

THURY M. and BOSSART P. (1999): Mont Terri rock laboratory: results of the hydrogeological, geochemical and geotechnical experiments performed in 1996 and 1997. *Geologische Berichte* Nr. 23. Bern, Switzerland: Swiss National Hydrological and Geological Survey.

TOURNASSAT C., TINNACHER R. M., GRANGEON S. and DAVIS J. A. (2018): Modelling uranium(VI) adsorption onto montmorillonite under varying carbonate concentrations: a surface complexation model accounting for the spillover effect on surface potential. *Geochimica et Cosmochimica Acta* 220, 291–308. DOI: 10.1016/j.gca.2017.09.049

TOURNASSAT C., BOURG I. C., STEEFEL C. I. and BERGAYA F. (2015): Surface properties of clay minerals. *Developments in Clay Science*. Vol. 6. Elsevier. Chap. 1, 5–31. DOI: 10.1016/B978-0-08-100027-4.00001-2

TOURNASSAT C. and STEEFEL C. I. (2019): Reactive transport modelling of coupled processes in nanoporous media. *Reviews in Mineralogy and Geochemistry* 85 (1), 75–109. DOI: 10.2138/rmg.2019.85.4

TURNER D. R. and SASSMAN S. A. (1996): Approaches to sorption modelling for high-level waste performance assessment. *Journal of Contaminant Hydrology* 21 (1–4), 311–332. DOI: 10.1016/0169-7722(95)00056-9

VAN LOON L. R., GLAUS M. A. and MÜLLER W. (2007): Anion exclusion effects in compacted bentonites: towards a better understanding of anion diffusion. *Applied Geochemistry* 22 (11), 2536–2552. DOI: 10.1016/j.apgeochem.2007.07.008

VAN LOON L. R., LEUPIN O. X. and CLOET V. (2018): The diffusion of SO_4^{2-} in Opalinus Clay: measurements of effective diffusion coefficients and evaluation of their importance in view of microbial mediated reactions in the near field of radioactive waste repositories. *Applied Geochemistry* 95, 19–24. DOI: 10.1016/j.apgeochem.2018.05.009

VAN LOON L. R. and MIBUS J. (2015): A modified version of Archie's law to estimate effective diffusion coefficients of radionuclides in argillaceous rocks and its application in safety analysis studies. *Applied Geochemistry* 59, 85–94. DOI: 10.1016/j.apgeochem.2015.04.002

VAN LOON L. R. and SOLER J. M. (2003): Diffusion of HTO, $^{36}Cl^-$, $^{125}I^-$ and $^{22}Na^+$ in Opalinus Clay: effect of confining pressure, sample orientation, sample depth and temperature. *Nagra Technical Report* NTB 03-07. Wettingen and Villingen, Switzerland: Nagra and PSI. URL: https://www.nagra.ch/en/download-centre (accessed on 16 February 2022)

VAN LOON L. R., SOLER J. M. and BRADBURY M. H. (2003a): Diffusion of HTO, $^{36}Cl^-$ and $^{125}I^-$ in Opalinus Clay samples from Mont Terri: effect of confining pressure. *Journal of Contaminant Hydrology* 61 (1-4), 73–83. DOI: 10.1016/S0169-7722(02)00114-6

VAN LOON L. R., SOLER J. M., JAKOB A. and BRADBURY M. H. (2003b): Effect of confining pressure on the diffusion of HTO, $^{36}Cl^-$ and $^{125}I^-$ in a layered argillaceous rock (Opalinus Clay): diffusion perpendicular to the fabric. *Applied Geochemistry* 18 (10), 1653–1662. DOI: 10.1016/S0883-2927(03)00047-7

VAN LOON L. R., WERSIN P., SOLER J. M., EIKENBERG J., GIMMI T., HERNÁN P., DEWONCK S. and SAVOYE S. (2004): In-situ diffusion of HTO, $^{22}Na^+$, Cs^+ and I^- in Opalinus Clay at the Mont Terri underground rock laboratory. *Radiochimica Acta* 92 (9-11), 757–763. DOI: 10.1524/ract.92.9.757.54988

VINSOT A., APPELO C. A. J., CAILTEAU C., WECHNER S., PIRONON J., DE DONATO P., DE CANNIÈRE P., METTLER S., WERSIN P. and GÄBLER H. E. (2008): CO_2 data on gas and pore water sampled in-situ in the Opalinus Clay at the Mont Terri rock laboratory. *Physics and Chemistry of the Earth* 33 (Supplement 1), S54–S60. DOI: 10.1016/j.pce.2008.10.050

VODYANITSKII Y. N. (2011): Chemical aspects of uranium behaviour in soils: a review. *Eurasian Soil Science* 44, 862. DOI: 10.1134/S1064229311080163

VOLKMER M. (2007): Kernenergie Basiswissen. Berlin, Germany: Informationskreis KernEnergie.

VON BERLEPSCH T. and HAVERKAMP B. (2016): Salt as a host rock for the geological repository for nuclear waste. *Elements* 12 (4), 257–262. DOI: 10.2113/gselements.12.4.257

WERSIN P., GAUCHER E. C., GIMMI T., LEUPIN O. X., MÄDER U. K., PEARSON F. J., THOENEN T. and TOURNASSAT C. (2009): Geochemistry of pore waters in Opalinus Clay at Mont Terri: experimental data and modelling. *Technical Report* TR 2008-06. St. Ursanne, Switzerland: Mont Terri Project.

WERSIN P., GIMMI T., MAZUREK M., ALT-EPPING P., PĘKALA M. and TRABER D. (2018): Multi-component diffusion in a 280 m thick argillaceous rock sequence. *Applied Geochemistry* 95, 110–123. DOI: 10.1016/j.apgeochem.2018.05.013

WERSIN P., LEUPIN O. X., METTLER S., GAUCHER E. C., MÄDER U., DE CANNIÈRE P., VINSOT A., GÄBLER H. E., KUNIMARO T., KIHO K. and EICHINGER L. (2011): Biogeochemical processes in a clay formation in-situ experiment: part A - Overview, experimental design and water data of an experiment in the Opalinus Clay at the Mont Terri underground research laboratory, Switzerland. *Applied Geochemistry* 26 (6), 931–953. DOI: 10.1016/j.apgeochem.2011.03.004

WERSIN P., MAZUREK M., MÄDER U. K., GIMMI T., RUFER D., LEROUGE C. and TRABER D. (2016): Constraining pore water chemistry in a 250 m thick argillaceous rock sequence. *Chemical Geology* 434, 43–61. DOI: 10.1016/j.chemgeo.2016.04.006

WERSIN P., SOLER J. M., VAN LOON L. R., EIKENBERG J., BAEYENS B., GROLIMUND D., GIMMI T. and DEWONCK S. (2008): Diffusion of HTO, Br^-, I^-, Cs^+, $^{85}Sr^{2+}$ and $^{60}Co^{2+}$ in a clay formation: results and modelling from an in-situ experiment in Opalinus Clay. *Applied Geochemistry* 23 (4), 678–691. DOI: 10.1016/j.apgeochem.2007.11.004

WERSIN P., TRABER D., MÄDER U. K., MAZUREK M., WABER H. N., RUFER D., GIMMI T. and CLOET V. (2017): Pore water chemistry in claystones in the context of radioactive waste disposal. *Procedia Earth and Planetary Science* 17, 718–721. DOI: 10.1016/J.PROEPS.2016.12.182

WIGGER C., KENNELL-MORRISON L., JENSEN M., GLAUS M. and VAN LOON L. R. (2018): A comparative anion diffusion study on different argillaceous, low permeability sedimentary rocks with various pore waters. *Applied Geochemistry* 92, 157–165. DOI: 10.1016/j.apgeochem.2018.02.009

WIGGER C. and VAN LOON L. R. (2018): Effect of the pore water composition on the diffusive anion transport in argillaceous, low permeability sedimentary rocks. *Journal of Contaminant Hydrology* 213, 40–48. DOI: 10.1016/j.jconhyd.2018.05.001

ZORN T. (2000): Untersuchungen der Sorption von Uran(VI) an das Gestein Phyllit zur Bestimmung von Oberflächenkomplexierungskonstanten. Ph.D. thesis, Dresden, Germany: Technische Universität Dresden.

Appendix A

Supplementary S-1: Surface parameters and reactions

As already mentioned, we consider sorption on binding sites of the clay minerals due to their relevance. According to Bradbury and Baeyens (2005a,b), weak (98%) and strong (2%) binding sites are distinguished for illite and montmorillonite. For kaolinite, the SCM data is based on Turner and Sassman (1996). There, the two edge surface sites, aluminol (AlOH) and silanol (SiOH), are distinguished.

Table A.1: Summary of the surface reactions and cation exchange used for modelling U(VI) sorption onto Opalinus Clay as well as specific surface area SSA (m^2/g) of the clay minerals.

Mineral	Surface reaction			log K
Illite	*Weak sites*			
SSA 100 m^2/g [a,b]	Ill^{w1}-OH + H^+	⇔	Ill^{w1}-OH_2^+	4.59 [c]
	Ill^{w1}-OH	⇔	Ill^{w1}-O^- + H^+	-7.11 [c]
	Ill^{w1}-OH + UO_2^{2+}	⇔	Ill^{w1}-O-UO_2^+ + H^+	-0.81 [c]
	Ill^{w1}-OH + UO_2^{2+} + H_2O	⇔	Ill^{w1}-O-$UO_2(OH)$ + $2H^+$	-6.21 [c]
	Strong sites			
	Ill^{s}-OH + H^+	⇔	Ill^{s}-OH_2^+	4.90 [c]
	Ill^{s}-OH	⇔	Ill^{s}-O^- + H^+	-6.80 [c]
	Ill^{s}-OH + UO_2^{2+}	⇔	Ill^{s}-O-UO_2^+ + H^+	2.00 [c]
	Ill^{s}-OH + UO_2^{2+} + H_2O	⇔	Ill^{s}-O-$UO_2(OH)$ + $2H^+$	-4.20 [c]
	Ill^{s}-OH + UO_2^{2+} + $2H_2O$	⇔	Ill^{s}-O-$UO_2(OH)_2^-$ + $3H^+$	-10.90 [c]
	Ill^{s}-OH + UO_2^{2+} + $3H_2O$	⇔	Ill^{s}-O-$UO_2(OH)_3^{2-}$ + $4H^+$	-18.10 [c]
	Cation exchange reactions			
	CE: Ill-clay + H^+	⇔	H-Ill-clay	0.00 [d]
	CE: Ill-clay + Na^+	⇔	Na-Ill-clay	0.00 [d]
	CE: Ill-clay + K^+	⇔	K-Ill-clay	0.92 [d]
	CE: 2Ill-clay + Ca^{2+}	⇔	Ca-Ill-$clay_2$	0.24 [d]
	CE: 2Ill-clay + Mg^{2+}	⇔	Mg-Ill-$clay_2$	0.58 [d]
	CE: 2Ill-clay + Sr^{2+}	⇔	Sr-Ill-$clay_2$	0.24 [d]
	CE: 2Ill-clay + Fe^{2+}	⇔	Fe-Ill-$clay_2$	0.70 [e]
	CE: 2Ill-clay + UO_2^{2+}	⇔	UO_2-Ill-$clay_2$	0.65 [c]

Continued on next page

Mineral	Surface reaction			log K
Montmorillonite	*Weak sites*			
SSA 100 m^2/g [a,b]	Mnt^{w1}-OH + H^+	⇔	Mnt^{w1}-OH_2^+	3.98 [f]
	Mnt^{w1}-OH	⇔	Mnt^{w1}-O^- + H^+	-8.42 [f]
	Mnt^{w1}-OH + UO_2^{2+}	⇔	Mnt^{w1}-O-UO_2^+ + H^+	0.18 [f]
	Mnt^{w1}-OH + UO_2^{2+} + H_2O	⇔	Mnt^{w1}-O-$UO_2(OH)$ + $2H^+$	-6.22 [f]
	Strong sites			
	Mnt^{s}-OH + H^+	⇔	Mnt^{s}-OH_2^+	4.34 [f]
	Mnt^{s}-OH	⇔	Mnt^{s}-O^- + H^+	-8.06 [f]
	Mnt^{s}-OH + UO_2^{2+}	⇔	Mnt^{s}-O-UO_2^+ + H^+	2.94 [f]
	Mnt^{s}-OH + UO_2^{2+} + H_2O	⇔	Mnt^{s}-O-$UO_2(OH)$ + $2H^+$	-3.56 [f]
	Mnt^{s}-OH + UO_2^{2+} + $2H_2O$	⇔	Mnt^{s}-O-$UO_2(OH)_2^-$ + $3H^+$	-11.16 [f]
	Mnt^{s}-OH + UO_2^{2+} + $3H_2O$	⇔	Mnt^{s}-O-$UO_2(OH)_3^{2-}$ + $4H^+$	-20.66 [f]
	Cation exchange reactions			
	CE: Mnt-clay + H^+	⇔	H-Mnt-clay	0.00 [d]
	CE: Mnt-clay + Na^+	⇔	Na-Mnt-clay	0.00 [d]
	CE: Mnt-clay + K^+	⇔	K-Mnt-clay	1.10 [d]
	CE: 2Mnt-clay + Ca^{2+}	⇔	Ca-Mnt-$clay_2$	0.42 [d]
	CE: 2Mnt-clay + Mg^{2+}	⇔	Mg-Mnt-$clay_2$	0.36 [d]
	CE: 2Mnt-clay + Sr^{2+}	⇔	Sr-Mnt-$clay_2$	0.37 [d]
	CE: 2Mnt-clay + Fe^{2+}	⇔	Fe-Mnt-$clay_2$	0.80 [g]
	CE: 2Mnt-clay + UO_2^{2+}	⇔	UO_2-Mnt-$clay_2$	0.15 [f]
Kaolinite	*Aluminol sites*			
SSA 11 m^2/g [h]	Kln^{a}-OH + H^+	⇔	Kln^{a}-OH_2^+	8.33 [h]
	Kln^{a}-OH	⇔	Kln^{a}-O^- + H^+	-9.73 [h]
	Kln^{a}-OH + UO_2^{2+}	⇔	Kln^{a}-OH-UO_2^{2+}	9.20 [h]
	Kln^{a}-OH + UO_2^{2+}	⇔	Kln^{a}-O-UO_2^+ + H^+	2.18 [h]
	Kln^{a}-OH + UO_2^{2+} + H_2O	⇔	Kln^{a}-O-$UO_2(OH)$ + $2H^+$	-4.74 [h]
	Silanol sites			
	Kln^{s}-OH + H^+	⇔	Kln^{s}-OH_2^+	-
	Kln^{s}-OH	⇔	Kln^{s}-O^- + H^+	-6.90 [h]
	Kln^{s}-OH + UO_2^{2+}	⇔	Kln^{s}-OH-UO_2^{2+}	6.03 [h]
	Kln^{s}-OH + UO_2^{2+}	⇔	Kln^{s}-O-UO_2^+ + H^+	1.26 [h]
	Kln^{s}-OH + UO_2^{2+} + H_2O	⇔	Kln^{s}-O-$UO_2(OH)$ + $2H^+$	-5.45 [h]
Chlorite	Chl-OH + H^+	⇔	Chl-OH_2^+	10.20 [i]
SSA 1.8 m^2/g [j]	Chl-OH	⇔	Chl-O^- + H^+	- [j]
	Chl-OH + UO_2^{2+}	⇔	Chl-O-UO_2^+ + H^+	4.51 [i]

[a] Hartmann (2010); [b] Payne et al. (2011); [c] Bradbury and Baeyens (2005a); [d] Wersin et al. (2009); [e] Pearson et al. (2011); [f] Bradbury and Baeyens (2005b); [g] Baeyens and Bradbury (2017); [h] Turner and Sassman (1996); [i] Arnold et al. (2001); [j] pzc (chlorite) >9.5, in the investigated pH range, only X-OH_2^+ species on the clay surface are relevant (Zorn, 2000)

To compare the surface reaction constants for such heterogeneous systems like the Opalinus Clay, we normalized all protonation and stability constants following Kulik (2002) to a reference surface site density (SSD) of 2.31 sites/nm^2 as recommended by Davis and Kent (1990) and Turner and Sassman (1996). Due to the 1:1 SiOH/AlOH ratio derived from the layer structure of kaolinite, the respective log K values for the two sorption sites were corrected to a reference SSD of 1.155 sites/nm^2 (Joseph et al., 2013a). All SCM-values were corrected to infinite dilution (ionic strength 0 mol/L) using the Davies equation (Davies, 1962).

Following Joseph et al. (2013a), the log K for the cationic exchange reactions of uranyl on illite ($\log K_c = 0.65$) was taken from Bradbury and Baeyens (2005a) and for montmorillonite ($\log K_c = 0.15$) from Bradbury and Baeyens (2005b). For the exchange of the main cations, except iron, on illite and montmorillonite, the log K values presented in Wersin et al. (2009) were used. The log K for iron was selected from Pearson et al. (2011) for illite and for montmorillonite from Baeyens and Bradbury (2017). According to Wersin et al. (2009), the exchange of H^+-ions is also taken into account in the model. As already applied by Hartmann et al. (2008), Joseph et al. (2013a) and Wersin et al. (2016), a cation exchange capacity CEC of 22.5 meq/100g for illite and a CEC of 87 meq/100g for montmorillonite was used. Both parameters were determined by Bradbury and Baeyens (2005b).

Appendix B

Supplementary S-2: Self-diffusion coefficients in water D_w

Table B.1: Summary of the self-diffusion coefficients in water D_w (m^2/s) required for the multi-component diffusion approach.

Species	D_w (10^{-10} m^2/s)	Reference	Comments
H^+	93.1	a	
H^2	51.3	a	
OH^-	52.7	a	
O_2	23.5	a	
CO_3^{2-}	8.1	b	
HCO_3^-	11.8	a	
CO_2	19.2	a	
CH_4	18.5	a	
Ca^{2+}	7.9	a	
$CaHCO_3^+$	5.1	a	
$CaCO_3$	4.5	a	
$CaSO_4$	4.7	a	
Cl^-	20.3	a	
Fe^{2+}	7.2	a	
K^+	19.6	a	
KSO_4^-	15.0	a	
Mg^{2+}	7.1	a	
$MgHCO_3^+$	4.8	a	
$MgCO_3$	4.2	a	
$MgSO_4$	4.5	a	
Na^+	13.3	a	
$NaHCO_3$	6.7	a	
$NaCO_3^-$	12.0	a	
$NaSO_4^-$	13.3	a	
PO_4^{3-}	6.12	a	
HPO_4^{2-}	6.9	a	
$H_2PO_4^-$	8.5	a	
SO_4^{2-}	10.7	a	
HSO_4^-	13.3	a	
S^{2-}	73.1	a	
HS^-	17.3	a	

Continued on next page

Species	D_w (10^{-10} m^2/s)	Reference	Comments
H_2S	21.0	a	
Sr2+	7.8	a	
UO_2^{2+}	7.7	b	
UO_2CO_3	6.7	b	
$UO_2(CO_3)_2^{2-}$	5.5	b	
$UO_2(CO_3)_3^{4-}$	5.6	b	
$MgUO_2(CO_3)_3^{2-}$	5.1	b	
$CaUO_2(CO_3)_3^{2-}$	5.1	b	
$Ca_2UO_2(CO_3)_3$	4.6	b	
$SrUO_2(CO_3)_3^{2-}$	4.8	b	
$U(OH)_3^+$	7.7	b	analogous to UO_2^{2+}
$U(OH)_4$	7.7	b	analogous to UO_2^{2+}
$UCO_3(OH)_3^-$	7.7	b	analogous to UO_2^{2+}
UO_2^+	7.7	b	analogous to UO_2^{2+}

[a] taken from database *phreeqc.dat* distributed with PHREEQC (Parkhurst and Appelo, 2013); [b] Kerisit and Liu (2010); [c] Liu et al. (2011)

Supplementary S-3: Data summary of pore water components

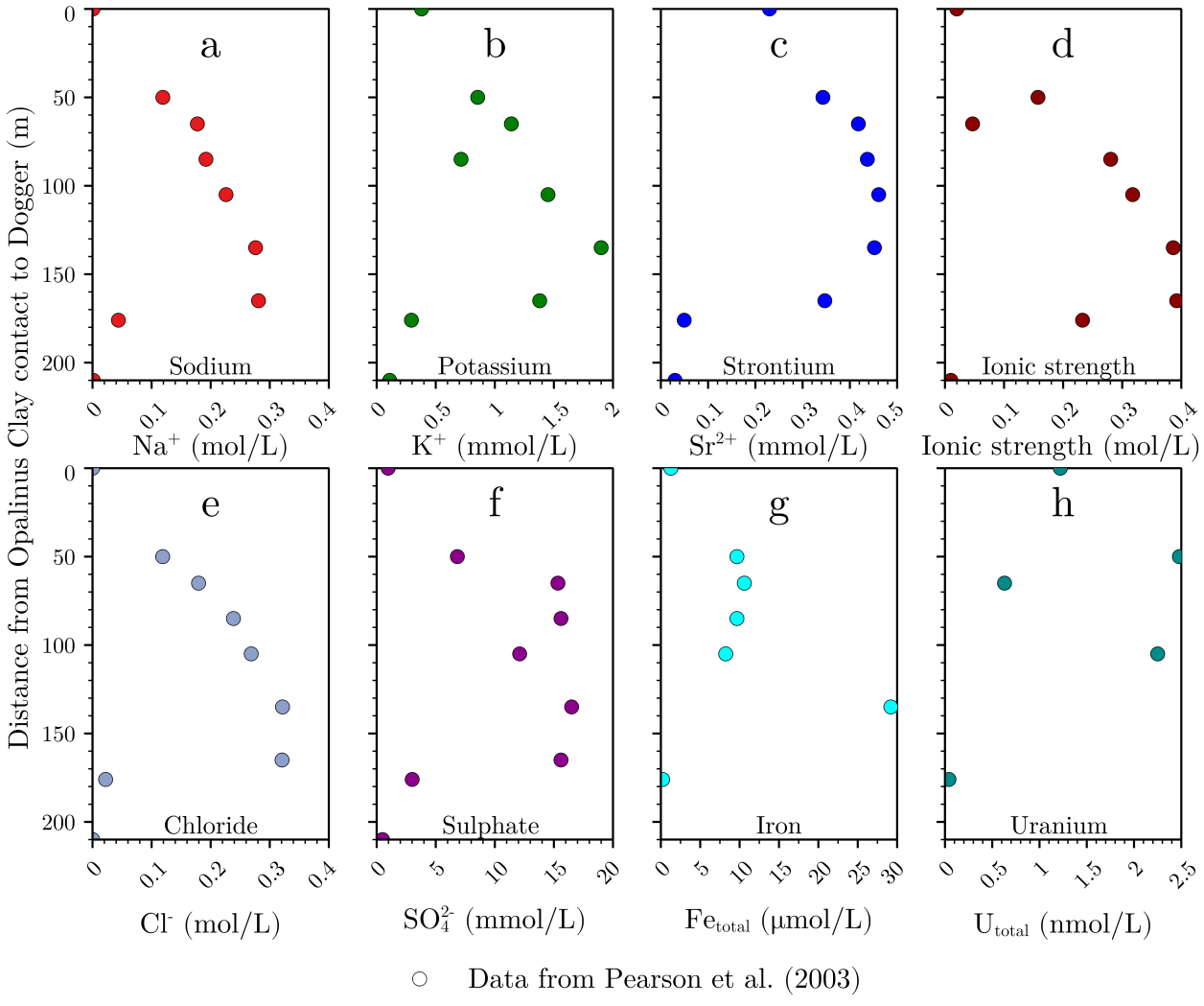

Figure C.1: Concentration profiles of pore water components used for model calibration. The data stems from borehole analyses at the underground laboratory Mont Terri. The y-axis is the distance perpendicular to the contact between Opalinus Clay and Dogger limestones.

Table C.1: Summary of the pore water components used for model calibration. Concentrations are given as averaged values from borehole analyses at the underground laboratory Mont Terri (Switzerland).

Parameter	Unit	BK[a] (Dogger aquifer)	BWS-A3[a,b] (OPA sandy)	BWS-A2[a] (OPA sandy)	BGP-1[a] (OPA carb-rich)	BWS-A1[a,b] (OPA shaly)	BPC-C1[c] (OPA shaly)	E6[a] (Liassic shales)	JM[a] (Liassic shales)	G2[a] (Liassic aquifer)
pH	-	7.38	7.39	7.55	7.28	7.49	7.13	7.78	7.96	7.44
Na^+	mmol/L	0.83	121	197	195	230	276	281	43.8	1.29
K^+	mmol/L	0.38	0.87	1.14	0.73	1.47	1.93	1.28	0.29	0.11
Mg^{2+}	mmol/L	2.65	5.91	11.01	15.89	16.79	21.97	24.71	0.71	0.67
Ca^{2+}	mmol/L	1.99	6.73	8.23	16.37	16.03	18.91	19.28	0.69	2.09
Sr^{2+}	mmol/L	0.23	0.35	0.42	0.44	0.47	0.46	0.35	0.05	0.03
Fe_{total}	μmol/L	1.27	9.81	10.57	n.a.	8.37	29.62	n.a.	0.23	n.a.
Cl^-	mmol/L	0.09	121	321	242	273	327	321	22.19	0.18
SO_4^{2-}	mmol/L	0.97	6.94	15.34	16.03	12.29	16.79	15.63	3.01	0.49
U_{total}	nmol/L	1.22	2.52	0.63	n.a.	2.28[c]	n.a.	n.a.	0.04	n.a.
pCO_2	bar	$10^{-1.7}$	$10^{-2.3}$	$10^{-2.2}$	$10^{-2.4}$	$10^{-2.8}$	$10^{-1.9}$	$10^{-2.5}$	$10^{-2.3}$	$10^{-1.9}$
I[d]	mol/L	0.02	0.16	0.23	0.28	0.32	0.38	0.39	0.05	0.01
Distance[e]	m	0	50	65	85	105	135	165	176	210

n.a. = no data available; OPA = Opalinus Clay; [a] Data from Pearson et al. (2003); [b] Data from Wersin et al. (2009);[c] Data from Vinsot et al. (2008); [d] calculated in PHREEQC; [e] Distance from contact between Dogger limestone and OPA

Supplementary S-4: Adapted stability constant of calcite

The solubility of calcite increases in solutions containing magnesium compared to the pure mineral due to the exchange of Ca^{2+} with Mg^{2+} on the surface of the calcite lattice (Möller and De Lucia, 2020). Therefore, the stability constant of calcite given in the PSI/Nagra thermodynamic database Version 12/07 (Thoenen et al., 2014):

Calcite (pure)
CaCO3 = +1.000 Ca+2 - 1.000 H+ + 1.000 HCO3-
log K = 1.8490

is adapted based on the Mg^{2+}/Ca^{2+} ratio in the pore waters of the Opalinus Clay formation at Mont Russelin representing old chemical signatures (Koroleva and Mazurek, 2009; Mazurek et al., 2011). According to the approach presented in Möller and De Lucia (2020), the new stability constant for calcite is about 0.2 log units higher:

MgCalcite
CaCO3 = +1.000 Ca+2 -1.000 H+ +1.000 HCO3-
log K = 2.01672

Supplementary S-5: Measured pore water profiles confirmed

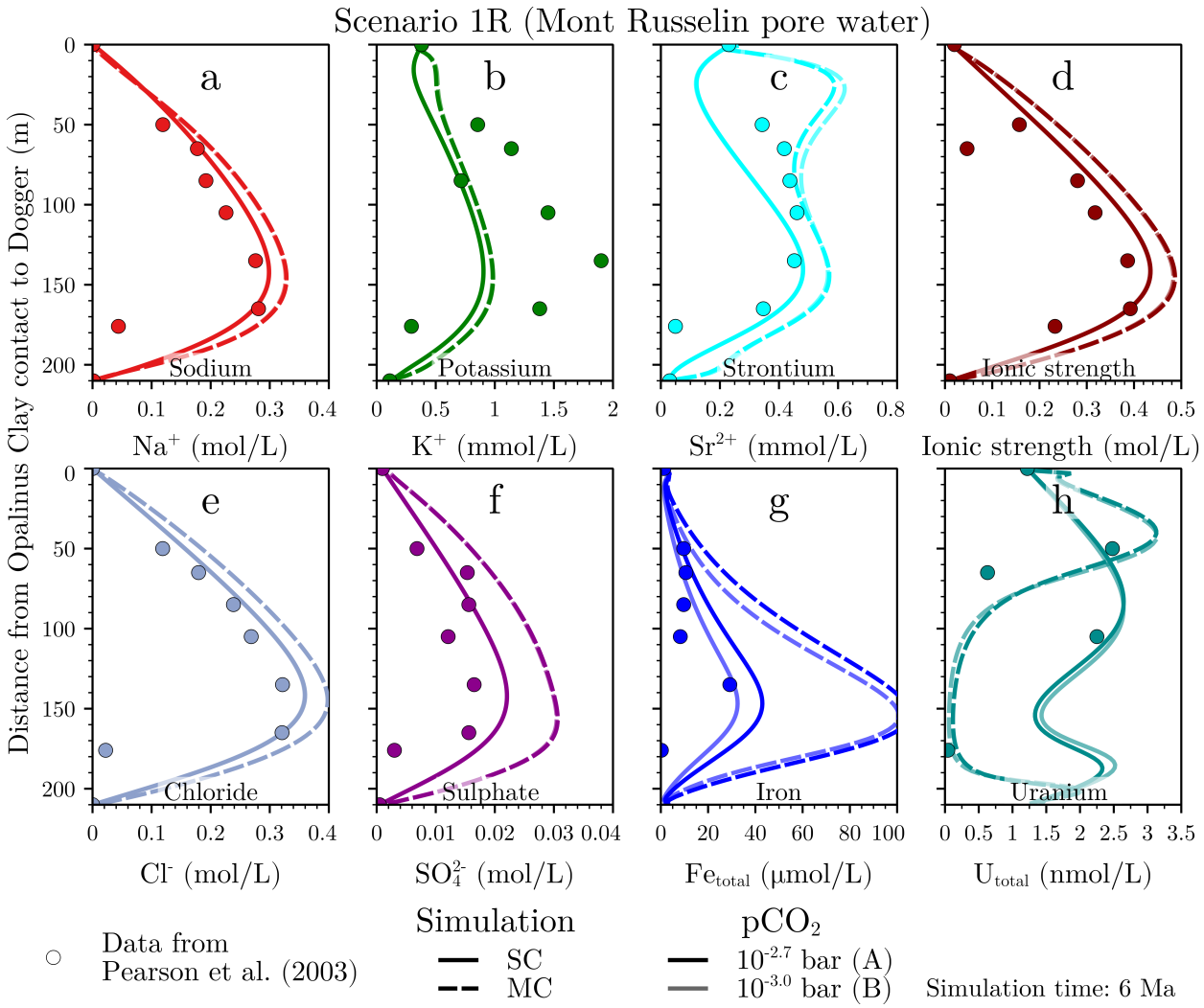

Figure E.1: Modelled concentration profiles of SC simulations coincide with measured data using initial pore water composition according to Scenario 1R. With MC diffusion, transport towards the embedding aquifers is decreased leading to higher concentrations, especially for sulphate and iron.

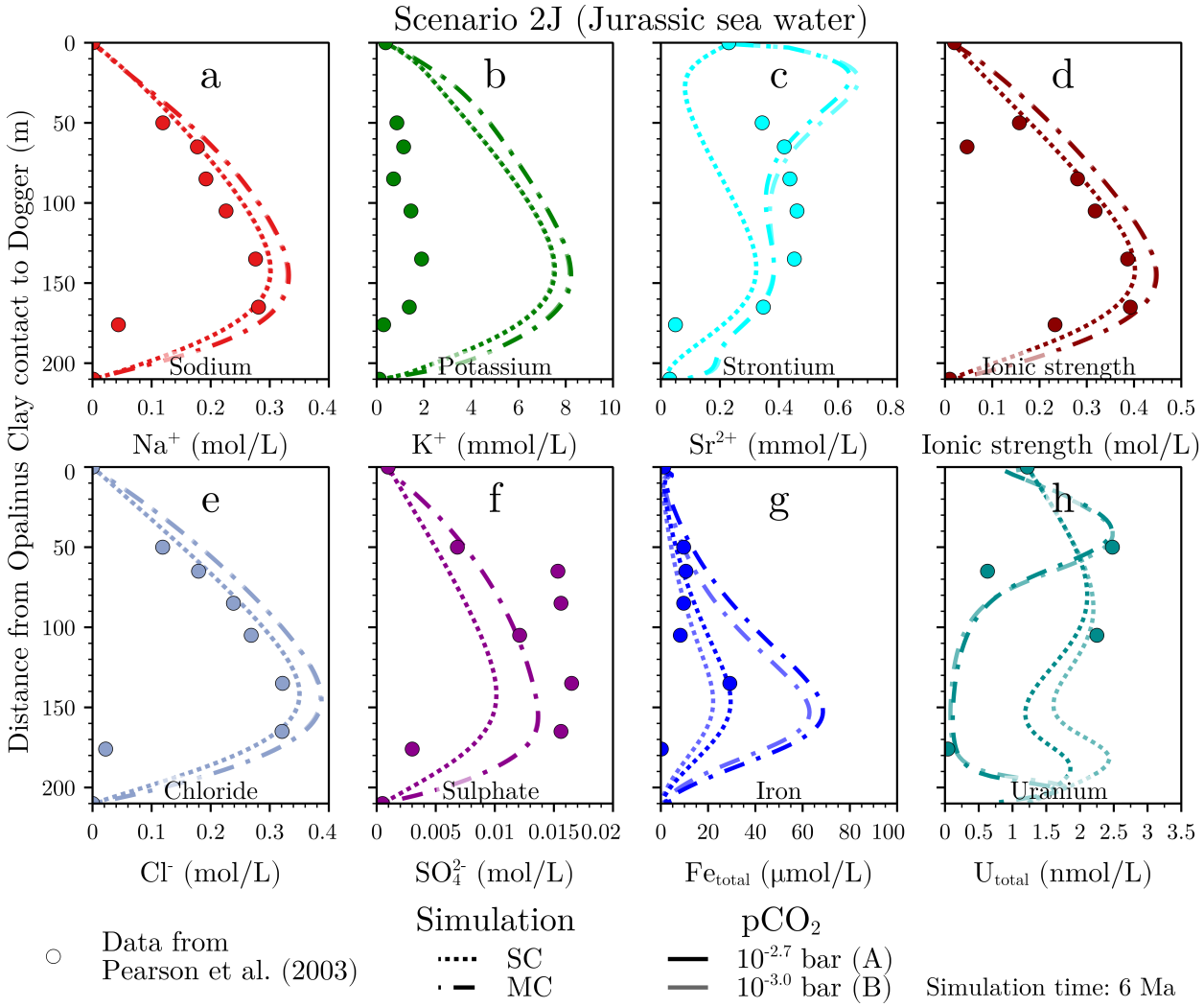

Figure E.2: Modelled concentration profiles of SC simulations coincide with measured data using initial pore water composition according to Scenario 2J, except for potassium and sulphate. With MC diffusion, transport towards the embedding aquifers is decreased leading to higher concentrations, especially for potassium and iron.

Publications of the author

Hennig, T. and Kühn, M. (2021a): Surrogate model for multi-component diffusion of uranium through Opalinus Clay on the host rock scale. *Applied Sciences*, 11, 786. DOI: 10.3390/app11020786

Hennig, T. and Kühn, M. (2021b): Uranium migration through the Swiss Opalinus Clay varies on the metre scale in response to differences of the stability constant of the aqueous, ternary uranyl complex $Ca_2UO_2(CO_3)_3$. *Advances in Geosciences*, 56, 97-105. DOI: 10.5194/adgeo-56-97-2021

Hennig, T. and Kühn, M. (2021c): Potential uranium migration within the geochemical gradient of the Opalinus Clay system at the Mont Terri. *Minerals*, 11, 1087. DOI: 10.3390/min11101087

Kühn, M., **Hennig, T.**, Heidbach, O. and Scheck-Wenderoth, M. (2021): Modelle simulieren die Zukunft. *System Erde*, 11, 2, 30-35. DOI: 10.48440/GFZ.syserde.11.02.5

Hennig, T., Stockmann, M. and Kühn, M. (2020): Simulation of diffusive uranium transport and sorption processes in the Opalinus Clay. *Applied Geochemistry*, 123, 104777. DOI: 10.1016/j.apgeochem.2020.104777

Acknowledgements

The present thesis was financed by the German Research Centre for Geosciences (GFZ) Potsdam, and thus I want to thank the GFZ for the received funding. Further, I would like to acknowledge the Mont Terri Project and the Helmholtz-Zentrum Dresden-Rossendorf for providing data and the chemical thermodynamic database, respectively.

I would like to take the opportunity to thank all those who supported me over the past years. Therefore, this is ”probably” the most important part of the thesis.

I am very grateful to my first supervisor Prof. Michael Kühn for the trust he placed in me and profusely offering his time and expertise. His continous encouragement, enthusiastic manner and valuable ideas supported me to stay motivated and focused. I am very appreciative for his empathy, especially in difficult times. I also want to thank Dr.-Ing. Thomas Kempka for his support and accepting to be the second supervisor. Further, I would like to acknowledge Prof. Thomas Neumann and Prof. Vinzenz Brendler for accepting to review this work.

My thanks goes to Dr. Claudia Joseph for the helpful discussions regarding the uranium diffusion experiment and her time answering all my questions. To my co-author Dr. Madlen Stockmann, I am very grateful for the pleasant cooperation, proofreading parts of the thesis and for always having an open ear for me.

Many special thanks to the working group of section Fluid Systems Modelling. The pleasant atmosphere, valuable discussions and motivating support embellished the everyday work life and after work life as well. In particular, I would like to thank Maria, Marco and Elena for proofreading parts of this thesis as well as Jenny, Peter, Christopher and Benjamin for supporting me in different ways over the past years.

Marielle and Sophia, thank you for proofreading parts of the manuscript and your deep friendship since the beginning of our student life. Michael and Anne, I am very grateful for your support and that you are always by my side as friends.

Finally, my deepest gratitude goes to my mother, Rosemarie, and, of course, to my mental support and personal graphic designer, my boyfriend Stefan. You two had my back the whole time. I cannot even begin to tell you how grateful I am.

Selbstständigkeitserklärung

Hiermit erkläre ich, Theresa Hennig, dass ich als Autorin der vorliegenden Dissertation mit dem Titel "*Uranium migration in the Opalinus Clay quantified on the host rock scale with reactive transport simulations*", die Arbeit selbstständig und ohne unerlaubte Hilfe angefertigt habe.

Ferner versichere ich, keine anderen als die angegebenen Quellen und Hilfsmittel benutzt zu haben. Alle Ausführungen, die anderen Schriften wörtlich oder inhaltlich entnommenen wurden, sind als solche kenntlich gemacht. Die vorliegende Arbeit wurde in keinem anderen Promotionsverfahren angenommen oder abgelehnt.

_____

Potsdam, 22.02.2022